University of Strathclyde

Strathclyde Institute of Pharmacy and Biomedical Sciences

Formulation of Bacteriophage for Application in Bacterial Lung Infection

by

Utsana Puapermpoonsiri

A thesis presented in fulfilment of the requirements for the degree of Doctor of Philosophy

2011

This thesis is the result of the author's original research. It has been composed by the author and has not been previously submitted for examination which has led to the award of a degree.

Signed:

Date:

ACKNOWLEDGMENTS

First, my thanks go to Dr. Christopher F. van der Walle for providing me the opportunity to undertake this Ph.D project, accompanied by his precious supervision and guidance. I would like to express a special gratitude to him for giving me a positively attitude in life, for having believed in me, for being my friend. He always motivates and encourages me to go forward when I felt bad in life. He also teaches me what a good teacher is! He really is!

I acknowledge all the help from all my friends and colleagues I have shared the lab with: Ju Yen, Hiba, Ebtihaj, Heba, Manal, Mohammed, Farah. I also wish to thank Magaret Nutley (University of Glasgow, UK) for the technical assistance in SEM. I wish to specially thank David Blatchford for technical assistance with CLSM. Heartfully thanks for Dr. Steven Ford for scientific support provided during the lyophilisation experiment. I wish to thank to Dr. Janice Spencer who trained and supported me in bacteriophage techniques in the beginning of my Ph.D. I cannot wait to thank for Dr. Nontima Vardhanabhuti who always support me with her love and her kindness. She always gives me a useful advice and moral support when I missed my home. To my best friend, Tantima Kumlung, I would like to thank her for all of her supports, her warm and her friendship.

I would like to thank Thai Government for the funding of my study.

Last, but certainly not least, I am grateful to my mom (Pataya) and dad (Prawit) and my brother (Apisit) for their unconditional love and carefulness. It is very difficult to explain how much I love you….mom..dad…bro…I..LOVE..YOU..THANKS FOR ALL.

TABLE OF CONTENTS

LIST OF FIGURES

LIST OF TABLES

LIST OF ABBREVIATIONS

alv	alveolus
ATCC	American Type Culture Collection
BaCl	barium chloride
brn	bronchiole
ca.	approximately
CF	cystic fibrosis
cf.	compare
CFC	critical flow controller
CFTR	cystic fibrosis's transmembrane conductance regulator
CFU	colony forming unit
CLSM	confocal electron microscopy
cm	centimetre
CNT	connective tissue
CsCl	cesium chloride
d_a	aerodynamic diameter
DCM	dichloromethane
d_g	geometric mean weight diameter
DLS	dynamic light scattering
DNA	deoxyribonucleic acid
d_{pd}	diameter of the primary emulsion
DPI	dry powder inhaler
DSC	differential scanning calorimetry

d_{sd}	diameter of the secondary emulsion
FITC	fluorescein isothiocyanate
g	gram
g/cm^3	gram per cubic centimetre
g/mL	gram/millilitre
h	hour
H&E	hematoxylin and eosin
HCl	hydrochloric acid
HPLC	high pressure liquid chromatography
e.g.	for example
i.v.	by intravenous
ID	inner diameter
K_2SO_4	potassium sulphate
KCl	potassium chloride
LB	Luria Bertani
$MgCl_2$	magnesium chloride
min	minute
mL or ml	millilitre
mm	millimetre
mM	millimolar
MSLI	multi-stage liquid impinge
mTorr	millitorr
Na_2HPO_4	disodium hydrogen phosphate
NaCl	sodium chloride

NCIMB	National Collectional Industrial, food and Marine Bacteria
nm	nanometer
^{o}C	degree celsius
OD	outer diameter
p.o.	‘by mouth’ , oral route
PBS	phosphate buffer saline
PEG 6000	polyethylene glycol MW 6000
Pfu	plaque forming unit
PLGA	poly (D,L-lactic-co-glycolic acid)
PVA	polyvinyl alcohol
Q	flow rate
rpm	rotations per minute
SD	standard deviation
SDC	deoxycholic acid, sodium salt
SEM	scanning electron microscopy
TEM	transmission electron microscopy
Tg	glass transition
TMDSC	temperature-modulated DSC
TSB/TSA	tryptone soya broth/agar
v/v	volume by volume
VMD	volume median diameter
w/o	water-in-oil
w/o/w	water-in-oil-in-water
w/v	weight by volume

ABSTRACT

This thesis first describes the encapsulation of bacteriophage into the biodegradable polyester microspheres for the use in phage therapies. The focus was on bacteriophage selective for *Staphylococcus aureus* or *Pseudomonas aeruginosa,* encapsulated with PLGA via a modified water-in-oil-in-water double emulsion (w/o/w) solvent extraction technique. The bioactivity of the bacteriophage and the physicochemical properties of the microspheres containing bacteriophage were determined. The bacteriophages were shown to retain lytic activity following the modified w/o/w emulsification process. Fluorescently labelled bacteriophages were distributed entirely within the internal porous matrix of the microspheres, which had the appropriate size and density for inhalation (d_a ~ 3.6 μm and d_g ~ 6.6 μm). An initial burst release of bacteriophage was observed over the first 30 min (55-63% release), followed by a sustained release was quite short, with plateau at around 6 h. The stability of the encapsulated bacteriophage lytic activity lost after 7 days during storage at either 4 °C or 22 °C.

In the second part of this thesis, the lyophilisation of bacteriophage was investigated, examining the drying cycle, moisture content and cake stability. In an attempt to improve the stability of freeze-dried bacteriophage, stabilisers such as sucrose and poly(ethylene glycol) 6000 were added before lyophilisation. The addition of sucrose and PEG 6000 with high concentration (0.5 M and 5%, respectively) produced a stable cake, but the lytic activity of bacteriophage rapidly declined over the first 7-14 days of storage. No distinct change in the glass transition temperatures (T_g) was observed between the blank formulations and formulations containing bacteriophage. Imaging of cakes containing fluorescently labelled bacteriophage did not show gross aggregation or phase separation of bacteriophage during lyophilisation. However, the moisture content of the cake did correlate with lytic activity, with a 4-6% moisture content proving least detrimental. We propose that moisture is a key determinant of bioactivity following

lyophilisation of bacteriophage from solutions containing minimal concentrations of excipient.

In the third part of this thesis, the *in vivo* study, a murine model of lung disease was used to show that the bacteriophage solution could treat the *P. aeruginosa*-infected lung via intranasal administration or nebulisation. However, the reconstituted freeze dried bacteriophage did not show efficacy for treatment in the same manner.

In conclusion, the thesis has explored novel dry powder and solid state formulations for bacteriophages. Key determinants of stability of the formulated bacteriophages have been described. The future development of robust animal models of chronic bacterial lung infection is critical to establishing bacteriophage therapies.

Publications and presentation

Puapermpoonsiri, U., Spencer, J., van der Walle, C.F. (2009). A freeze-dried formulation of bacteriophage encapsulated in biodegradable microspheres. *European Journal of Pharmaceutics and Biopharmaceutics, 72* (1), 26-33.

Puapermpoonsiri, U., Ford, S.J., van der Walle, C.F. (2010). Stabilization of bacteriophage during freeze drying. *International Journal of Pharmaceutics, 389* (1-2), 168-175.

Work from this thesis has already been presented and reported in conference abstract.

Puapermpoonsiri, U., Spencer, J., van der Walle, C.F. A release study of bacteriophage-containing microspheres. Presented as a poster presentation at the 36th *Annual meeting & Exposition of the Controlled Release Society* in Copenhagen, Denmark, on the 18th-22nd July, 2009.

Chapter 1: Introduction

1.1. The pathology of cystic fibrosis

Cystic fibrosis (CF) is an inherited disease affecting infants, children and young adults. It is characterized by the widespread secretion of abnormally viscous mucus and by sweat containing high electrolyte concentrations. Approximately 1 in 20 people carry the gene and 1 in 1600 Caucasian births are affected (Massie, et al., 2000; Welsh, et al., 2001; Massie, et al., 2005). It is a multisystem disease affecting many organ systems including the lungs, pancreas, male genital tract, sweat glands, liver, and intestine.

This inherited autosomal-recessive disease is only expressed when the individual is homozygous for a defective gene located on the long arm of chromosome 7. This gene will produce the membrane protein which is widely known as the CF transmembrane conductance receptor (CFTR) (Kerem, et al., 1989; Riordan, et al., 1989; Kerem, 2006). The CFTR is required for the regulation of sodium and chloride ion transport across the cell membrane: the CFTR serves as the chloride channel in lung epithelium and other organs. Congenital absence or a defect of CFTR in the lung leads to decrease chloride secretion and increased reabsorption of sodium. This leads to the production of a thick mucus secretion by the dehydrated epithelium and predisposes the patient to develop impaired mucociliary clearance and bacterial infections (Puchelle, et al., 2002).

The major cause of mortality of CF is the lung disease, which is responsible for more than 95% of mortality (Welsh, 1994). In recent years, Lyczak, et al. (2002) mentioned that the airways of cystic fibrosis (CF) patients are colonised by pathogenic micro-organisms in infancy, and in the vast majority of cases chronic infections are

established. Most CF patients experience recurrent acute respiratory episodes and eventually die of respiratory failure resulting from infection. Particularly, the obstruction of the respiratory airways from a thick mucus results in chronic infection, and in time this leads to progressive deterioration of lung function. Prevalent CF pathogens most commonly studied and characterised include: *Staphylococcus aureus*, *Haemophilus influenzae*, *Pseudomonas aeruginosa, and Burkholderia cepacia* complex (BCC). The prevalence of these species in the airway changes over time, as illustrated in Figure 1.1 (Harrison, 2007). CF patients are infected early in life with *Staphylococcus aureus* and *Haemophilus influenzae* and later with the opportunistic bacterial pathogen, *Pseudomonas aeruginosa*. *P. aeruginosa* colonisation in the lung which is the principal cause of mortality in CF patients (LiPuma, et al., 1990; Franz, et al., 1994; Nixon, et al., 2001; Davies, 2002; Salunkhe, et al., 2005).

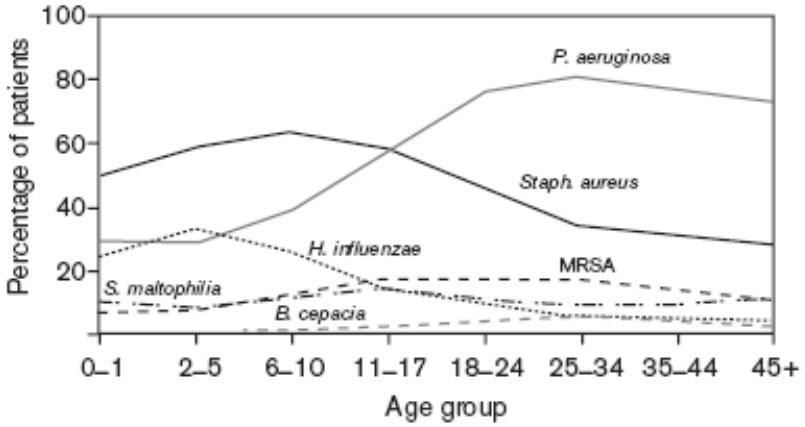

Figure 1.1. Bacterial respiratory infectious types for each range of age (Harrison, 2007).

Recently, some CF centres have reported early, aggressive antibiotic treatment or prophylactic administration of antibiotics can delay or prevent chronic colonization by *P. aeruginosa* and *S. aureus* (Döring and Hoiby, 2004; Hoiby, et al., 2005; Lebecque, et al., 2006). Several studies explicitly report coinfections of more two or more bacterial

species. The results of reported co-infections are summarized in Figure 1.2. *P. aeruginosa* infections generally persist despite the use of long-term antibiotic therapy and induce a host inflammatory response by the elaboration of the bacterial products, particularly the exopolysaccharide alginate. As a result of inflammation the lung extracellular matrix is degraded, as occurs in emphysema, by protease neutrophil elastase released by neutrophils recruited to the lung during the immune response. This protease also damages neutrophils and cleaves complement, resulting in an impaired ability to destroy lung pathogens (Alexis, et al., 2006).

The problem of eradication of *P. aeruginosa* from chronically infected patients has also been shown to be due to bacterial mucoid secretions (Bjarnsholt, et al., 2009). Exposure of non-mucoid *P. aeruginosa* to oxygen radicals from hydrogen peroxide or activated polymorphonuclear leukocytes (PMN) induces mutations in the *muc*A gene. *Muc*A encodes an anti-sigma factor of *Alg*U required for expression of the alginate biosynthetic operon, leading to a mucoid phenotype (Mathee, et al., 1999). As a result, *P. aeruginosa* mutate to a mucoid type that is resistant to opsonization and phagocytosis by cells of the immune system, and increases tolerance to toxic oxygen radicals and antibiotics. Thus, over time, mucoid *P. aeruginosa* strains colonise the CF lung in structures referred to as biofilms, making chronic infections very difficult to treat (Hoiby, 2002). Drenkard and Ausubel (2002) discovered that the phenomena of antibiotic resistance and biofilm formation are genetically linked, and that antibiotic-resistant phenotypic variants of *P. aeruginosa* with enhanced ability to form biofilms arise at high frequency both in vitro and in the lungs of CF patients.

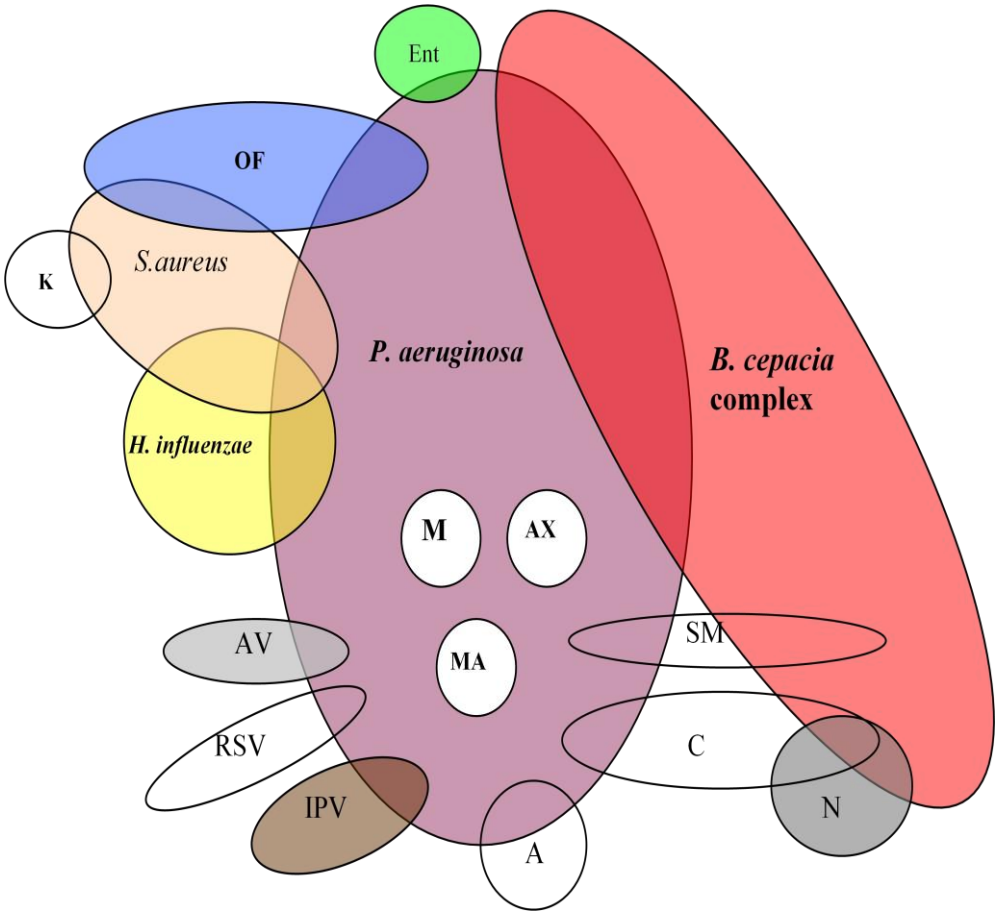

Figure 1.2. Venn diagram depicting the coinfections of the CF airways. A, Aspergilus spp.; AV, adenovirus; AX, A. xylosoxidans; C, Candida spp.; Ent, enterobacteria; IPV, influenza and/or parainfluenza virus; K, Klebsiella spp.; M, mycoplasma; MA, Mycobacterium abscessus; N, Neisseria spp.; OF, oropharyngeal flora; RSV, respiratory syncytial virus; SM, S. maltophilia (adapted from Harrison, 2007).

1.2. Animal models of CF

To develop new treatments, animal models are required for investigation of lung inflammation and the pathogenesis of lung disease in CF. The appropriate animal model should be representative for the human disease and several models exist. For example, Johansen et al. described new strategies for the treatment of chronic infection in CF patients following improved therapy of chronic *P. aeruginosa* lung infection in the rat model (Johansen 1995, 1996). In the animal model, the rapid clearance of the infective organism or acute sepsis and death can take place if free *P. aeruginosa* is administered (Schook, et al., 1977; Dunn, et al., 1985).

As stated in section 1.1, the cause of mortality of CF is the chronic bacterial lung infection. Although the animal model with deficiency of CFTR gene is a good representative for study, in this study we focus on the development of bacteriophage therapy forbacterial lung infection. To overcome the problem of eradication of bacterial lung infections, the animal model lacking the genetic deficiency for CF was used for this study, so it may be not the suitable model for the lung infection with CF condition.However, the chronic bacterial lung infection model for the bacteriophage therapy would be established by this study. Thus, to model chronic infection, agarose beads are used as carriers of the pathogenic bacteria and avoid physical elimination; this leads to a persistent stimulation of the host defense, typical of CF. Cash and colleagues originally employed the agarose beads embedded with *P. aeruginosa* with a rat model of chronic bronchopulmonary infection in rats (Cash, et al., 1979). Subsequently, Starke, et al. (1987) also used agarose beads for use in a murine model of chronic pulmonary infection with either *P. aeruginosa* or *P. cepacia*. The results showed that the mice model with agarose beads was a useful tool for the study of the pathology of chronic pneumonia with *Pseudomonas* species. The bacteria can migrate from the agarose beads, or grow slowly within the beads *in vivo* (Hodgson, et al., 1995). As a

variation on this model, Nacucchio, et al. (1984) suggested that free-living *P. aeruginosa* in the presence of sterile agar beads was sufficient to induce lung infection the same as using *P. aeruginosa*-laden agar beads in rat model by intratracheal injection; i.e. it was not necessary for the bacteria to be embedded, but simply the presence of the beads reduced mechanical airway clearance. To date, there are several reports using the agarose bead model of chronic pulmonary infection with mucoid *P. aeruginosa* to model CF lung infection (Pennington, et al., 1981; Klinger, et al., 1983; Iwata and Sato, 1991; Johansen, et al., 1995; Beaulac, et al., 1996; Song, et al., 1998; Cantin and Woods, 1999; Meers, et al., 2008). Seaweed alginate beads containing *P. aeruginosa* have also been compared with agarose beads, the rationale being that the alginate beads are similar in chemistry to the alginate produced by mucoid *P. aeruginosa* (Pedersen, et al., 1990; Wu, et al., 2001, 2004; Ciofu, et al., 2002; Song, et al., 2005). Bragonzi and colleagues (2005) also studied the alginate expression of nonmucoid *P. aeruginosa* in lung CF patient and in a mouse model via the agar bead. It was reported that the anaerobic conditions in the lung is able to induce a rapid production of alginate in *P.aeruginosa* and that this response is initially reversible but can become stable after 2 weeks of chronic lung infection in mice. It was suggested that the exopolysaccharide has to be considered since this phenomenon was also found in the analysis of nonmucoid *P. aeruginosa* isolates from patients with CF. The agarose bead model of (murine) lung infection has been successfully employed to investigate the safety and efficacy of various pharmacological and gene-therapy protocols in chronic pulmonary infection. For instance, CF mouse models have been used to examine gene targeting - to disrupt the murine CFTR locus by homologous recombination (Dorin, et al., 1992; Snouwaert, et al., 1992; O'Neal, et al., 1993; Hasty, et al., 1995; Rozmahel, et al., 1996). Recently, Debarbieux et al. (2010) was successful to introduce the luminescent *P.aeruginosa*infection in murine model for determination the bacteriophage therapy via the bacterial intranasally administration. This model illustrated that the intranasal administration practically produced the lung infection.

Other animals have also been used, such as the ferret, to evaluate the secretion of mucous from serous cells in trachea after *P. aeruginosa* alginate exposure (Kishioka, et al., 1999), or the cat, to study the role of macrophage activation in chronic lung disease (Thomassen, et al., 1984). The role of submucosal glands which are only found in the proximal trachea in mice can be studied in sheep, pig, or cat models (Hug and Bridges, 2001; Joo et al., 2001).

Till now, 'natural' animal models of this disease have not yet been identified, despite extensive screening of non-human primates (Glavac, et al., 2000). Although the discovery of the CFTR gene lead to rapid progress in understanding the molecular basis of CF, the recurrent lung infections with *P. aeruginosa* remain the major cause of morbidity and mortality. However, progress towards an understanding of the inflammatory and immunological events, and the relationship between CF mutation and infection, remains largely undefined due to a lack of appropriate animal models (Stotland, et al., 2000). Stoltz, et al. (2010) recently attempted to overcome this limitation by using a pig model which harboured the mutated CFTR gene. They found that these pigs had a host defense deficiency against bacteria within an hour of birth. However, it may be useful to develop the bacterial lung infection animal model and investigate the efficiency of bacteriophage therapy or the other therapeutic agents which can be benefit for the antibiotic bacterial resistant condition.

1.3. The treatment of CF

1.3.1. Antibiotics

Due to airway infection and airway obstruction CF, the treatment strategies include aggressive airway clearance by using antibiotics, mucolytics, physical therapy, anti-inflammatory agents, and increasing airway surface liquid. Much of the treatment for CF is supportive, including intensive antipseudomonal/ antibiotic therapy, anti-pseudomonal vaccines and physical therapy. These measures have been primarily responsible for the increase in the median age of death from under 10 to 28 years in the last three decades (Ravilly, et al., 2005). Recently, a phase III clinical study of a flagella-based *P. aeruginosa* vaccine revealed that the vaccination of a flagella-based *P. aeruginosa* failed to reduce infection rates for chronic *P. aeruginosa* colonisation (Döring, et al., 2007). Furthermore, the Cochrane database has also asserted that vaccines against *P. aeruginosa* cannot yet be fully recommended (Johansen and Gøtzsche, 2008). However, it should be noted that antibiotics further reduce the influx of neutrophils to the lungs, which in turn slows the rate of progression of proteolytic lung destruction by neutrophil elastase (NE) (Meyer, et al., 1991).

Antibiotics may be administered for treatment of pulmonary exacerbation with TOBI® (Novartis Pharmaceuticals). Intravenous antibiotics active against *P. aeruginosa* are used immediately when symptoms of an impending exacerbation of infection first appears in the patient, and are usually given for 2 weeks or longer. Suggested antibiotic regimens include an aminoglycoside such as tobramycin sulfate or amikacin sulfate, administered with an extended-spectrum penicillin such as ticarcillin disodium or piperacillin sodium (Franz, et al., 1994). Moreover, nebulised antibiotics have been shown to maintain lung function between courses of antibiotics and are in widespread use as prophylaxis in adult clinics (Taylor and Hodson, 1993). One study showed an

improvement in lung function during high dose aerosolized tobramycin with a concomitant decrease in sputum density of *P. aeruginosa* (Lenoir, et al., 2007). The drawback of this study was that patients had to receive 600 mg of aerosolized tobramycin three times a day, which involved a 30 mL volume of nebulisation (Pai and Nahata, 2001).

Established *P. aeruginosa* infections are rarely eradicated by antibiotics but chronic infections can usually be well controlled (Hoiby, et al., 2005). Problems arise when the *Pseudomonal* strains become resistant to the antibiotics (McManus, et al., 2005; Sener, et al., 2005). In many centres, *Pseudomonas cepacia* has emerged as a serious problem in patients with CF because this organism tends to develop resistance to multiple antibiotics. Furthermore, in some centres, infection with *P. cepacia* has been associated with a severe, frequently fatal, pneumonia (Downey, et al., 2007; Paschoal, et al., 2007).

Table 1.1. Antibacterial agent in management of *P. aeruginosa* lung infections in CF

Antibiotic group	Antibiotic names	Antibiotic mechanism(s)	Route of administration
Aminoglycoside	Amikacin / liposomal amikacin Netilmicin Tobramycin	Inhibit protein synthesis by irreversibly binding to the 30S ribosomal subunit and preventing the 30S initiation complex, thereby inhibiting tRNA translocation and interfering with the proof reading process.	i.v./ liposomal amikacin for inhalation i.v. i.v., p.o., inhaled
β-lactam	Aztreonam Cefepime Ceftazidime Imipenem (β-lactam)/cilastatin Ticarcillin piperacillin	Interfere with bacterial cell wall biosynthesis, specifically the peptidoglycan layer which is important for cell wall structural integrity, especially in Gram-positive bacteria.	i.v. i.v. i.v. i.v. i.v. i.v.

This table is continued in page 11

Macrolide	Azithromycin	Primarily protein synthesis inhibitors by blocking the action of peptidyltransferase (transfer of the peptide unit to tRNA) and ribosomal translocation. Secondary effects on glutathione-S-transferase, chemokine release, nitric oxide (bronchoconstriction and airways remodelling).	p.o.
Quinolone	Ciprofloxacin Levofloxacin (MP-376)	Bind to the A subunit of DNA gyrase (topoisomerase) and so prevent the supercoiling of DNA and inhibit DNA synthesis.	p.o./inhaled liposomal
Polymyxins	Colistin sulfate/ sulphomethate	Isolated from Gram positive bacteria and specific for Gram-negative bacteria since they target a lipopolysaccharide in their outer membrane. Also generally interact with cell membrane phospholipids.	Inhaled
Chloramphenicol	Chloramphenicol	Inhibits protein synthesis by binding to 30S bacterial ribosomal subunit and also inhibiting peptidyl transferase activity.	p.o.

- i.v. = intravenous administration, p.o. = oral administration

With the problem of antibiotic resistance mentioned above, a novel amikacin formulation was developed called "Arikace™," as shown in Table 1.1 (Transave Inhalation Biotherapeutics, Monmounth Junction, NJ, USA). Arikace™ composed the anti-*P. aeruginosa* aminoglycoside Amikacin encapsulated in neutral liposomes (DPPC) and cholesterol. With a Phase II clinical trial, the European and U.S. trials were performed across 15 and 18 centres in paediatric and adult CF patients, respectively. The studies indicated that Arikace™ significantly improved the lung function and reduced of *P. aeruginosa* density in the sputum (Clancy, 2009).

1.3.2. Mucolytic agents

Infections caused by multiresistant bacteria that cannot be treated by antibiotics combined with very few discoveries of truly novel antibiotics during the last 20 years have forced the exploration of alternative therapies. The pathophysiological properties of CF, as a result of the viscous mucus, have been successfully treated with human recombinant deoxyribonuclease (rhDNase), which digests linear DNA (a product of neutrophil lysis and bacterial secretion) to reduce mucus viscosity, so enhancing mucociliary clearance and improving lung function. Pulmozyme™ (rhDNase produced by Genetech Inc.) is administered by nebulisation and has been shown to improve the forced expiratory volume in one second (FEV_1) and the forced vital capacity (FVC), albeit a small but significant improvement (Fuchs, et al., 1994; Henry, et al., 1998; Quan, et al., 2001; Hodson, et al., 2003; Suri, 2005; Frederiksen, et al., 2006). Fuchs, et al. (1994) reported a Phase III study in 968 adults and children with CF treated by rhDNase twice-daily for 24 weeks (Fuchs, et al., 1994); the treatment could slightly improve in lung function whereas the exacerbation of respiratory symptoms was not eliminated. Similarly, Quan, et al. (2001) also revealed that nebulised Dornase alfa can maintain lung function and reduce the risk of exacerbations. rhDNase is also used in long term (12-month) treatment and may help in preventing gradual tissue damage and irreversible loss of lung function, which is the consequence of a sustained presence of

pathogens in the lower respiratory tract (Frederiksen, et al., 2006). Patients also experience an enhanced quality of life: decreased cough frequency and severity, and improved expectoration, dyspnea, energy levels and appetite. Recently, Rozov, et al. (2010) also reported that Dornase alfa improved the Health-related quality of life (HRQOL) of the patients with CF during the first year of treatment through measuring about the psychological and social impact of treatment on patients with CF.

Although clinical trials have shown that rhDNase significantly improves lung function in patients with CF, it does not mean that all patients benefit from this treatment (Fuchs, et al., 1994; Shah, et al., 1995; Harms, et al., 1998). Many studies have been performed to evaluate the effect of ions (calcium, magnesium) on the structure and stability of rhDNase to overcome the failure of the rhDNase in CF patients (Chen, et al., 1999; Sanders, et al., 2006). However, the cost of Pulmozyme is high and guidelines for prescription of this drug must be carefully considered.

1.3.3. Anti-inflammatory agents

In the CF airway, the inflammatory response will lead to the lung damage. Therefore anti-inflammatory agents are necessary for CF lung disease while the adverse effects need to be concerned. The anti-inflammatory agents including corticosteroids and NSAIDs were used for CF lung disease.

Lai, et al. (2000) reported that oral prednisolone could reduce the rate of decline in lung function for children with CF. However, the adverse effects from prednisolone included growth retardation, cataract formation and the development of glucose intolerance. A Phase III study of high dose NSAIDs (ibuprofen) also failed to improve in FEV1

(Lands, et al., 2007). Currently, high dose ibuprofen was also reported to down-regulate IL-8 production in response to TNF-α and IL-1 β in the CF epithelium (Dauletbaev, et al., 2010). It indicated that the efficacy of these agents has not been proven and the balance between reducing the damage from a heightened inflammatory response while conserving the protective effects of the host against infections is important.

1.3.4. Airway rehydrators

As described above in section 1.1, depletion of the airway surface liquid layer due to defective chloride secretion and sodium hyperabsorption leads to diminished mucociliary transport. Airway surface liquid can be augmented by activating chloride secretion via non-CFTR dependent pathways, inhibiting sodium absorption or by the addition of osmotic agents that work by increasing water influx. The net result would be an increase in mucociliary clearance of bacteria, mucus and inflammatory products that would ultimately preserve lung function (Ratjen, 2006, 2009).

1.3.4.1. Osmotic agents

An alternative route to increasing airway surface liquid is to use osmotic agents. Inhaled hypertonic saline (7% saline) was found in many studies to improve mucociliary clearance and is currently a standard therapy in CF (Donaldson, et al., 2006; Elkins, et al., 2006; Amin, et al., 2010). Another type of inhaled osmotic agent that is now in Phase III trials is inhaled mannitol (Wills, 2007). In a 2-week crossover trial in 48 patients with CF lung disease, inhaled mannitol (400 mg twice daily) demonstrated improvement in lung function parameters with the percent change of FEV1 and FVC being 8.75 and 8.14 %, respectively (Teper, et al., 2010). Teper, et al. (2010) also reported that the safety profile of high doses is the same as for lower doses.

1.3.4.2. Ion channel modulating agents

The activation of purinergic receptors in airway epithelia by extracellular nucleotides (adenosine triphosphate/uridine triphosphate) has beneficial effects on mucus clearance in CF. Denufosol tetrasodium is a puridinine triphosphate derivative and agonist of purinergic ($P2Y_2$) receptors. Denusol demonstrated that inhibit acceleration of Na^+ transport via inhibition of epithelial sodium channel (ENaC) and alternation of chloride channels in respiratory epithelium (Kunzelmann and Mall, 2003). In Phase II studies, Kellerman et al. suggested that nebulised Denufosol provided a significant difference in FEV1 between treatment and placebo subjects (Kellerman, et al., 2008). The other agents that act on ion channels either block sodium reabsorption, such as amiloride, or increase chloride secretion, such as adenosine triphosphate, Uridine triphosphate is in the early stages of investigation (Ghosal, et al., 2000; Rodgers and Knox, 2001; Harris, et al., 2007). Amiloride was also suggested by Mall (2009) for preventive therapy in CF, however, adverse effects such as cough were found.

1.3.5. Gene therapy

Gene replacement therapy was also explored by replacing the defective CFTR with wild-type CFTR and transferring this gene by viral vectors such as adenovirus (Ad) and adeno-associated virus (AAV) or non-viral vectors such as cationic liposome and cationic polymer vectors (Rosenfeld, et al., 1991, 1992; Flotte, et al., 1993; Porteous, et al., 1997). In early studies on gene therapy for CFTR function, they demonstrated that the replacement of absent CFTR developed chloride secretion in airway. However, routine, successful gene delivery has not been established because many factors need development: the gene, vector and host factors (reviewed in Griesenbach and Alton, 2009; Mueller and Flotte, 2008). The barriers for effective and safe gene transfer (such as the host cellular immune response against vectors and/or transgene antigens, and the mechanisms of delivering gene transfer vectors to the lung) were also demonstrated in

several studies. These include the innate defense mechanisms of mucociliary clearance, cough, and secreted antimicrobial peptides (Bartlett, et al., 2008). Boucher (2004) demonstrated that mucus adherent to the epithelium could generate biofilm formation, but inflammation occurred in either the presence or absence of infection (Armstrong, et al., 2005; Brennan, et al., 2009; Rosenfeld, et al., 2001). Thus, treatment must not only target infection but also inflammation.

Although repeated doses are required, due to the limited life span of the vectors, the antibody response was detectable with repeated administration of viral transfer vectors (Flotte, et al., 2003; Moss, et al., 2004). The lungs have a strong adaptive immunity to respiratory viruses (reviewed in Kohlmeier and Woodland, 2009) in which the host defenses lead to difficulty in gene transfer by viral vectors.

1.3.5.1. Viral-based gene therapy

Replication-deficient adenovirus-based vector is the first generation viral-based gene therapy. Adenovirus is naturally efficient at *in vivo* infection of the respiratory tract, where it cause symptoms generally associated with the respiratory epithelium. However, Walters, et al. (1999) also demonstrated that the adenovirus would penetrate to the cell via the basolateral surface via specific receptors, whereas the apical surface of epithelial cells was devoid of these receptors. This may cause poor gene transfer efficacy by aerosolized adenovirus vector (Walters, et al., 1999).

Patients who received 2 separate doses of vector demonstrated inefficient gene transfer (Joseph, et al., 2001), and progressive decrease in gene transfer with repeated administration that did not correlate with the appearance of adenovirus vector-specific neutralizing antibodies (Harvey, et al., 1999). Furthermore, adenoviral vectors elicited a dose-dependent inflammatory response in non-human primates and humans (Brody, et al., 1994; Joseph, et al., 2001). Pickles (2004) showed that the adenoviral vectors to be

ineffective and inefficient and there have been concerns about immunologic responses and toxicity.

Adeno-associated virus (AAV) has emerged to improve gene transfer efficacy. The rationale for developing AAV as a vector for gene transfer is based on an increase in duration of activity and improved safety (Flotte and Laube, 2001). With AAV administration, Moss et al. showed that a humoral immune response was not elicited (Moss, et al., 2004). Although AAV encoding CFTR was found to be safe in Phase II trials, it did not show the improvement of lung function when compared between control and treatment groups (Moss, et al., 2007). Furthermore, the novel AAV (AAV serotype 9) preparations showed efficacy in gene transfection (Limberis, et al., 2009) and can be re-administered despite the presence of neutralizing antibodies in the serum in mice (Limberis and Wilson, 2006). Recently, Mitomo et al. (2010) have developed a novel gene transfer vector (a lentiviral vector) which shows many advantages, such as longer expression, repeat administration and transfection of the respiratory epithelium of the (murine) nose, which was beneficial for clinical use.

1.3.5.2. Nonviral vectors

1.3.5.2.1. Cationic lipids complexed with plasmid DNA

Cationic liposomes are lipid:DNA complexes that were developed for transfection of eukaryotic cells *in vitro*. Typically, the positive charges of the liposome would complex and condense negatively charged DNA, while the hydrophobic group would either enhance DNA condensation of or promote membrane fusion and cell uptake (Simões, et al., 2005).

Studies of cationic lipid mediated DNA transfer to the nasal epithelium of CF patients were performed but found to be inefficient for CF treatment, although the safety profile was good (Caplen, et al., 1995; Goddard, et al., 1997). However, Ruiz et al. (2001)

investigated the inflammatory response of inhaled lipid-based DNA transfer to the lower airways, and demonstrated that administration was associated with an innate inflammatory response (Ruiz, et al., 2001). The efficacy of cationic liposomes for CF treatment in Phase I clinical trial has also reported by Rosenecker et al. (2006) that the level of CFTR expression in respiratory epithelium is low and limit of duration. Although several researchs were successful in gene delivery by cationic liposomes such as the mesenchymal stem cell and siRNA for tumor treatment, the improvement of cationic liposome for CF treatment is necessary (Hattori, 2010; Madeira, et al. 2010).

1.3.5.2.2. Compacted DNA nanoparticles

The first generation of cationic gene delivery polymers such as poly(ethylenimine) (pEI), poly(2-dimethylaminoethyl methacrylate) (pDMAEMA), and poly-L-lysine (pLL) were the non-degradable polymers that might cause of the accumulation in body after administration. As this property, it leads some cytotoxicity due to the adverse interactions with membranes. The biodegradable polymer was developed consequently to reduce the toxicity and avoid the accumulation of polymer in the cells. Moreover the degradation of the polymer also was used as a tool to release the plasmic DNA into cytosol. The degradable polymers that are used for this purpose are poly(4-hydroxy-L-proline ester) (PHP), poly(γ-(4-aminobutyl)-L-glycolic acid) (PAGA), polyurethane, PEG-pLL and homopolymer of poly(N-2-hydroxypropyl methacrylamide) (pHPMA). The degradable polymers provide a higher transfection activity than the first generation (Fischer, et al., 2003; Luten, et al., 2008; Kuo, et al., 2010). Furthermore, a cationic polymer (a polyethylene glycol-substituted poly-L-lysine 30-mer) was proposed as a candidate to form complexes with DNA. DNA nanoparticles in preclinical studies with CFTR knockout mice showed transient dose dependent correction of cAMP-stimulated chloride transport (Ziady, et al., 2002).

1.3.6. CFTR modulators

CFTR modulators are aimed at the specific defects in CFTR transcription, processing or function. The compounds currently in development are small molecules taken in oral form and can be classified into three mechanisms dependent on the defective CF lung. In Class I, nonsense mutations lead to premature termination of mRNA translation and result in truncated, nonfunctional CFTR protein. Based on this defect, the compound should allow the reading through of premature stop codons which produce the full length CFTR that can move to the cell surface. PTC124® (Ataluren, USA) has been shown to improve the chloride flux in a Phase II study (Kerem, et al., 2008). In Class II, the CF mutation at F508del leads to misfolded CFTR which is degraded before moving to the apical cell membrane. Thus compounds called 'correctors' would be used to proper folding of the CFTR and allow the CFTR to move to the cell surface. Some examples of correctors identified by high-throughput screening include the aminoarylthiazoles, quinazolinylaminopyrimidinones, and bisaminomethylbithiazoles (Pedemonte, et al., 2005b), the sildenafil analog, KM11060 (Robert, et al., 2008), and the quinazoline VRT-325 (Van Goor, et al., 2006). In Class III, mutations lead to reduced opening of the CFTR channel, with resultant reduced chloride flux into the airway lumen. 'Potentiators' are compounds that increase the function of CFTR correctly located at the cell membrane. Recently, VX-770 demonstrated the improvement of the nasal potential difference and lung function in a clinical Phase II study (Clancy, 2009).

1.3.7. CF therapy from biological derivatives

The alternative therapies such as the chest physical therapy and biological derivatives for CF such as the blocking agent for quarum sensing, bacteriocin, phage therapy and biological control weredemonstrated in Table 1.2. The biofilm formation of *P.*

aeruginosa is produced by cell-to-cell signaling called quorum-sensing (QS). QS associates with the virulence of bacterial infection so the reduction or control of QS will lead to decreased of exacerbation in CF with infection (Eberl, 2006). Furanone and derivatives were demonstrated as biofilm control agents and QS inhibitors, enhancing bacterial clearance in lung infection with *P. aeruginosa* (Wu, et al., 2004; Kim, et al., 2008).

Bacteriocins can act against other bacteria dependent on the type of pyocin. Pyocins are produced mostly by *P. aeruginosa* strains and are located on the *P. aeruginosa* chromosome. Pyocins have three types; R-type pyocins resemble non-flexible and contractile tails of bacteriophage; F-type pyocins also resemble phage tail but are flexible and non contractile; rod-like stricter and S-type pyocins are colicin-like, protease-sensitive proteins (Michel-Briand and Baysse, 2002). Williams, et al. (2008) revealed that engineered R-type pyocin has potential in bactericidal activity.

A bacteriophage is specific for a particular bacterial host (Toro, et al., 2005) and can demonstrate anti-biofilm activity in bacterial infection (review in Donlan, 2009). With this advantage, bacteriophages are good candidates and alternative agents for bacterial infections, particularly in antibiotic resistance. *Bacteriovorus vibrios* reduce biofilm biomass by paretic life cycle; these bacteria such as *Bdellovibrio spp.* will attach to other gram negative cells, penetrate their periplasm, multiply in the periplasmic space, and finally burst the cell envelope to start the new cycle (Kadouri and O'Toole, 2005) (Table 1.2).

Table 1.2. Alternative therapies in CF

Treatment (s)	Purpose (s)	Material (s)/Agent (s)
Chest physical therapy/chest clapping or percussion	To dislodge the mucus from the lungs so that the patient can better expectorate.	A physiotherapist/an electric chest clapper, known as a mechanical percussor.
Biologically derived treatments	Block bacterial quorum sensing.	furanone
	Bacteriocins; S-type is limited only to *P. aeruginosa* strain but R-type can kill other gram negative bacteria.	Bacteriocin; pyocin
	Phage therapy; use viruses that infect and kill solely bacterial cells.	Bacteriophage
	Biological control.	Bacteriovorus

1.4. Bacteriophage therapy

With regards to the treatment of antibiotic resistant *P. aeruginosa* and other pathogenic strains, phage therapy may prove a useful supplementary therapy to the current antibiotics used in chronic infectious disease. Treatment of infections by bacteriophages that specifically kill the infecting pathogen, 'phage therapy', is not new – it has been practiced in Eastern Europe (the old Soviet states) since the early 1900s, but in 'the West' was superseded by the emergence of sulphonamide, penicillins and aminoglycosides. Phage therapy would be particularly useful in treating chronic bacterial infections that are resistant to other treatments and possibly in controlling disease outbreaks in developing countries (Skurnik, et al., 2007).

Typical phage was depicted in Figure 1.3. The bacteriophage consists of an outer protein (capsid, head) including genetic material such as ssRNA, dsRNA, ssDNA, or dsDNA. The tail of bacteriophage is also the protein shell covering the internal structure of bacteriophage but it will be found in some bacteriophages. Tailed phage is the most widespread group of the bacterial viruses. Typical tail phages infect both Eubacteria and Archaea (Table 1.3). Virions consist of a protein shell and linear dsDNA only. Phage particles are not enveloped, and they are said to have a "binary" symmetry since their heads (capsids) have a cubic symmetry and their tail are helical. The DNA composition of tailed phages generally resembles that of their host bacteria. The bacteriophage host range is primarily determined by surface proteins and carbohydrates that the phage uses as ligands to dock onto bacterial surface receptors (Merril, et al., 2006; Hyman and Abedon, 2010). O antigens masking on the host and the presense of restriction endonucleases were demonstrated to associate with the titer of phage activity (Kutter, 2009). It indicates that the specificity to bacterial host of bacteriophage is affected by the biological material presented on the surface of host.

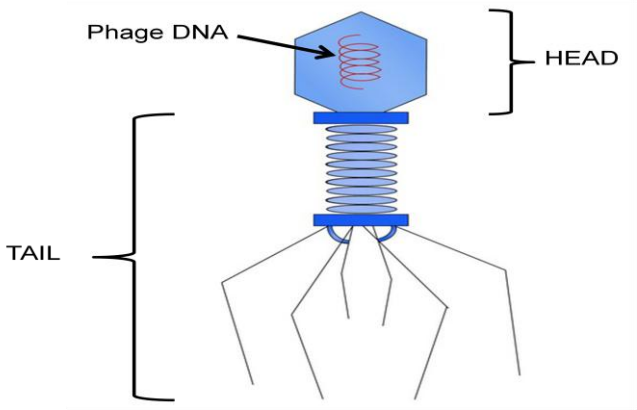

Figure 1.3. Common structure of a bacteriophage (‘phage’)

Table 1.3 shows the host range of the bacteriophage that can infect Eubacteria and Archaea which is the prokaryote bacteria so they may also be defined as “a virus of prokaryotes”. The bacteriophage can infect more than 140 bacterial genera (Ackermann, 2003). In addition to, the bacteriophages are extremely heterogenous in their structural, physicochemical, and biological properties, filamentous, and pleomorphic.The bacteriophage was classified base on the morphology as seen in Figure 1.4 for example; the tailed phages (Order Caudovirale) present into 3 families; Myoviridae, Siphoviridae, Podoviridae.

Table 1.3. Host range of phages by group and host genus (from Ackermann, 2003).

Phage group or family	**Eubacteria**	**Archaea**
Caudovirales	Any (ubiquitous)	Extreme halophiles and methanogens
Microviridae	Enterobacteria, *Bdellovibrio, Chlamydia, Spiroplasma*	
Corticoviridae	*Alteromonas*	
Tectiviridae	a. Enterics, *Acinetobacter, Pseudomonas, Thermus, Vibrio* b. *Bacillus, Alicyclobacillus*	
Leviviridae	Enterics, *Acinetobacter, Caulobacter, Pseudomonas*	
Cystoviridae	*Pseudomonas*	
Inoviridae: Inovirus *: Plectrovirus*	Enterics, *Pseudomonas, Thermus, Vibrio, Xanthomonas* *: Acholeplasma, Spiroplasma*	
Plasmaviridae	*Acholeplasma*	
Lipothrixviridae		*Acidianus, Sulfolobus, Thermoproteus*
Rudiviridae		*Sulfolobus*
Fuselloviridae		*Acidianus, Haloarcula Sulfolobus*

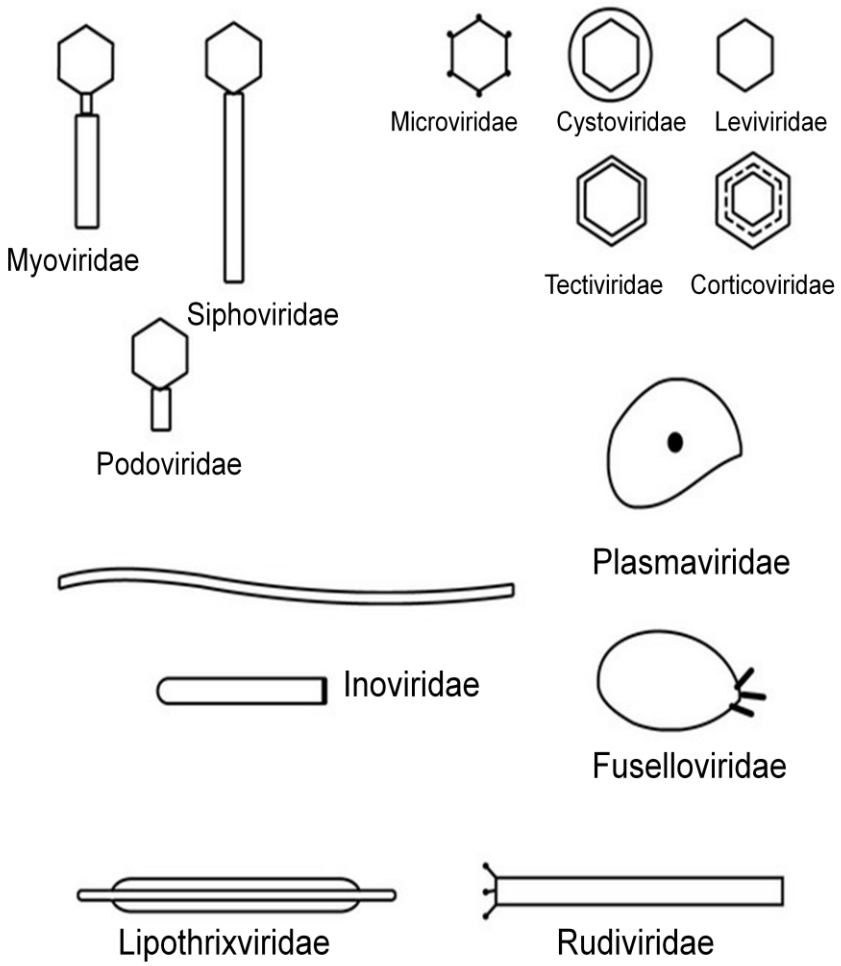

Figure 1.4. Bacteriophage morphology, adapted from Ackermann, 2003.

The phages may have lytic or lysogenic cycle. Lytic phage will directly work for the lytic cycle by the infection via tail which specialised adsorption structure will bind to the specific surface molecules on the target bacteria (as shown in Figure 1.5). In gram-negative bacteria, oligosaccharides and lipopolysaccharides can act as the receptors for some phage. The more complex of gram-positive bacteria offer a very different set of

potential binding sites. Adsorption efficacy and the rate depend on the external factors and host physiological state such as the presence of sugar, specific conditions or specific cofactors. Following the adsorption, the injection process of DNA or the genetic material through the bacterial host will be taken place. Generally, the tail tip has an enzymatic mechanism for penetrating the peptidoglycan layer into the cell target. The replication of phage and the interruption of metabolism in host will be found due to the inactivated host proteases and block restriction enzymes so the host macromolecular biosyntheses was destroyed. The DNA is packaged into preassembled icosahedral protein shalls (procapsids). At last, the lysis of host cell was happen. The lytic cycle is so quick (within 20-30 min). In contrast, the lysogenic cycle did not produce the lysis of host cell immediately. The phage following this cycle is called temperate phage. This phage will integrate its genome with host DNA and replicate themselves by host division (the phage in this state is called "prophage"). The phage will be active again when host conditions deteriorate or the depletion of nutrients (Figure 1.5).

Phages may have some advantages over conventional antibiotics where the treatment of multi-drug-resistant pathogenic bacteria is concerned. For example, the restricted host specificity also means that phages generally will not affect beneficial bacteria, like commensals in the gastrointestinal tract. It is also possible to construct phages that kill, but do not lyse, their target host bacteria (temperate or lysogenic phages as opposed to lytic phages). Furthermore, phage-associated side effects are apparently uncommon in the limited number of high quality clinical investigations (Dancer et al., 2003; Inal, 2003).

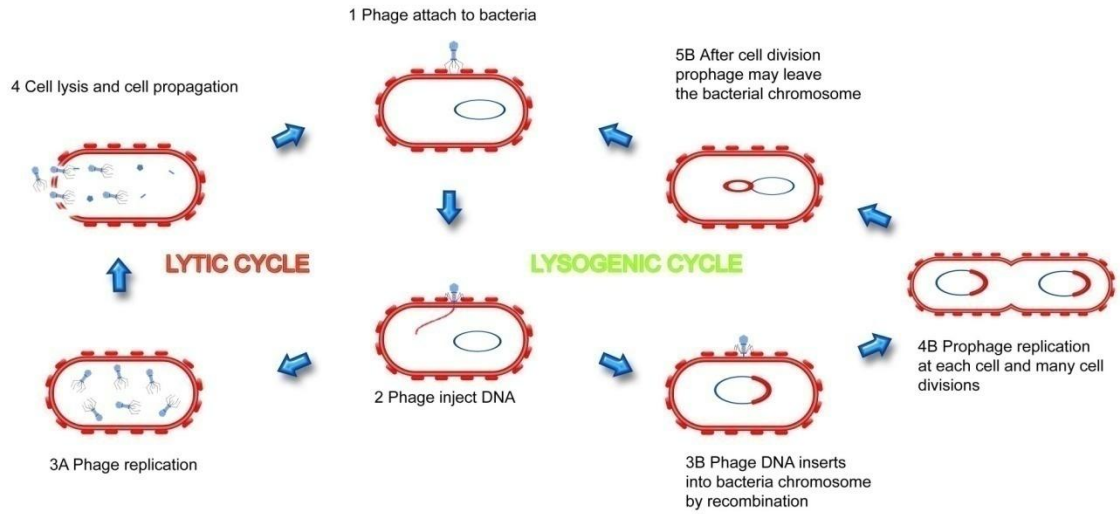

Figure 1.5. Diagram of bacteriophage lytic and lysogenic cycles

For each phage, pharmacokinetic information and understanding is required to design the most effective ways to apply phage therapy. Phage therapy challenges current pharmacokinetic studies because it behaves as a self-amplifying drug (due to *in vivo* replication when target bacteria is present) which can lead to unfamiliar kinetic phenomena. The self-replicative nature of phage therapy may mean that there is a reduced need for multiple doses but, conversely, immune responses may neutralize repeated administration (Payne and Jansen, 2001, 2003).

Phages have been reported to be more effective than antibiotics in treating certain infections in humans (Meladze, et al., 1982; Kochetkova, et al., 1989; Sakandelidze, 1991; Weber-Dabrowska, et al., 2003) and experimentally infected animals (Soothill, et al., 2004; Smith and Huggins, 1982). For example, in one study (Meladze, et al., 1982), phages selective for *S. aureus* were used to treat patients with purulent disease of the lungs, comparing clinical outcomes for patients receiving either phages or antibiotics; this clinical trial was one of few studies using intravenous phage administration and it

was shown that the percent recovery for patients receiving phages was higher than for antibiotic treatment. Interestingly, some whole-phage products have already been used in the clinic to treat topical infections of patients with antibiotic-resistant bacteria. For example, biodegradable patches composed of polymeric scaffolds impregnated with phage (licensed in the Republic of Georgia as Phage BioDerm®) have been used in Tbilisi to treat patients with chronic skin infection unresponsive to antibiotic therapy. Furthermore, a recent study reported that a Phase I/IIa clinical trial targeting *P. aeruginosa* infections of the human ear was completed in November 2007 (Wright, et al., 2009). Pet dogs have also undergone phage therapy trials for the treatment of antibiotic-resistant ear infections (Soothill, et al., 2004).

Since in the past (1968-1991), phage therapy was used and studied in many kinds of bacterial infections about the phage efficacy. For instance, Babalova, et al. (1968) found that *Shigella* phage was successfully to use for prophylaxis of bacterial dysentery. Ten years later, Litvinova, et al. (1978) also succeeded to utilize phage to treat antibiotic-associated dysbacteriosis in 500 low-birth-weight infants. Furthermore, in the same year Zhukov-Verezhnikov, et al. (1978) used the adapted phages, selected against bacterial strains isolated from individual patients, to treat 60 patients having suppurative infections and the results also succeeded.

The clinical studies in the treatment of lung and pleural infections, suppurative skin infection, and postoperative wound infections in cancer patients (Ioseliani, et al., 1980; Meladze, et al., 1982; Cisło, et al., 1987; Weber-Dabrowska, et al., 1987; Kochetkova, et al., 1989) all reported the successful treatment of infection using phages. In 1990's, the phages were developed to treat infectious allergies, infection of skin and nasal mucosa, bacterial dysentery and salmonelosis, recurrent subphrenic abscess, inflammatory urologic diseases and cerebrospinal meningitis (Sakandelidze, 1991; Bogovazova, et al., 1992; Miliutina and Vorotyntseva, 1993; Kwarciński, et al., 1994;

Perepanova, et al., 1995; Strój, et al., 1999). The commercial potential of phage therapy is demonstrated by PhageBioderm, for treatment of wounds and ulcers in 2002 (Markoishvili, et al., 2002). Golshahi and co-workers have reported that *Burkholderia cepaci* complex (BCC) bacteriophage by nebulisation was also successful in treatment of CF patients (Golshahi, et al., 2008). With the first, successful Phase I/IIa clinical trial reported the successful to target the bacteriophage to the human ear infection (Wright, et al., 2009). Examples of current and potential targets for phage therapy are summarised in Table 1.4 and Table 1.5. Although, the resistance to phage is unclear and rarely observed from several works, Cairns et al. (2009) presented that the resistance of phage to host is possible from the mathemetic model. It agrees with the observation from the phage used in the treatment of *C. jejuni* in poutry (Scott, et al., 2007). However, the bacteriophage therapy remains interesting for the optional to the antibiotic resistant treatment condition.

Table 1.4. Phage therapy related to the dieases. Adapted from (Sulakvelidze, et al., 2001).

Reference(s)	Infection(s)	Etiologic agent(s)	Comments
Weber-Dabrowska, Mulczyk, Gorski (2003)	Septic infection	*S. aureus, P. aeruginosa, E. coli, K. pneumonia, P. mirabilis, M. morganii, Enterobacter*	Successful prevention and treatment of septicaemia in humans.
Marza, et al., (2006)	Skin burn with infection	*P. aeruginosa*	A 27-year old with 50% surface area burns. After skin graft and excision, the wound became infected. Purified phage suspension could heal the wound with no adverse effects.
Marza, et al., (2006)	Chronic bilateral otitis externa	*P. aeruginosa*	A 5-year-old dog presented with chronic bilateral otitis externa was given a phage suspension. After treatment the ear was dry and the inflammation disappeared.
Weber-Dabrowska, et al., (2006)	External ear infection	*S. homes, S. epidermidis*	A 24-year-old woman who suffered from post-influenza otitis media infection. Specific bacteriophage combined with lactoferrin administration improved the treatment of infection.
Biocontrol. Ltd.UK.(2007)	Otitis	*Pseudomonas*	The first completed phase II clinical trial testing the efficacy of phage therapy, in this case for human ear infections.
Grandgirard, et al., (2008)	Meningitis	*Streptococcus pneumoniae*	Phage lysin specific for *S. pneumonia (recombinant Cpl-1)* was used with infant rat to treat pneumococcal meningitis. Cpl-1 decreases the pneumococci in cerebrospinal fluid.

Table 1.5. Some examples of preparations used at the Eliava Institute, Tbilisi, Georgia from (Kutateladze and Adamia, 2008)

Phage preparation	Component	Application
Phage mixtures (cocktails)-pyophage	Five components; phage against *S. aureus, Streptococcus, Proteus, P. aeruginosa, and E. coli*	Purulent-septic infections (wounds, infectious dermatological complications), and also to treat problems dealing with the urinary tract, the digestive system, and bronchopneumonia Digestive tract infections: stomatitis esophagitis, gastritis, enterocolitis.
Phage mixture(cocktails)-intestiphage	Various phage preparation	Treatment and prophylaxis of intestinal problems caused by various pathogens, such as *Shigella (Flexner, Newcastle, sonnei), Salmonella (paratyphi A and B, typhimurium, enteritidis, cholera suis, oraneiburg), proteus (valgaris, mirabilis), Staphylococcus, Pseudomonas* and various serovars of *enteropathogenic E.coli.*

This table is continued in page 32

Monoclonal preparations-staphylococcal bacteriophage	Staphylococcal phage preparation	Traumatic osteomyelitis (intra-artery) Lung disease (intravenous) Against various complications of acute and chronic sepsis, septic staphylodermia, septicopaenia, peritonitis, osteomyelitis, mastitis, purulent arthritis, acute and chronic lung abscesses, chronic pneumonia and bronchitis, bronchoectasis, purulent cysis, chronic inflammation of the female reproductive system
Composed preparations-PhageBioderm	Biodegradable polymer impregnated with bacteriophages (pyophage, plus different phage components)	Wounds and ulcer healing and infected radiation burns.

With the phase II clinical trial completed by Biocontrol Ltd., phage therapy is now truly gaining momentum in 'the West'. However, there is to date little data regarding the formulation of phages, and few infectious diseases have been studied. Lack of information on suitable formulations of phage have been a stimulus for the work in this thesis. A particularly promising area for phage therapy, which is also being targeted by companies such as Biocontrol, is the pulmonary delivery of phage to the infected CF lung. The potential for phage therapy in this area is high due to the chronic nature of infection and widespread antibiotic resistance.

1.5. Pulmonary Drug Delivery

The respiratory tract is an attractive site for protein and peptide drug delivery due to its large surface area which can be exposed to drug almost simultaneously. The lung also has a high blood flow which does not directly expose absorbed drug to the clearance mechanisms present in the liver, and has less metabolic activity relative to the intestine and liver. The upper respiratory tract including the trachea and large bronchi has a relatively limited surface area for absorption compared to the alveolar region which provides more that 95% of the surface area of the lung (Weibel, 1979). These results suggest that systemic absorption of peptides and proteins occurs in the alveolar region of the lung but the site of action for agents with local effects may be in either the alveolar region or in the larger airways.

The respiratory route of drug administration by inhalation (pulmonary delivery) is well established (e.g. sulbutamol and steroids in asthma patients). Particularly, CF patients with chronic pulmonary infection with *P. aeruginosa* benefit from the inhalation of antibiotics (Touw, et al., 1995; Mukhopadhyay, 1996). Pulmonary delivery has recently been shown to be an effective route for the administration of biopharmaceuticals, particularly proteins (e.g. Pulmozyme® and Exubera®) and in these cases is

advantageous over oral routes (due to protein degradation in the intestine and hepatic first-pass elimination) and parenteral routes (due to patient compliance and risk of direct infection into the bloodstream). The drug dose may also be less than those for oral or parenteral routes, minimising the risk of systemic side effects or toxicity. In addition, inhalation is also recommended in the European Consensus document on antibiotic therapy against *P. aeruginosa* in CF (Doring, et al., 2000). Recently, Golshahi et al. (2010) successfully developed the dry powder inhalers dosage form forbacteriophages that selective for *B. cepacia* complex and *P. aeroginosa* via the lyophilisation.

Effective delivery generally requires deposition of the drug into the peripheral regions of the lungs, enabling maximum surface area for absorption. The respiratory tract is a series of airways, subdividing from the trachea to bronchi to bronchioles and terminating at the alveolar sacs. From the trachea to alveoli, the airways diameter decreases from about 1.8 cm. to 0.04 cm; but the surface area increases to about 140 m^2. Figure 1.6 illustrates that the segmental bronchi diameter decrease from approximately 4 to 1 mm and the diameter of the bronchioles in the lobe become less than 1 mm (Hickey and Thompson, 1992; Washington, et al., 2001).

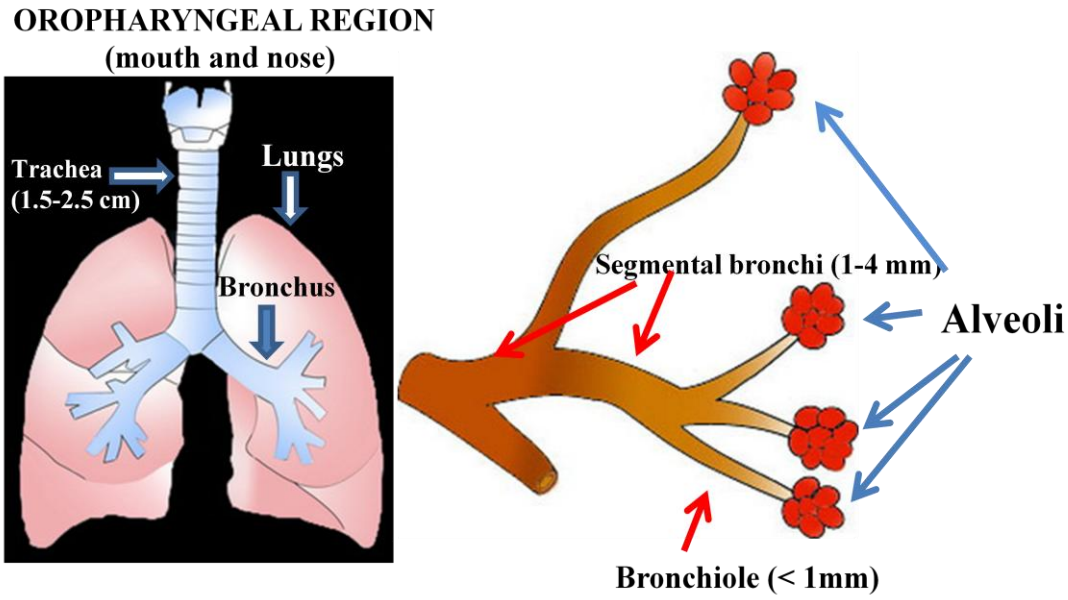

Figure 1.6. Diagram of the respiratory tract and the fractionation of particle size in each region following inhalation.

Whereas the primary function of the respiratory tract is to facilitate gas exchange, the large surface area and two-cell thickness of the alveolar region as well as the high blood flow also provide for a useful route of drug administration.

Particle size and distribution are important considerations in pulmonary delivery. Deposition in the respiratory tract occurs via five physical mechanisms: inertial impaction, sedimentation, diffusion, interception, and electrostatic deposition (Bailey, 1997). Deposition by inertial impaction is dependent on the momentum of the aerosol particles. In general, large particles (above 5 μm) with high velocity are deposited in the back of the mouth and upper airways by inertial deposition (Heyder, 1982). Deposition by sedimentation is described by Stokes' law:

$$v = 2ga^2(\rho_1-\rho_2)/9\eta$$

Where v is the particles' settling velocity, a is the particle radius, η is the viscosity of dispersion medium, ρ_1 is the density of the particles, ρ_2 is the density of the medium and g is the gravitational constant.

Smaller particles (0.5 to 3 μm) are deposited in the bronchial and alveolar regions by sedimentation (Heyder, 1982). Sedimentation increases during either holding of the breath or slow tidal breathing (Newman, 1985; Darquenne, et al., 2000). Deposition by diffusion is due to Brownian motion, caused by constant random collisions of gas particles with small aerosol particles, it is independent of particle density and increases with decreasing particle size. Generally, inertial impaction and sedimentation dominate the deposition of particles larger than 1 μm and diffusion dominates the deposition of particles smaller than 0.1 μm (Tsuda, et al., 1994; Finlay and Gehmlich, 2000).

Small molecule drug absorption following pulmonary delivery occurs in the main by passive diffusion (Heyder, 1982; Tronde, et al., 2003), giving consideration to the molecular size, charge and lipophilicity of molecule. Other absorption routes include transport through aqueous pores, Receptor Mediated Endocytosis (RME – an active transport process), and lymphatic transport (Gonda, 1990).

In additional to the physical characteristics of a particle, drug deposition in the lung is also dependent on the kinetics of absorption and non-absorption clearance mechanisms such as mucociliary clearance, phagocytosis and metabolism. The occurrence of these processes depends on the region of the lung and drug type (Patton, 1996; Sakagami, et al., 2002; Pang, et al., 2005). The clearance of substances by enzymatic degradation for

example is important for molecules like vasoactive intestinal polypeptide (Wall, 1995). The mucociliary escalator is the primary innate defensive system of the lung. It consists of two intrinsically linked components that are the ciliated epithelium and the airway surface liquid (ASL). They have a function to remove the foreign material and cellular debris from the lungs. The ciliated epithelium extends from the inferior turbinate in the nose to the distal small airways. This epithelium covered by the ASL, which is composed of two distinct layers: the periciliary liquid (PCL) and the mucus layer (Knowles and Boucher, 2002). The cilia bodies are surrounded by the PCL, which is approximately the same height as an outstretched cilium, whilst the tips are in contact with the overlying layer of mucus. The mucus layer consists of heavily glycosylated macromolecules known as mucins that behave as a complicated network of polymers, binding and trapping inhaled particles to facilitate clearance from the lung (Kim, et al., 1997). Thus, the efficiency of mucociliary clearance (MCC) depends on the interaction of the airway epithelium including the cilia, the PCL (which must be of normal depth and chemical composition), and airway mucus which has to have a normal composition and rheology.

The lack of a normal CFTR function within the CF airway leads to increased sodium and water absorption resulting in reduced ASL volume (Matsui, et al., 1998; Tarran, et al., 2001; Tarran, et al., 2001). The same CFTR defect also leads to PCL depletion, which causes the cilia to become embedded in the dehydrated mucus, uncoupling the ciliamucus interaction and impairing MCC (Matsui, et al., 1998). This gluing or 'velcro' effect between mucins also inhibits cough clearance (expectoration). The depletion of the ASL volume and impaired MCC can be found in the CF lung disease. Thus, inhaled pathogens fail to be eliminated and can be a cause of chronic infection consecutively.

Bronchus-associated lymphoid tissue (BALT) is the secondary lymphoid tissue in bronchial mucosa. In the adaptive immune response, naive T cells will migrate through

blood vessel high endothelia venules (HEVs) into secondary lymphoid tissue which is stimulated by antigen-bearing dendritic cells. Following this process, the antigen-specific effectors and memory T cells and B cells will be generated and migrate to non-lymphoid tissue containing the cognate antigen or pathogen (Sprent and Surh, 2002). BALT is commonly found in the normal lung of healthy animal such as rabbits and rat, whereas in the normal lung of adult humans, cannot be observed (Bienenstock and Johnston, 1976; Plesch, et al., 1983; Tschernig and Pabst, 2000; Pabst and Tschernig 2010). The BALT will be induced in response to microbial exposure or other types of pulmonary inflammation called "inducible BALT (iBALT)". Inhaled antigens are presented at the BALT initially and are then transported from the bronchial lumen by specialized M cells and dendritic cells in the epithelium (Lugton, 1999; Teitelbaum, et al., 1999; Lührmann, et al., 2002-2003). In viral infection, the presence of BALT leads to accelerate the immunity in response to influenza, mouse-adapted SARS coronavirus, and mouse pneumovirus provided the reduction of morbidity and improve the survival of these animals (Wiley, et al., 2009). It indicated that BALT generally protected the respiratory from viral infection. In humans, chronic bacterial stimulation also leads to the BALT development. For example, BALT was observed in fetus lung without infection 3% but was significantly difference in bacterial lung infection which presents 30-60%. This development (BALT development) will facilitate the local immune response to eliminate the bacterial infection (Gould and Isaacson, 1993; Ersch, et al., 2005).

Phagocytosis is a passive mechanism of immunology and appears in the deep lung region, especially the alveoli, where there are many macrophages and (drug delivery) particles. The phagocytosis of particles diminishes precipitously as particle diameter increases beyond 3 μm (Edwards, et al., 1997). Due to low clearance in the CF lung the drug/carrier may deposit at the site of target and prolong action longer than normal lung. However, toxicity and adverse effects also have to be considered.

1.6. Polyester microparticles for controlled drug delivery

Biodegradable poly-(lactic-co-glycolic acid) (PLGA) microspheres and microparticles have been described for many years and have shown promise for the encapsulation and controlled release of drugs and for passive or active drug-targeting strategies (Okada, et al., 1994; Okada and Toquchi, 1995; Cleland, 1997; Kostanski, et al., 2000; Sinha and Trehan, 2005; Degim and Celebi, 2007; Mundargi, et al., 2007; Mohamed and van der Walle, 2008). Microspheres have been prepared from polyesters (e.g. PLGA, poly ε-caprolactone (PLE), and poly (DL-lactic acid) (PLA)) by various fabrication methods including phase separation, solvent evaporation, and cold precipitation (Chen and Lu, 1999; Ruan and Frenq, 2003; Rahman and Mathiowitz, 2004; Lee, et al., 2006).

Table 1.6. Polyesters used in drug delivery

Polymer	Chemical structure
Poly(lactic-co-glycolic acid)/PLGA	-(-O-C(CH_3)H-CO-O-C(CH_3)H-C-O-CH_2-CO-O-CH_2-CO-O-)$_n$- OR -(-O-C(CH_3)H-C-O-CH_2-CO-O-)$_n$-
Poly(glycolic acid)/PGA	-(-O-CO-CH_2-)$_n$-
Poly(lactic acid)/PLA	-(-O-CO-C(CH_3)H-)$_n$-
Poly(ε-caprolactone)/PLE	-(-O-CO-(CH_2)$_5$-)$_n$-
Poly(*para*-dioxanone)	-(-O-CO-(CH_2)$_2$-O-CH_2)$_n$-
Poly(hydroxybutyrate)	-(-O-CO-C(CH_3)H-CH_2-)$_n$-
Poly(β-malic acid)	-(-O-CO-C(COOH)H-CH_2-)$_n$-

Many microencapsulation processes are a modification of the three basic techniques: solvent extraction/evaporation, phase separation (coacervation) and spray-drying. Supercritical carbon dioxide may avoid toxic solvents (Davies, et al., 2008). Each of these methods employs a similar first step that is the formation of a water-in-oil dispersion (W1/O). In solvent extraction/evaporation, the primary emulsion (W1/O) from the initial step is dispersed into a large volume of aqueous phase containing the stabiliser/emulsifier which commonly is poly (vinyl alcohol) to produce a secondary emulsion (W1/O/W2). Microsphere formation and polymer hardening occur by solvent extraction into the W2 phase. Solvent extraction can also occur via a cosolvent or via evaporation. At the final step of this technique, microspheres will be harvested, washed and dried.

In spray-drying, the primary emulsion (W1/O) is atomized in a flow of air with gradually increasing temperature. In the drying chamber, the organic solvent is rapidly vaporized and the solidified microspheres are completely separated from the drying air in a cyclone chamber (Shi and Hickey, 2010).

Supercritical fluid technology may include rapid expansion of supercritical carbon dioxide (RESS), anti-solvent technique (eg. GAS, SAS, PCA, ASES and SEDS), and particle from gas saturated solution (PGSS). In the process of RESS, the drug and polymer are solubilised in the supercritical carbon dioxide ($scCO_2$) and then expand through a capillary nozzle into a chamber. The rapid decompression of the solution leads to supersaturation, nucleation and microsphere formation. With the limitation of drug/polymer solubility in $scCO_2$, Mishima, et al. (2000) attempted to use another system called rapid expansion of supercritical solutions with a nonsolvent (RESS-N), in which the drug/polymer in $scCO_2$ would be improve the solubility by co-solvent (low molecular weight alcohol) (Mishima, et al., 2000; Matsuyama, et al., 2003). The anti-solvent technique uses a dense gas as an anti-solvent to precipitate the polymer which is

dissolved in an organic solvent. Precipitation occurs as the gas is absorbed by the organic solvent thus expanding the liquid phase and reducing the solvent power until nucleation and microspheres were formed (Chen, et al., 2007). In the solution-enhanced dispersion by supercritical fluids (SEDS), solubilisation of PLGA in dichloromethane before spraying is required. Following the solubilisation of polymer, scCO2 and solvent are mixed in a tube-in-tube injector and then the mixture is sprayed through a nozzle (Ghaderi, et al., 1999).

The single emulsion-solvent evaporation process has found widespread application as a technique for the microencapsulation of low molecular weight, hydrophobic molecules such as progesterone and hydrocortisone (Witschi and Doelker, 1998; Benita, et al., 1984; Cavalier, et al., 1986). However, this method is not generally suitable for the preparation of microparticles containing high molecular weight, hydrophilic biopharmaceuticals. Particularly, the macromolecule such as protein may be loss of activity or less entrapment due to the process of a single emulsion (higher exposure of o/w interface and leakage during solidification as shown in Figure 1.7). A modification of this technique, double emulsion-solvent evaporation, may be employed with the aim of entrapping biopharmaceuticals, and has been widely employed (Witschi and Doelker, 1998). The water-in-oil-in-water (w/o/w) double emulsion systemas shown in Figure 1.7 produces microspheres or microcapsules with controllable diameter, matrix porosity and drug content (Billon, et al., 2005; Giovaqnoli, et al., 2007). In this technique the polyester is dissolved in an organic solvent with low boiling point (ethyl acetate or methylene chloride are favoured) and homogenised with an aqueous phase containing emulsifying agent (e.g. polyvinyl alcohol) and the active drug. This primary emulsion is then poured into a large aqueous phage and homogenised (the transient “secondary emulsion”) to facilitate microparticle formation concomitant with solvent evaporation.

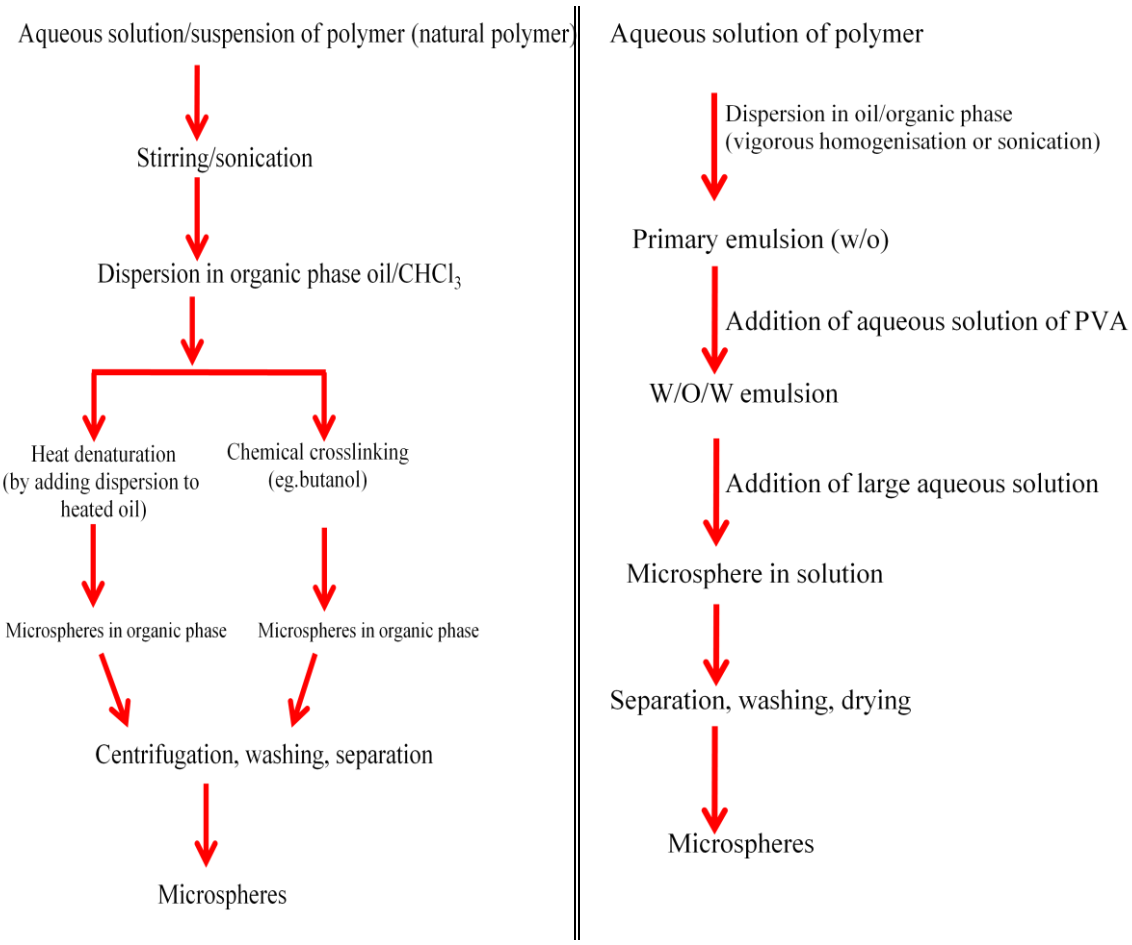

Figure 1.7. Microparticle preparations by single emulsion (left) and water in oil in water (w/o/w) (right)

Many reports have described the application of microspheres prepared by this technique; for example, the controlled release of therapeutic proteins, antigens, and DNA (Dunne, et al., 2003; Wang, et al., 2002; Kissel, et al., 1997; Blanco and Alonso, 1998; Capan, et al., 1999; Jung, et al., 2002; de Boer, et al., 2010; Yang, et al., 2010; Thomas, et al., 2010).

All biodegradable polyesters contain hydrolysable bonds, the most important degradation mechanisms are chemical degradation via hydrolysis or enzyme-catalysed hydrolysis. Degradation of PLGA and PLA occurs via hydrolysis of the polyester backbone, leading ultimately to non-toxic lactic acid and glycolic acid, which are excreted in the urine or respired as CO_2. Degradation *in vivo* has been followed using ^{14}C labelled PLA: 36.8% of the radioactivity was lost in 168 days, with only 7.4% was accounted for via the urine and faeces, whereas only 0.3% was found in the tissue (Brady, et al., 1973). It was suggested that the main route of elimination was by respiration as CO_2. Makino, et al. (1986) further showed that microsphere degradation was slowest at pH 5 and was partially dependent on the thickness of the charges surface double layer and the temperature. The hydrolysis of the polymer produces acidic oligomers, leading to microsphere degradation from the 'inside out': an acidic environment leads to autocatalysis. When the water-soluble polymers are small enough, the polymer fragments will diffuse from the internal to the external medium. However, the diffusion of these segments out of the matrix is limited by their size relative to the pore diameter and tortuosity (Wang, et al., 2002).

The glass transition temperature (Tg) is important to characterise in amorphous materials because it can be used to determine the stability and release mechanism. The Tg can be observed as a transition in the heat capacity of a polymer during heating and is distinct from melting which is exhibited by crystalline substances. Physically, the polymer chains exist in a 'glassy state' below the Tg and 'rubbery state' above. The Tg decreases in association with both the reduction of PLGA molecular weight and increasing chain motility due to water uptake (Deng and Uhrich, 2002). Similarly, residual water within the microspheres remaining after freeze-drying or acquired during storage lowers the Tg of PLGA (Passerini and Craig, 2001). In general, low molecular weight of PLGA (14 kDa; 50:50 lactide:glycolide) has a Tg around body temperature. The ratio of lactide:glycolide of PLGA is also considered because a higher lactide content leads to as increase in the Tg. The temperature of the environment therefore

affects drug release. Aso, et al. (1994) reported that the exposure of PLA microspheres with temperatures higher than the Tg of the polymer show a faster release of drug (Aso, et al., 1994).

Higher ratios of lactic acid: glycolic acid (75:25) slow degradation. It was noted that ester bonds neighbouring glycolic acid units have a high hydrolytic reactivity. Similarly, it is known that scission of the chain-end is faster than the degradation of the internal bonds. Consequently, end-capped polymer with lactic-acid-ethyl-ester, in contrast to the free COOH-terminal, delays degradation (Park, 1995; Göpferich, 1996; Shih, et al., 1996). Furthermore, the hydrophobic lactide group in PLGA can retard water uptake and sustain drug release. Similarly, cumulative DNA release from microspheres containing PLGA (lactide: glycolide, 50:50) was less than from microspheres containing PLGA (lactide: glycolide, 75:25) (Li, et al., 2004). It seems contradict from explanation above but Li also explain that the encapment efficiency of DNA from microspheres containing PLGA (lactide:glycolide, 50:50) (lower lactide group) is less than from microspheres containing PLGA (lactide:glycolide, 75:25) so the microspheres containing PLGA (lactide:glycolide, 50:50) produces a lower release.

Degradation of PLGA particles appears to be biphasic: an initial rapid degradation of polymer appears during the first 20-30 days, followed by a much slower degradation phase (Panyam, et al., 2003). To classify the degradation of microspheres, a distinction is made between surface (or heterogeneous) and bulk (or homogeneous) eroding materials (Figure 1.8). In surface erosion, there is loss of material from the surface, the particle becomes smaller in size but maintains its original geometric shape. In bulk erosion, on the material becomes less dense, while maintaining particle size and shape (Göpferich, 1996). Hence, knowledge of erosion mechanisms is useful for pulmonary drug delivery since this affects drug release of drug and particle clearance.

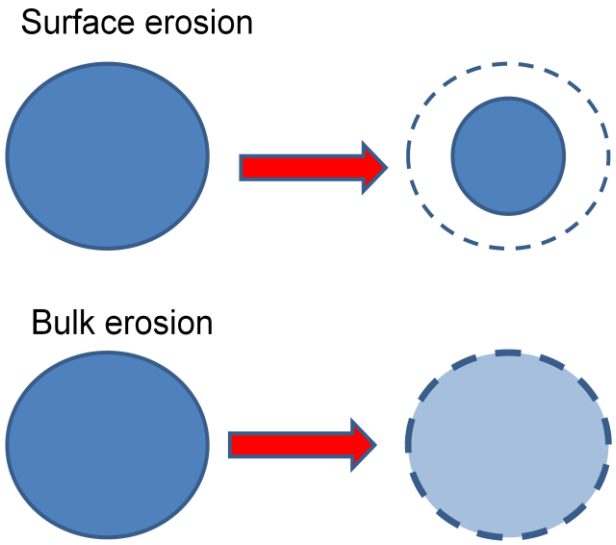

Figure 1.8. Schematic illustration of Surface erosion and bulk erosion adapted from (Göpferich, 1996)

For microsphere characterization, the drug distribution is needed to predict the release mechanism. Confocal Laser scanning microscopy (CLSM) can visualize fluorescent in both the z-axis and x-y axes. CLSM eliminates out of focus fluorescent light from the focal plane and produces non-destructive three dimensional optical sections without prior sample preparation. It is possible to obtain thin (0.5–1.5 µm) or thick (up to 100 µm) optical sections of a specimen along the *z* axis ('slicing' across) which can be compiled to reconstruct the three-dimensional (3D) structure (Jenkins and Egelhaaf, 2008). Fluorescent labelling is required for the encapsulated drug or biological material within microsphere, and drug release and drug distribution can then be examined (Mao, et al., 2007; Liu, et al., 2009).

Release from PLGA microspheres occurs via diffusion, polymer erosion or a combination of these. It has been shown that release from low MW PLGA (e.g., 5 kDa) microspheres is diffusion controlled whereas, release from high MW PLGA (e.g., 25 kDa) microspheres typically occurs via a combination of diffusion and erosion (Zolnik,

et al., 2006). The initial "burst release" may be associated with surface pores formed during formulation of the microspheres as well as other surface associated drug. Fick's second law of diffusion is often used to describe the drug release mechanism from PLGA microparticles. This diffusion law is suitable for non-steady state diffusion, i.e. drug concentration within the diffusion volume changes with time Fick's second law is described by:

$$dC/dt = D\ (d^2C/dx^2)$$

Where, C and D are the concentration and the diffusion coefficient of the drug, respectively; t represents time, and x is the position of a drug.

Mollica and his colleagues (2008) described protein distribution and release via CLSM data and Fick's second law. PLGA microspheres encapsulating tetramethyl rhodamine-labelled bovine serum albumin (BSA-Rhod) were used as a model. The mobilization of protein from inside to out occurred via PLGA degradation and macropore evolution. The mobilized protein diffused via the network of hydrated micropores, formed due to local degradation of polymer. Fick's second law diffusion was used to fit the release data and predict the release of drug over time (Klose, et al., 2008; Kalaji, et al., 2010).

During the encapsulation of a protein, it was found that surface porosity and surface morphology could be controlled by substituting various non-ionic surfactants for PVA (Bouissou, et al., 2004). This demonstrated that microsphere morphology could be engineered and led to the development of microcapsules with dimpled surfaces for pulmonary delivery (Mohamed and van der Walle, 2006), using Pluronic L92 as the surfactant in the primary emulsion.

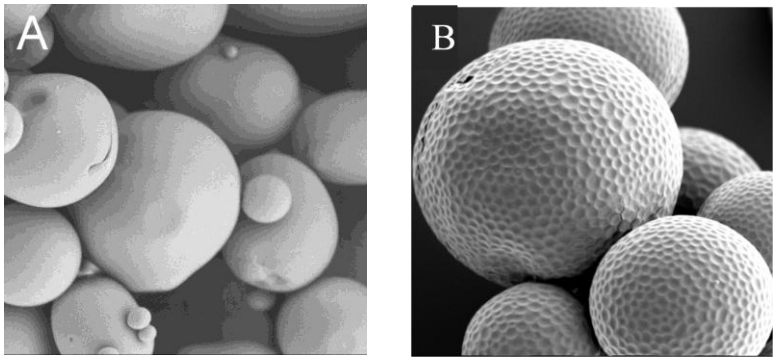

Figure 1.9. A microsphere with a smooth surface fabricated with PVA; B dimpled microspheres fabricated with Pluronic-L92 (reprinted from Mohamed and van der Walle, 2006).

Surface dimpling may improve particle dispersion via reduction in particle-particle contact energies, similar to that described for corrugated BSA microspheres (Chew and Chan, 2001; Chew, et al., 2005). The presence of a stabiliser in the external water phase is critical for the successful formation of individual spherical microspheres during the emulsification process. The role of the stabiliser is to prevent the coagulation of microspheres during emulsification and solvent removal process (Parikh, et al., 1993). PVA is the most commonly used stabiliser mainly due to its low toxicity, good solubility in water and its availability in a range of molecular weights (Singh and O'Hagan, 1998). Lui, et al. (2005) investigated the effect of the PVA concentration in the external water phase and found that if PVA concentrations exceeded 1.0 % w/v, the size distribution of microcapsules obtained was narrow. Although the results mentioned above demonstrated that a higher concentration of PVA was favourable for the formation of more uniform microcapsules, it may be better to use PVA in lower concentrations in some cases since PVA is easily bound onto the microcapsules and not easily washed away (Singh and O'Hagan, 1998). Therefore, by optimizing the conditions for preparing uniform-sized microcapsules, 1.0% PVA was used in the external water phase during the microcapsule preparation in this work.

1.7. Inhaler devices

There are three key devices for pulmonary delivery by inhalation: (1) Nebulisers which deliver aerosolised drug to the lungs; (2) Metered Dose Inhalers (MDIs), and (3) Dry Powder Inhalers (DPIs); the latter two being most convenient for the patient and commonly used. The formulations prepared for these devices can be classified as solutions or suspensions (dispersion systems), in liquid propellant mixture for MDIs and as solid dosage forms (dried powders) for DPIs.

To formulate a drug for a MDI, the drug solution or suspension has to be considered carefully regarding particle size (if suspension), cosolvent, valve clogging, moisture content, solubility or suspension of active compound in propellant, the relative density of propellant and drug, and the surfactant used as suspending agents. These factors may cause problems in drug delivery such as drug aggregation and poor deposition due to an unsuitable propellant. The propellant is the key excipient, since it must generate the aerosol cloud and also suspend or dissolve the drug, and may make up to 99 % of the delivered dose. Typical propellants have a boiling point from -100 to 30 °C, a density similar to the drug (ca. 1.2 to 1.5 g/cm^3), a high vapour pressure (40 to 80 psi). The switch from chlorofluorocarbon propellants, which deplete the ozone layer, to hydro-fluoroalkane (HFAs) is well documented. In contrast, DPIs deliver a cloud of fine particles and the drug in this system is not exposed via any propellant and other excipients except the carrier, which is commonly lactose. To improve the dry power for DPI, the particle size should be micronized. The high-energy powders produced have poor flow properties due to their static, cohesive and adhesive nature. The flowability of powder depends on the physical properties of powder (particle size and shape, density, surface roughness, hardness, moisture content and bulk density). The larger carrier particles impact in the throat, whereas smaller drug particles are carried in the inhaled air deeper into respiratory tract. There is a strong field of research which examines the

balance between cohesive and adhesive forces (CAB) between the drug-drug and drug-carrier, respectively. Such CAB ratios have been able to predict the performance of carrier-based DPI formulations in a number of studies (Hooton, et al., 2006; Hooton, et al., 2008; Jones, et al., 2008).

Inhalation therapy has become a mainstay in respiratory infection disease since the aerosol is delivered directly to the site of infection. Moreover, the adverse effects of some drugs can be improved by inhalation directly to the site of action since there is the opportunity to reduce the dose (avoidance of liver metabolism) and so lower systemic drug concentrations (Le Brun, et al., 2000; Thorsson and Geller, 2005). Practically, aerosolized antibiotic agents are extensively used for patients chronically infected with *P. aeruginosa* (Banerjee and Stableforth, 2000; Geller, et al., 2007). Touw, et al. (1995) reported from 12 studies of nebulised antibacterials for maintenance treatment in CF patients and showed that treatments using inhaled antibiotics can reduce the number of hospital admissions, while improving lung function. It has also been shown that the penetration of an aerosolized solution in the human lung is more efficient when aerosolisation is preceded by physiotherapy and a bronchodilator (Kuni, et al., 1992). The size of aerosol is crucial for nebulisation reaching the smaller bronchioles, which are commonly the sites of pulmonary infection in CF patients (Touw, et al., 1995). In addition to particle size, which is usually in the range of 1-5 μm for effective CF treatment, the osmolarity of formulation is also important for several reasons. First, the aerodynamics of hygroscopic therapeutic aerosols is affected by exchange of water vapour in lung where there is a high humidity (Ferron, 1994). Secondly, bronchial secretions are iso-osmolar so either adding large amounts of hypotonic or hypertonic solutions causes mucosal irritation (Matthews and Doershuk, 1967).

Nebulisation of phages would provide a potential route for the pulmonary delivery of phages. However, solid state formulation of proteins and DNA may increase shelf life

and negate the need for bulky or refrigeration transport. For these reasons we have initially chosen to formulate phages into a dry powder via encapsulation in biodegradable polyester microcapsules, which have previously been shown to be suitable for pulmonary delivery from a Dry Powder Inhaler (DPI) (Mohamed and van der Walle, 2006)**.**

1.8. Lyophilisation

Due to the bacteriophage structure in section 1.4, the bacteriophages compose of the protein/DNA material in either the head or tail. Thus the lyophilisation of bacteriophage has to consider under the protein condition.The thermodynamic stability of a protein is described by Lumry and Eyring (1954) following two-step equilibrium process:

$$N \leftrightarrow D \rightarrow A$$

where N is the native (folded) state, D the denatured (unfolded) state and A represents theirreversible aggregated state. At the folded stated of protein 80% of nonpolar side chains (Ala, Val, Ile, Leu, Met, Phe, Trp, Cys), 60 % of the polar side chains (Asn, Gln, Ser, Thr, Tyr), 50 % of the charged side chains (Arg, Lys, His, Asp, Glu) and 70 % of the peptide backbone groups are buried in the core of the molecule to prevent the water exposure. Whilst the hydrophobic residues are buried in the interior of the molecule at the state of a protein unfolding, it enhances the exposure of molecule to the solvent environment so the denaturation may take place due to the lower solibility. The folded state of a protein has conformational stability, defined by the free energy change, $\Delta G_{f\rightarrow u}$, of the denaturation/unfolding reaction under physiological conditions. The larger this value the more stable the protein is against denaturation. However, $\Delta G_{f\rightarrow u}$ is generally small, which means that the folded state is only slightly more stable than the denatured state. The aggregation can also occur by the specific interaction of conformational

protein intermediate states and accordingly, be divided into three steps: initiation, propagation and termination. The unfolding and aggregation processes can be reversible or irreversible, depending on:

• The equilibrium described above is in close connection with the temperature of the system, among other variables, through the dependence of both intramolecular interactions (enthalpic, stabilising) and dissipating forces (entropic, destabilising the native folded state). The unfolding of proteins is normally an endothermic process that occurs at a certain temperature, termed T_m or "melting temperature", defined as the temperature at which 50% of molecules are unfolded ($\Delta G = 0$). For most proteins, the T_m values are located between 40 and 80 ºC, and logically, more stable proteins hold higher melting temperatures.

• Temperature can also induce chemical modifications on proteins, such as increased hydrolysis of aspartate (Asp) residues, deamidation of asparagine (Asn) and glutamine (Gln) residues in RNAse and lysozyme and insulin covalent polymerisation at temperatures higher than 25 ºC.

1.8.1. Stabilisation of proteins in aqueous solution

Proteins from hyperthermophilic organisms such as archaebacteria function normally at temperatures near or above 100 ºC. The mechanisms on the basis of this extreme stabilisation can involve intrinsic factors such as high molecular packing, increased hydrophobic interactions, hydrogen bonds or salt bridges, or extrinsic factors, related with the high cellular content of either salts, sugars or other organic molecules.

Intrinsic protein stabilisation involves structural modifications of the protein, in an attempt to increase the stabilising forces, without changing the overall conformation. These structural modifications can increase $\Delta G_{f \rightarrow u}$ of the protein, leading to a stabilisation of the native structure translated by $\Delta G = \Delta Gmut - \Delta Gnat$. The most common way of achieving this, is by performing single or multiple mutations on the

protein amino acid sequence. The increase in stability afforded by mutations can derive from a decreased external hydrophobicity (reinforcement of the internal hydrophobic core), from enhanced interactions between amino acid residues close on the sequence, or from a decrease on the structural mobility of some flexible (labile) areas in the protein molecule – often substitution for proline. The basic principle of *extrinsic* protein stabilisation is the same as for *intrinsic* stabilisation, that is, whether by enhancing stabilising forces or by disturbing the stability of the unfolded state. In thermodynamic terms, stabilisation has the objective to shift the two-state Lumry-Eyring equilibrium towards the left, N, the native state of the protein, raising $\Delta G_{f \rightarrow u}$. Although several excipients can be used to achieve this goal, this thesis will focus on particularly three types: buffer pH, sucrose and polyethyleneglycol (PEG). As the statement in buffer pH, the incorporation of protein in both basic and acidic functional groups, the ionisation state of the molecule in an aqueous solution will depend on the pH of the solution. At a characteristic pH, called the isoelectric point (pI), the negatively and positively charged molecular species are present in equal concentration and the protein molecule is said to have zero net charge and consequently, minimal solubility. Thus, at pH values below the pI, proteins carry a positive net charge and accordingly, when the pH is above the pI, the net charge is negative. In the folded state of protein, the isoelectric point of a protein depends on the conformational position of the amino acid side chains. The pH can also affect the rate at which some chemical degradation reactions take place. For example, deamidation of Asn-X appears mostly favoured at neutral or alkaline conditions. The oxidation rate can also be enhanced, in some cases, at alkaline pH. Thus either the type or the concentration of the solute in buffer preparation may affect the physical and chemical protein stability (deamination and oxidation) (Florence and Attwood, 2006; Mulinacci, et al., 2011).

1.8.2. Solid state formulation

To overcome the instability of protein molecules in solution, one option is to formulate in the solid state. The most commonly used process to achieve this is lyophilisation or freeze-drying. The lyophilisation or freeze-drying process consists of two different phases: freezing of the protein solution and subsequent drying under vacuum. The drying process takes place in two different steps: the first, called primary drying, involves the removal of bulk frozen water through sublimation and the second, called secondary drying, the removal of non-frozen "bound" water (Tang and Pikal, 2004). Lyophilisation generates a variety of stresses which tend to denature the protein. Due to this, cryo- and lyo-protectants ("additives") are frequently a necessity.

1.8.2.1. Sources of protein denaturation

Low temperature

Similar to unfolding at high temperatures, proteins are also unstable at low temperatures. The reasons by which this occurs are still unclear, but one proposed mechanism is the decrease of the solvophobic interactions that stabilise the protein conformation, since the hydration of non polar residues increases with the decrease in temperature (Dill, et al., 1989, Graziano, et al., 1997). It has been stated that, contrary to what happens with denaturation at high temperatures, protein denaturation at low temperatures is not entropy but enthalpy driven, since in this case the lower value for the denatured state shifts the equilibrium towards the right (Shortle, 1996).

Formation of ice-water interface

Freezing of a solution generates the formation of an ice-water interface; consequently interactions between the protein and ice-water interface arise. One way this interaction can take place is by the adsorption of protein molecules to ice crystals, leading to its

surface-denaturation. The protein will be distributed between the liquid and solid phases and the extent of adsorption will depend on the volume of liquid water present and on the surface area of ice. Alternatively, the protein structure can be physically distorted due to its confinement to the intergranular spaces between ice crystals, when these have a molecular volume similar or smaller than that of the protein molecules, a phenomenon also known as "molecular crowding" (Strambini and Gabellieri, 1996). The cooling rate will have an impact on the extent of surface or physical distortion induced denaturation, since rapid cooling will generate small ice crystals (increased ice surface area and decreased intermolecular pores) and oppositely, slow cooling will provide crystals with a bigger size (lower ice surface area and larger intermolecular pores).

Concentration effects during freezing

The formation of ice during freezing increases the concentration of all solutes in a solution. Similarly, an increase on protein concentration can increase the interaction between protein molecules, raising their tendency to unfold. If a solution is buffered, the differential crystallization of the buffer species during freezing can cause modifications on the pH of a formulation. According to the magnitude of this change, protein stability will be more or less affected. If the pH is far away from the protein pI, repulsion between like-charges increases, leading to unfolding. Shift in the pH can also affect, as stated before, the rate of chemical reactions taking place on a protein formulation.

If polymeric stabilisers are present in the formulation, another effect derived from the concentration of species during freezing is phase separation. Because the solubility of the polymers changes at low temperatures, liquid-liquid phase separation can occur (Heller, et al., 1997). Strategies to avoid this phenomenon include the use of alternative salts (Heller, et al., 1997), the addition of crystallizing agents such as mannitol (Heller, at al., 1999a) or the PEGylation of proteins (Heller, et al., 1999b).

Drying

When in solution, proteins are said to be fully hydrated, this is, having a monolayer of water molecules covering their surface, called the hydration shell (Rupley and Careri, 1991). Lyophilisation removes part of the hydration shell, since the water content of a lyophilised product is usually less than 10%. This can lead to destabilisation of the folded state. It is also worth noting that the distribution of water in a product during lyophilisation may be uneven, causing an overdrying of the protein at the top of the vials, whilst the moisture at the bottom has an optimal value (Pikal and Shah, 1997). This can contribute to a further dehydration-induced protein denaturation.

1.8.2.2. Stabilisation of proteins in the solid state

Due to the effect of the stresses suffered by a protein during lyophilisation, stabilisers are frequently needed. These stabilisers or excipients can afford protection during the freezing step, being called cryo-protectants, or during the drying step, termed lyo-protectants in this case. The excipients that combine these two functions are known as both cryo- and lyo-protectants. Similarly to what has been done for the liquid state formulation, our discussion will focus only on the effects of pH, buffers, sucrose and PEG.

pH and buffer choice

The optimal pH for a protein in solution may not be the same for when the protein is lyophilised (Townsend and DeLuca, 1990), since the mechanisms of destabilisation in the liquid and solid state can be different. When choosing a buffering agent, some special considerations are required, and a compromise must be reached between the desired pH and the agents buffering capacity. For example, sodium phosphate should be

used carefully, given the fact that selective crystallization of Na_2HPO_4 compared to NaH_2PO_4 during freezing (Franks, 1993) can cause abrupt decreases on the pH and possible protein denaturation. Changes in pH during lyophilisation can be minimised by the correct choice of buffer salts, citrate being preferred to phosphate, succinate and tartrate (Shalaev, et al., 2002) or by reducing their concentration (Murase and Franks, 1989).

Sucrose

Sucrose is known to have both cryo- and lyo-protectant effects. The protection of compounds against drying stresses has long been known from natural occurring processes: anhydrobiotic microorganisms normally possess high concentration of this dissacharide as a mechanism of survival (Crowe, et al., 1998). During the freezing step, sucrose protects the molecules by its preferential exclusion from the surface, increasing the free energy of denaturation and consequently minimising this process (Lee and Timasheff, 1981). During the drying stage, protein 'protection' from sucrose is thought to occur via one or both of the following mechanisms: i) by forming a highly viscous glass around the protein molecules, preventing protein-protein interactions (Allison, et al., 1998) or ii) via the establishment of hydrogen bonds with polar groups at the surface of the protein, replacing water molecules (Allison, et al., 1999). The stabilisation is dependent on the concentration of sucrose and some authors have proposed the need of a specific molar ratio of sugar to protein to attain adequate stabilisation (Cleland, et al., 2001). Sucrose has also the advantage of being a non-reducing sugar, avoiding the potential occurrence of the Maillard reaction with the dried proteins and also of not crystallizes at the general temperatures used for lyophilisation (avoiding phase separation).

Polyethylene glycol (PEG)

PEG is mainly considered a cryo-protectant but the mechanisms by which this occurs can widely vary. They derive from its polymer characteristics and can be related to steric hydrance of protein-protein interactions, preferential exclusion, surface tension

reduction and increased solution viscosity, which can inhibit the crystallization of other components and thus prevent changes in the pH during freezing (Wang, 2000). During the drying step, PEGs can potentially also protect the protein by raising the glass transition, Tg, of the formulation. The protection afforded via PEGs is once again concentration dependent, and high quantities of the polymer can have an adverse effect on stabilisation.

Protein concentration

Another consideration is the concentration of protein in the formulation. Although in solution high protein concentrations increase the tendency for unfolding and aggregation, alternatively, concentrated protein solutions may be more resistant to freezing-induced aggregation (Carpenter, et al., 1990). Allison, et al., 1996, proposed two explanations accounting for this increased resistance. The first was that the unfolding of proteins can be temporarily inhibited due to steric repulsion of protein molecules at high concentrations. Secondly, the area of the formed ice-water interface is finite, limiting the amount of protein being accumulated and denatured at the interface.

Increasing concentrations of ovalbumin from 0.5 to 2.5 mg/ml at pH 1.9 (in the acidic pH range, ovalbumin has an increased tendency to unfold) decreased the structural changes suffered by the protein upon freezing at -40 ºC (Koseki, et al., 1990). Likewise, aggregation during lyophilisation was seen to decrease with increasing concentrations of both human and bovine IgG (Sarciaux, et al., 1999). Last, as a result of protein-protein interactions, monomers may dimerise or multimerise (Mozhaev and Martinek, 1984).

Residual Moisture

Protein has both strong and weak binding sites to accommodate unfrozen water. The weak binding sites include carbonyl backbone plus hydrophilic –OH and –NH- groups, while the strong binding sites include ionisable groups in amino acids such as Glu, Asp, Lys and Arg (Careri, et al., 1979). Careri et al. (1979) also reported that the residual moisture is a small portion of strong bond water molecules in protein because water in

secondary drying was removed only weakly bound and some of strongly bound of water molecules. The residual moisture content for lyophilized protein products is usually below 10%. Generally, lower moisture content leads to more stability of products. However, some of proteins such as lyophilized BSA and bovine γ-globulin formulations were more stable with moisture content about 10% (Yoshioka, et al., 1997).

Storage temperature

Since high temperature also enhances the physical aggregation of protein in solid state due to increasing of protein mobility and promote protein protein interaction. For example; the aggregation and chemical degradation (deamidation) of lyophilized rhIL-1ra increased when the temperature increased (Chang, et al., 1996). Thus, the storage temperature is one of important factor affecting the protein stability.

1.8.2.3. Design of the lyophilisation cycle

To minimise the freezing and drying stresses on the protein and to have a reproducible and feasible cycle, a careful design of the critical parameters of lyophilisation is needed. This optimisation requires the prior knowledge of some important characteristics, namely the glass transition temperature (Tg') of the protein being formulated, the properties of the excipients (including their Tg) and also the appropriate rates of cooling and drying. Although theoretical knowledge is used as a way to begin the design of a lyophilisation cycle, the correct optimisation derives from experimental work, where the different variables and consequent outcomes are actually measured.

Protein glass transition temperature (Tg') and collapse temperature (Tc)

The glass transition is a phenomenon that can potentially occur in all noncrystalline or semicrystalline materials, providing there is a sufficiently high degree of molecular

disorder. As temperature decreases during freezing, the formation of ice concentrates all solutes, decreasing the molecular movement, and the solution changes from a viscous liquid to a brittle glass. This reversible process takes place at a precise temperature, termed the glass transition or vitrification temperature. This temperature is known for proteins as Tg', to differentiate it from the true glass transition of a polymer (Hill, et al., 2005). The positioning of the protein molecules in a glassy-like environment has though a potential stabilising effect through the decrease in molecular vibrations and rotations (Duddu, et al., 1997). It is commonly accepted that the higher the glass transition temperature of a protein formulation, the more stable it is. Polymers with high glass transition temperatures can be used to stabilise a protein formulation by increasing its Tg'.

The most widely used method for the determination of Tg and Tg' is differential scanning calorimetry (DSC) (Wang, 1999). The glass transition temperature causes an increase in the heat capacity of the sample, and is displayed to the user as an endothermic shift in the baseline. This measurement might prove difficult to perform, since glass transition temperatures take place very close to the minimum limits of detection and also because they can be influenced by other parameters, such as solutes, the moisture content of the sample, the conditions of glass formation, the rate of cooling (Her and Nail, 1994) and the thermal history of the samples.

The collapse temperature of the formulation, Tc, is the temperature above which the lyophilised product looses macroscopic structure during freeze-drying and collapses. It is usually higher than Tg' by 2 ºC (Pikal and Shah, 1990) or has the same value as the eutectic temperature (T_{eu}) if all the solutes in the frozen solution are in the crystalline state (Tang and Pikal, 2004). The eutectic crystallization/melting temperature is defined as the temperature at which the least soluble component crystallizes simultaneously with water, forming a mixture (Wang, 2000) (Figure 1.10).

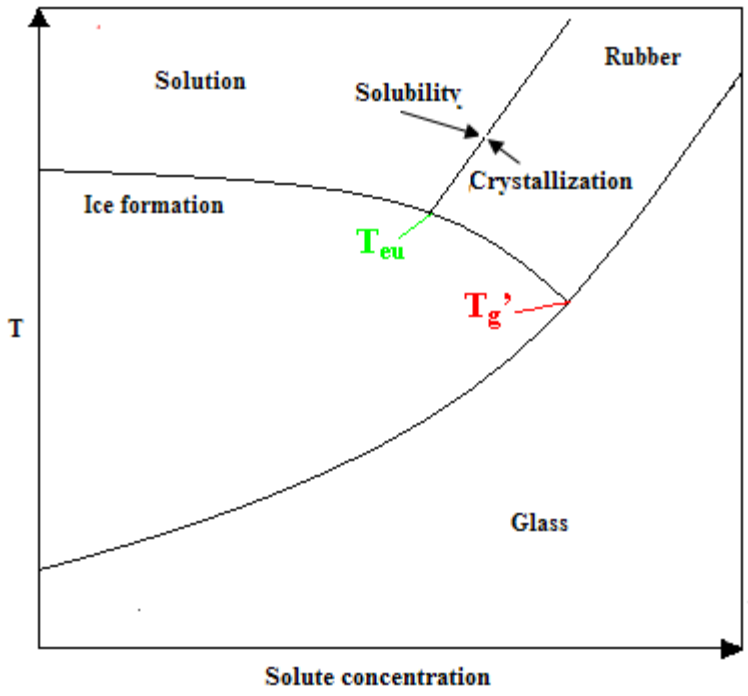

Figure 1.10. Theoretical phase diagram, show the relationship between Tg' and Teu (Adapted from (Wang, 2000)).

Selection of stoppers

The correct choice of a stopper is of extreme importance, due to the possibility of increased moisture during storage of a product. This can occur mainly via three processes: a) transfer of moisture from the stopper to the formulation; b) moisture diffusion or transmission through the stopper material or c) microleaks generated at the stopper-vial seal (House and Mariner, 1996). Stopper leakage or oxygen permeation can increase the oxidation potential of proteins during storage (Wang, et al., 1997). Also, an increase in the moisture content of a lyophilised product can cause a dramatic change in the Tg of the formulation, compromising its stability during storage (Kreilgaard, et al., 1998).

From the different types of stopper materials available, butyl or halobutyl rubber is often chosen due to low moisture absorption and vapour transmission (DeGrazio and Flynn, 1992). Among the latter, bromobutyl stoppers have shown to be more resistant to moisture absorption during storage, when compared to chlorobutyl ones (Corveleyn, et al., 1997).

Cooling rate, freezing temperature and time

If a protein is cooled quickly (e.g. by immersion in liquid nitrogen), small ice crystals will result, yielding a high surface area for ice and this can lead to surface induced denaturation. On the other hand, if a protein is cooled too slowly and if the system is prone to phase separation, denaturation will result from this phenomenon, since the time scale is not a limiting factor (Heller, et al., 1999a). Tang and Pikal (2004) have proposed that a moderate cooling rate of 1 ºC/min is a good compromise in moderating the effects derived from both super- and slow-cooling, providing a uniform and reproducible ice structure. Since the major goal of freezing is to have all the components of a solution in the solid state, this step should be conducted below the Tg of the formulation and kept at this temperature for a time long enough to solidify the whole solution. The freezing time will depend on the depth volume of the vials. Naturally, a higher volume of solution will take longer to freeze than a smaller one. Nevertheless, the total freezing time should never be inferior to one hour. If there are bulking agents in the formulation (cake promoting agents), an annealing step might be required to ensure their crystallization. Annealing consists in holding the product temperature above the final freezing temperature allowing the potential crystalline components to crystallize. The non crystallization of bulking agents during freezing can have catastrophic effects on the formulation, especially when this process occurs during the drying step, resulting in vial breakage due to a volume expansion (Williams, et al., 1986), or compromising stability during storage of the solid product (Lueckel, et al., 1998).

Primary drying

The primary drying or ice sublimation is often the most time-consuming step in a lyophilisation cycle. Its basic aim is to choose the correct temperature, quickly bring the product to this value and hold it throughout the whole duration of the step. The primary drying step in a lyophilisation cycle will reach its end point when all the frozen water has been removed, this is, when there is no ice present in the vials and the sublimation rate has been reduced to a minimum. Two widely used methods to confirm this are based on direct observation of changes in the product temperature and/or chamber pressure. When no ice is present, the temperature of the product will be very similar to the shelf temperature, since heat transfer is made easier across the sample. At the same time, if the vacuum is disconnected from the system, the rise in chamber pressure will be proportional to the moisture content of the sample. As primary drying ends, this rate will decrease and approach zero. Bearing in mind the inter vial differences in temperature during the process, it is advisable to allow an extra two to three hours to the drying time, to avoid premature ending.

Due to stability concerns, theoretically, the drying temperature of a formulation should be several degrees below its temperature of collapse (Tc). In practice, if the drying temperature is too low, the primary drying can be a very long, unfeasible process. Nevertheless, proteins can be dried well above Tg' without undergoing detrimental denaturation (Chang, et al., 2005). An optimal drying temperature should result from a compromise between safety, this is, the possibility of collapsing, and time required for freeze-drying. Also, the shelf temperature set in the freeze-dryer very often does not equal the actual temperature of the product. Measurements *in situ* (normally by the use of thermocouples) should be made in order to correct any temperature discrepancies. Ice sublimation in lyophilisation is driven by the temperature differences between the condenser and the product. The condenser temperature is normally set to a minimum of 20 ºC below the product temperature, this is, between -50 and -60 ºC.

The rate of ice sublimation, *v*, (weight of ice sublimed/hour) can be defined by the following equation:

$$v = \frac{P_{ice} - P_c}{R_p + R_s}$$

where P_{ice} is the equilibrium vapour pressure of the ice, P_c the chamber pressure, R_p the dry layer resistance and R_s the stopper resistance to vapour water transport (both in Torr.g/h) (Tang and Pikal, 2004). As P_{ice}, R_p and R_s are normally fixed for a certain formulation at the drying temperature, the sublimation rate of ice can only be controlled by changing P_c. If R_p changes during drying, the rate of sublimation and temperature values will change accordingly. Thus, a low chamber pressure will provide a high sublimation rate. However, very low pressures can cause a heterogeneous heat transfer between vials (Pikal, et al., 1984) and contamination of the product by the components of the stoppers or by the oil from the pump. Pikal, et al. (1984) have proposed the use of a moderate chamber pressure, 100-150 mTorr, as a way of achieving a balance between a relatively high sublimation rate and an acceptable homogeneous heat transfer inter vials (Pikal, et al., 1984). Tang and Pikal (2004) have presented an equation for the calculation of the optimal chamber pressure value:

$$P_C = 0.29.10^{(0.019Tp)}$$

where T_p is the primary drying temperature (in ºC).

Care must be taken also to not overload the freeze-dryer, since the ice sublimation rate will be compromised and the cycle take longer than expected.

Secondary drying

The objective of secondary drying is to remove the non-frozen water by desorption from the product. The optimal residual moisture for the formulation (Hsu, et al., 1992) will dictate the duration of this step. The temperature required is much higher than for primary drying, to allow the water to be desorbed at a practical rate.

A heating rate of 0.1 to 0.15 ºC/min is normally advisable for amorphous products to avoid collapse during secondary drying. For crystalline products, a higher rate of 0.3 to 0.5 ºC/min should be used (Tang and Pikal, 2004). It is not necessary to change the chamber pressure during secondary drying, since below 200 mTorr this parameter has no influence on the rate of water desorption (Pikal, et al., 1990).

Secondary drying temperature and time will depend on the residual moisture level desired and on the characteristics of the formulation. For amorphous products, higher temperatures and times are required to achieve full dryness. Temperature values can vary from 20 to 50 ºC, and once the final temperature value has been reached by the product, secondary drying can take place during a time period of 3 to 6 hours. Longer drying times have proven to have little effect on the residual moisture of the sample (Tang and Pikal, 2004).

The residual moisture of a product can be measured in situ, by the use of residual gas analysers or electronic hygrometers (Nail and Johnson, 1992) or by sampling the product without interrupting the lyophilisation cycle, followed by analysis with either thermal gravimetric methods, Karl Fisher titration, near infrared (IR) spectroscopy or gas chromatography. To have an insight of the residual moisture impact on the stability of a

lyophilised product during storage, long term stability studies with different moisture values are often required.

1.9. Aims and Objectives

In this thesis, we hypothesize that bacteriophages may be encapsulated into polymeric microspheres or nebulised from reconstituted lyophilised formulations, to achieve pulmonary administration while maintaining their bioactivity. The experimental objectives will be to: i) encapsulate phage into PLGA microparticles and characterise the physical nature and deposition of the particles, the *in vitro* release profiles and the biological activity; ii) to formulate phage via lyophilisation using cryo- and lyo-protectants, for reconstitution and nebulisation; iii) develop animal models of bacterial lung infection for *in vivo* testing of the phage formulations.

Chapter 2 : Materials and methods

2.1. Materials

2.1.1. Microsphere formulations

PLGA (50:50 poly(D,L-lactic-co-glycolic acid), carboxy terminal, inherent viscosity 1.05 dl/g) was purchased from Purac Biochem, Netherlands and stored at -80 °C with desiccant. Poly(vinyl alcohol) (PVA) (MW 25000, 88% hydrolysed), gelatin, sucrose, polyethylene glycol MW 6000 (PEG6000), and fluorescein isothiocyanate (FITC), were purchased from Sigma-Aldrich Chemical Company (Dorset, UK), sodium chloride, Tris.HCl, were obtained from Sigma-Aldrich or Melford Laboratories Ltd., Suffolk, UK, at analytical grade or equivalent. Water was purified to > 17 MΩ-cm (Purite, UK). Dichloromethane (DCM), analytical grade, ethanol, propanol and acetone, reagent grade, were obtained from Fisher Scientific, UK. Pluronic-L92® PEO-PPO-PEO triblock copolymer (MW PPO:3000-3600) was received as a kind gift from BASF, USA.

2.1.2. Microbiology

Tryptone, yeast extract, granulated agar, peptone, glycerol, sodium phosphate, sodium chloride, sodium bicarbonate and Tris.HCl (Tris(hydroxymethyl) aminomethane HCl) were purchased from Melford laboratories Ltd., Suffolk, UK. Tryptone soya broth was supplied by Oxoid Ltd., Cambridge, UK. DPX solution (DPX mountant for histology, a synthetic resin), sulphuric acid, glacial acetic acid, hydrochloric acid, ethanol, magnesium sulphate, sodium bicarbonate, potassium chloride, barium chloride, formaldehyde, hematoxylin and eosin were obtained from Sigma-Aldrich Chemical

Company, Dorset, UK. Histo-Clear™ II was supplied by Fisher Scientific, UK. All other chemicals were purchased from either Sigma-Aldrich or Fisher Scientific at analytical grade or equivalent.

Bacteriophage selective for *Staphylococcus aureus* strain FDA209P variant were kindly provided from laboratory of Prof. Mattey, University of Strathclyde, UK, but originally obtained from the National Collection of Industrial, food and Marine Bacteria (NCIMB), Aberbeen, UK with accession numbers 9563 and 8588, respectively (American Type Culture Collection (ATCC) accession numbers 6538-B and 11522, respectively). Mucoid *Pseudomonas aeruginosa* strain 217M, a clinical isolate, was kindly donated by Dr Tyrone Pitt, Laboratory of HealthCare Associated Infection, Health Protection Agency, Colindale, London, UK. A second mucoid *Pseudomonas aeruginosa* strain was obtained as a kind gift from the Strathclyde Institute for Drug Research, but was originally obtained from the ATCC, accession number 39324, and is a clinical isolate. The bacteriophage selective for both mucoid *P. aeruginosa* strains was isolated from Clyde river water by Dr McColm, University of Strathclyde, UK.

2.2. Methods

2.2.1. Bacteria

2.2.1.1. Bacterial preparation

A frozen bacterial stock was diluted with media broth and streaked over the surface of media agar plate. Following the incubation at 37 ^{o}C overnight, the isolated colony (single colony) of bacteria would be deposited on the surface of the medium. A single colony was harvested and diluted with media borth overnight, 180 rpm in a shaking

incubator. The bacteria suspension would be determined the bacterial concentration by McFarland standards and 100 µL of bacteria suspension would be incorporated in molten agar (40-50 ^{o}C) for plaque assay.

For the *in vitro* experiments, *S. aureus* and *P. aeruginosa* strain 217M were incubated in Luria Bertani (LB) broth at 37 °C overnight, 180 rpm in a shaking incubator, and harvested while they were in the exponential growth phase for subsequent phage preparation or plaque assay. For the *in vivo* experiments, *P. aeruginosa* strain 39324 was used for infection and incubated in Trytone Soya Broth (TSB) at 37 °C overnight, 180 rpm in a shaking incubator.

For long term storage at -80 °C, the bacteria were harvested following overnight incubation, washed in sterile PBS and resuspended in sterile 15% (v/v) glycerol in PBS or saline.

2.2.1.2. Preparation of media

Luria Bertani (LB) broth

9 g of tryptone extract, 4.5 g of yeast extract and 9 g of NaCl were dissolved in 700 mL of water then adjusted to 900 mL (pH ~7.4). The broth was autoclaved (121 °C for 20 min) and stored at room temperature.

Luria Bertani (LB) agar

9 g of tryptone extract, 4.5 g of yeast extract, 9 g of NaCl and 13.5 g of bacterial grade agar were dissolved in 700 mL of water then adjusted to 900 mL (pH ~7.4). This mixture would be sterilized by autoclaving. Following sterilization, molten agar would

be cooled to 50-60 °C and ~25 mL poured into an aseptic polystyrene Petri dish. The agar plate would be kept under a laminar flow cabinet for 1-2 hours until solidified and then storage at 4 °C for no more than 2 weeks.

Bacteriophage storage medium

50 mL of 1 M Tris HCl (pH 7.5), 5.8 g of NaCl, 0.98 g of anhydrous $MgSO_4$, and 0.1 g of gelatin were dissolved in 900 mL of water then adjusted to 1 L (pH 7.5). The solution was autoclaved and stored at room temperature.

King's A media (broth)

18 g of peptone, 9 g of glycerol, 9 g of anhydrous K_2SO_4, and 12.6 g of anhydrous $MgCl_2$ were dissolved in 700 mL of water then adjusted to 900 mL (pH 7.4). The broth was then autoclave and stored at room temperature.

King's A media (agar)

18 g of peptone, 9 g of glycerol, 9 g of anhydrous K_2SO_4, 12.6 g of anhydrous $MgCl_2$, and 18 g of bacterial grade agar were dissolved in 700 mL of water then adjusted to 900 mL (pH 7.4). This mixture would be sterilized by autoclaving. Following sterilisation, molten agar would be cooled and poured as described above.

TSB

9 g of TSB was dispersed in 700 mL of water then adjusted to 900 mL (pH 7.4). The broth was then autoclave and stored at room temperature.

TSB agar (TSA)

9 g of TSB and 13.5 g of granulated agar were dissolved in 700 mL of water then adjusted to 900 mL (pH 7.4). This mixture would be sterilized by autoclaving. Following sterilization, molten agar would be cooled and poured as described above.

All broths and agars were made in distilled water (> 17 MΩ-cm).

2.2.1.3. McFarland standards

McFarland standards were used as a reference to adjust the number of bacteria in suspension for the *in vivo* experiments (Chapin and Lauderdale, 2007). Specified amounts of 1% anhydrous barium chloride ($BaCl_2$) and 1% sulfuric acid (H_2SO_4) were mixed and produced a precipitation of barium sulphate. For example, a 0.5 McFarland standard was prepared by mixing 0.05 mL of 1% anhydrous barium chloride with 9.95 mL of 1% sulfuric acid. After the mixture was shaken well, the absorbance was measured at 625 nm (ThermoSpectronic, Cambridge, UK). A bacterial suspension adjusted to a particular absorbance value equivalent to a McFarland standard can then be said to have a particular concentration of bacteria according to those in Table 2.1 (also Figure 2.1).

Table 2.1. McFarland standards

McFarland Standard	**1% anhydrous $BaCl_2$ (mL)**	**1% H_2SO_4 (mL)**	**Absorbance at 625 nm**	**Equivalent bacterial concentration (10^8 CFU/mL)**
0.5	0.05	9.95	0.087	1.5
1	0.1	9.9	0.141	3
2	0.2	9.8	0.265	6
3	0.3	9.7	0.383	9
4	0.4	9.6	0.528	12
5	0.5	9.5	0.699	15
6	0.6	9.4	0.812	18
7	0.7	9.3	0.913	21
8	0.8	9.2	0.977	24
9	0.9	9.1	1.18	27
10	1.0	9.0	1.26	30

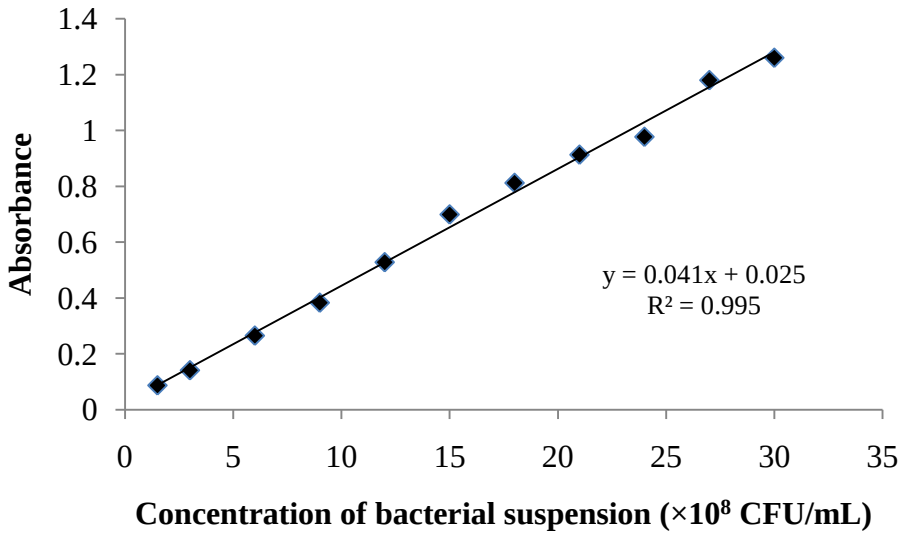

Figure 2.1. The absorbance of the McFarland standards (at 625 nm) correlated to the equivalent concentration of bacteria in suspension.

2.2.2. Bacteriophage

2.2.2.1. Phage preparation

A single *S. aureus* or *P. aeruginosa* strain 217M colony was picked from an agar plate with a sterile loop and inoculated in 5 ml LB broth, incubated at 37 °C overnight at 180 rpm. 0.3 mL of the overnight culture was mixed with 0.45 mL of phage stock solution (aliquot/freshly prepare from the phage stock solution which was previously stored at -80°C) and incubated at 37 °C for 10-20 min (with left standing). Following the incubation, 200 µl of the bacteria/phage mixture was mixed with 4 mL of molten top agar at 40-50 °C, poured onto a LB agar plate and incubated at 37 °C overnight. When phage active against *P. aeruginosa* strain 39324 were required, LB broth and agar was replaced with TSB and TSA for bacterial culture.

2.2.2.2. Phage Harvest

After overnight incubation of the bacteria-phage mixture in top agar (2.2.2.1), the resultant extent of the bacterial 'lawn' (that is, closely packed bacterial microcolonies) was observed and checked for the presence of phage plaques (seen as small, clear zones in the lawn). 5 mL of sterile storage medium would be used to flood the plates and placed at 4 °C for 3-4 h with gentle swirling every 0.5 h. Storage medium containing phage was then decanted and extruded through a 0.22 μm sterile filter. The phage activity in this solution was determined by the plaque assay technique (below), using a series of dilutions of the phage solution.

2.2.2.3. Plaque Assay

The plaque assay was used as a technique for counting the numbers of plaques and thereby calculating the concentration of active phage in terms of plaque forming units per mL (pfu/mL). A series of twelve 10-fold dilutions would be made of the harvested phage stock and a 100 μL aliquot of each dilution would be mixed with an equal amount of overnight bacterial culture, and then poured with 4 mL molten top agar onto an agar plate (as above) and kept at 37 °C for 12 h. The number of visible plaques was then counted and used to calculate the concentration of phage as pfu/ml. To minimise the number of counts required, the agar plate was divided into quadrants. At high concentrations of phage, the plaques were seen to merge, to the extent that the bacterial lawn was no longer continuous. Accurate counts would then be made from an agar plate with a higher dilution of phage.

For assessment of bacteriophage activity following encapsulation in PLGA microspheres, 100 μL of the reconstituted, centrifuged formulation would be mixed with an equal amount of overnight bacterial culture and 4 mL molten top agar, poured onto an agar plate and kept at 37 °C for 12 h. Negative and positive controls substituted sterile storage medium and a known concentration of phage for the test formulation, respectively.

2.2.2.4. Bacteriophage purification

0.5 g of CsCl was added to 1 mL of freshly prepared phage and placed on a rocking platform until the CsCl completely dissolved. To fractionate the phage solution, a CsCl step gradient was made using the CsCl solutions one third (1/3) of phage solution used in each gradient solution shown in Table 2.2, either by layering three CsCl solutions of decreasing density on top of one another or by layering solutions of increasing density under one another, into a Beckman centrifuge tube, thick wall, polycarbonate, 32 mL, 25 x 89 mm. On top of the least dense solution, the phage-CsCl solution was carefully pipetted and for each layer (which remained visible) a mark at the interface with the next layer was made on the outside of the tube. After centrifugation at 22,000 rpm (64000 × g) in a Beckman SW 28 rotor for 2 h at 4 °C, a thin bluish band could be observed between the 1.4 and 1.5 g/mL CsCl density layers. This band was carefully aspirated using a Pasteur pipette. One millilitre of this band including purified bacteriophage was kept at 4 °C a day before labelling with fluorescein.

Table 2.2. Step gradients of CsCl solutions in storage media (Sambrook and Russell, 2000)

Density (g/mL)	CsCl (g)	vol. storage media (mL)*	Refractive Index
1.45	60	85	1.3768
1.50	67	82	1.3815
1.70	95	75	1.3990

*, the final volume of each solution is 100 mL.

2.2.2.5. Fluorescein labelling of phage

Fluorescein isothiocyanate (FITC) is a free amine-reactive derivative (–N=C=S) of fluorescein. A 0.5 g excess of FITC was added to 1 mL of purified bacteriophage equilibrated in 46 mM $NaHCO_3$ (pH 9) in a total volume of 10 mL. The mixture was agitated continuously for 2 h and then (whole mixture was dialyzed) dialyzed against PBS in a dialysis bag having a MW cut off of 12,400 Dalton (D9777, Sigma-Aldrich, UK). PBS was continuously stirred and changed every ~8 h over 24 h to remove unbound fluorescein. The solution in the dialysis bag was then removed and the phage activity determined by plaque assay. The fluorescence of the labelled phage sample was verified using an excitation wavelength of 495 nm and an emission wavelength 525 nm (Varian Cary Eclipse fluorometer, Oxford, UK). The labelled phage would be kept at 4 °C and used within 2 days.

2.2.2.6. Transmission electron microscopy (TEM)

A negative staining technique was employed to visualise the bacteriophage by TEM. 10 µL of phage sample were dropped onto the surface of a Formvar/carbon coated 300 mesh grid. The sample was allowed to settle for 30 seconds and excess sample was then drained away from the grid carefully. The sample was then stained with 10 µL methylamine vanadate negative stain (NanoVan®, Nanoprobes, Universal Biologicals, Cambridge, Ltd.), with excess strain removed by wicking and the sample left to dry before viewing on TEM.

2.2.3. Fabrication of microspheres containing bacteriophage

For experiments investigating the effect of emulsification alone on the lytic activity of bacteriophage (selective for *S. aureus*), addition of bacteriophage (10^9 pfu/ml) to the aqueous phase of either the primary or secondary emulsions was performed and examined the lytic activity to select the appropriated method bacteriophage inclusion. Experiments were repeated for four independently prepared batches.

For experiments investigating the effect of lyophilisation alone on the lytic activity of bacteriophage (selective for *S. aureus*), 0.5 ml of bacteriophage in storage medium at concentrations of 5×10^9, 5×10^7 and 5×10^3 pfu/ml were frozen and lyophilised using a Micromodulyo (ThermoSavant, UK) with a vacuum of 30 mTorr, condenser -40 ^oC and sample compartment at 10 °C, for periods of 24 and 96 h. Each dried powder was then reconstituted in storage medium for measurement of lytic activity by plaque assay.

Following studies on the effect of emulsification on bacteriophage stability (above), a modified water-in-oil-in-water (w/o/w) double-emulsion solvent evaporation method as shown in Figure 2.2 was employed to fabricate the bacteriophage-containing microspheres. This modified method was intended to minimize the bacteriophages exposure to organic solvent in the primary emulsion, which is well known to cause denaturation at the w/o interface. The modification then involved a two-step secondary emulsion process, during which point the bacteriophage were added.

The primary emulsion was prepared by adding 200 µL 1% w/v of surfactant in water (Pluronic L92) into 2 mL 5% PLGA in DCM and homogenising using an Ultra Turrax IKA T18, at 22000 rpm for 15 s. In the first step of the secondary emulsion, the primary emulsion was added to an aqueous phase composed of 22 mL 1% PVA in storage medium containing 1×10^9 pfu/ml phage, and immediately homogenised (14,000 rpm, 3 min). This secondary emulsion (w/o/w) was then injected immediately into a non-solvent bath containing 200 mL 1% w/v aqueous PVA (hardening tank) and continuously stirred using an overhead stirrer (IKA RW11, 500 rpm). Stirring was continued for 4 h (per total volume of 2 mL DCM), the microcapsules were then harvested by centrifugation (5000 × g, 2 min) and washed by gentle resuspension in 50 mL of storage medium (repeated twice). For the purpose of comparison, blank polymeric microcapsules were also fabricated, substituting water for bacteriophage solution. Following washing, the microsphere slurry (*ca*. 1:1 microspheres:water by volume) was frozen in liquid nitrogen and lyophilised for 72 hours using a Micromodulyo, ThermoSavant, UK (vacuum of 30 mTorr, condenser -40 °C, sample compartment 10 °C). Lyophilised microspheres were kept at 4 °C in a sealed container with silica gel. Three batches of microspheres for each experiment were prepared in similar condition (room temperature, ~20 °C).

For the biological assay of phage activity (plaque assay), all (approximately 1 mL) of the lyophilised microspheres were reconstituted with 1 mL of storage medium.

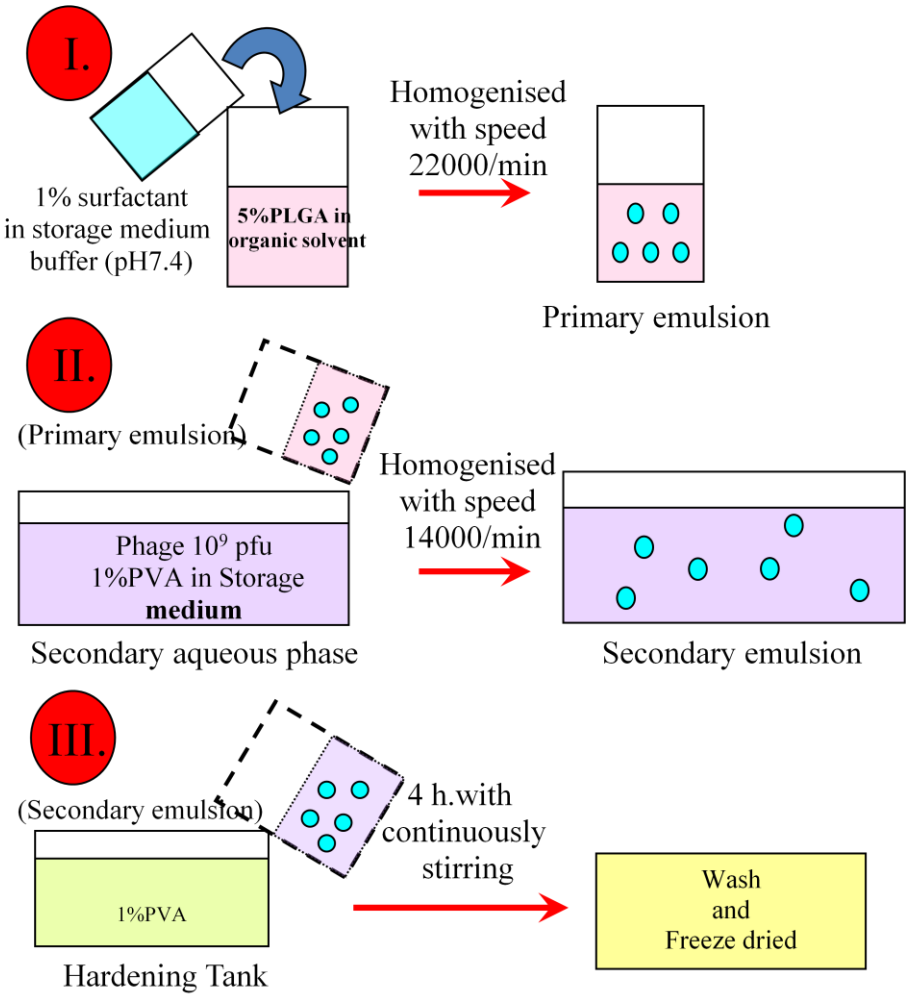

Figure 2.2. PLGA microspheres containing bacteriophage fabrication by w/o/w emulsion solvent extraction method

2.2.3.1. Physicochemical characterization of microspheres

2.2.3.1.1. Particle size analysis

Non-lyophilised microspheres were routinely sized prior to freeze-drying by laser diffractometry using Mie scattering theory (Mastersizer 2000 Version 5.00, Malvern Instruments Ltd., UK). The microsphere suspension was dispersed into water in the chamber till a laser obscurity between 10-20% was reached and data acquired. The size was reported as the volume median diameter (VMD) with the span. The median diameter was measured for three independent batches, calculating the average median diameter and standard deviation.

Span value represents the width of the size distribution. Size distribution was evaluated with span value, as shown with equation below;

$$span\ value = \frac{d(0.9) - d(0.1)}{d(0.5)}$$

Where $d_{(N)}$ (N = 0.1, 0.5, 0.9) is the diameter at the fraction cumulative volume.

2.2.3.1.2. Scanning electron microscopy (SEM)

Morphological examination of microspheres was performed by SEM (Model Jeol JSM-6400). Microspheres were mounted onto metal stubs using double-sided adhesive tape. After being vacuum-coated with a thin layer (100-150 Å) of gold, the microcapsules were imaged on a Jeol JSM-6400 operating at 6 kV, 20 °C and 10^{-5} Torr.

2.2.3.1.3. Confocal Electron Microscopy (CLSM)

Fluorescein-labelled bacteriophages were encapsulated as above and the lyophilised microspheres viewed on a Leica DM6000B microscope equipped for epifluorescence and TCSSP5 confocal laser scanning systems. The fluorescein conjugates were excited with an Argon laser line set to 488 nm and with an emission bandwidth of 521-616 nm which was tailored to provide the best image. Leica (HCX Plan Fluotar) 20× and 40× dry objectives were used and the pinhole was set automatically for optimal performance. The images were converted with Volocity software. The fluorescence was transient and photo-bleaching was rapid and no quantitative analysis of encapsulation was made. The phage activity by plaque assay was also determined at the end of the study.

2.2.3.1.4. In vitro release profile

Phages were labelled with FITC and purified by $CsCl_2$ as previously described. Phages loaded at 10^9 pfu per 100 mg of PLGA would be employed to fabricate the microspheres in each batch. Freeze drying was continued for 3 days (72 hours) as above. For each batch, approximately 10 mg of lyophilised microspheres were accurately weighed and resuspended in 500 µL PBS (pH 7.4) in Eppendorf tubes, in triplicate (n = 3 for each batch tested). The tubes were rotated end-to-end at room temperature for 2-3 weeks. At the predetermined time points (30, 60, 90, 120, 150, 180, 210, 240 min, then 5, 6, 7, 8 h, then 10, 12, 14 h, then 19, 24 h), Eppendorfs were centrifuged (12,000 × *g*, 5 min) and the supernatant was removed then put into 0.45 µm Whatman VectaSpin Micro™ and re-centrifuged at the same condition to clarify the sample. Bacteriophage yields were measured by fluorescence using an excitation wavelength of 495 nm and an emission wavelength 525 nm (Varian Cary Eclipse fluorometer, Oxford, UK).

2.2.3.1.5. Stability study

Microspheres encapsulating bacteriophage selective for *S. aureus* were prepared as above and, following completion of the lyophilisation cycle, were immediately stored in sealed containers with silica gel at 4 °C and room temperature (22 °C). After 1, 3 and 7 days, the dried microspheres were redispersed in 1 mL storage medium and lytic activity determined by plaque assay as above. Experiments were repeated for four independently prepared batches.

2.2.3.1.6. Cascade impaction

Cascade impaction was employed for particle flow measurement using a Multi-stage Liquid Impinger (MSLI) (Copley Scientific, UK), with a Critical Flow Controller (CFC) (model TPK, Copley Scientific, UK), a high capacity pump (model HCP4, Copley Scientific, UK), a flowmeter (model DFM2, Copley Scientific, UK) and a flowmeter adapter to the induction port (Copley Scientific, UK).

Three independently prepared batches were tested for each formulation using 30 hard gelatin capsules (type 3, Capsugel, Belgium), each loaded with 30 ± 2 mg of dried PLGA microcapsules harbouring phage. These microcapsules contained in these capsules would flow through the induction port via the Monodose™ inhaler (MIAT SpA, Italy) with an inhaler adapter fashioned from Silastic S Base used with Silastic S Curing agent green (Dow Corning, USA), as shown in Figure 2.2. The Monodose™ inhaler is a passive, capsule based dry powder inhaler (DPI) and consists of a mouthpiece, dispersion chamber and puncturing mechanism (red buttons located at the base of the inhaler).

As Figure 2.4, the CFC was connected to the vacuum pump and MSLI via the silicone tubing (B in Figure 2.3: inner diameter (ID) = 8 mm, outer diameter (OD) = 14 mm). Pressure tab tubing (P1: 2.2 mm ID, 3.1 mm OD, 59 mm length) at the back of CFC was inserted to the hole of the fourth stage. When the system was enclosed, the pressure (P1) was adjusted to 3.8-4.0 kPas by means of turning the flow control valve of the CFC clockwise/anticlockwise (D). The flow rate stability was also determined so that the ratio of P3/P2 should be 0.5 or less.

Once the required pressure has been established, the inhaler mouthpiece was detached and replaced by a flow meter to measure the flow rate (Q). Commonly, the flow rate (Q) was 60 ± 5 L/min, so that the effective cut-off diameters at stages 1, 2, 3, 4, 5 were 13, 6.8, 3.1, 1.7, and < 1.7 microns, respectively. Based on the value of Q, the time was adjusted corresponding with the total volume of air in MSLI (4L of air is drawn in into MSLI per actuation). So, four litres of air in MSLI would be calculated to open the valve inside the CFC for 4 seconds. Once the time was established and the pump on, the inhaler mouthpiece with adapter replaced the flowmeter.

The capsule in the dispersion chamber (A; in Figure 2.3) was punctured by pressing the red buttons to discharge the microspheres into the MSLI via the induction port during the valve opened for the pre-determined time. These steps were repeated twenty-nine times. Following the completion of these 30 capsule tests, 20 ml of water was dispersed onto each stage of the MSLI impinger (stage 1-4) and the glass fibre filter (Gelman Sciences, USA) placed onto stage 5 (MSLI impinge stage 1 to 5; Figure 2.5). The microsphere suspension from each stage was collected and lyophilised in order to measure the weight fraction of dried microspheres collected at each stage and the glass filter. Calculation of geometric mean weight diameter (d_g) and the geometric standard deviation (σ_g) was made from the log-probability plot for cumulative % frequency undersize versus particle size, as described by Martin (Martin, et al., 1983)

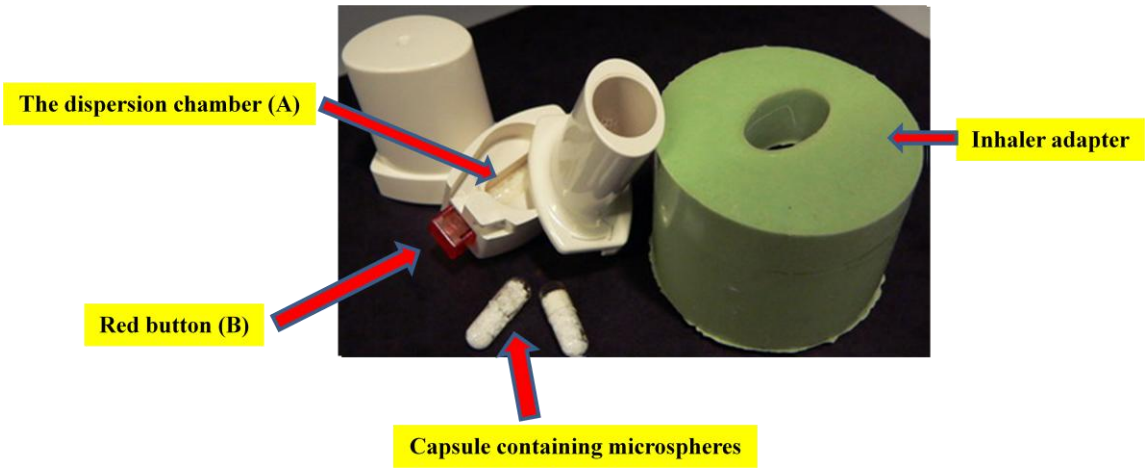

Figure 2.3. MIAT patented delivery system, Monodose™ inhaler; A. The dispersion chamber for insert the capsule; B. Red buttons to puncture the capsule into the dispersion chamber (this figure shows only one side)

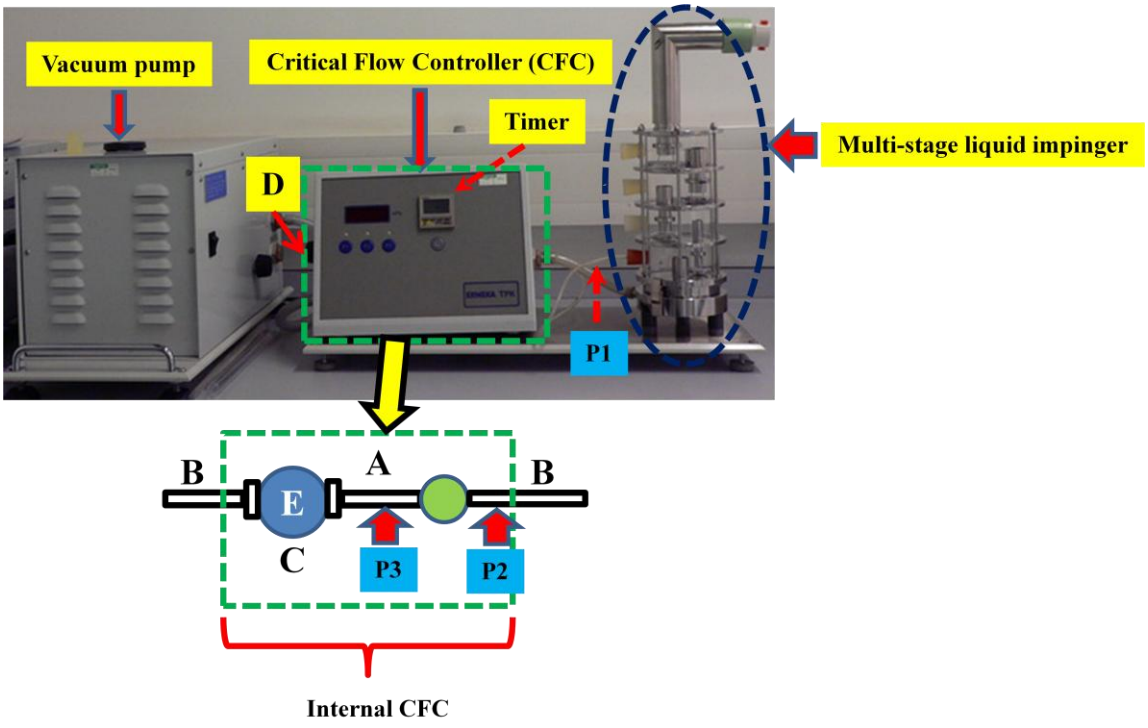

Figure 2.4. Image and Diagram of a dry powder particle sizing apparatus; A. connector (ID = 8 mm short metal coupling); B. vacuum tubing; C. two-way solenoid valve; D. flow control valve of CFC (green box); E. timer

2.2.3.1.7. Density measurement

The density of lyophilised microspheres was calculated from the volume occupied by a known mass of microspheres loaded into a measuring cylinder and tapped 10,000 × (Tap Density Volumeter, Copley Scientific, UK).

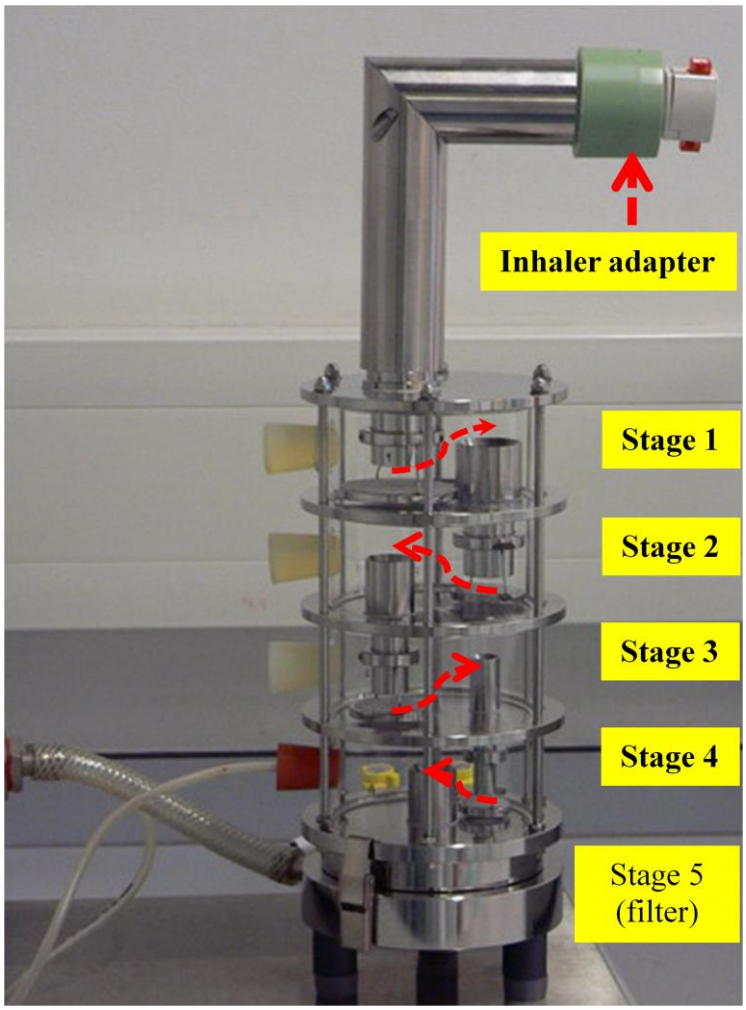

Figure 2.5. MSLI impinger shows the powder flow into the stage from stage 1 to 5 (Red arrow)

2.2.4. Lyophilisation of bacteriophages from aqueous solutions

One millilitre of bacteriophage solution (~3.3×10^8 pfu/mL) composed of 700 µL of additives (0.1 M or 0.5 M for sucrose or 1% or 5% for PEG 6000) and 300 µL of bacteriophage stock solution was lyophilised in a 10 mL borosilicate glass vial with a crimp top (Chromacol, Hertfordshire, UK) using an AdVantage benchtop freeze dryer (VirTis, US). The initial freezing steps involved cooling of the shelf holding the samples to 5 °C, held for 30 min, before further cooling to -5 °C, 30 min, and then to -30 °C at a rate of 1 °C/min, and maintained for 1 h. Primary drying was initiated at -30 °C over 1000 min, with a chamber pressure of 100 mTorr. Secondary drying involved subsequent heating of the shelf to 25 °C at a 0.1 °C/min, maintained under vacuum for a further 6 h, with final equilibration of pressure and temperature.

Lyophilised bacteriophages selective for *S. aureus* and *P. aeruginosa* were prepared as above and, following completion in each lyophilisation cycle, were immediately stored in sealed containers with silica gel at 4 °C. To test the lytic activity of bacteriophage, lyophilised bacteriophage selective for *S. aureus* and *P. aeruginosa* were kept for 2, 7 and 14 days. Following the storage in each point of time, the dried cake was reconstituted in 1 mL sterile water and lytic activity for bacteriophage was determined by plaque assay as above. For the purpose of comparison, negative control samples included storage medium, with and without gelatin and sucrose or PEG 6000. Experiments were repeated for three independently prepared batches.

2.2.4.1. Examination of bacteriophage following lyophilisation

2.2.4.1.1. Confocal laser scanning microscopy (CLSM)

For each formulation, a drop of 40 µL of fluorescein-labelled bacteriophage on a glass coverslip was lyophilised as above (2.2.4) and imaged on a Leica DM6000B microscope equipped for epifluorescence and TCSSP5 confocal laser scanning systems. The fluorescein conjugates were excited with an Argon laser line set to 488 nm and with an emission bandwidth of 521-616 nm which was tailored to provide the best image. Leica (HCX Plan Fluotar) 10× dry objectives were used and the pinhole was set automatically for optimal performance. The images were converted with Volocity® software.

2.2.4.1.2. Particle size measurements

The hydrodynamic diameters of the bacteriophage following reconstitution of the freeze-dried cakes in distilled water were determined by dynamic light scattering (DLS) with a Zetasizer Nano ZS (Malvern Instruments, UK). Values are given as the average of two measurements. It should be noted that analysis of DLS assumes a perfect sphere, which is not the case for the tailed bacteriophages; nevertheless, the data were of a sufficient quality to allow determination of aggregation or dispersion.

2.2.4.1.3. Moisture content

Freeze-dried cakes from method 2.2.4 stored in 10 mL sealed vials at 4 °C were redispersed in 3 ml anhydrous methanol and the water content of each cake determined by Karl Fischer (KF) titration (Mettler Toledo DL 37, Leicester, UK). The apparatus

was calibrated with Karl Fisher water standard (2-methoxy ethanol) and blanked with the addition of anhydrous methanol. The water content was determined for each formulation from three independently prepared samples. The samples were also prepared prior the measurement less than 24 hour.

2.2.4.1.4. Differential scanning calorimetry (DSC)

The glass transition (T_g) for the lyophilised samples was determined with a Mettler Toledo DSC822e calorimeter. Temperature-Modulated DSC (TM-DSC) was used to determine the mid point of the T_g, observed without superposition of the enthalpy relaxation and so circumventing the need to undergo a quench-cool step to remove thermal history for the material (Rouse, et al., 2007). Specifically, the T_g is represented by the reversible contribution that derives from the heat capacity, whereas the relaxation endotherm is represented by the non-reversing heat flow that derives from kinetic events. Samples were prepared by carefully weighing ~3-5 mg of powder into a 40 µl aluminium pan, which was then hermetically sealed with a pin-hole in the lid. An empty pin-holed 40 µl aluminium pan was used as a reference. To determine the T_g the pans were heated at a rate of 2 ºC/min from 40 ºC to 100 ºC for sucrose samples, or from -55 to 0 ºC for the PEG 6000 samples. The accuracy of the DSC sensor is 0.1 °C and measurements were performed in duplicate with the results analyzed using Mettler STAR software.

2.2.5. Animal models of lung infection

2.2.5.1. Rat model

2.2.5.1.1. Alginate beads encapsulating *P. aeruginosa*

One colony of *P. aeruginosa* strain 217M was picked from an agar plate and inoculated in 5 mL LB broth with shaking at 37 °C overnight to grow to late log phase, and then aliquoted to prepare the gel beads. Two percent agarose (10 mL; low electroendoosmosis) in PBS pH7.4 was mixed with 1 mL of bacterial broth. The agarose–broth mixture was added to heavy mineral oil that was equilibrated at 50-60 °C, rapidly stirred at maximum speed (IKA RW11) for 6 min at room temperature.

This emulsion was cooled over 10 min and the agarose beads were washed once with 0.5% deoxycholic acid, sodium salt (SDC) in PBS, and once with 0.25% SDC in PBS, Washing from performed by first allowing the beads to sediment for separation from the oil using a separating funnel (Figure 2.5), and then centrifuging the beads collected (3000 × g, 4 min) and resuspending in PBS at 3000 g for 4 min. The bead slurry was allowed to settle and diluted in PBS to 5 mL (shown in Figure 2.5). The bead diameter was determined using laser diffractometry (2.2.3.1.1). An inverted light microscope (Polyvar®, Reichert-Jung, Austria) was used to characterise the beads' physical morphology. To check the integrity of the bacteria in the agarose beads, the beads were used to inoculate 5 mL King's A media at 37 °C overnight. Bacteria were encapsulated into agarose beads 24 h prior to *in vivo* experiments (stored at 4 °C).

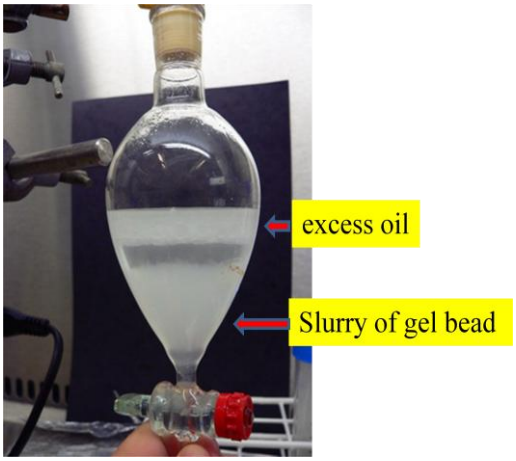

Figure 2.3. Slurry of gel beads during washing with SDC in PBS solution.

2.2.5.1.2. *In vivo* procedure for agarose bead model

All procedures were first subjected to scrutiny by the local ethics committee and approved by the Home Office. Male Sprague-Dawley rats weighing 300-400 g were housed for 12 h in a light/dark, constant temperature environment prior to the experiment, with free access to food and water *ad libitum*. Each rat was weighed and anesthetized by intraperitoneal administration using a fresh preparation of 1 mL Hypnorm® (0.315 mg fentanyl: 10 mg fluanisone/mL), 1 mL Midazolam® (5mg), and 2 mL water for injection, at a dose of 0.27 mL/100 g weight of animal. The depth of the anaesthesia was examined by tail pinch or pedal withdrawal reflex.

Following complete anaesthesia, a 1 mL syringe would be attached to the round-tipped cannula which was a part of insufflator device (Figure 2.6). 30-50 µL of air would be predrawn followed by 30 µL of diluted agarose bead slurry. Blank and bacterial gel beads (100-200 µL, total volume) would be introduced into the trachea through the mouth using the round-tipped cannula. The syringe with cannula was then removed and

the rat allowed to recover. The rat would be observed for 14 days. If there were no signs and symptoms of infection, the rats were re-infected and monitored for 14 days. At the end of experiment, the rats were sacrificed and lung histopathology studied with hematoxylin-eosin (H&E) staining.

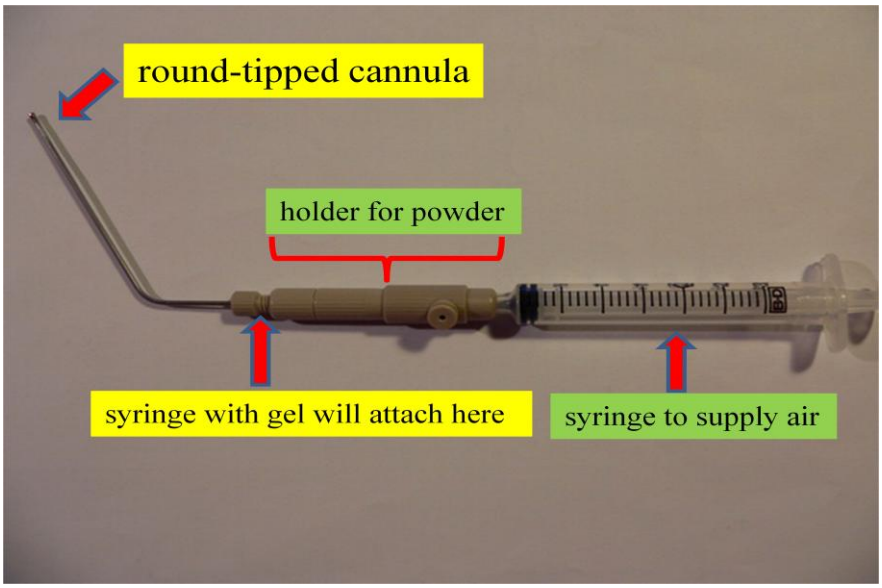

Figure 2.4. The 'insufflator' device that was used to deliver the agarose gel beads by intra-tracheal administration.

2.2.5.2. Mouse model

2.2.5.2.1. Bacterial preparation

Both mucoid strains of *P. aeruginosa* (P39324 and 217M), picked as single colonies from an agar plate, were cultured in TSB at 37 °C with shaking overnight. The concentration of bacteria was examined and compared with the McFarane standards by spectrophotometry at wavelength 625 nm. Cultured bacteria would be harvested by

centrifugation (4000 × *g*, 2 min) and resuspended with PBS pH7.4 to make a required concentration.

2.2.5.2.2. Preparation of bacteriophage for animal model

Two preparations of bacteriophage were used for in this mouse model. A volume of bacteriophage solution equivalent to 5×10^{10} pfu was employed for either intranasal administration (30 µl volume) or by nebulisation (2 mL). To compare the in vivo activity of freeze-dried bacteriophage, the freeze-dried cake (section 2.2.4) was redispersed with 1 mL of PBS pH7.4 and then adjusted to 2 mL for nasal nebulisation. Both routes of administration were given to mice 24 h after infection.

2.2.5.2.3. In vivo procedure

Since the rat model provided the uncertain outcome so the mouse model would be developed for this study. Male BALB/C mice (20-25 g) were housed for 12 h in a light/dark, constant temperature environment prior to the experiment, with free access to food and water *ad libitum*. Each mouse was anesthetized by isoflurane inhalation and the depth of the anaesthesia was examined by tail pinch or pedal withdrawal reflex (recovery normally occurred within 60 s).

On day one, each mouse in the treatment group was infected with 5×10^8 CFU of mucoid *P. aeruginosa* (strain 39324) intranasally by applying 15 µL of the bacterial suspension to each of the nares (30 µl total) using a plastic pipette. Sterile PBS was substituted for bacterial suspension in control mice. Clinical symptoms, particularly weight loss and body temperature would be observed carefully, and other signs such as behaviour, eye colour, and (laboured) breathing were also observed every 3-4 hours for 24 hours.

Twenty four hours following infection, the treatment group were administered with 5 × 10^{10} pfu bacteriophage, either with 30 µL intranasally or with 2 mL by nebulisation. For the purpose of comparison, the control group of mice were dosed with PBS pH 7.4 instead of bacteriophage at the same volume as in the treatment group. With the nebulisation technique as shown in Figure 2.7, mice would be put in the Volumatic (Allen & Hanburys, UK) spacer device and so become exposed to the nebulised phage. Mice inhaled the nebulised droplets (PARI BOY® SX compressor in combination with PARI LC SPRINT® Nebuliser, PARI GmbH., Germany. Total output rate, 590 mg/min; mass median diameter, 2.9 µm; mass percentage below 5µm, 75%) for 15 min and were then kept dry and warm under a lamp. In the case of intranasal administration, bacteriophages were directly placed at each nare of an anesthetized mouse, as above. For both routes of administration, a second dose of bacteriophage was introduced 24 h after the first dose and clinical signs were monitored. Mice were sacrificed 24 h following the second dose and the left and right lobe of the lung tissue harvested separately.

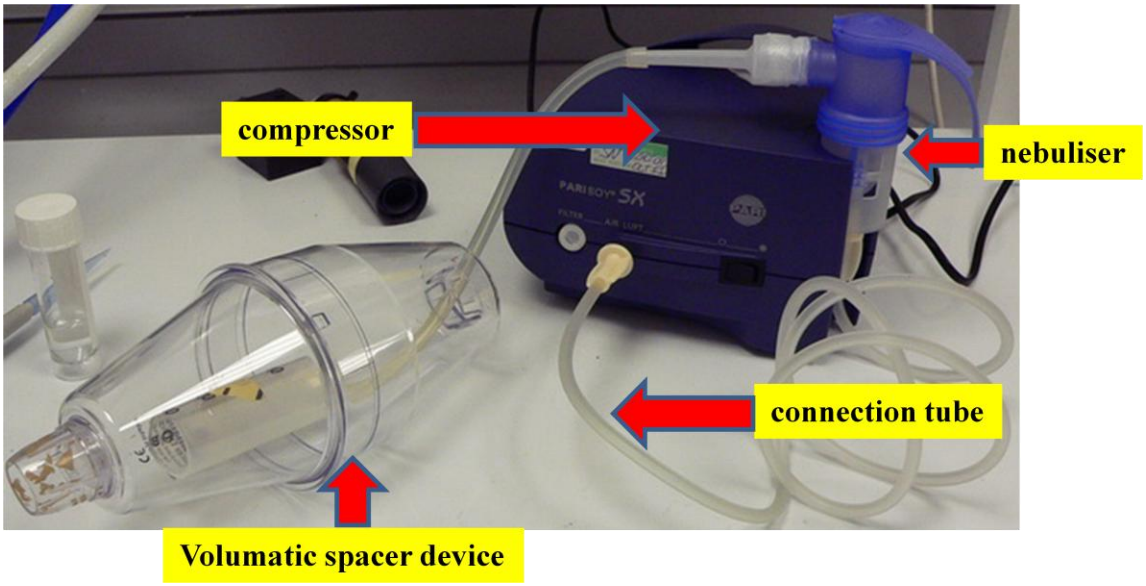

Figure 2.5. Nebuliser with improvised nebulisation chamber (Volumatic, Allen & Hanburys, UK) where keep the mouse to inhale preparation.

2.2.5.2.4. Collection of lung tissue

The lung tissues were harvested 3 days after infection to enumerate the bacterial colonies and investigate the lung histopathology by hematoxylin-eosin (H&E) staining.

2.2.5.2.5. Lung bacteriology

The right lobe lung of each mouse was excised aseptically and homogenised (IKA T18 5700 rpm, 20 s) in 10 mL of sterile PBS pH 7.4. The homogenised tissue was allowed to settle under gravity and 10-fold serial dilutions of the supernatant (each 200 µl total volume) were plated on tryptone soya agar (TSA) and incubated at 37 °C overnight. Colonies on each plate were counted to enumerate the CFU per ml in the original supernatant for each mouse, repeated for three samples.

2.2.5.2.6. Histopathologic autopsy of lungs from infected mice

The left lobe of the mouse lung was studied by HE-staining using 5 µm sections of lung tissues. To preserve the microstructure of the lung tissue, 10% formaldehyde was used as the chemical fixative agent. Fixation was performed rapidly when the lung was harvested and kept at room temperature for 24 h (for the formaldehyde to penetrate into the whole sample).

Following the tissue fixation, tissue dehydration would be conducted by sequential immersion in ethanol solution at 70%, 90%, and 100% ethanol, respectively. With the dehydrated tissues, the ethanol was removed by incubation of the sample in a solution of ethanol:Histoclear® (50:50) and 100% Histoclear, respectively.

When the lung tissues were properly dehydrated and cleared, they would be embedded with paraffin wax to mount and section by microtome. With tissue sections of 5 µm, staining would be carried out with hematoxylin-eosin (H&E) following the length of time shown in Table 2.3. Histopathology inspection would then make and images were taken to illustrate the lung histopathology.

Table 2.3. Hematoxylin and Eosin (H&E) Staining Protocol

Step and Chemical	**Length of time (minute)**
1. Histoclear	1
2. Histoclear	1
3. Histoclear	1
4. 100% Ethanol	1
5. 100% Ethanol	1
6. Distilled water	1
7. Haematoxylin	1
8. Distilled water	1
9. 0.5% Acid alcohol	1
10. Distilled water	1
11. Scots tap water	2
12. Distilled water	1
13. 3% Eosin	1
14. 100% Ethanol	1
15. 100% Ethanol	1
16. 100% Ethanol	1
17. Histoclear	1
18. Histoclear	1
19. Histoclear	1
20. Histoclear	1

Chapter 3: Results

3.1. Encapsulation of bacteriophage in PLGA microspheres

3.1.1. Defining "bacteriophage activity"

Formulation of bacteriophages by encapsulation in polymeric micropheres will result in either biologically active or inactive bacteriophage. The plaque assay is an enumeration of the lytic activity of bacteriophage, with each plaque arising from a single infectious bacteriophage when co-incubated with properly viable bacteria. Thus, the observation of many plaques demonstrates strong phage activity and also retention of phage viability. However, the plaque assay will only yield quantitative data for lytic activity over a narrow range wherein the number of plaques for a particular dilution of a bacteriophage sample can feasibly be counted. Making further dilutions of a bacteriophage sample to bring the number of plaques into a countable range following the initial overnight co-incubation carries uncertainty due to the drop in bacteriophage activity over time. Thus, the approaches to measuring and interpreting the efficiency of bacteriophage encapsulation and rate of release are inherently more complicated when compared to the well established spectroscopic assays that can be employed for protein- or DNA-loaded microspheres (e.g. Barman, et al., 2000; Duncan, et al., 2005). Measurement of the total encapsulated bacteriophage via dissolution of the microspheres followed by a protein- or DNA-based assay will not distinguish between active and inactive populations. In this study, to characterize the bioactivity and release profile of the bacteriophage-loaded microspheres two approaches were adopted: 1) semi-quantitative measurement (plaque assay) of the lytic activity of the bacteriophages released within a 1 h period from the microspheres, and 2) quantitative measurement of fluorescently-labelled bacteriophages released as a percentage of the total encapsulated, making no distinction between active and inactive populations. As regards the semi-quantitative measurement of the lytic

activity of the bacteriophages in this study, the symbols used in this study are first defined in Table 3.1 (the lytic activity of bacteriophage will be reported from minimum to maximum activity with –P, P, +P, and ++P, respectively).

Table 3.1. Definition of the symbol used to describe the lytic activity of bacteriophage by plaque assay

Symbol	-	-P	P (number of plaque)	+P	**++P**
Definition	Clear (negative control, no bacteria plated out)	Bacterial lawn, no plaques	Countable number of plaques	Uncountable number of plaques (>400 per plate)	Confluent lysis (fragmented bacterial lawn)

3.1.2. Effect of process parameter on size and lytic activity

First, the appropriate process of bacteriophage loading was performed for bacteriophage selective for *S. aureus.* The initial bacteriophage loadings in the primary emulsification were 10^7, 10^8 and 10^9 pfu/formulation. During the primary emulsion, the influence of homogenisation speed (10000 and 22000 rpm) on particle size and lytic activity was investigated. The volume median diameter (VMD) and span were obtained as measures of microsphere size and size distribution (equation 1). The mean median diameter determined at 50% cumulative volume for repeated measurements of three batches is shown in Table 3.2.

$$Span = \frac{d(0.9) - d(0.1)}{d(0.5)}$$ ….Equation 1.

Where $d_{(N)}$ (N = 0.1, 0.5, 0.9) is the diameter at the fraction cumulative volume.

Table 3.2. Effect of phage loading and homogenisation speed on microsphere size and size distribution.

Phage amount (pfu/formulation)	Microsphere diameter and span (µm)					
	at 11000 rpm			at 22000 rpm		
	Exp1	Exp2	Exp3	Exp1	Exp2	Exp3
1×10^{9}	17.55 (1.23)	21.94 (1.17)	17.75 (1.01)	10.16 (1.15)	8.74 (1.19)	10.09 (1.31)
1×10^{8}	16.15 (1.23)	14.32 (1.53)	15.85 (1.12)	9.80 (0.98)	9.88 (1.18)	10.25 (1.24)
1×10^{7}	17.66 (1.02)	15.48 (1.40)	17.14 (1.02)	9.81 (1.15)	9.57 (1.19)	9.98 (1.12)
0 (blank)	18.55 (0.91)	19.66 (1.20)	18.76 (1.04)	11.45 (1.02)	11.04 (1.15)	10.32 (1.26)

Data shows the microsphere diameter (span value).

The size of the microspheres fabricated from higher homogenisation speeds was dramatically smaller than for low homogenisation speeds. This is consistent with emulsions in general, wherein the higher energy used in droplet dispersion supports a greater oil-water interface and thereby smaller droplet size. There did not appear to be a conclusive trend between the concentration of bacteriophage added to the emulsion and the final microsphere size (d(0.5)). This is probably because the phage concentrations remain insignificant with regard to a change in viscosity of the solution, as may be expected for very high protein/DNA concentrations. However, with respect to the intended purpose of pulmonary delivery, microspheres produced at higher homogenisation speeds (22000 rpm) would be considered to more appropriate since since their diameter approaches that required for deposition to the peripheral lung. It must be remembered that these direct measurements of diameter must be converted to

the aerodynamic diameter (d_a) (equation 2); i.e. the geometric diameter, density and shape of the microspheres have to be considered. The size distribution (span) of the preparations was nearly 1.00, indicating a monodispersed particle size with reasonably narrow size distribution and uniformity of batches.

Calculated aerodynamic diameter (d_a) = $\sqrt{\rho/x}$ (d) ….Equation 2

Where; ρ is the apparent density (g/cm^3), x is the shape factor (for spherical species, x=1) and d is the median diameter (μm).

The lytic activity of the bacteriophage recovered following encapsulation into microspheres was determined immediately after preparation and lyophilisation (Table 3.3). All loadings resulted in the production of microspheres with lytically active bacteriophage, meaning that the bacteriophage had survived in particular the homogenisation process. The highest loading of bacteriophage yielded corresponding high lytic activities, though a linear trend between loading and lytic activity was not observed. It is interesting to note that a higher lytic activity was retained following microsphere preparation at the higher homogenisation speed. This would suggest that a simple hypothesis of bacteriophage inactivation at the oil/water interface (as occurs for proteins in general) is not entirely sufficient to explain the data. However, it was considered that methods which minimise exposure of the phage to the oil/water interface would still be an important goal for this work. Thus, from these data, a bacteriophage loading 10^9 pfu/ml with homogenisation speed of 22000 rpm would appear to be providing initial encapsulation parameters.

Table 3.3. The effect of bacteriophage loading and homogenisation speed on the lytic activity of phage recovered from microsphere formulations

Initial phage additional amount in primary emulsification process (pfu)	Lytic activity					
	Speed 11000 rpm			Speed 22000 rpm		
	Exp1	*Exp2*	*Exp3*	*Exp1*	*Exp2*	*Exp3*
1×10^{9}	P(37)	P(49)	P(44)	P(51)	P(49)	P(45)
1×10^{8}	P(8)	P(15)	P(12)	P(26)	P(17)	P(29)
1×10^{7}	P(11)	P(6)	P(6)	P(15)	P(19)	P(15)
0 (blank)	-P	-P	-P	-P	-P	-P

3.1.3. Effect of lyophilisation on the lytic activity of bacteriophage

The integrity of the protein coat of the bacteriophage will presumably be challenged by the lyophilisation (freeze-drying) process, as is the case for many other proteins (e.g. Chang, et al., 2005; Pereira, et al., 2007). Thus, since lyophilisation is the final process of PLGA microsphere fabrication, this process needed to be considered in an isolated fashion (i.e. the effect of lyophilisation alone). In this regard, simple solutions of bacteriophage were used to determine the effect of lyophilisation over 24 and 96 hours, which corresponds to the lyophilisation protocols that may be commonly used for the freeze-drying of PLGA microspheres.

For bacteriophage selective for *S. aureus*, a range of concentrations in 0.5 mL storage medium were lyophilised as described in the methods over periods of 24 and 96 h. Reconstitution of the dried powder with water and measurement of lytic activity by plaque assay showed good retention of lytic activity of the bacteriophages for both lyophilisation periods (Table 3.4). As commonly observed, the number of plaques decreased for decreasing concentrations of bacteriophage. The maximum lytic activity was observed as a confluent lysis of bacteria (++P), for phage freeze-dried from concentrations of 5×10^9 pfu/mL over either 24 or 96 hours. An uncountable number of plaques (+P) was observed for phage freeze-dried from concentrations of 5×10^7 pfu/mL. A difference in stress caused by longer lyophilisation times was most clearly observed only for bacteriophage freeze-dried from low concentrations of 5×10^3 pfu/mL: six plaques were observed following 24 h lyophilisation but no plaques were observed following 96 h lyophilisation.

From this result, it can be implied that the lyophilisation step following microsphere fabrication does not significantly affect the lytic activity of the bacteriophages encapsulated in this study, particularly as high phage concentrations are used for encapsulation.

Table 3.4. Effect of lyophilisation on bacteriophage lytic activity

Time of lyophilisation (hour)	Bacteriophage concentration (pfu/mL)		
	5×10^9	5×10^7	5×10^3
24	++P	+P	P(6)
96	++P	+P	-P

3.1.4. Effect of emulsification type on the lytic activity of bacteriophage

Given the putative loss of lytic activity of bacteriophage following exposure at the oil-water interface (considering in particular denaturation of the protein coat), careful consideration of the double emulsion process was required. Therefore, it was interesting to investigate the effect of addition of the bacteriophage during either the primary or secondary emulsion steps on their resultant lytic activity. It was decided to test the effect of the emulsion protocol on the lytic activity of bacteriophage.

The plaque assay clearly demonstrated that addition bacteriophage selective for *S. aureus* to the internal aqueous phase resulted in poor lytic activity (Table 3.5). In contrast, addition of bacteriophage to the external aqueous phase of the secondary emulsion resulted in a much higher retention of lytic activity: seen as an uncountable number of plaques or confluent lysis of the bacteria in the assay (Figure 3.1, A). From this result, it was asserted that the method wherein bacteriophages were added to the external aqueous phase caused less denaturation of the bacteriophage than the method wherein the bacteriophages were added to the internal aqueous phase. This result does provide evidence that exposure to the oil/water interface is key to bacteriophage inactivation, since exposure of bacteriophage to the interface will be higher for bacteriophage added to the internal aqueous phase than for addition to the continuous, external aqueous phase. This is also consistent with the maximum lytic activity being observed for non-emulsified bacteriophage (freeze-dried bacteriophage from solution). It should be noted that the negative control (blank microspheres) did not show any evidence of lytic activity, i.e. soluble PLGA fragments that may arise from erosion/degradation of the microspheres did not perturb the plaque assay. Thus, our results show that the lytic activity of the bacteriophage can be better maintained during encapsulation into PLGA microspheres by simple modification of the double emulsion-solvent evaporation protocol to minimise exposure at the solvent interface. The emulsion

protocol wherein bacteriophages were added to the continuous aqueous phase of the secondary emulsion was therefore adopted for all future experiments.

Table 3.5. Effect of emulsification type on lytic activity of bacteriophage

Formulations	Experiments (N=4)			
	Exp1	Exp2	Exp3	Exp4
Bacteriohage added to internal aqueous phase	P (7)	P(56)	P (45)	-P
Bacteriophage added to external aqueous phase	P (360)	+P	++P	+P
Non-emulsified bacteriophage solution	++P	++P	++P	++P

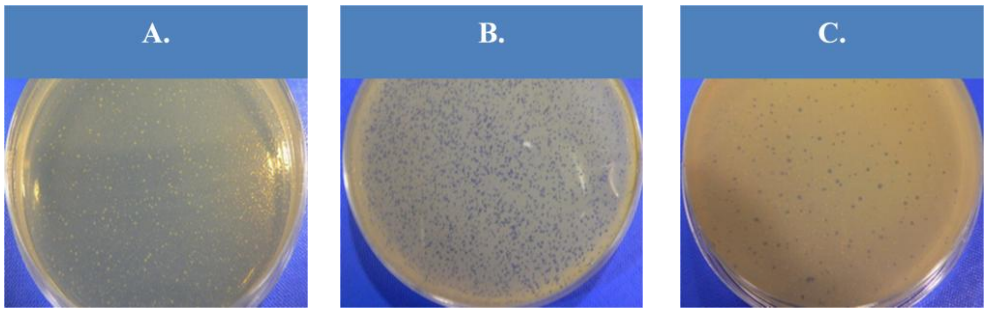

Figure 3.1. Plaque assay showing the lytic activity of bacteriophage for the two routes of encapsulation. A. the confluent lysis for the non-emulsified bacteriophage solution (++P); B. uncountable plaques for bacteriophage added to the external aqueous phase (+P); C. countable plaques (low activity) for bacteriophage added to the internal aqueous phase (P).

3.1.5. Comparison of the lytic activities of both bacteriophage strains following encapsulation into microspheres.

A comparison of bacteriophages selective for *S. aureus* and *P. aeruginosa* strain 217M was made following encapsulating both strains into microspheres. The emulsification protocol developed above was employed and measurement of the resultant lytic activity immediately after the lyophilisation step was complete was made (for four independent batches). Interestingly, the appearances of the plaques of bacteriophage selective for *P. aeruginosa* were dissimilar in appearance from plaques of bacteriophage selective for *S. aureus*, mainly with respect to their larger size. Figure 3.2 shows the plaque characteristics for the two bacteriophage strains. The characteristics of these plaques did not change following encapsulation and release. Note that the mucoid forms of *P. aeruginosa* grow as green colonies due to the production of pyocyanin, a water-soluble green pigment. In both cases the plaques are, typically, seen as clear zones within the bacterial lawn.

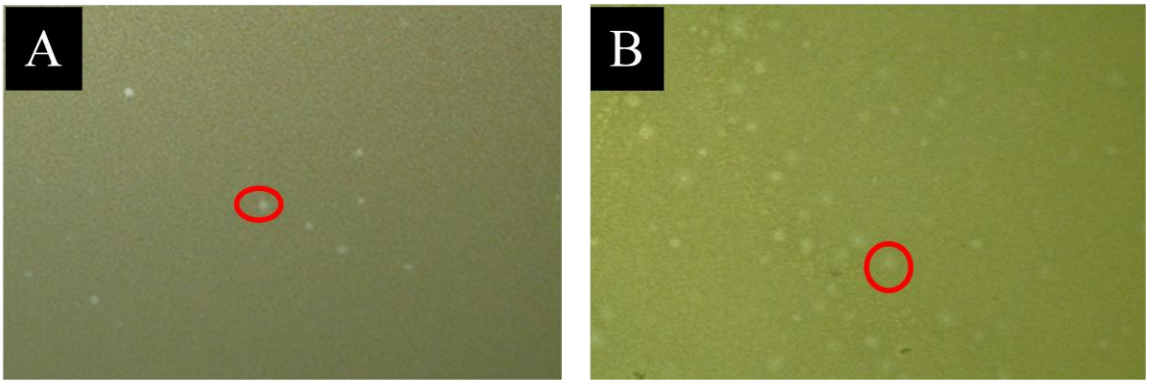

Figure 3.2. Plaques of bacteriophage (following formulation) selective for *S. aureus* (A) and *P. aeruginosa* strain 217M (B). Within the red circle is depicted a single, clear zone (one plaque), representing phage lytic activity.

In addition to the observed differences between the appearances of the plaques from the two phage strains, the lytic activity of both bacteriophages following encapsulation into microspheres could also be distinguished. Although both encapsulated bacteriophage strains retained lytic activity, this was less that the lytic activity observed for the non-formulated (positive control) bacteriophage in solution, and bacteriophage selective for *S. aureus* retained greater lytic activity than those for *P. aeruginosa* following encapsulation into microspheres (Table 3.6): the plaque assay showing either confluent lysis of bacteria (++P) or an uncountable number of plaques (+P) for bacteriophage selective for *S. aureus* following formulation. As observed previously, any degradation products from the PLGA microspheres that were present had no visible influence on the plaque assay (negative control).

Table 3.6. Lytic activity of bacteriophage immediately following encapsulation and release.

Formulation	expt. 1	expt. 2	expt. 3	expt. 4
P. aeruginosa bacteriophage, microspheres	P(200)	+P	P(300)	P(300)
P. aeruginosa bacteriophage, solution	++P	++P	++P	++P
S. aureus bacteriophage, microspheres	P(400)	+P	+P	++P
S. aureus bacteriophage, solution	++P	++P	++P	++P
Blank microspheres	–P	–P	–P	–P

3.1.6. The stability of bacteriophages encapsulated into microspheres

The stability of the encapsulated bacteriophages selective for *S. aureus* over a 7-day period was examined. It is acknowledged that a 7 day period can be considered as a very short period of time for a stability study. However, it must be remembered that biopharmaceuticals (particularly some protein therapeutics) are inherently unstable and we anticipated that the complex self-assembling nature of the bacteriophage would be no different. Microspheres loaded with bacteriophage were stored at 4 or 22 °C for 7 days, during which samples were taken for determination of the lytic activity by plaque assay.

Table 3.7 clearly shows that the bacteriophages were very unstable in PLGA microspheres over the 7 day period, though interestingly, the lytic activity was not different between storage temperatures of 4 and 22 °C. The loss of activity during storage at either temperature was consistent between all four independently prepared batches.

This shows that the storage temperature had no effect on the lytic activity of bacteriophage loaded microsphere selective for *S. aureus.* The initially high lytic activity seen on day 1 is consistent with the high lytic activity seen in the previous experiments above. Given the large number of counts that were needed for this work, and the rapid decline in activity over time, these stability experiments were not repeated for the bacteriophage strain selective for *P. aeruginosa*.

Table 3.7. Lytic activity of the bacteriophage following storage of microspheres formulations

Storage time (days)	Storage at 4 ^{o}C				Storage at room temp. (22 ^{o}C)			
	expt. 1	expt. 2	expt. 3	expt. 4	expt. 1	expt. 2	expt. 3	expt. 4
1	++P	++P	++P	++P	++P	++P	++P	++P
3	+P	++P	+P	+P	+P	+P	+P	+P
7	–P	–P	–P	–P	–P	–P	–P	–P

3.1.7. Comparison of microsphere morphology for the two bacteriophage strains.

3.1.7.1. The size determination and size distribution

Previous characterisation of microsphere size was made for addition of bacteriophage to the internal aqueous phase of the primary emulsion (above). In this section, the same characterisation is made but for both bacteriophages added to the continuous aqueous phase of the secondary emulsion. Figure 3.3 shows that bacteriophage-loaded microspheres were similar in size to blank microspheres: 10 μm, similar to the size previously determined (cf. Table 3.2) as may be expected given that the same homogenisation speed and emulsion systems were used. There was no statistical difference between the average median diameters ($P > 0.05$ using Friedman's analysis with Dunn's post test). Therefore, microsphere size was independent of the addition of bacteriophage and of the bacteriophage encapsulated. For each batch of microspheres, the size-distribution profiles showed one major peak with a span value (Figure 3.4). The average span was 1.14, 1.19 and 1.22 for the blank microspheres and the microspheres

encapsulating bacteriophages selective for *S. aureus* and *P. aeruginosa*, respectively. These span values were similar to those obtained previously (Table 3.2) and indicated that batches had narrow size distributions (span value nearly 1) and could be produced with quite consistent characteristics.

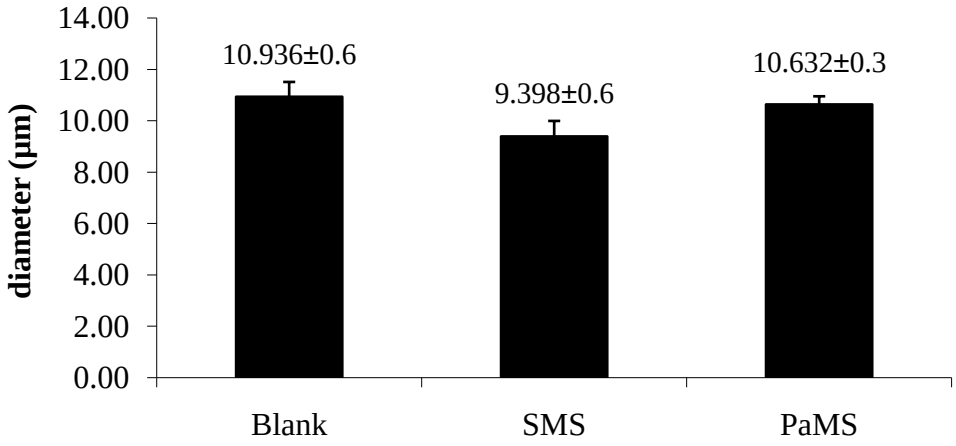

Figure 3.3. Comparison of the average median diameter of blank microspheres (Blank) and bacteriophage loaded microspheres selective for *S. aureus* (SMS) and *P. aeruginosa* (PaMS). The data represent the average median diameter and standard deviation (± SD).

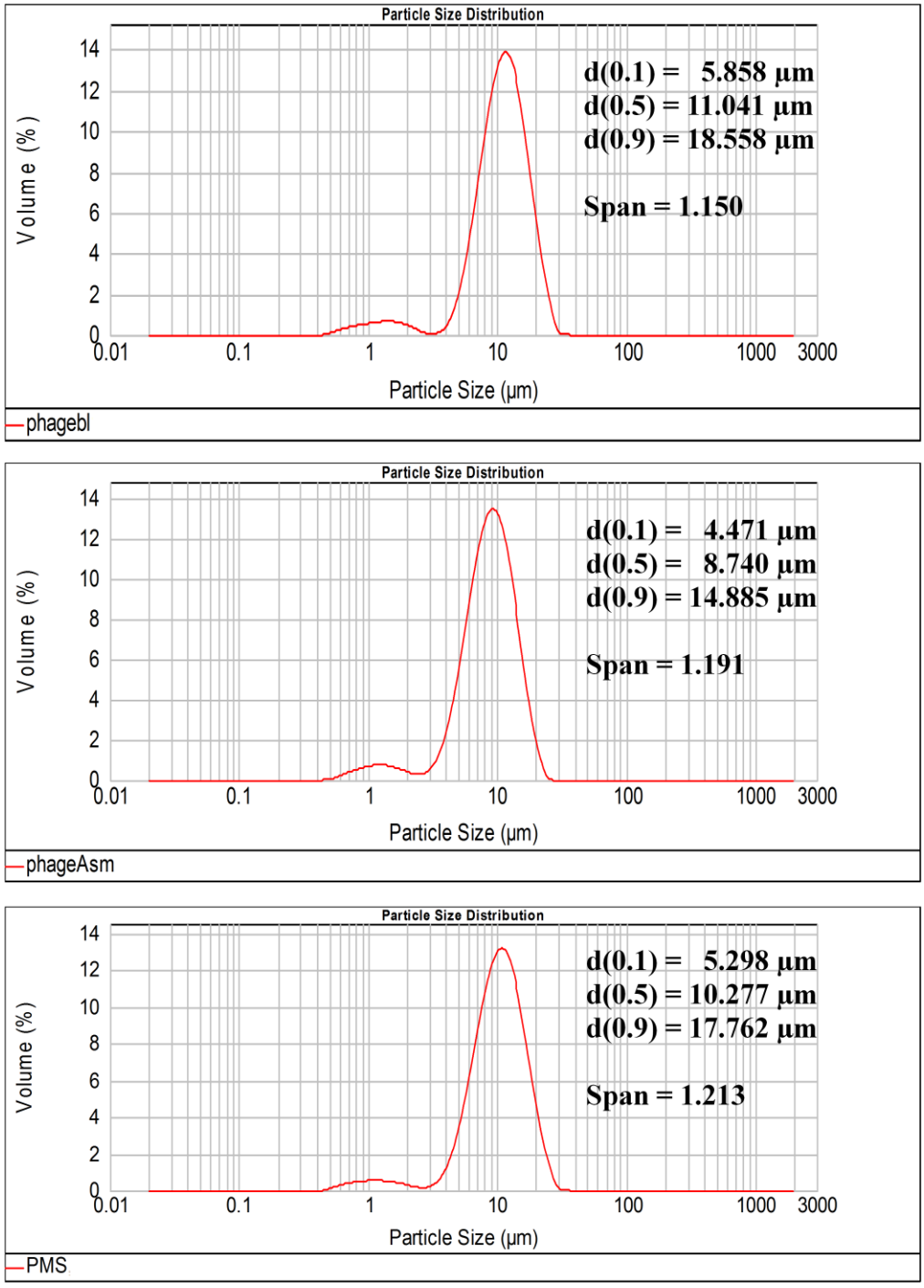

Figure 3.4. Representative size distribution profiles blank microsphere and bacteriophage-loaded microspheres. Cumulative volume diameters are shown at d(0.1), d(0.5), and d(0.9), alongside the calculated span value.

3.1.7.2. Morphological characteristic of bacteriophage loaded microsphere

The morphology of microspheres fabricated using the protocol described above (section 3.1.4) are shown in Figure 3.5. Micrographs were obtained for at least three different batches of microspheres, to ensure that the morphologies produced were consistent. The external morphology of microspheres encapsulating bacteriophage was markedly different to the blank microspheres; the latter being consistent with previous work showing that Pluronic L92 generates dimpled, non-porous surfaces (Fig 1, A) (Mohamed and van der Walle, 2006). Microspheres encapsulating bacteriophage showed smooth to slightly irregular surfaces with some external pores (Fig 1, B-D). A fraction of the blank microspheres showed complete internal collapse, indicating a hollow interior as observed previously. Similar collapse of microspheres prepared with storage medium as the aqueous phage, of with bacteriophage in storage medium, was not observed, suggesting an internal matrix; i.e. by SEM, the interior of the microspheres was hollow only for blank microspheres. This observation can be related to the distribution of bacteriophage examined by CLSM, as described in section 3.1.7.3. Since addition of storage medium alone produced this change in external/internal morphology, it would appear that one or more constituents of the storage medium in some way alter the emulsion system and prevent surface dimpling/hollow microsphere interiors: the addition of bacteriophage does not seem to further perturb the morphology. Thus, for bacteriophage-loaded microspheres, the surface was less dimpled and the interior was macroporous.

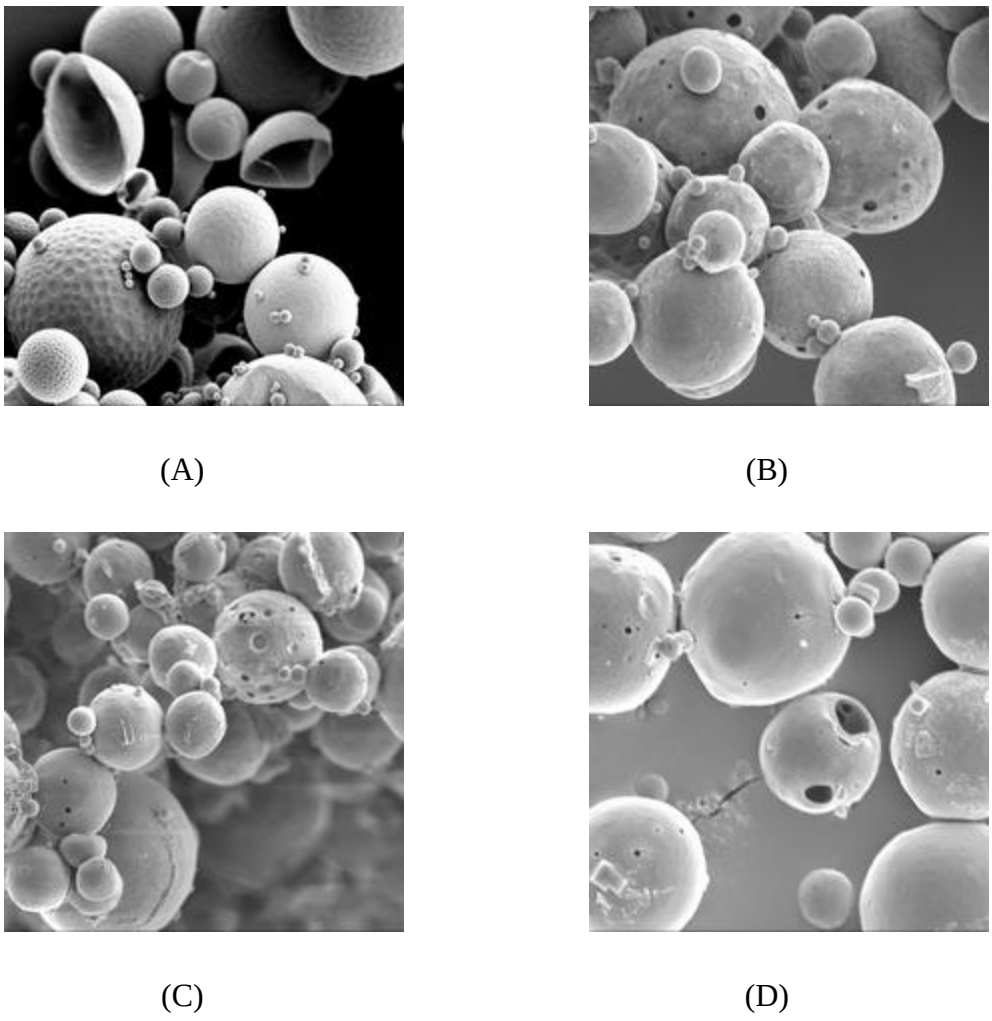

(A) (B)

(C) (D)

Figure 3.5. Scanning electron micrographs of PLGA microspheres: (A) prepared with 1% PVA as the aqueous phase (magnification 2000×), (B) prepared with storage medium, as the aqueous phase (magnification 3000×), (C and D) prepared with bacteriophage selective for *S. aureus* in storage medium as the aqueous phase (magnification 2000× and 3500×, respectively).

3.1.7.3. The distribution of bacteriophage within microsphere formulation

The distribution of fluorescein-labelled bacteriophages within the microspheres was investigated by CLSM. The confocal photomicrographs shown in Figure 3.6 represent an equatorial slice of the microspheres and demonstrate that the bacteriophages were entirely encapsulated within the internal matrix, rather than simply being surface adsorbed. These photomicrographs are also consistent with the interpretation of the SEM micrographs, showing that the interior of the bacteriophage-loaded microspheres was not hollow. A punctuate distribution was apparent at higher magnification photomicrographs (Figure 3.6, B and D), rather than a homogeneous distribution. This may reflect the macroporous nature of the internal porous matrix of the microspheres as suggested above (section 3.1.7.2). The photomicrographs are also useful for the interpretation of the release study (below) since it is useful to know the initial distribution of phage (either surface bound or encapsulated) before release from the microsphere.

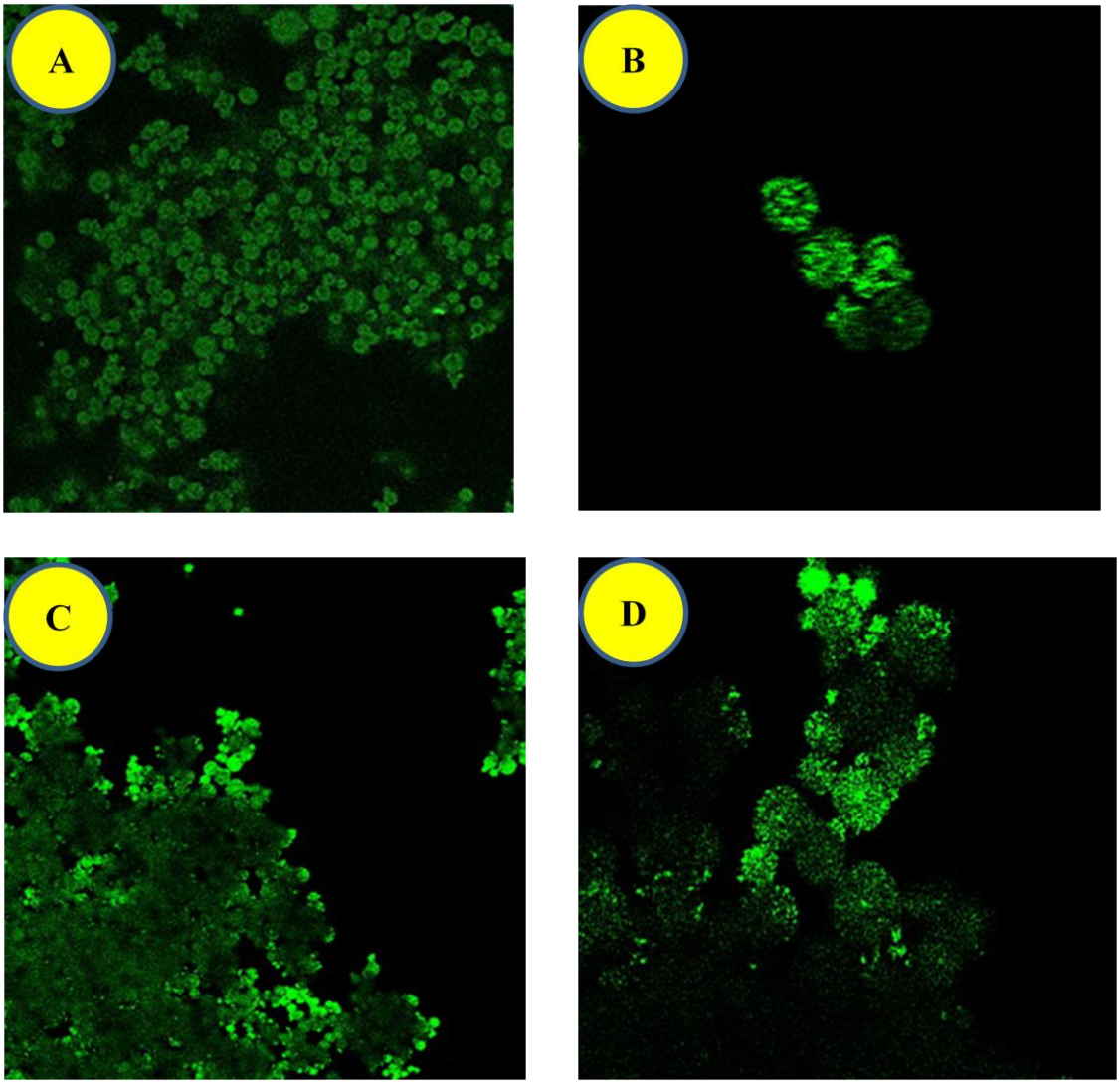

Figure 3.6. Confocal photomicrographs of microspheres encapsulating fluorescein-labelled bacteriophages selective for *S. aureus*. (A and B) and *P. aeruginosa* (C and D) at 20× (A and C) and 40× (B and D) magnification.

3.1.7.4. Aerodynamic diameter (d_a) and geometric mean weight diameter (d_g)

From equation 2 (above) measurement of the apparent density of the microspheres is required to calculate the aerodynamic diameter (d_a). Bulk density of the microsphere dry powders were simply calculated prior to tapping and re-calculation of the apparent density, used to calculate d_a. Table 3.8 shows that the calculated densities for both blank and phage-loaded microspheres were quite low (around 0.1 g/cm^3). The low apparent density of the blank and bacteriophage-loaded microspheres was in agreement with previous work for microspheres produced in a similar manner (Mohamed and van der Walle, 2008). Pairwise comparisons using the Kruskal-Wallis test revealed that the densities (bulk density or tapped, apparent density) were not significantly different between the blank microspheres and bacteriophage-loaded microspheres ($p > 0.05$). This is consistent with the various microsphere formulations being statistically indistinguishable with respect to their directly measured diameters (d), above.

Table 3.8. Bulk and tapped densities of microspheres

The average density (g/cm^3)	Blank	*SMS*	*PaMS*
Bulk density	0.0935 ± 0.003	0.0902 ± 0.005	0.0867 ± 0.006
Tapped/apparent density	0.1233 ± 0.004	0.1136 ± 0.003	0.1236 ± 0.004

**data express the value of density ± SD of three independent bactches in each formulation (N=3). Blank, SMS, and PaMS represent blank microsphere, bacteriophage loaed microsphere selective for S. aureus and P. aeruginosa, respectively.*

As the apparent density in Table 3.8, the aerodynamic diameter (d_a) would be calculated from the equation (2)

The calculated aerodynamic diameters of these formulations are shown in Table 3.9 and it can be seen to lie within the general diameter required for deposition to the lung periphery (ca. 3 μm). Because the density of the microspheres is low, d_a is much less than the measured diameter (d).

We compared the value for d_a to the geometric mean weight diameter (d_g), which is an experimentally determined measurement made using cascade impaction, and calculated from log-probability graph plot (as shown in Figure 3.7). The geometric mean weight diameter for phage-loaded microspheres selective for *S. aureus* was 6.6 μm, which is nearly two-fold greater than the corresponding value of d_a; in contrast d_g for the blank microspheres was similar to the calculated d_a value (Table 3.9). The calculated geometric standard deviation (GSD or σ_g), which is a measure of the spread of the particle sizes measured by cascade impaction, for blank and bacteriophage-loaded microsphere formulations was the same and consistent with the span calculated for direct measurement of particle diameter (span as shown in Table 3.9). The relatively high value of d_g for phage-loaded microspheres may be a reflection of the ease of dispersion; the blank microspheres appeared to disperse completely since d_g and d_a were similar, but the phage-loaded microspheres may have partially clumped together leading to a higher value for d_g.

Table 3.9. Physical characteristics of the microspheres

Microsphere formulation	d (μm)	Span	ρ (g/cm^3)	d_a (μm)	d_g (μm)	σ_g
PaMS	9.4 ± 0.6	1.22 ± 0.02	0.12 ± 0.004	3.30	nd	nd
SMS	10.6 ± 0.3	1.19 ± 0.08	0.11 ± 0.003	3.57	6.6	1.5
blank	10.9 ± 0.6	1.14 ± 0.12	0.12 ± 0.004	3.83	3.4	1.5

Data are expressed as the mean ± standard deviation for 3 independent batches; nd, not determined.

From log-probability graph plot the MMAD was observed at 50% cumulative mass and then the geometric standard deviation (GSD) was also determined by equation (3);

MMAD = 50% size = 6.6 μm.

Geometric standard deviation, GSD (σ_g) $= \frac{50\%\ size}{16\%\ undersize}$ …Equation 3

$= \frac{6.6}{4.4} = 1.5$ μm.

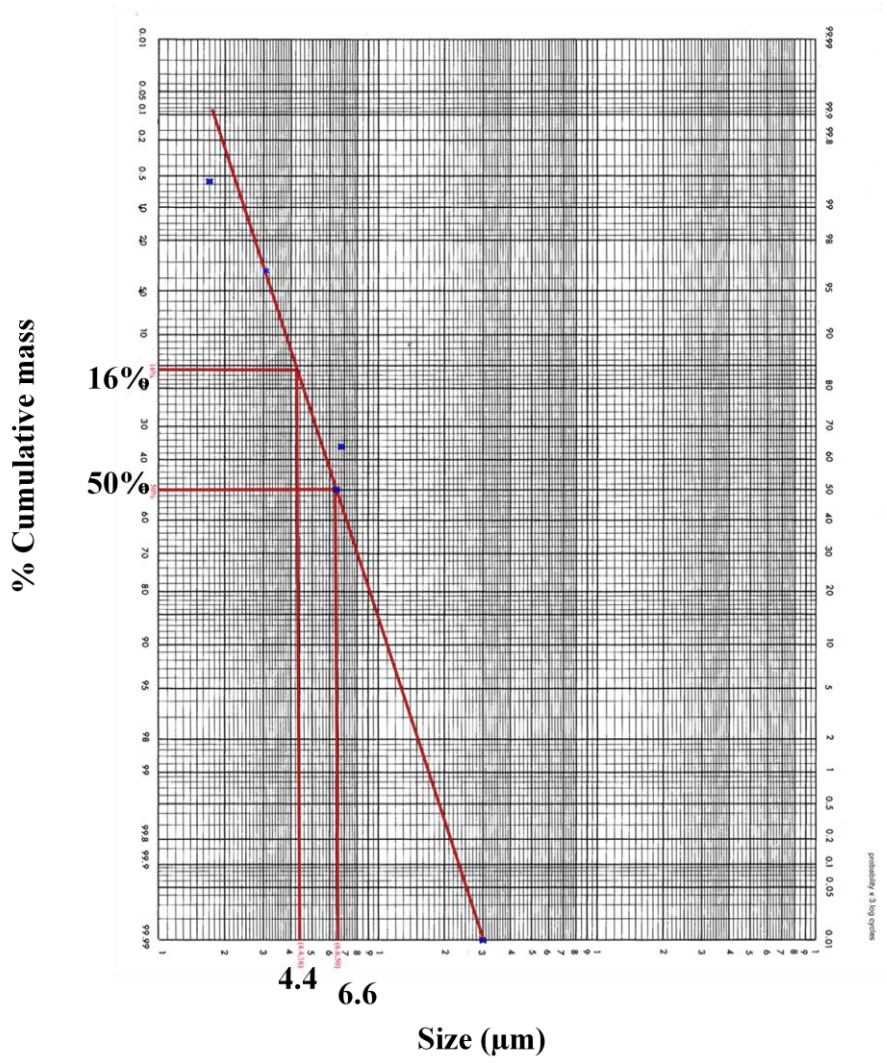

Figure 3.7. Log-probability graph plot for bacteriophage loaded microsphere selective for *S. aureus*.

3.1.6.5. Release study of phage-containing microsphere

The release profile of bacteriophages from the microspheres was examined by quantitative measurement of fluorescence, using fluorescein-labelled bacteriophages selective for *S. aureus*. In order to generate a quantitative measurement, it was required to construct a calibration curve of fluorescence versus concentration. While this is straightforward for fluorescently-labelled proteins whose extinction coefficient at 280 nm can be calculated, this is not the case for bacteriophage. Instead we made a calibration curve of the concentration of fluorescein versus fluorescence ($\lambda_{ex}/\lambda_{em}$ 495/525 nm). Constructing the calibration curve in this manner (Figure 3.8) yielded a straight line of the form $y = 5.820x + 0.843$, where y is the fluorescence intensity and x is the concentration. With this calibration curve, it was possible to measure the fluorescence of bacteriophage released from the microspheres over time, and relate the fluoresence to a concentration.

Figure 3.9 shows the release profiles for both bacteriophage formulations, which indicate an initial 'burst release' – that is, a relative rapid release over the first 30 min. Following this burst release, for both bacteriophage formulations a slower sustained release phase was observed, approaching plateau after ~6 h. Note that the release profiles are not normalised to the maximum cumulative release; instead the fluorescence measured during release of bacteriophage from the microspheres is expressed as a percentage of the known amount of fluorescently-labelled bacteriophage that was added to the emulsion.

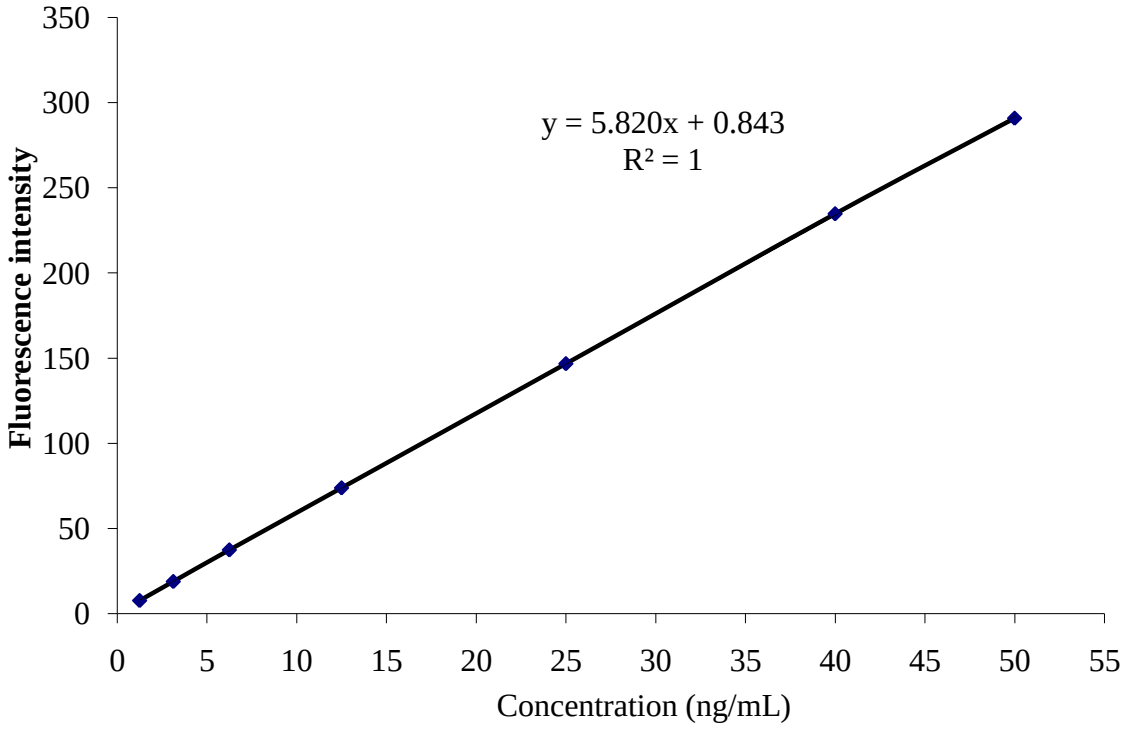

Figure 3.8. Calibration curve of FITC solution as shown the fluorescence intensity and concentration of FITC at the excitation wavelength 495 nm and emission wavelength 525 nm.

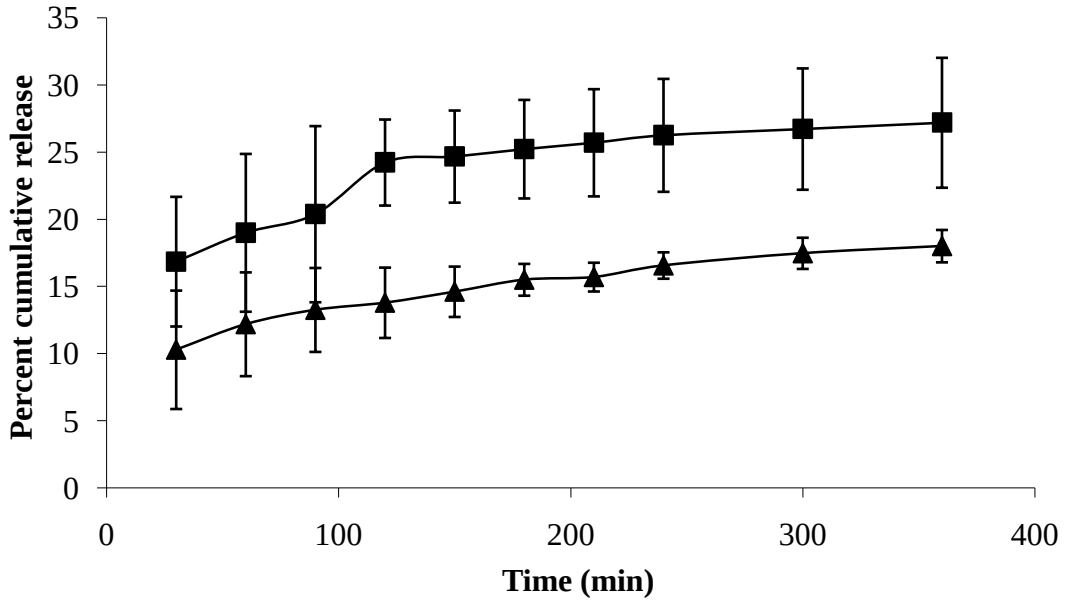

Figure 3.9. In vitro release profiles of bacteriophage selective for *S. aureus* (SMS, ▲) and *P. aeruginosa* (PaMS, ■), shown as the cumulative percentage of the total added during the encapsulation process. The data shows as mean ± SEM.

The encapsulation efficiency (a value typically reported for microsphere formulations, representing the total amount of drug encapsulated as a fraction of that added to the emulsion) is also more difficult to calculate for bacteriophage. For proteins and peptides, extraction from PLGA microspheres using solvent and measurement of concentration by High Performance Liquid Chromatography or UV absorbance would typically be performed this calculation. However, the concentrations of phage added are very low and HPLC is not practical, nor is UV absorbance for reasons described above. For this reason, it was assumed that the release profiles gave the closest possible measurement of the encapsulation efficiency, thus inferred near the plateau and being around 18% and 27% for bacteriophages selective for *S. aureus* and *P. aeruginosa*, respectively.

3.2. Stabilisation of bacteriophage during freeze drying

3.2.1. Morphology of bacteriophage

To classify the bacteriophages, Transmission Electron Microscopy (TEM) was used with negative staining of the sample. Observation of the bacteriophage morphologies enabled the classification of the NCIMB 9563 bacteriophage into the Siphoviridae family: having an isometrically hexagonal head ~80 nm in diameter and a long, noncontractile tail ~200 nm in length with a knoblike structure at its distal end (Figure 3.10, A). Similarly, the bacteriophage isolated against *P. aeruginosa* strain 217 M was classified into the Myoviridae family: having a smaller icosahedra head ~55 nm in diameter and a shorter, contractile tail of ~110 nm in length consisting of a sheath and central tube (Figure 3.10, B) (Ackermann, 2005).

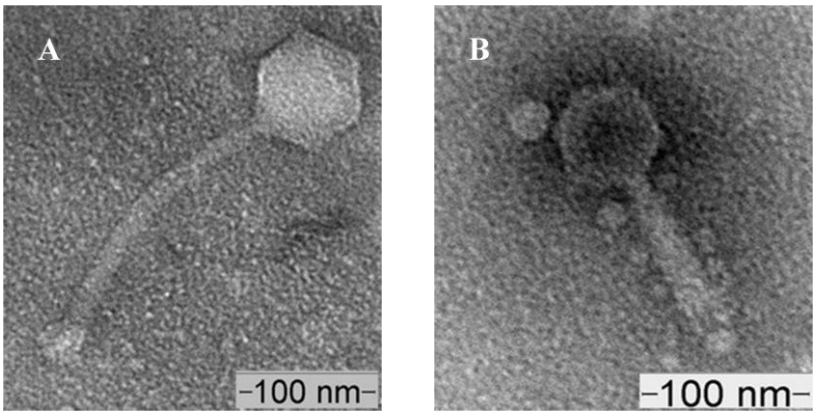

Figure 3.10. Transmission electron micrograph of the two bacteriophages employed in this study and selective against *S. aureus* (A) and a mucoid *P. aeruginosa* (B).

3.2.2. Lytic activity of freeze-dried bacteriophage

In the initial stability study (Table 3.10), bacteriophages were lyophilised from storage medium (SM) with or without gelatin. The lytic activity of the freeze-dried bacteriophages was compared against non-lyophilised bacteriophages, with both liquid and freeze-dried bacteriophage being stored at 4 °C. The effects of drying cycles on lytic activity were also determined by comparison against previous study in this work.

Extending the primary drying cycle with a typical secondary cycle was seen to be beneficial for the stability of both bacteriophages; particularly the phage active against *S. aureus*, which was seen to rapidly lose lytic activity when not fully dried (Table 3.10). The freeze-dried formulations are clearly much more stable than the dry powder (PLGA microsphere) formulations, which lost lytic activity after 7 days (Puapermpoonsiri et al., 2009). For both freeze-dried bacteriophage formulations, lytic activity was seen to begin to fall after 30 days, irrespective of whether gelatin was added into the storage medium or not. Since these data on lytic activity showed that the presence of gelatin in the lyophilised formulation had an effect, that is, bacteriophage lyophilised from storage medium without gelatin retained a higher lytic activity on reconstitution, stabilisers/bulking agents (PEG and sucrose) were introduced to generate a pharmaceutically elegant cake (Table 3.11 and 3.12).

Table 3.10. The lytic activity of bacteriophages lyophilised from storage media (SM)[a].

Freeze-dry cycle	Phage selective for:	SM with gelatin				SM without gelatin			
		d 2	d 7	d 14	d 30	d 2	d 7	d 14	d 30
primary	*S. aureus*	+P	+P	P<100	P<100	++P	++P	+/++P	+P
	P. aeruginosa	++P	++P	+P	+P	++P	++P	+/++P	+P
primary & secondary	*S. aureus*	++P	++P	+/++P	+P	++P	++P	+/++P	+P
	P. aeruginosa	++P	++P	++P	+P	++P	++P	++P	+P
control[b]	*S. aureus*	++P	++P	++P	+P	++P	++P	++P	+P
control[b]	*P. aeruginosa*	++P	++P	++P	+P	++P	++P	++P	+P

[a], where variation in lytic activity for the three independent experiments was observed, this is shown as +/++P (high titers) or P<100 (low titers); [b], bacteriophage in SM at 4 °C.

However, the lytic activities of bacteriophage lyophilised in the presence of 1% and 5% PEG 6000 were poor (Table 3.11), although PEG did form an elegant cake (see section 3.2.3). Indeed, the addition of PEG 6000 at both concentrations tested appeared to be detrimental, irrespective of the lyophilisation cycle adopted; although we note that secondary drying yielded a relatively greater lytic activity (Table 3.11). Nevertheless, the final measurement of lytic activity at day 30 showed an activity similar to that observed at the same stage for freeze-dried bacteriophage in storage media alone (+P). Thus, while PEG 6000 caused a greater loss of activity over the first 14 days, thereafter the relative stabilities of the various bacteriophage formulations appeared to converge.

Data for the stabilising effect of sucrose also showed, in general, a detrimental effect on bacteriophage lytic activity though it was possible to retain good lytic activity through optimization of sucrose concentration and lyophilisation cycle (Table 3.12). A high sucrose concentration of 0.5 M caused a general decrease in the lytic activity of the

reconstituted bacteriophage, relative to phage lyophilised from 0.1 M sucrose or storage media alone. Lower concentrations of sucrose maintained good lytic activity of the bacteriophage over the 30 day period, similar to activities seen in Table 3.10. The appearance of the cake from lyophilisation cycles containing sucrose was also pharmaceutically acceptable (see section 3.2.3). Sucrose would therefore appear to be favour over PEG 6000 for the stabilisation of bacteriophage during lyophilisation.

Table 3.11. The lytic activity of bacteriophages lyophilised using PEG 6000 as a stabiliser[a].

Freeze-dry cycle	Phage selective for:	SM, no gelatin, 1% PEG				SM, no gelatin, 5% PEG			
		d 2	d 7	d 14	d 30	d 2	d 7	d 14	d 30
primary	*S. aureus*	+P	+P	+P	+P	+P	+P	+P	+P
	P. aeruginosa	+P	+P	+P	+P	+P	+P	+P	+P
primary & secondary	*S. aureus*	++P	+/++ P	+P	P<100	++P	+/++ P	+/++ P	+P
	P. aeruginosa	++P	+P	+P	+P	++P	+P	+P	+P

[a], variation in lytic activity between the three independent experiments is shown as in Table 3.10.

Table 3.12. The lytic activity of bacteriophages lyophilised using sucrose as a stabiliser[a].

Freeze-dry cycle	Phage selective for:	SM, no gelatin, 0.1 M sucrose				SM, no gelatin, 0.5 M sucrose			
		d 2	d 7	d 14	d 30	d 2	d 7	d 14	d 30
primary	*S. aureus*	++P	++P	+P	nd	+/++ P	+P	+P	nd
	P. aeruginosa	++P	++P	+P	nd	+P	+P	+P	nd
primary & secondary	*S. aureus*	++P	++P	++P	+P	+P	+P	+P	+P
	P. aeruginosa	++P	+P	+P	+P	++P	+P	+P	+P

[a], variation in lytic activity between the three independent experiments is shown as in Table 3.10; [b], nd = not determined.

3.2.3. Physical characterization of freeze-dried bacteriophage/cakes

3.2.3.1. Cake structure

A proper, elegant cake structure for the freeze-dried bacteriophage was one aim of the lyophilisation process. Collapse or eutectic melting of the cake may lead to high residual moisture and prolong the reconstitution time of the dried powder, influencing the physical and biological stability of the bacteriophage formulation. Therefore, the appearance of the cake was also examined, shown in Figures 3.11-3.14.

The appearance of the cake for bacteriophage lyophilised from storage media was poor, being entirely collapsed (Figures 3.11 and 3.12). The intention of adding a non-protein stabiliser was to produce a pharmaceutically acceptable, elegant freeze-dried cake for reconstitution. The cakes observed for bacteriophage lyophilised from 0.5 M sucrose and

5% PEG 6000 remained stable after pressure and temperature (Figure 3.13). A little collapse for dried bacteriophage containing 5% PEG was found in the primary drying cycle alone (Figure 3.14). It was noted that the bacteriophage themselves caused collapse of the cake for lower concentrations of sucrose, and the same effect was seen for 1% PEG 6000 either in the primary drying cycle alone or in the primary and secondary drying cycles (Figure 3.13 and 3.14). It should be noted that minor collapse was also observed as the cake 'pulling away' from the wall of the vial, without gross collapse of the cake thickness. Ideally, the cake should be entirely free of collapse.

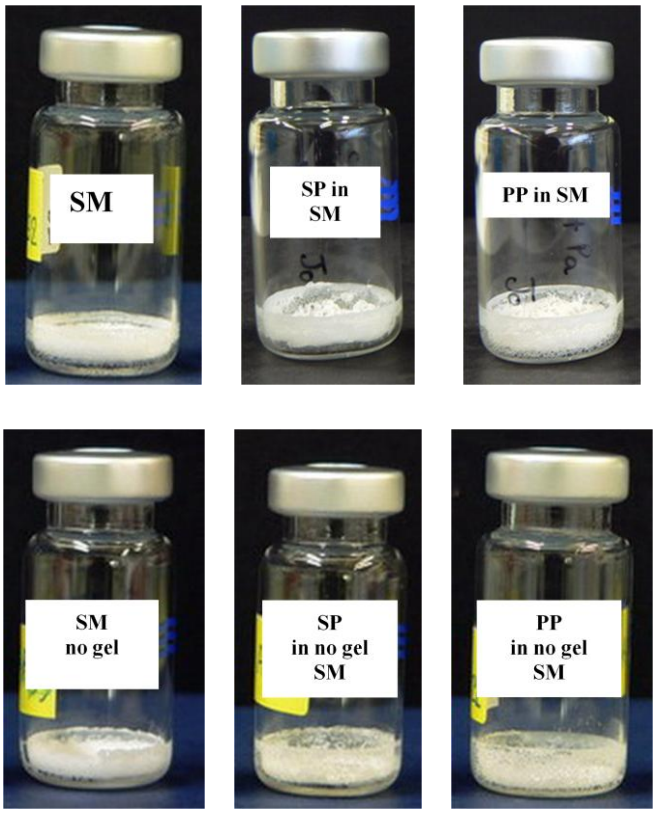

Figure 3.11. Images of the freeze-dried cakes following primary drying cycle. Top row from left to right: storage medium with gelatin (SM), bacteriophage selective for *S. aureus*, and *P. aeruginosa* in SM with gelatin, respectively. Bottom row from left to right: storage medium without gelatin (SM no gel), bacteriophage selective for *S. aureus*, and *P. aeruginosa* in SM with gelatin, respectively.

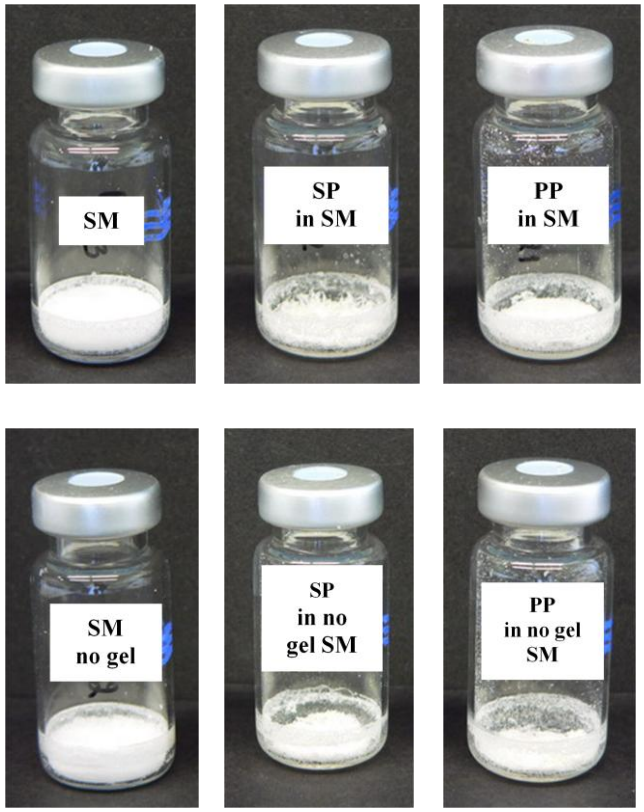

Figure 3.12. Images of the freeze-dried cakes following primary and secondary drying cycles. Top row from left to right: storage medium with gelatin (SM), bacteriophage selective for *S. aureus*, and *P. aeruginosa* in SM with gelatin, respectively. Bottom row from left to right: storage medium without gelatin (SM no gel), bacteriophage selective for *S. aureus*, and *P. aeruginosa* in SM with gelatin, respectively.

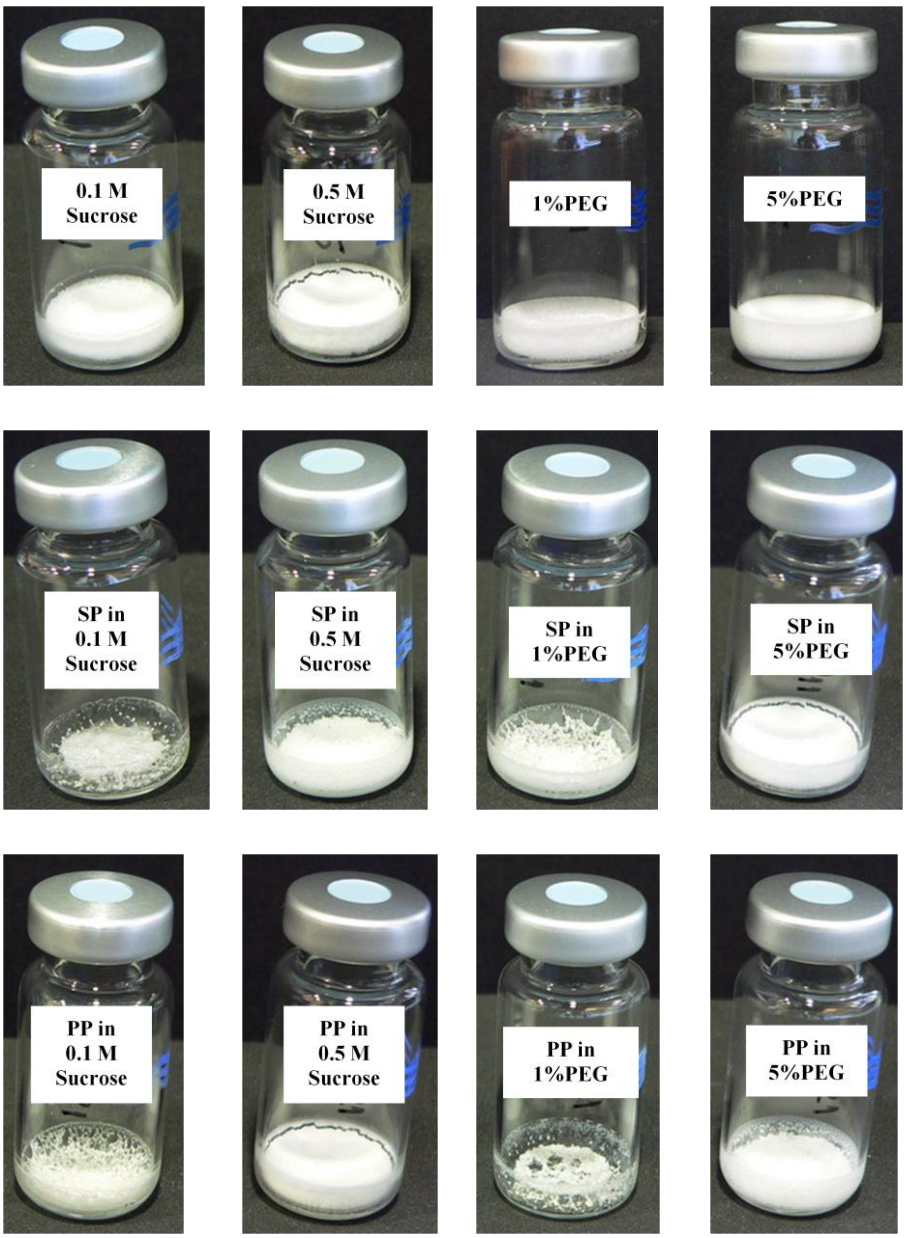

Figure 3.13. Images of the freeze-dried cakes following primary and secondary drying cycles. Top row from left to right: 0.1 M sucrose, 0.5 M sucrose, 1% PEG, and 5% PEG. Middle row from left to right: additive as above but containing bacteriophage selective for *S. aureus* (SP). Bottom row from left to right: additive as above but containing bacteriophage selective for *P. aeruginosa* (PP).

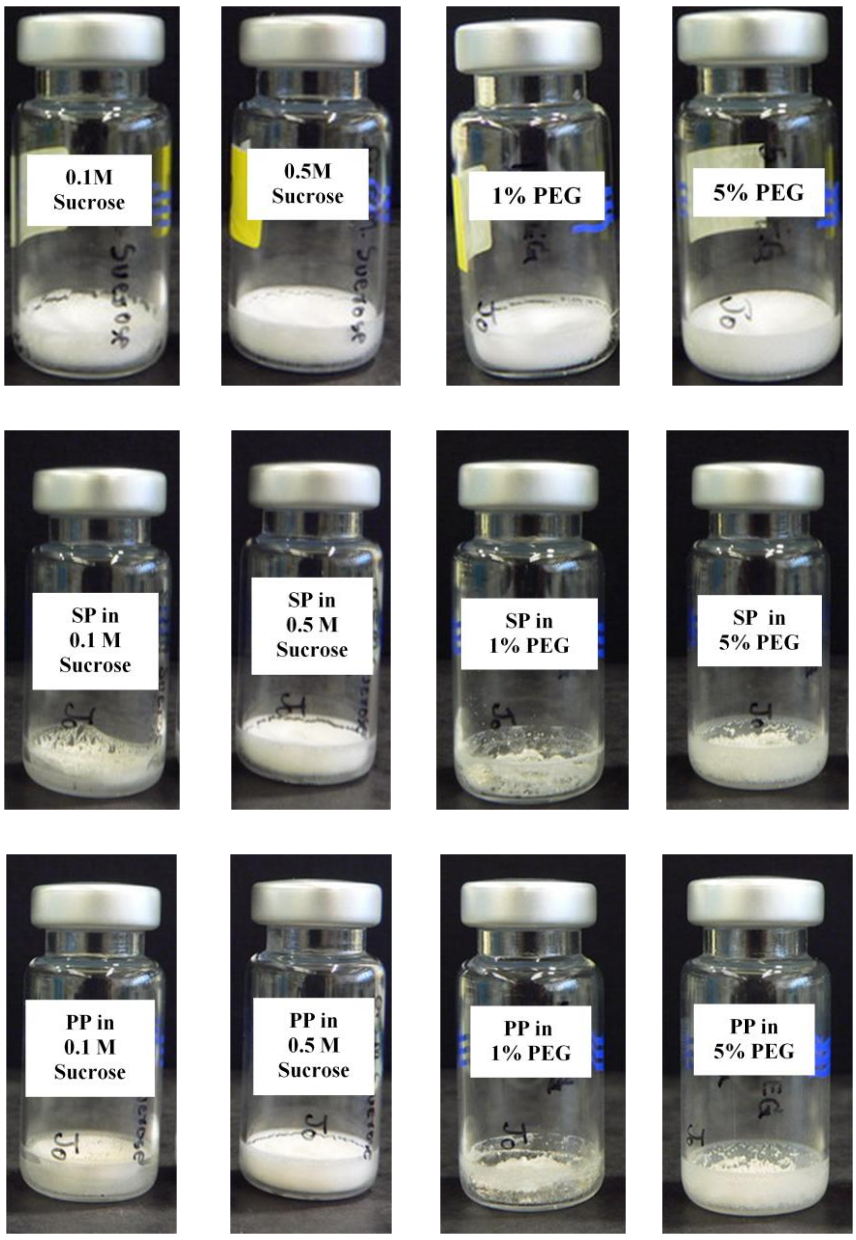

Figure 3.14. Images of the freeze-dried cakes following primary drying cycle. Top row from left to right: 0.1 M sucrose, 0.5 M sucrose, 1% PEG, and 5% PEG. Middle row from left to right: additive as above but containing bacteriophage selective for *S. aureus* (SP). Bottom row from left to right: additive as above but containing bacteriophage selective for *P. aeruginosa* (PP).

3.2.3.2. Glass transition

The collapse phenomenon is most accurately measured by the collapse temperature (Tc), using a microscope with a freeze-drying stage. In the absence of this specialized equipment, the glass transition temperature of the frozen solution (Tg') is determined (since Tc and Tg' are generally close to each other) (Fonseca, et al., 2004).

In this study, the stability of the final freeze-dried product was examined by determination of the residual water content and the glass transition temperature (Tg), in order to relate the two parameters. The Tg of representative sucrose samples from different formulations, determined by Temperature modulated DSC (TMDSC), were 47 and 51 °C for 0.1 and 0.5 M sucrose in SM, respectively (Figure 3.17). It is interesting that the DSC thermogram has shown the increasing of heat near the end of running time for bacteriophage formulations with sucrose (Figure 3.17). Therefore the duration of running system was increased in Figure 3.18. Unfortunately, the heat flow change did not clear with the freeze dried bacteriophage with the addition of 0.1 M sucrose while Figure 3.18 has revealed that the heat flow was changed between 72-80 °C for bacteriophage formulations for the addition of 0.5 M sucrose. With the no-pin hole of pan in the experiment the Tg of bacteriophage formulation was shown 72 ± 2°C whereas the pan with small pin hole will provide the Tg 80 and 75 °C for bacteriophage formulation selective for *S. aureus* and *P. aeruginosa*. This value is typical of previous data for similar sucrose samples acquired by DSC (Saleki-Gerhardt and Zografi, 1994). The Tg from the pans with no-pin hole provide a narrow range of value than a small pin hole because they also loss of heat transfer less than in the pans with small pin hole. Therefore, although the bacteriophage caused collapse of the lyophilised cake this was not through a plasticizing effect wherein the Tg of the sucrose sample was markedly lowered.

Figure 3.15 has shown that the melting point (mp) of bacteriophage formulations with the inclusion of 1% and 5% PEG 6000 did not alter from the blank of PEG 6000 (mp 61

± 1 °C). Similarly, the inclusion of bacteriophage did not alter the Tg of the samples containing PEG 6000, which remained at −25 ± 1 ◦C (Figure 3.16), close to that determined for lyophilised PEG 8000 (−16 °C) using DSC and thermally stimulated current spectrometry (Amin, et al., 2004). In these amorphous samples, residual water would in any case be expected to lower the Tg, consistent with previous work (Rouse, et al., 2007). Furthermore, the melting points of the bacteriophage including PEG 6000 were also found that they had apparently no differences for these formulations (61 ± 1 °C, Figure 3.15).

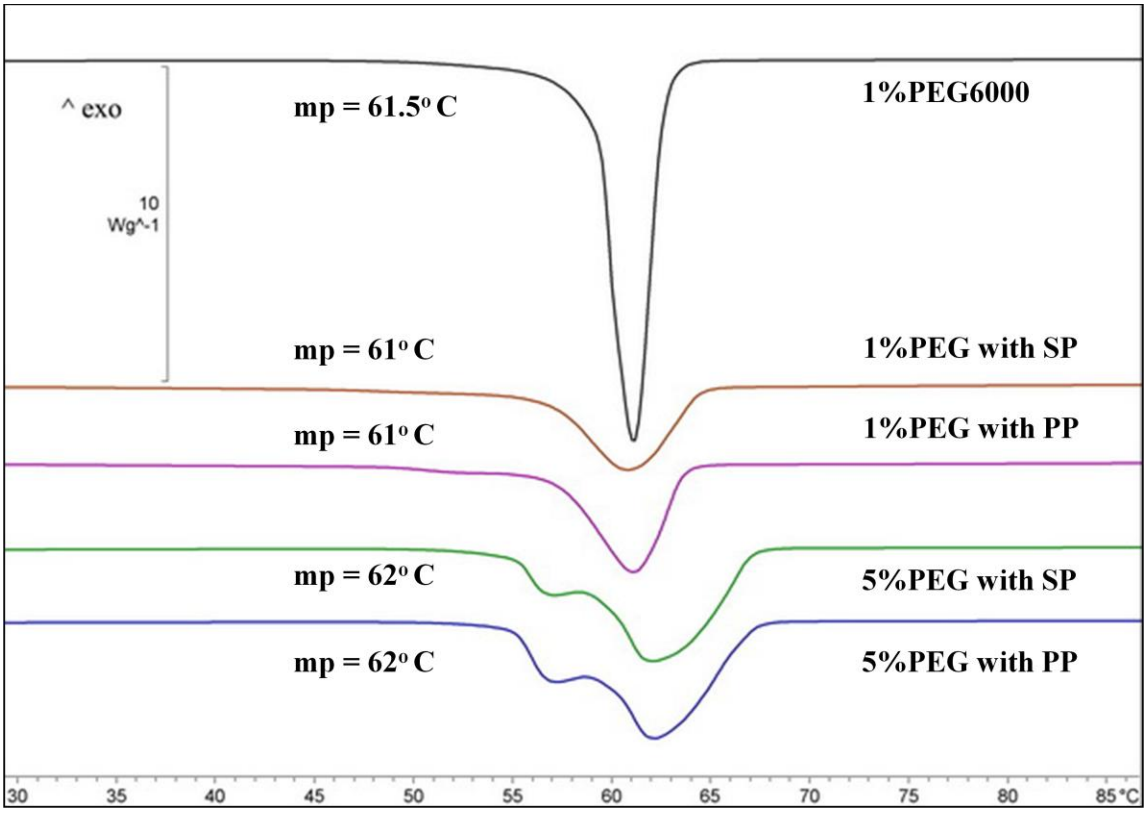

Figure 3.12. DSC thermograms of freeze-dried 1% PEG 6000 and bacteriophage selective for *S. aureus* (SP) or *P. aeruginosa* (PP). Bacteriophage formulations compose of 1% PEG 6000 (1% PEG) or 5% PEG 6000 (5% PEG) and SP or PP by volumetric ratio 3:7.

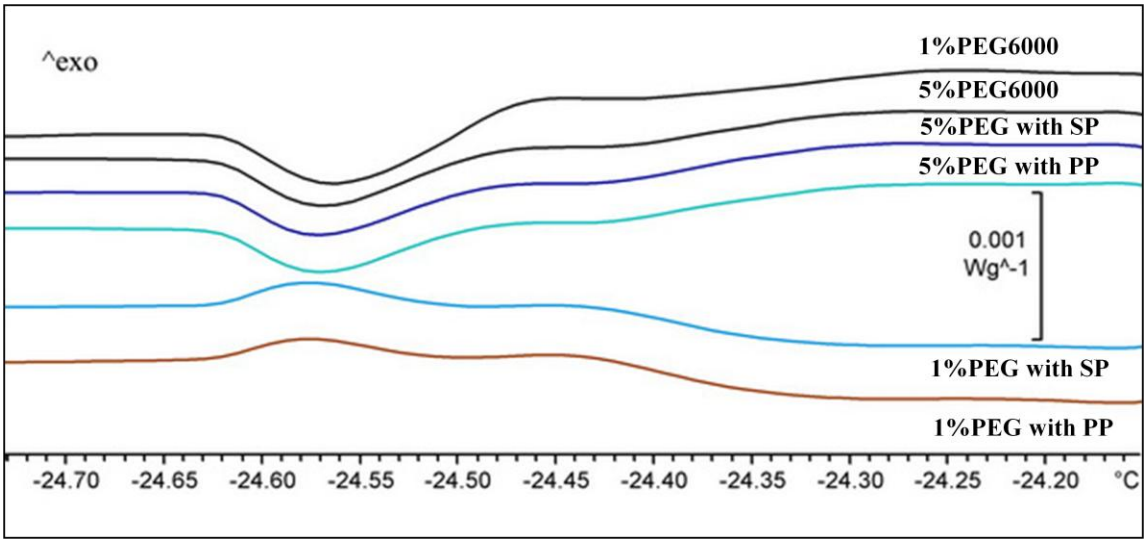

Figure 3.13. TMDSC thermograms of freeze-dried bacteriophage selective for *S. aureus* (SP) or *P. aeruginosa* (PP) with the addition of 1% and 5% PEG 6000, respectively.

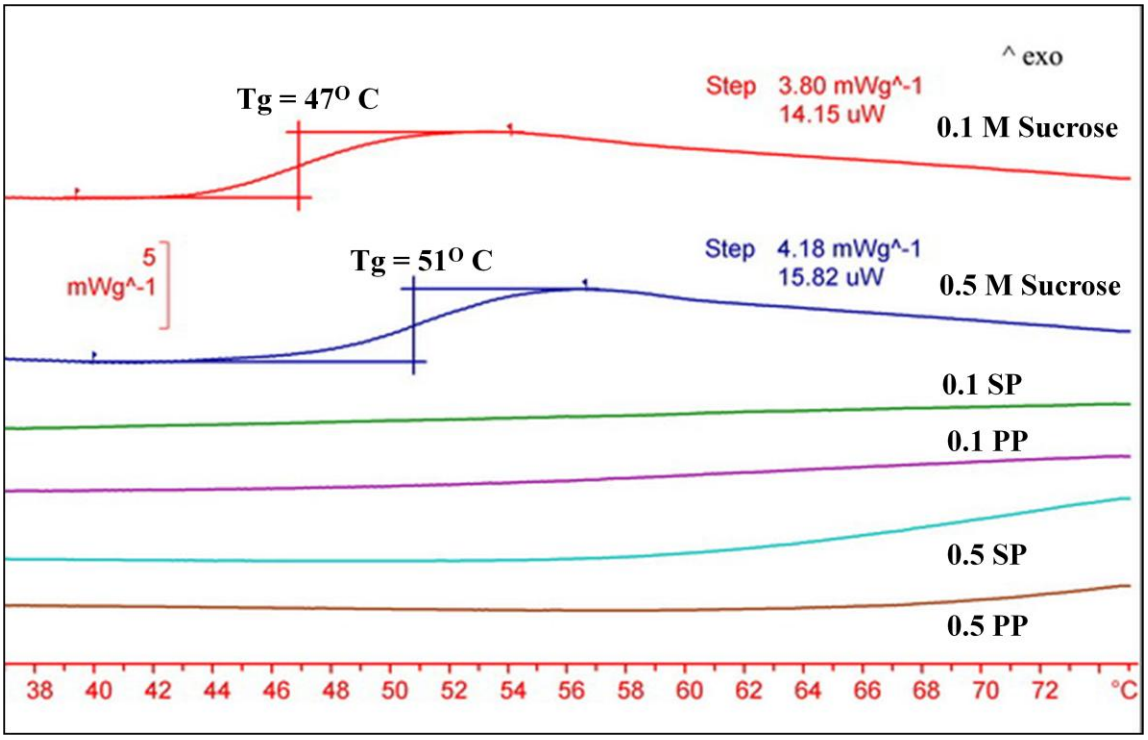

Figure 3.14. TMDSC thermograms of freeze-dried bacteriophage selective for *S. aureus* (SP) or *P. aeruginosa* (PP) with the addition of 0.1 and 0.5 M sucrose, respectively.

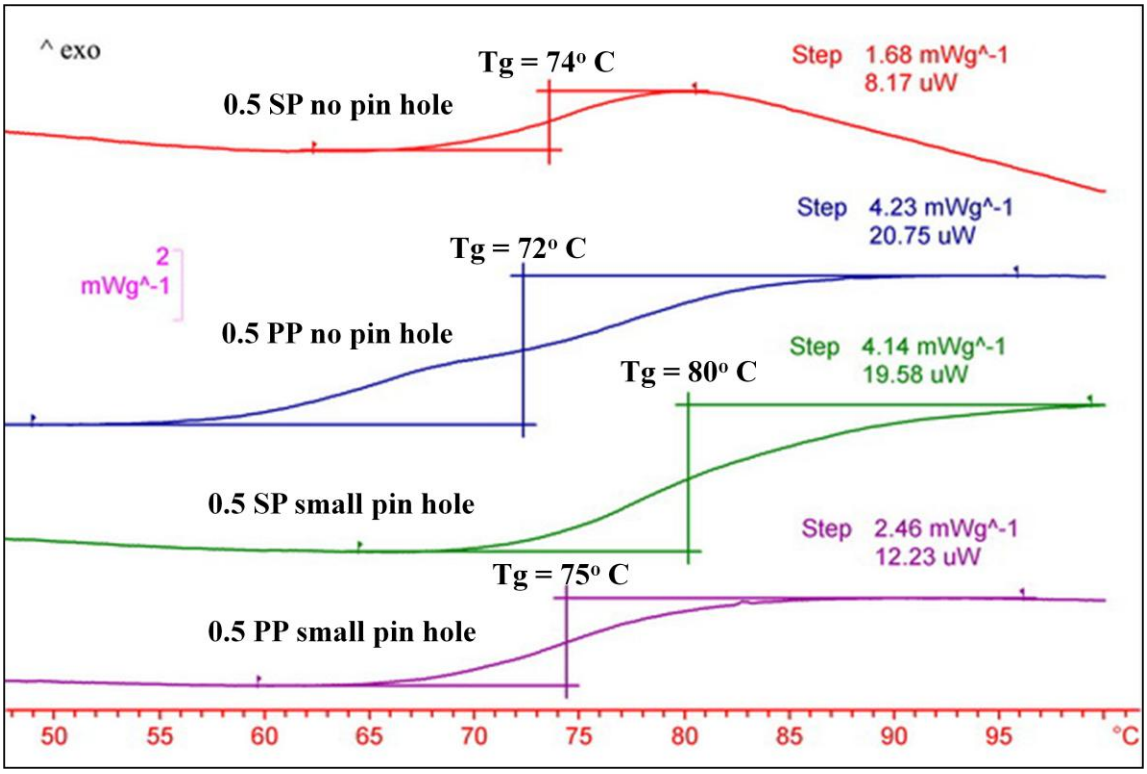

Figure 3.15. TMDSC thermograms of freeze-dried bacteriophage selective for *S. aureus* (SP) or *P. aeruginosa* (PP) with the addition of 0.5 M sucrose. Red and Blue lines demonstrate the thermograms with no-hole pin on the experiment. Green and purple lines illustrate the thermogrms with small-hole pin on the experiment.

3.2.3.3. Distribution of bacteriophage

To investigate the possibility that loss of lytic activity of the bacteriophage was caused through aggregation or phase separation during lyophilisation, we labelled the phage with fluorescein and imaged their distribution throughout freeze-dried thin films, for the same formulations. Thin films were required for imaging on the particular microscope stage used. Images are shown for labelled bacteriophage (selective for the *S. aureus* and *P. aeruginosa*) lyophilised from PEG 6000 and storage media with and without gelatin alone, clearly showing their amorphous and crystalline nature, respectively (Figure 3.19 and 3.20). The images from Figure 3.19 and 3.20 present the fluorescence apparently through the matrix of the crystalline structure either in the storage medium (Figure 3.19) or in the condition containing PEG 6000 (Figure 3.20). Images for freeze-dried sucrose containing labelled bacteriophages showed thin, homogenous films, unrepresentative of the porous nature of the corresponding cakes in Figure 3.11-3.14. Nevertheless, for all freeze-dried films, the bacteriophage was dispersed throughout the matrix suggesting that there was no phase separation or aggregation.

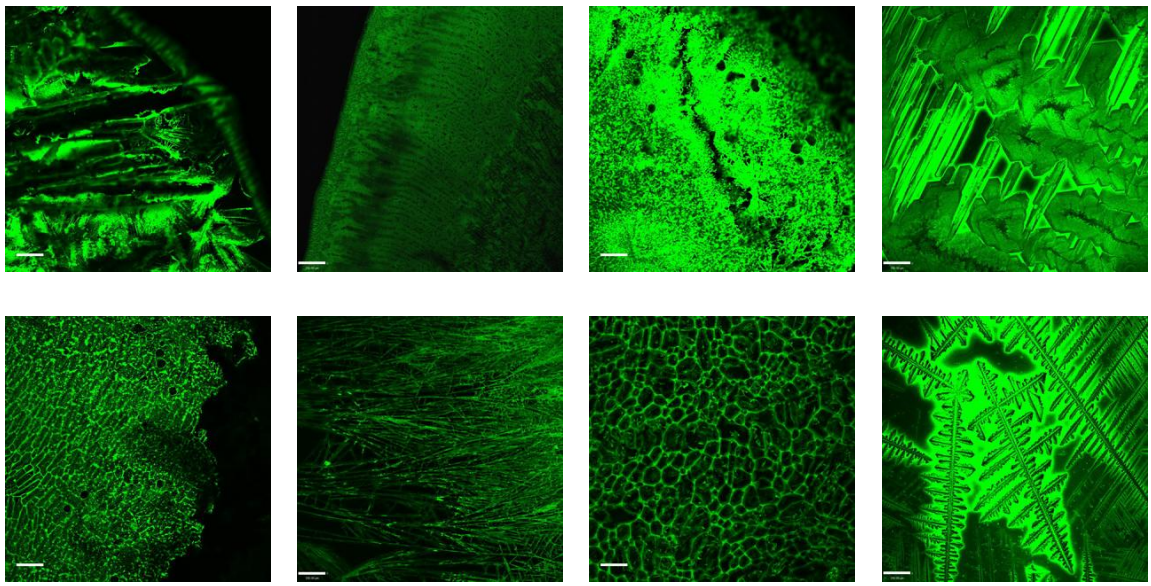

Figure 3.16. CLSM images of freeze-dried thin films of labelled bacteriophage in storage medium. Top row from left to right: bacteriophage selective for *S. aureus* with primary drying cycle, bacteriophage selective for *S. aureus* with primary and secondary drying cycles, bacteriophage selective for *P. aeruginosa* with primary drying cycle, bacteriophage selective for *P. aeruginosa* with primary and secondary drying cycles with storage medium containing gelatin. Bottom row from left to right: bacteriophage selective for *S. aureus* with primary drying cycle, bacteriophage selective for *S. aureus* with primary and secondary drying cycles, bacteriophage selective for *P. aeruginosa* with primary drying cycle, bacteriophage selective for *P. aeruginosa* with primary and secondary drying cycles with storage medium without gelatin. Bar = 150 µm.

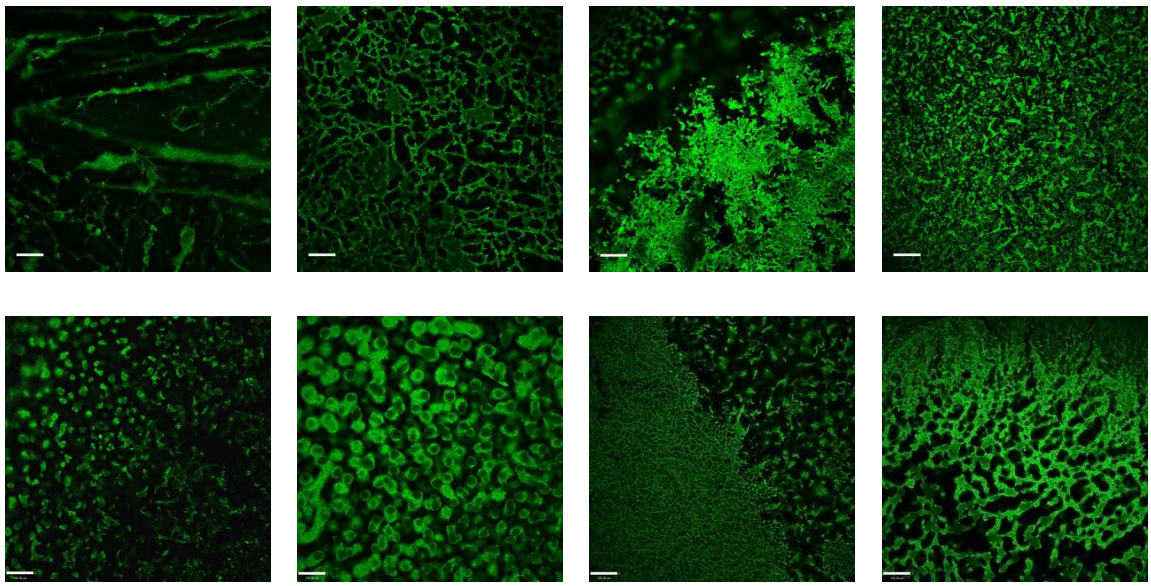

Figure 3.17. CLSM images of freeze-dried thin films of labelled bacteriophage in storage medium. Top row presents the primary drying cycle alone from left to right: bacteriophage selective for *S. aureus* containing 1% PEG, 5% PEG, bacteriophage selective for *P. aeruginosa* 1% PEG, and 5% PEG. Bottom row presents the primary and secondary drying cycle from left to right: bacteriophage selective for *S. aureus* containing 1% PEG, 5% PEG, bacteriophage selective for *P. aeruginosa* 1% PEG, and 5% PEG. Bar = 150 µm.

Evidence of aggregation was tested further by particle sizing of the reconstituted bacteriophage using DLS. Although data quality was poor for samples containing PEG 6000 or sucrose (null data not shown), reliable data could be acquired for samples lyophilised from storage medium, with or without gelatin. In these cases, no evidence of aggregation of the bacteriophage could be found (Table 3.13), since the mean particle diameter measured corresponded to the approximate sizes of the bacteriophages seen by TEM (note that DLS assumes a sphere during data interpretation). No particle sizing data could be acquired for the blank solutions of storage media, suggesting that the presence of low concentrations of gelatin did not interfere with particle sizing of the bacteriophage.

Table 3.13. Particle sizing data for bacteriophage following reconstitution of the freeze-dried cake.

Before lyophilisation	Phage selective for:	[a]mean diameter (nm)	[b]peak width (nm)
SM without gelatin	*S. aureus*	134	48
SM without gelatin	*P. aeruginosa*	140	78
SM with gelatin	*S. aureus*	133	45
SM with gelatin	*P. aeruginosa*	131	62
After lyophilisation			
SM without gelatin	*S. aureus*	202	149
SM without gelatin	*P. aeruginosa*	124	54
SM with gelatin	*S. aureus*	148	72
SM with gelatin	*P. aeruginosa*	126	38

[a], measured using the intensity distribution plot, the % intensity for each peak was ≥ 96%; [b], equivalent to the standard deviation of the peak

3.2.4. Residual moisture content of the freeze-dried formulations

An important parameter for lyophilised product development is the residual moisture content in the final product. There is no single, optimal residual moisture content for all biomolecules: some proteins show increased chemical stability as moisture content decreases with little change in physical stability (Breen, et al., 2001). In contrast, for other proteins, lyophilisation resulting in a moisture content of the cake which is below 10% results in protein denaturation and loss of activity (Jiang and Nail, 1998).

Clearly, when studying lyophilised biomolecules, including bacteriophage, a case by case assessment is required which aims to balance chemical stability (e.g. amino acid isomerisation) with physical stability (e.g. unfolding). We attempted to control the final moisture content of the cake by simply extending the primary drying cycle, during which bulk water sublimes, with a prolonged secondary drying cycle performed at elevated temperatures to remove unfrozen water adsorbed to the product surface (Pikal, et al., 1990). Given that the lytic activity for bacteriophage lyophilised from storage media only appeared to be dependent on the lyophilisation protocol (Table 3.10), we investigated the residual moisture content of the corresponding freeze-dried cakes. In the case of bacteriophage lyophilised in the presence of PEG or sucrose, only the moisture content of the cake following primary and secondary drying was measured, since lytic activity was more dependent on the additive than the lyophilisation cycle (Tables 3.12 and 3.13).

In figure 3.21 it can be seen that a secondary drying cycle consistently decreased the moisture content of the cake produced from storage media from approximately 7-9% to 5-6%. A clear correlation between moisture content and lytic activity can therefore be drawn. Thus, keeping the residual moisture to a level $\leq$ 6% may represent a good starting point for formulation of freeze-dried bacteriophage, since other formulation variables such as particle aggregation and T_g show no clear correlation with lytic activity. The usefulness of moisture content as an indicator of stability of freeze-dried bacteriophage is also supported when comparing formulations containing sucrose or PEG (Figure 3.22).

Here however, we see that the very low moisture contents (approximately 2-3%) of the cakes containing high additive concentrations (5% PEG 600 and 0.5 M sucrose) correlate with the lower lytic activities of the reconstituted bacteriophages (Tables 3.11 and 3.12). Therefore, reducing the moisture content below 4% is detrimental to bacteriophage stability, most likely due to the removal of nonfrozen water adsorbed to the bacteriophage tail/head. Consistent with this argument, is that the moisture content

of bacteriophage lyophilised from 1% PEG and 0.1 M sucrose was approximately 4-6% and correlated with the higher lytic activities observed for each additive.

As shown in Figure 3.23, a lower moisture content of the cake followed lyophilisation from higher concentrations of PEG. Both bacteriophages and drying cycles yielded lower moisture content from 5% PEG (approximately 1-2%), compared to the moisture content with 1% PEG (approximately 2-6%).

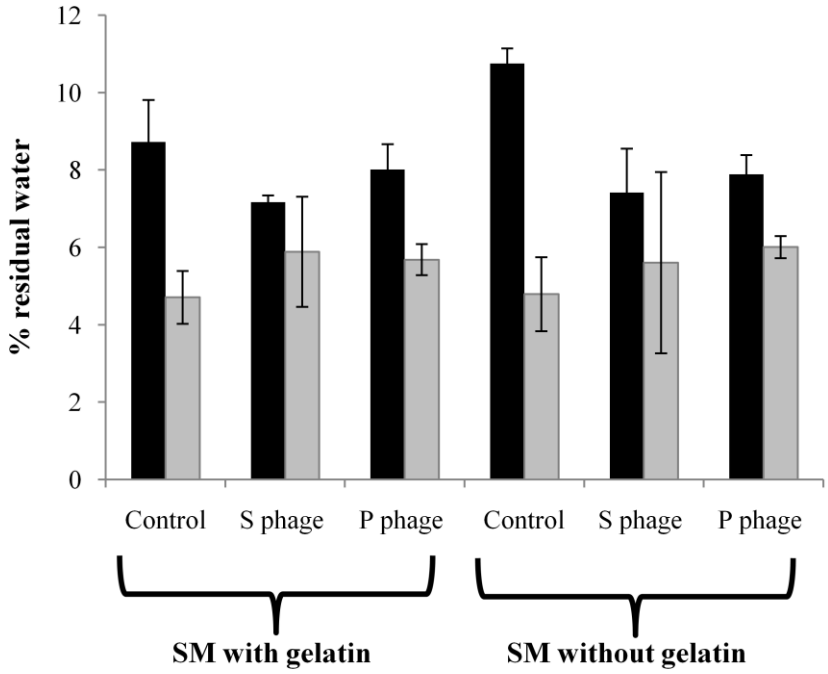

Figure 3.18. The moisture content of lyophilised cake from storage media following only a primary drying (black bars) or following primary and secondary drying (grey bars) with and without gelatin and containing bacteriophage selective for *S. aureus* (S phage), or *P. aeruginosa* (P phage), or control.

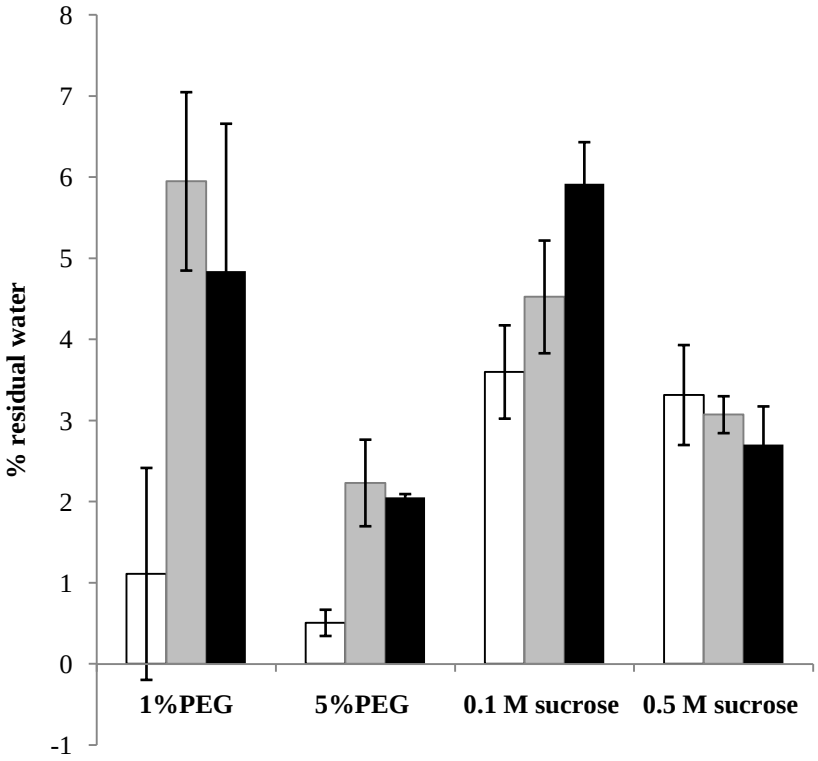

Figure 3.19. The moisture content of lyophilised cake from high and low PEG 6000 or sucrose concentrations, following primary and secondary drying cycles, and containing bacteriophage selective for *P. aeruginos*a (black bars), or *S. aureus* (grey bars), or neither (control, white bars).

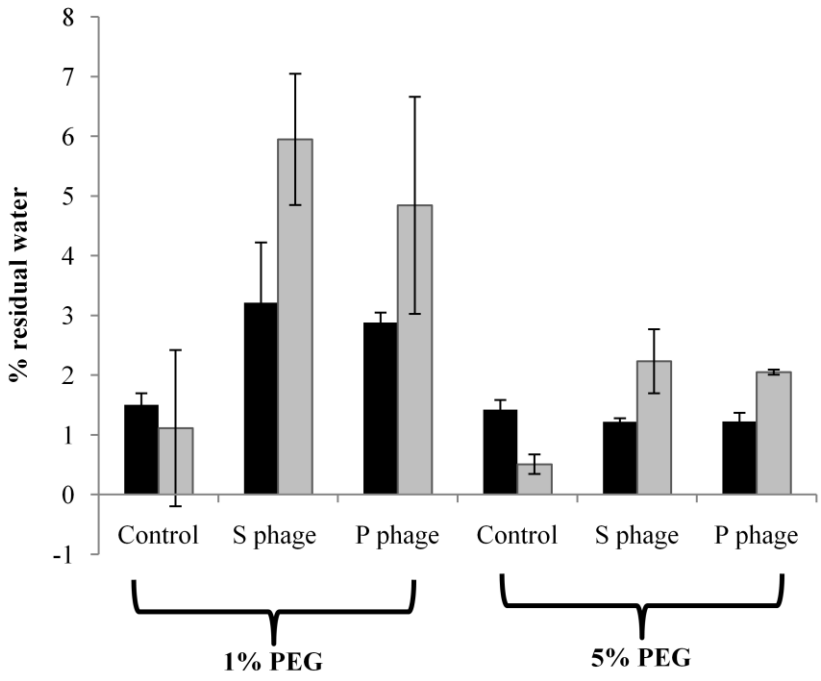

Figure 3.20. The moisture content of lyophilised cake from storage media following only a primary drying (black bars) or following primary and secondary drying (grey bars) with and 1% PEG 6000 and 5% PEG 6000 containing bacteriophage selective for *S. aureus* (S phage), or *P. aeruginosa* (P phage), or control.

3.3 In vivo studies

3.3.1 Rat model

3.3.1.1 Agarose bead preparation

P. aeruginosa-laden agarose beads were prepared by emulsification in mineral oil (see Methods) the day before inoculation and kept overnight at 4 °C. The morphology of the *P. aeruginosa*-laden beads was investigated with an inverted light microscope. Observation of many areas on sample slide showed that the agarose beads were reasonably uniform in size and shape (Figure 3.24). A monomodal size distribution was comfirmed by light scattering (Figure 3.25): the *P. aeruginosa*-laden beads having a median diameter of 37.65 μm with small size distribution (span value 1.274), with equivalent value of 39.58 μm and span value 1.165 for blank agarose gel beads.

The viability and sterility of the *P. aeruginosa*-laden and blank agarose beads, respectively, was assessed by bacterial culture on a King's A agar plate. Significant differences were observed between culture of empty and *P. aeruginosa*-laden agarose beads. The *P. aeruginosa*-laden agarose beads cultured at 37 °C for 18 hours showed the typical mucoid-green colonies of *P. aeruginosa* (Figure 3.26), whereas the blank agarose beads did not result in any visible colonies. This demonstrated that the agarose beads could be produced and stored at 4°C the day before use *in vivo*.

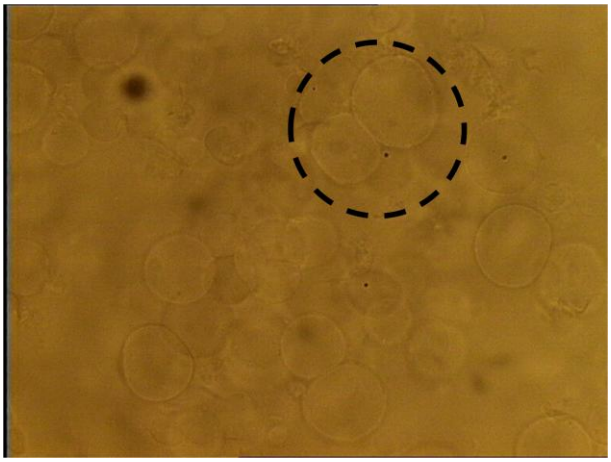

Figure 3.21. Inverted light microscopy image of the blank agarose beads. The dashed-line circle encompasses a pair of spherical beads (magnification ×25).

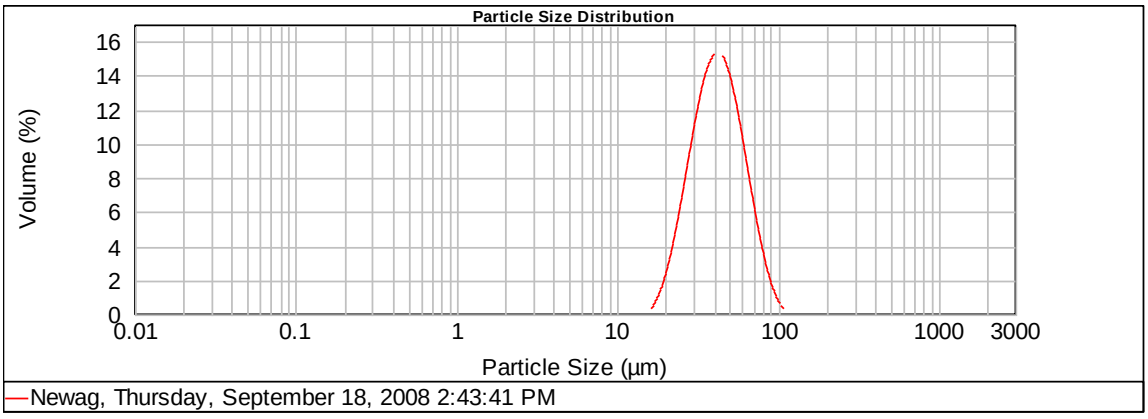

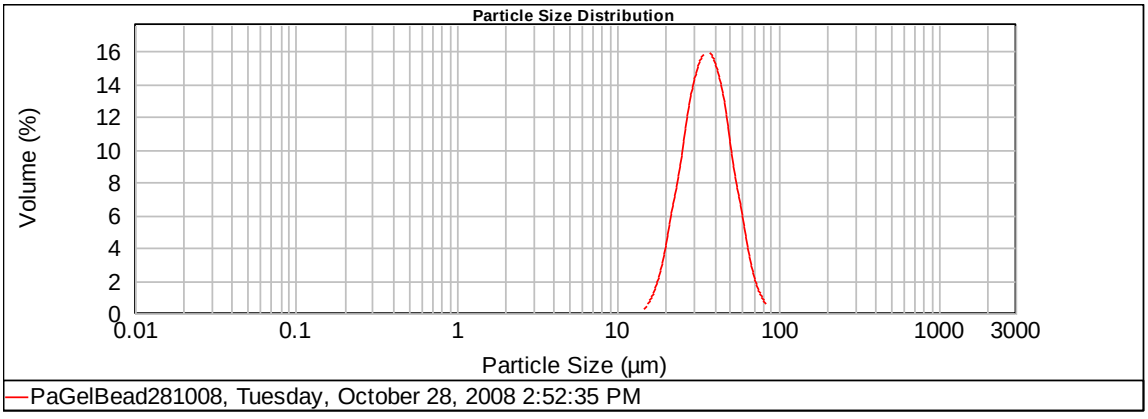

Figure 3.22. Size distribution profiles of blank (top) and *P. aeruginosa*-laden (bottom) agarose beads.

Figure 3.23. Colonies of *P. aeruginosa* cultured from overnight incubation of the *P. aeruginosa*-laden agarose beads on King's A agar at 37 °C.

3.3.1.2. Results of treatment

Initial experiments were conducted on only individual rats (2 test and 1 control), since the experimental technique had to be developed and the outcomes were uncertain. Sprague Dawley (SD) male rats were inoculated with *P. aeruginosa*-laden agarose beads by intra-tracheal instillation using the insufflator device; blank beads were used as the control. The rats were observed daily for 2 weeks after inoculation and then sacrificed. No difference either in physical visualization (e.g. eye colour, pilo-erection) or behaviour was observed between the treated and control rat. Because of this, it was decided that it would be not possible to continue study of lung infection in SD rats (see discussion). In this study, body weight loss was also measured and did not show significantly difference before and after treatment. However, the gross lung pathology of the rats having received *P. aeruginosa*-laden agarose beads showed enlargement of the lung, which was relatively pale with some localised white regions (Figure 3.27): this was

not observed in the control rat. A detailed histological examination using hematoxylin and eosin (H&E) staining was therefore undertaken in order to more fully understand the underlying processes and tissue changes that may be involved in progression of infection.

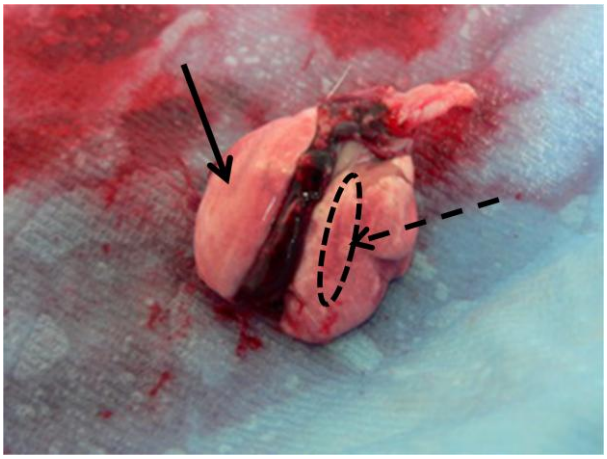

Figure 3.24. Representative of gross lung pathology in SD male mice inoculated with mucoid *P. aeruginosa*-laden agarose beads after 14 days. Arrow indicates the enlargement and the colour distinction of lung sample.

3.3.1.2.1. Histology of the control tissue

The histology of the lung tissue of the untreated rat showed a normal structure upon H&E staining, as depicted in Figures 3.28 and 3.29. The fine 'lace' structure of the lung sections is typically seen, because most of the lung is composed of thin-walled alveoli. The septum of the alveoli also shows the single layer of squamous epithelium. Many bronchioles were seen in this section, with various sizes. As shown in Figure 3.29, the large bronchiole was commonly lined with a ciliated columnar epithelium. With these sections, the internal cavities of the bronchioles or alveoli are clearly seen. No evidence of inflammation was observed for the lungs of the rat having only received blank agarose beads.

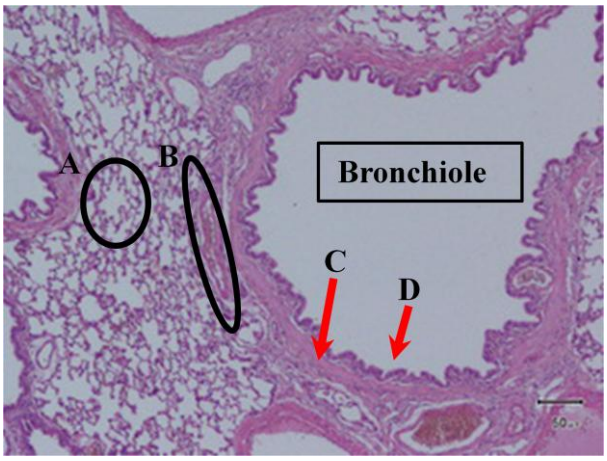

Figure 3.25. Representative section of non-infected rat lung section with H&E stain. Black circle A shows a single alveolus, with a typical thin epithelial lining. Black oval B represents the blood vessel which lines the connective tissue (C). Red arrow D points to the columnar epithelium lining the bronchiole. Scale bar = 50 µm

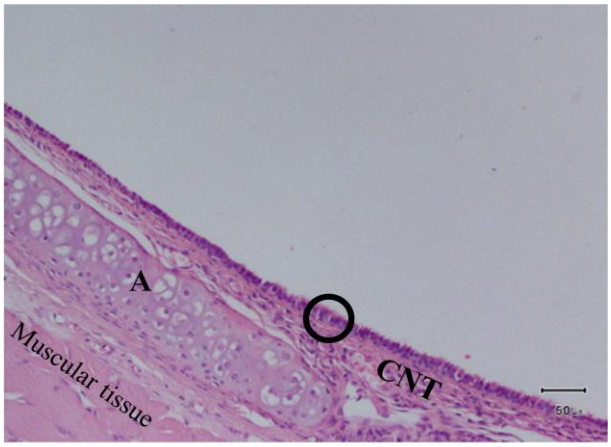

Figure 3.26. Representative section of non-infected bronchiole (H&E stained). The black circle illustrates the ciliated columnar epithelium lining the bronchiole, with the basement connective tissue (CNT) and cartilage (A) layers. Muscular tissue can be seen. Scale bar = 50 µm

3.3.1.2.2. Histology of the infected tissue

In contrast to the control, inoculation of *P. aeruginosa*-laden agarose beads resulted in coalescing large alveoli (bullae) within the parenchyma, which were observed for most of the lung lobe. Also, the multifocal area of eosinophilic material in the alveoli (oedema) was found around the bronchioles containing the emboli of bacteria (Figure 3.30 and 3.31). Larger bronchi had degenerating mucosal linings and contained plugs of mucus, cell debris and bacteria. There were surrounded by collections of inflammatory cells and eosinophilic materials (Figure 3.32).

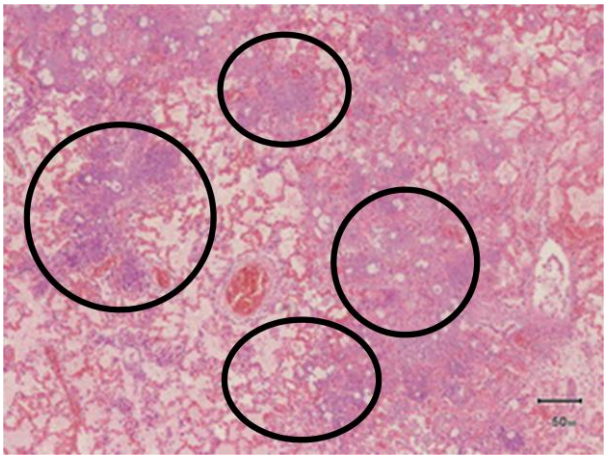

Figure 3.27. H&E staining of a section of lung of a SD rat following infection with *P. aeruginosa*-laden agarose beads. Black-ovals present the multifocal coalescing eosinophilic material (oedema) including inflammatory cells. Scale bar = 50 μm

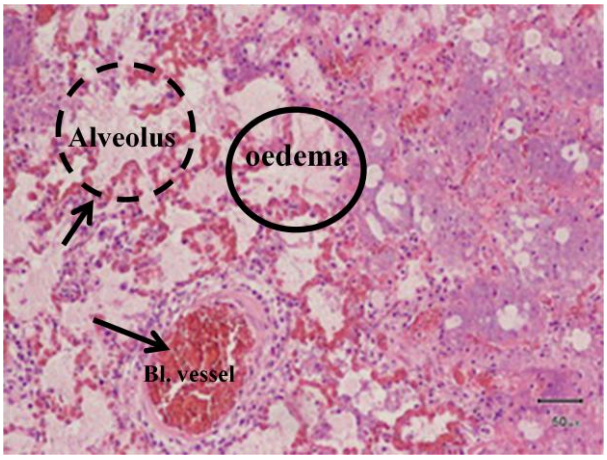

Figure 3.28. Representative oedema showing the mixture of debris and mucus produced from the lung tissue and bacteria (H&E stain, scale bar = 50 μm).

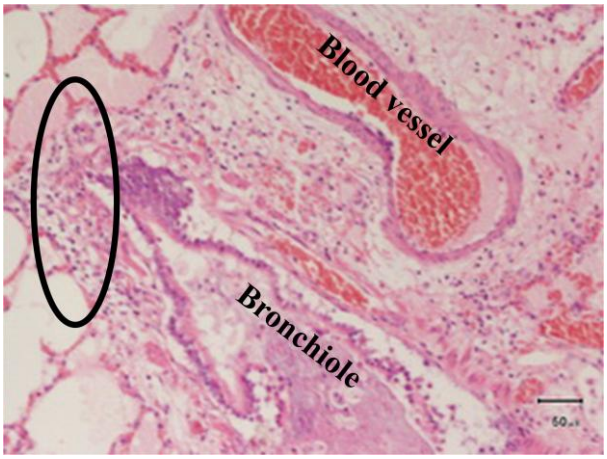

Figure 3.29. H&E stain of inflammatory cells and bacteria surrounding a bronchiole (scale bar = 50 μm).

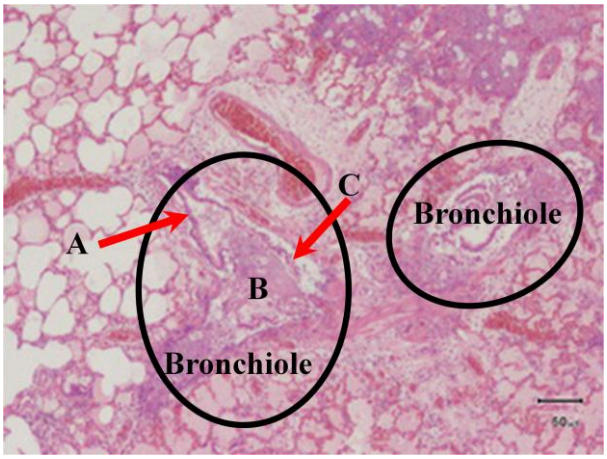

Figure 3.30. H&E staining of inflammed bronchiole (A) which appeared larger compared to the control section, and contained cell debris, mucus and bacteria (B), with a local loss of the mucosa (C). Scale bar = 50 μm

In all the infected rats, numerous sections of lung were examined and it was found that consolidation of the tissue around the bronchi and bronchioles was common. In addition, the coalescence of some alveoli was seen to form the larger bullae along with a minor thickening of the walls of alveoli, though no measurements were made from the stained images (Figure 3.34). A few macrophages were observed within the alveolar wall (Figure 3.35). In the consolidated areas, dense sheets of mostly lymphocytes and histocytes were seen, the latter containing multiple foci of large lymphocytes (neutrophils were seen rarely). These sheets mostly surrounded those airways with a prominent mucosal lining (hyperplasia) (Figure 3.36).

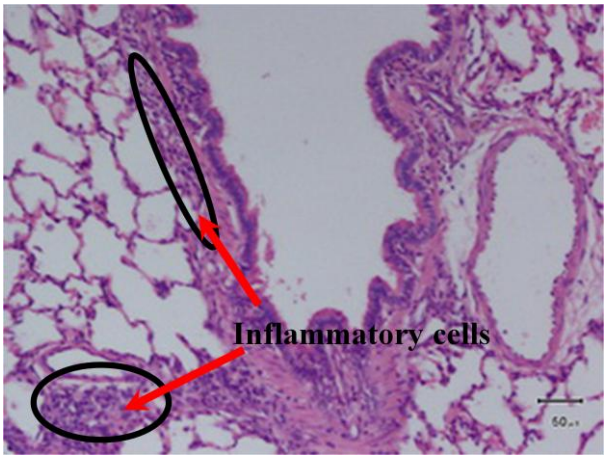

Figure 3.31. Inflammatory cells and the thickened epithelial in the infected rat lung (H&E stain, scale bar = 50 μm).

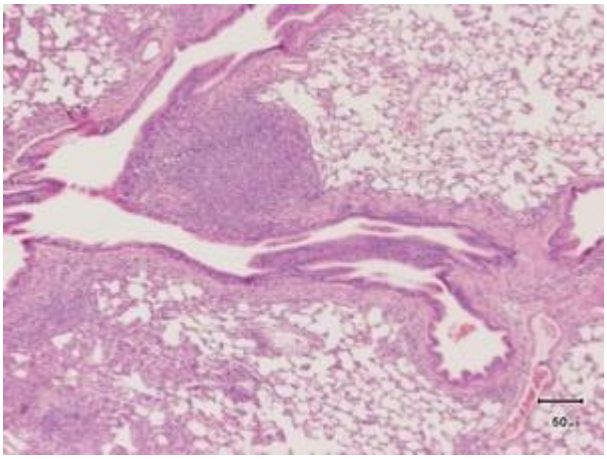

Figure 3.32. Areas circled show multifocal consolidation of the rat lung (H&E stain, scale bar = 50 μm).

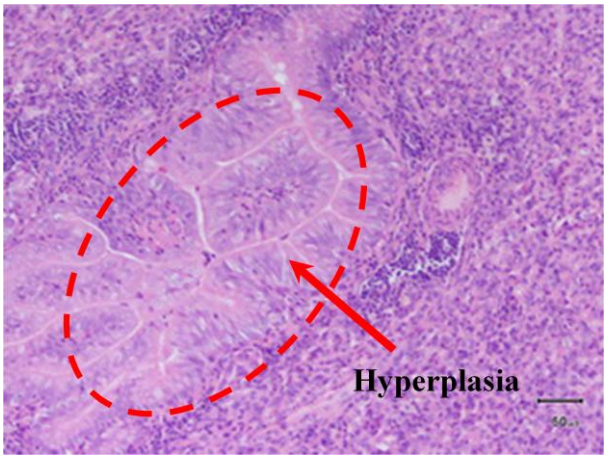

Figure 3.33. Area circled shows hyperplasia of the rat lung (H&E stain, scale bar = 50 μm).

3.3.2. Mouse model of lung infection

3.3.2.1. The bacteria infection with intra-nasal technique and the required amount of bacteria for infection

The mouse model was investigated since the SD rats did not (visibly) succumb to infection, at least using the method of infection used here. We examine by the clinical sign and symptom from the animal such as the hunched back of animal would be seen due to the destruction of lung structure or the breath pattern might show the obstruction of the airway or the temperature whichis the indicator for inflammation or infection or the behaviors of animal would indicate the abnormal condition physiopathology in the animal comparing with control animal. It was thought that mice would more readily and consistently succumb to infection and therefore present a more useful model for examination of phage therapy. Male Balb/C mice were used to investigate lung infection and histology after administration of *P. aeruginosa* and bacteriophage formulations by intra-nasal or nebulisation techniques. A control group involved mice treated with PBS (see Methods).

3.3.2.1.1. Histology of the control lung

As for the rat lung, a fine lace appearance was observed by H&E staining for the mice, which showed the thin-walled alveoli (Figure 3.37). The alveoli were composed of a single layer of squamous epithelium, lined with many capillaries. Figure 3.37 also shows the many bronchioles of various sizes: the larger bronchioles having a columnar epithelium whereas the smaller bronchioles have a cuboidal epithelium. The lumens of the alveoli or bronchioles are clear and free of oedema and cell infiltration.

3.3.2.1.2. Bacterial dosing of animals and histopathology

In accordance with the ethical guidelines agree for the project, careful monitoring of the mice was required to ensure that suffering (during infection) was kept to a minimum; i.e. scoring against clinical signs to a specified end-point, at which the mice were sacrificed. The criteria used to define the response to infection are described in section 2.2.5.2.3. It was decided to infect the mice with increasing numbers (CFU) of bacteria, and assess their subsequent responses. Similarly, bacteriophage-only dosing was assessed in order to monitor the animal responses to the phage alone. The highest dose of bacteria, 1.41×10^9 CFU/mouse, was administered intra-nasally after anesthetization by isofluorane inhalation. Within 12 h, the body weight fell by more than 10% and a low body temperature was recorded; the mice had to be sacrificed within 18 hours after infection. Examination of lung tissue showed multifocal coalescing eosinophilic-rich tissue - inflammatory cells were also clearly observed in the bronchioles (Figure 3.38 A/B). A thickening of the epithelium of the bronchioles was observed and the blood vessels were seen to be infiltrated with inflammatory cells and cell debris (Figure 3.38 C). Neutrophils were also found inside the lumen of alveoli (Figure 3.38 E/F). When compared to the control, these slides together indicate an acute phase of inflammation, as a result of bacterial infection.

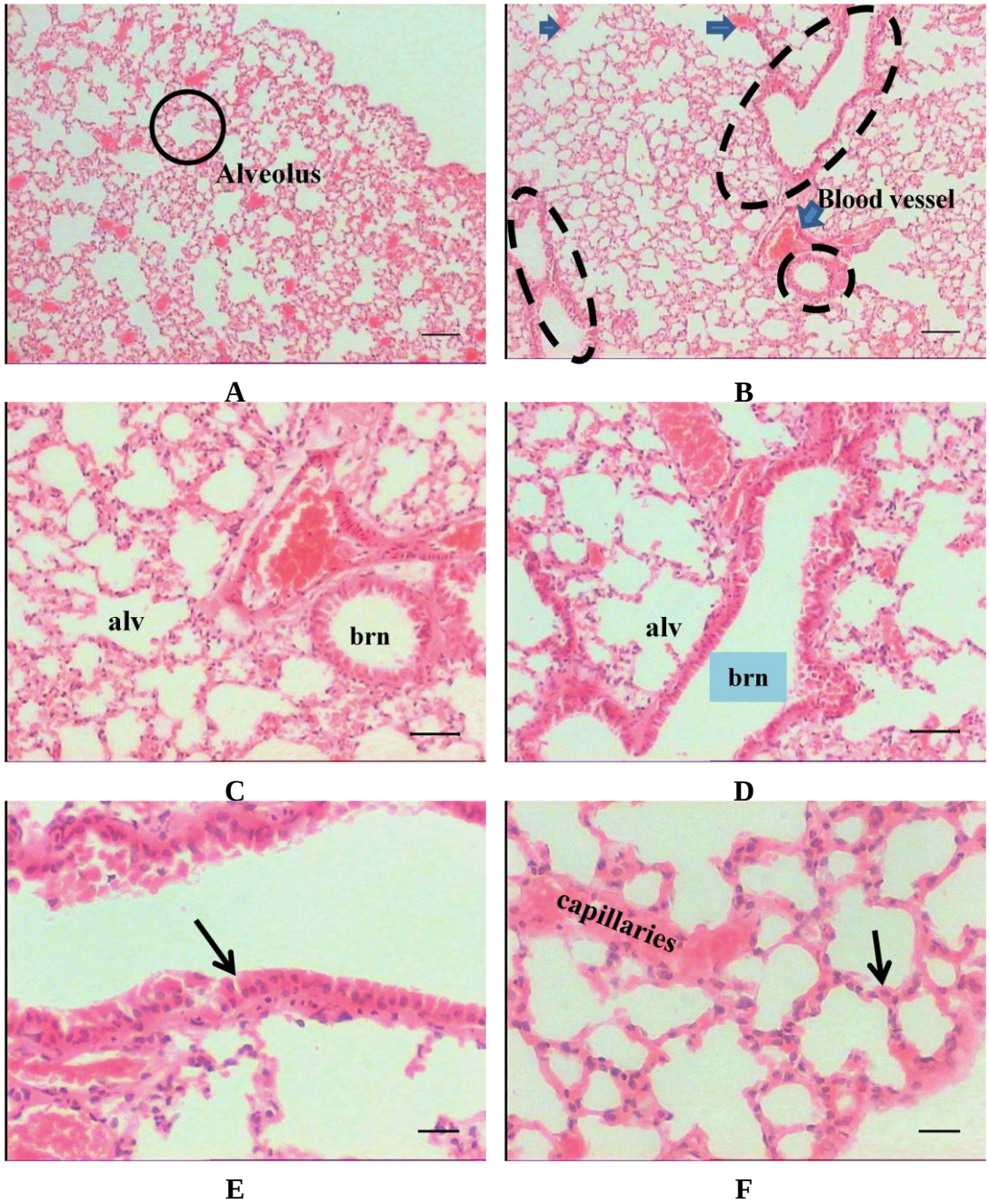

Figure 3.34. Representative lung histology by H&E stain for control mice; A) normal alveoli, circle depicts one alveolus; B) areas circled demonstrate the many sizes of bronchioles, the blue arrows illustrate the capillaries and blood vessel; C and D) lumens of the alveoli (alv) and bronchiole (brn); E) columnar epithelium of a bronchiole; F) single squamuos epithelium of the alveolar septum and capillaries between the walls. Scale bars for A/B, C/D, and D/F are 10, 5, and 2 µm, respectively.

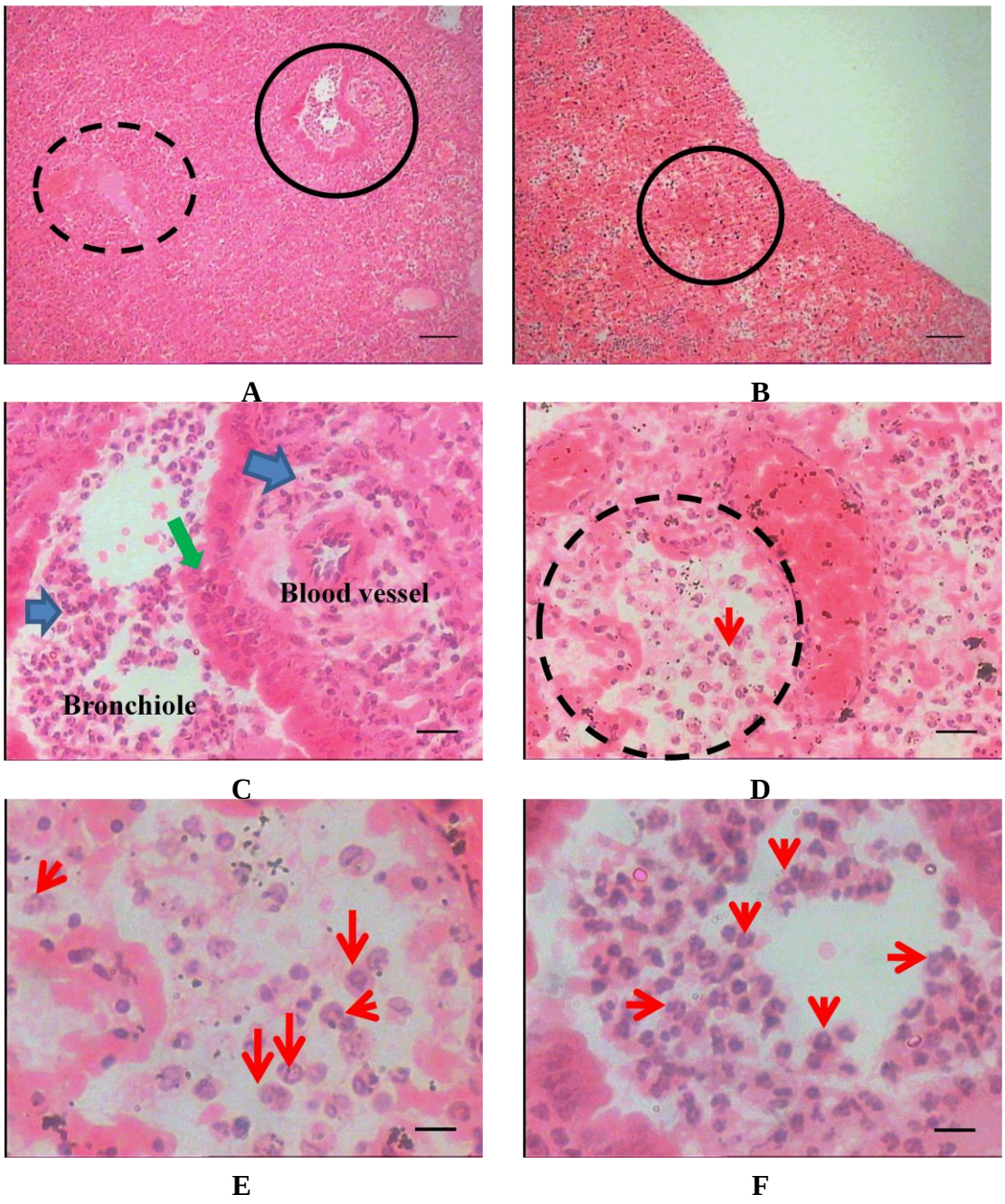

Figure 3.35. Lung histopathology of mice inoculated with a high dose of *P. aeruginosa*. A; the dashed-line oval shows multifocal coalescing eosinophilic material (oedema) with surrounding inflammatory cells. The solid-line circle shows inflammatory cells within a bronchiole. B; the circle shows oedema with cell debris and alveolar coalescence. C; The red, blue and green arrows show a thickened bronchiolar epithelium, inflammatory cell

infiltration within a blood vessel, and cell migration into a bronchiolar lumen, respectively. D and E; arrows show neutrophils within the alveoli lumen (circled in D) F; arrows show the inflammatory cells within a bronchiole. Scale bars for A/B, C/D and E/F are 10, 2, and 1 µm, respectively.

Given that the mice succumbed very quickly to infection with a dose of 1.41×10^9 CFU/mouse, a ten-fold reduction in the dose was made in order to define the clinical response to a weaker bacterial challenge. By observation, the mice recovered within 24 h post-inoculation and were completely recovered at day 4 of the experiment. Following the completion of experiment (i.e. sacrifice at day 7), the histopathology of the lungs was assessed. Thickened bronchiolar walls were observed but not oedema, infiltration of inflammatory cells or cell debris (Figure 3.39). Furthermore, the structure of alveolar network was 'normal' – similar to the control group. Together, these slides reflected the mild clinical signs and rapid recovery, demonstrating that this low dose could not be usefully employed.

On the basis of the clinical response and histology, it was considered that the bacterial doses of 1.41×10^8 and 1.41×10^9 CFU/mouse represented low and high doses. We therefore sought an intermediate dose of 5.7×10^8 CFU/mouse, to challenge the mice for infection before treatment with bacteriophage. Mice challenged with this intermediate dose of *P. aeruginosa* (followed by PBS instillation 24 and 48 h post infection – sham treatment) lost < 10% weight within 18 h, accompanied by mild clinical symptoms of infection such as body temperature (not less than 34 ^{o}C indicating the critical body temperature), breath pattern correlated with the hunched back pattern and the behaviours. After 3 days, the mice recovered the weight lost and improved with regards to clinical symptoms of infection. The mice were sacrificed at day 4 of the study, following their apparent recovery, and the right and left lobes of the lung separated for different purposes. The left lobe of the lung was sectioned (5 µm thickness) for

histopathology: as previously observed, multifocal coalescing eosinophilic material (oedema) was present and the fine lace structure had disappeared (Figure 3.40 A). Bronchioles had a thickened epithelium and were commonly associated with inflammatory cells inside the lumens (Figure 3.40). Neutrophils were observed around the blood vessels and had migrated through to the alveolar lumen; the alveolar epithelium was also infiltrated with inflammatory cells and macrophages (Figure 3.40).

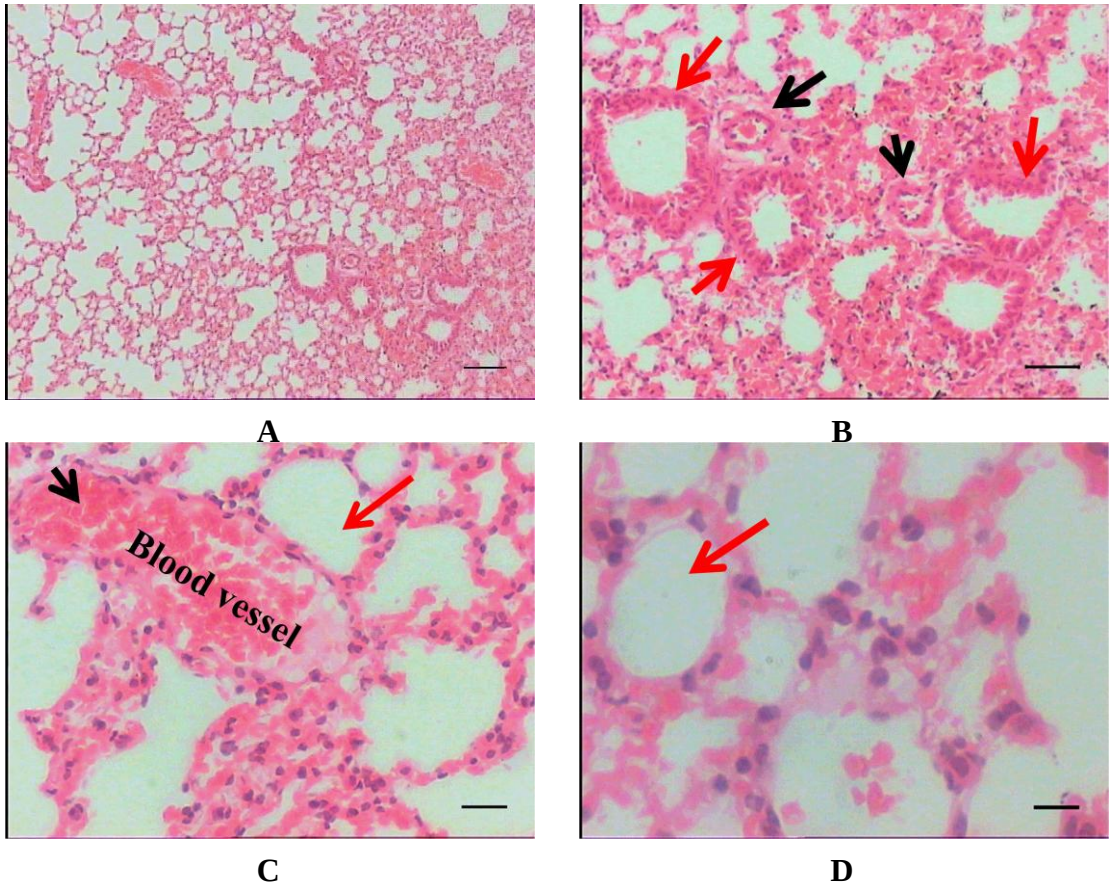

Figure 3.36. Lung histopathology of mice inoculated with low dose of *P. aeruginosa*. A; alveolar network without the presence of inflammatory cells/oedema phenomena. B; red arrow shows the thickened bronchiolar epithelia and black arrows the enlarged blood vessel; C-D; arrow show clear alveolar lumen and blood vessel. Scale bars for A, B, C and D are 10, 5, 2 and 1 µm, respectively.

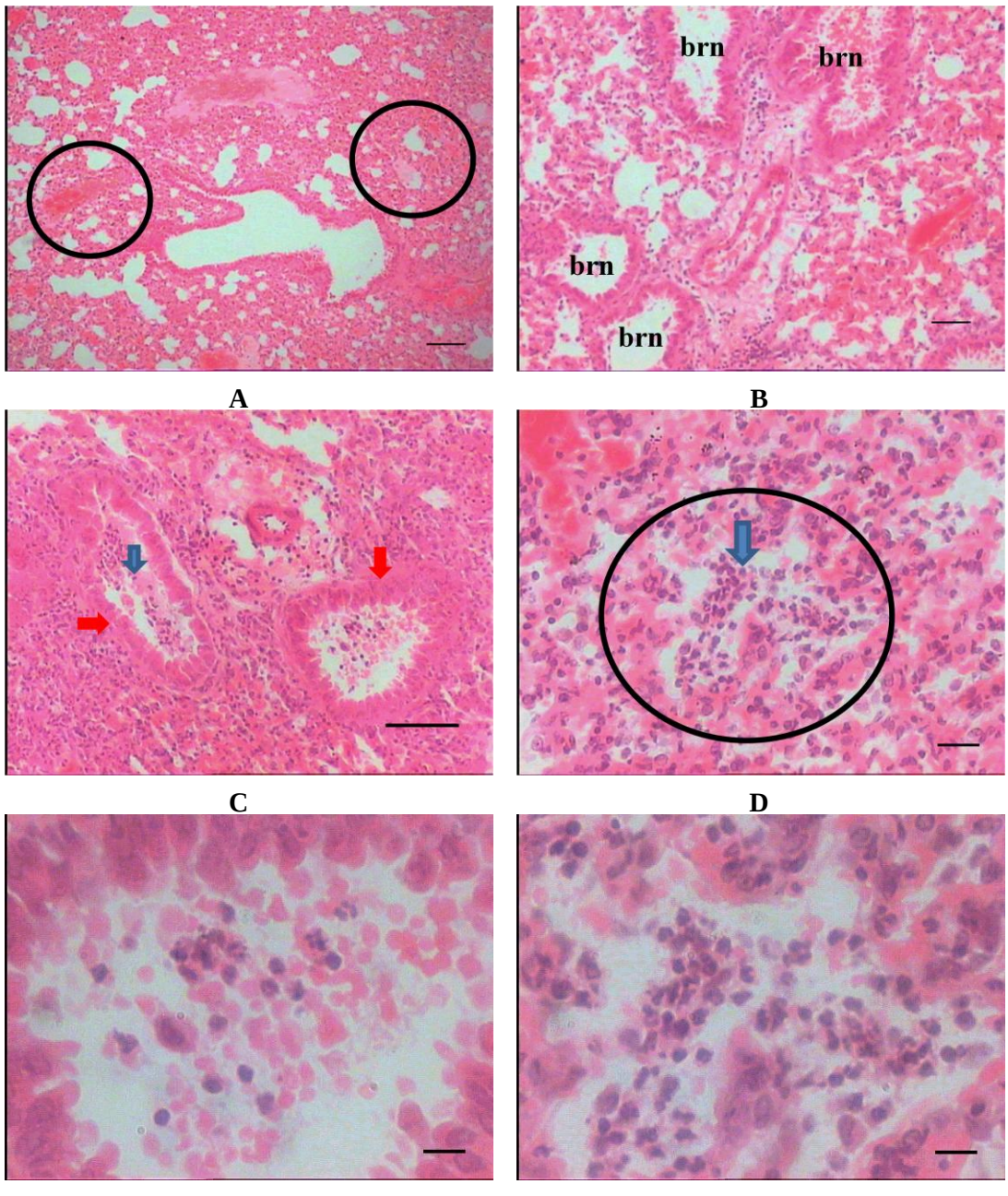

Figure 3.37. Lung histopathology of mice inoculated with an intermediate dose of *P. aeruginosa* (no subsequent bacteriophage treatment). A, black circle highlighting oedema and alveolar coalescence; B, abnormal bronchioles (brn); C, red arrow showing the thickened epithelium of bronchioles and blue arrow showing inflammatory cells inside the bronchioles; D, alveolus filled with inflammatory cells; E and F, infiltration of inflammatory cells and macrophages into the lumens of a bronchiole and alveolus, respectively. Scale bars for A/B, C/D and E/F are 10, 5, 2 and 1 µm, respectively.

3.3.2.1.3. Recovery of *P. aeruginosa* from infected lung tissue

The right lobe of the mouse lung was excised, homogenised and the supernatant cultured with appropriated media at 37 °C for 18 h, in order to enumerate the *P. aeruginosa* as CFUs. The phenotype of the bacterial colonies during incubation was indicative of mucoid *P. aeruginosa*: large, green colonies (Figure 3.41). This indicated that the method could readily discern *P. aeruginosa*, despite being an aseptic (rather than sterile) procedure, and colony counts could be made. For mice inoculated with 5.7×10^8 CFU/mouse, without subsequent bacteriophage treatment, the average *P. aeruginosa* count for the right lung lobe was 23,756 ± 2577 CFU (this number being calculated by, extrapolation back to total volume in which the lobe was homogenised).

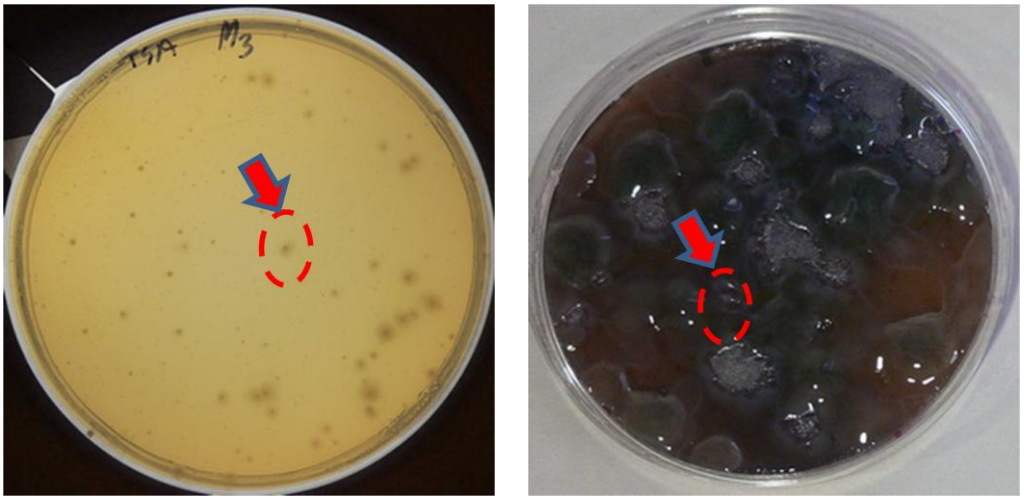

A **B**

Figure 3.38. Phenotype of the colonies cultured from the homogenised lung. A, after 18 h incubation colonies are green and relatively small. B, colonies after 48 h are green, confluent (large) and typical of the mucoid *P. aeruginosa* strains used in this study.

3.3.2.2. Bacteriophage therapy in vivo

3.3.2.2.1. Administration of simple bacteriophage solutions

For the treatment groups, infected mice (5.7×10^8 CFU/mouse) were administered the bacteriophage selective for *P. aeruginosa* 24 and 48 h post-infection, either intra-nasally or by nebulisation. Mice were sacrificed 24 h after the second dose of bacteriophage and the left and right lobes of the lung separated as above.

As for the treatment group above, mild clinical signs and symptoms were observed following infection and before treatment with bacteriophage. These included a weight loss of < 10% but with constant temperature, an irregular, laboured breathing pattern and an infrequently hunched back. Following sacrifice, the histopathology of the left lobe showed that the alveoli were enriched with mucus and inflammatory cells and coalescence of alveoli was seen along with oedema (Figures 3.42 and 3.43). Across the tissue section, inflammatory cells were present (though a reduction in number as a consequence of bacteriophage treatment was not immediately evident) and migration with macrophages to the bronchioles was observed (Figures 3.42 and 3.43). This suggests that the bacterial infection remained despite administration of bacteriophage.

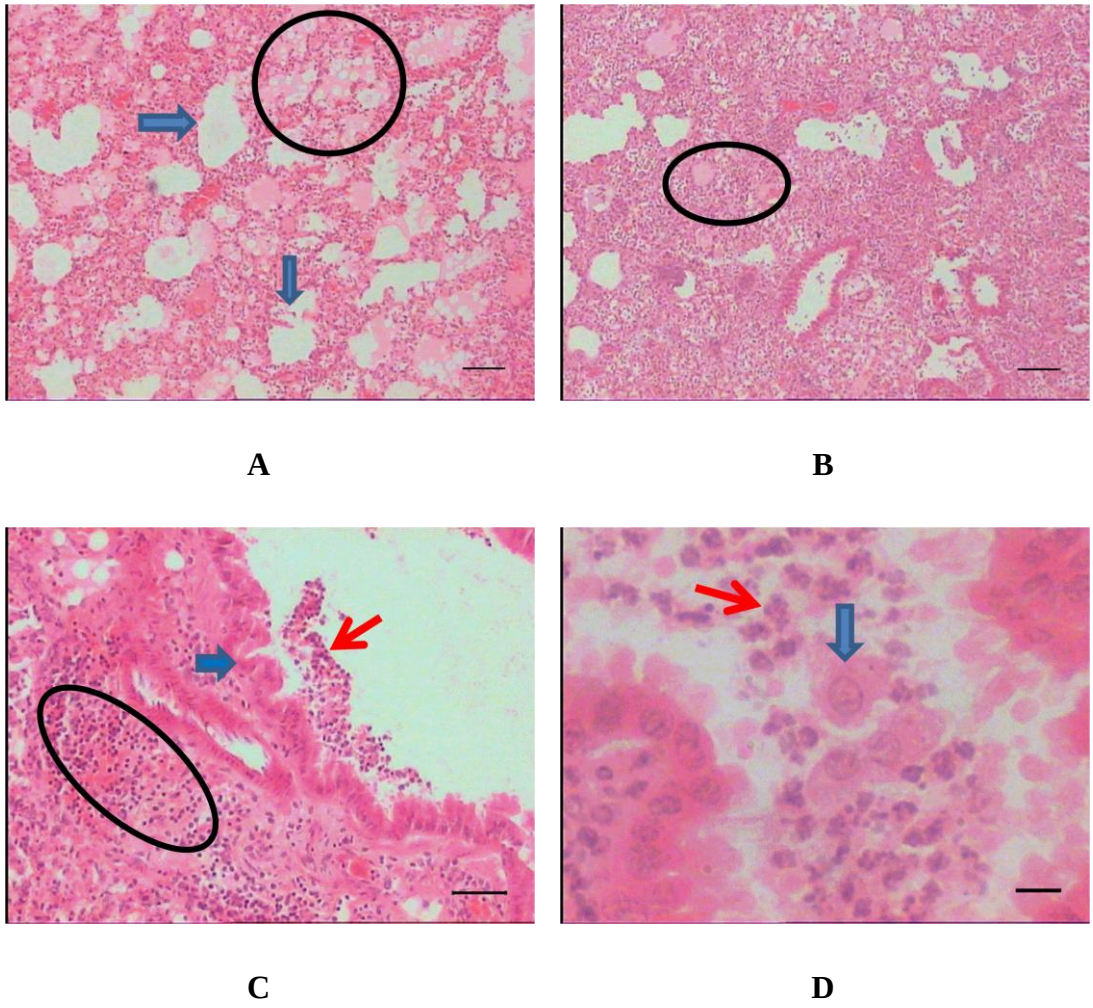

A **B**

C **D**

Figure 3.39. Lung histopathology of mice inoculated with an intermediate dose of *P. aeruginosa* followed with 2 intra-nasal doses of bacteriophage. A, the circled area shows oedema within an alveolus, with blue arrows showing coalescing alveoli; B; oedema and coalescence with inflammatory cells; C, red arrow and circled area show inflammatory cells inside a bronchiole and surrounding blood vessel, respectively, the blue arrow depicts the thickened the epithelium of the bronchiole; D, the blue arrow shows macrophages, with the red arrow showing neutrophils inside the bronchiolar lumen. Scale bars for A/B, C and D are 10, 5 and 1 µm, respectively.

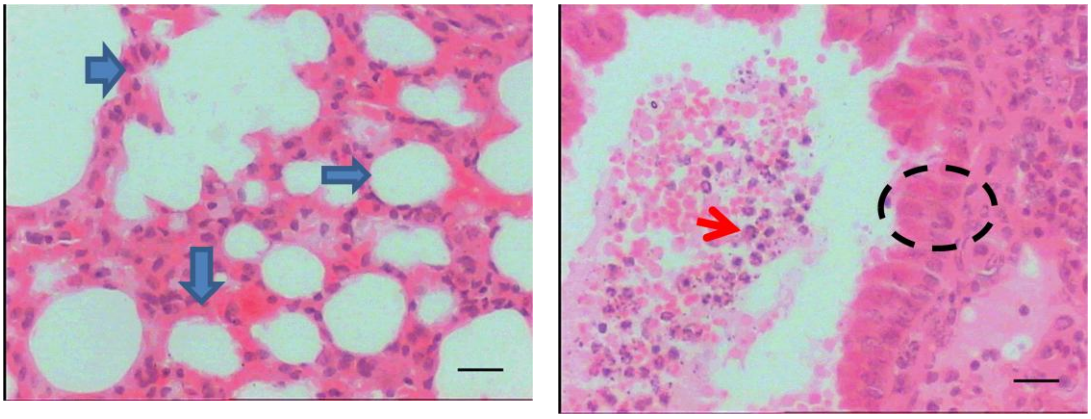

A **B**

Figure 3.40. Lung histopathology of mice inoculated with an intermediate dose of *P. aeruginosa* followed with 2 nebulised doses of bacteriophage. A; blue arrows show alveolar coalescence and infiltration by inflammatory cells in the alveolar wall; B, the red arrow shows oedema with inflammatory cells inside the bronchiole, the dashed circle depicts the thickened the epithelium of bronchiole. Scale bars = 2 µm.

Despite the histology and clinical symptoms being inconclusive with regard to the success of treatment with bacteriophage, the number of *P. aeruginosa* recovered from the right lobe was significantly less ($p < 0.05$, non-parametric Kruskal-Wallis test): 4783 ± 192 and 5822 ± 122 CFU/lobe for bacteriophage administered intra-nasally and by nebulisation, respectively (Figure 3.44).

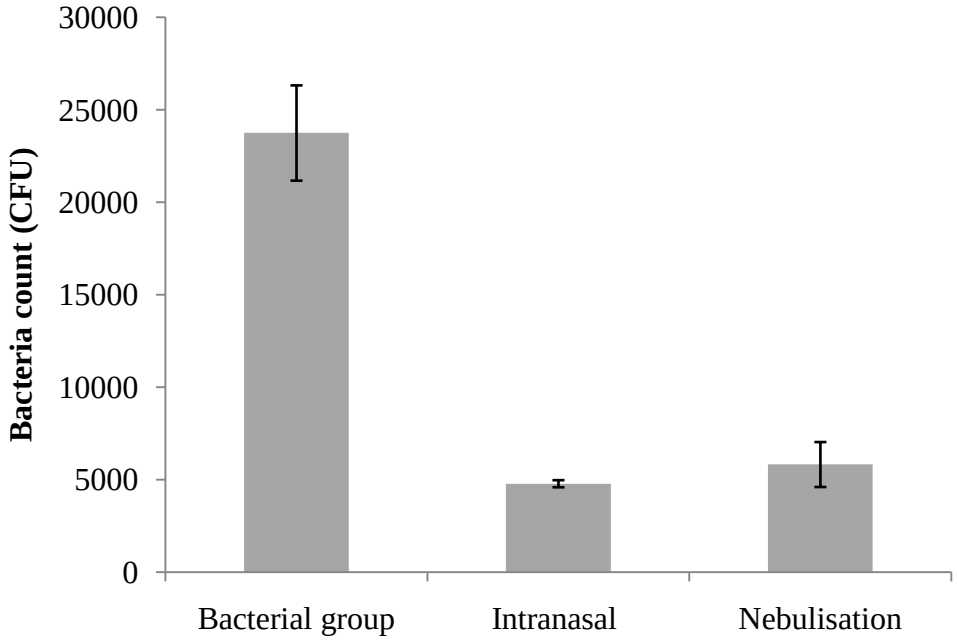

Figure 3.41. Counts of *P. aeruginosa* recovered from the right lobes of mice. The mice were administered by PBS for Bacterial control, bacteriophage solution for the treatment groups, via intranasal (middle bar) and nebulisation (right bar). Error bars show standard error of 3 samples.

3.3.2.2.2. Administration of formulated bacteriophage

Freeze-dried bacteriophage powders were redispersed with sterile PBS and administered by nebulisation to mice previously infected with *P. aeruginosa* (5.7×10^8 CFU/mouse) 24 h prior. Rather surprisingly, the mice presented a worsening of clinical symptoms compared to previous studies: piloerection, hunched back, lower activity and laboured breathing pattern. Mice were sacrificed in accordance with the end-point clinical scores at day 3 and the lungs excised for examination as above. The lung tissue sections showed many neutrophils, in accordance with the infection, and the alveolar epithelium was thickened and infiltrated with inflammatory cells (Figure 3.45). Thickening of the bronchiolar epithelium, oedema and alveolar coalescence were also observed, in a pattern as observed with the previously infected groups. Enumeration of *P. aeruginosa* from the homogenised right lobe revealed a colony count ten-times greater than for

infected mice treated with nebulised, non-lyophilised bacteriophage solutions (Figure 3.46). The large error bars for this group reflect the apparent worsening of clinical symptoms and variability within this treatment group; the reasons for which are not clear, though this may have been a consequence of bacteriophage formulation and further studies were therefore made.

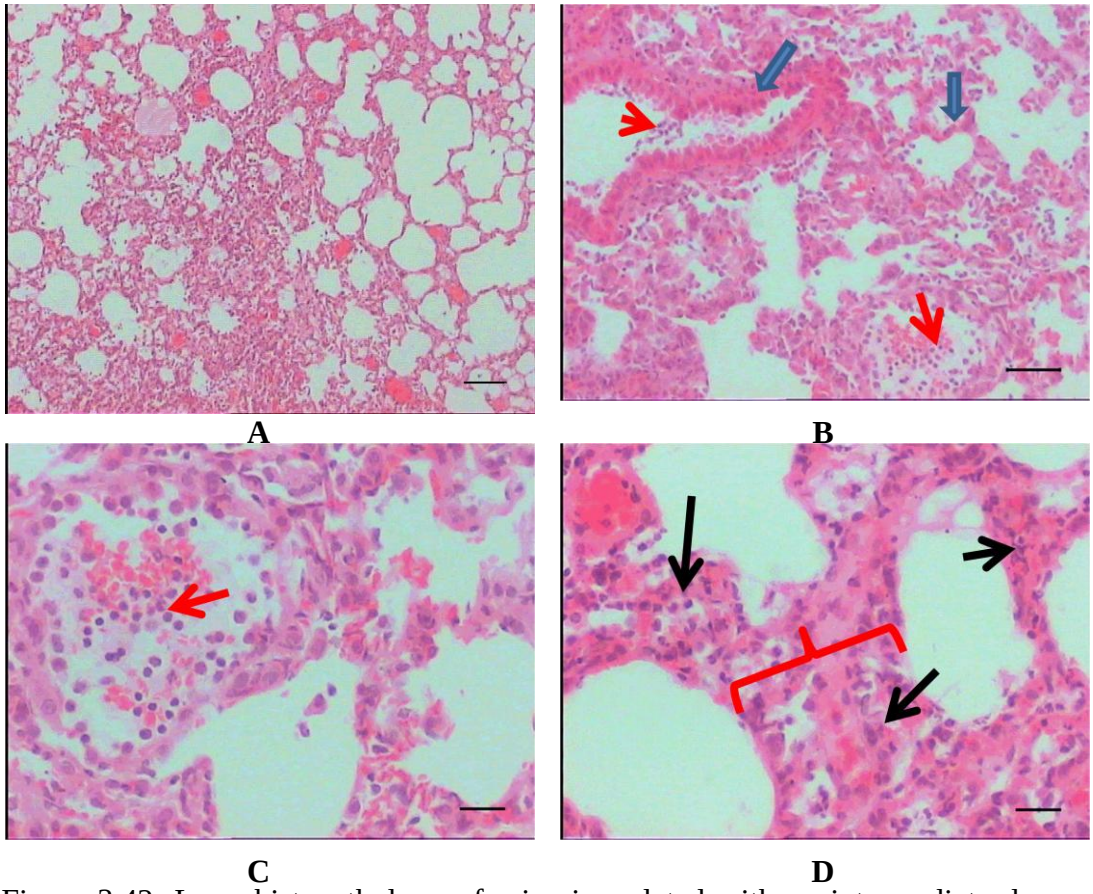

Figure 3.42. Lung histopathology of mice inoculated with an intermediate dose of *P. aeruginosa* followed with 2 nebulised doses of freeze-dried, reconstituted bacteriophage. A, abnormal alveolar structure showing coalescence and oedema; B, red arrows show oedema and inflammatory cells inside a bronchiole and alveolus, blue arrows show thicken bronchiolar and alveolar epithelia; C, oedema with inflammatory cells inside alveoli (red arrow); D, arrows point out inflammatory cells infiltrating the alveolar epithelium, which is thickened (red-bracket). Scale bars for A, B/C and D are 10, 5, and 21 µm, respectively.

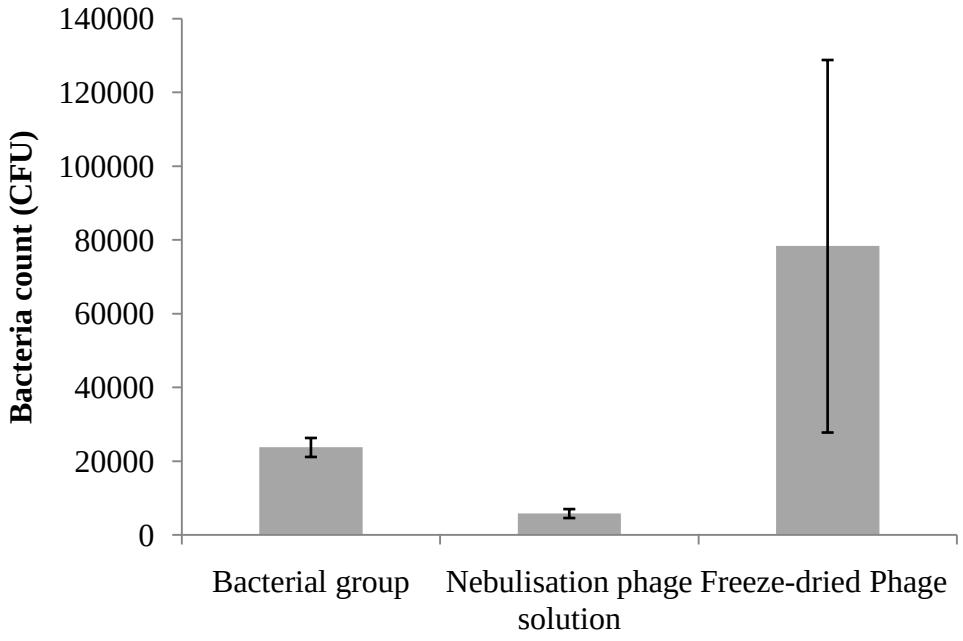

Figure 3.43. Counts of *P. aeruginosa* recovered from the right lobes of mice. The mice were administered by nebulisation comparing the bacteriophage solution (middle bar) and the reconstitution of lyophilised bacteriophage (right bar). The control group (bacterial group) was nebulised with PBS.Error bars show standard error of 3 samples.

Freeze-dried bacteriophage with inclusion of a stabiliser (1% PEG6000) was also studied *in vivo*. Freeze-dried bacteriophage were reconstituted and administered by nebulisation to infected mice as above. As for the previous administration of freeze-dried bacteriophage, the clinical signs and symptoms were more severe compared to the group of infected mice treated with simple (non-lyophilised) bacteriophage solutions. The mice reached their clinical end-points 48 h after infection and were sacrificed. Histological examination of the left lobe revealed that the fine lace structure of the alveoli had disappeared and the epithelia of the bronchioles and alveoli was thickened (Figure 3.47). This was accompanied by oedema and infiltration of inflammatory cells and neutrophils inside the bronchioles and surrounding blood vessels (Figure 3.47). Counts of *P. aeruginosa* recovered from the homogenised right lobe were very high and

variable (219889 ± 351065 CFU/lobe) and made further interpretation not meaningful; further *in vivo* experiments were not made.

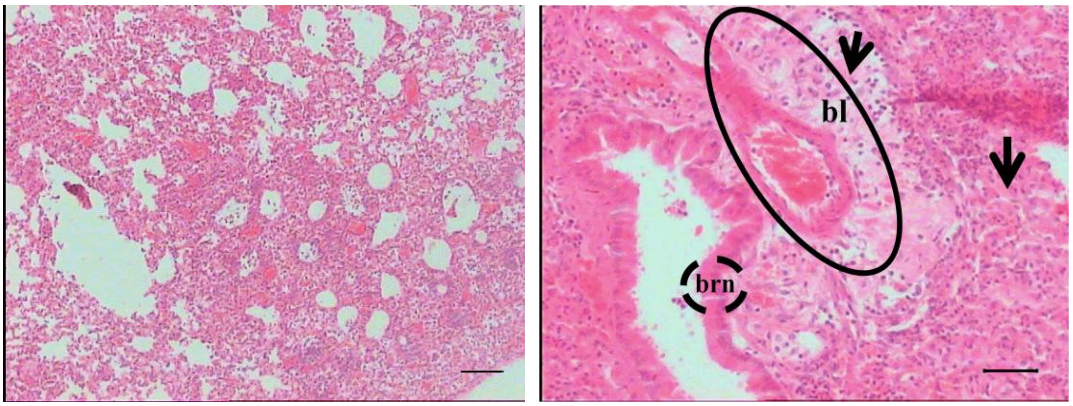

A **B**

Figure 3.44. Lung histopathology of mice inoculated with an intermediate dose of *P. aeruginosa* followed with 2 nebulised doses of freeze-dried, reconstituted bacteriophage/1% PEG. A, abnormal alveolar structure showing coalescence and oedema; B; the immigration of inflammatory cells surrounding blood vessel (bl) and bronchiolar epithelia (brn), arrows show oedema with inflammatory cells inside the bronchioles and alveoli. Scale bars for A and B are 10 and 5 µm, respectively.

The microsphere formulation including the bacteriophage did not perform in this study. Since the bacteriophage amount of microsphere formulation is uncertainly quantifed and in vitro results also shows that the lytic activity of the microsphere formulation is less than the lyophilized bacteriophage. Although the lytic activity of lyophilized bacteriophage demonstrates a greater lytic activity, the outcome in animal remain unsatisfied (the reduction of bacterial was not seen). Thus it is reasonable that the microsphere formulation may provide inappropriated amount of bacteriophage for this study.

3.3.2.3 Bacteriophage toxicity in vivo

Bacteriophage solutions (1.5×10^9 pfu/mouse) were administered to mice intra-nasally. Clinical observation and histopathological examination were made in order to determine the potential toxicity and/or adverse effects of bacteriophage administration. Weight loss, body temperature, eye colour, activity, breathing and other criteria (as described in section 2.2.5.2.3) were not apparently different to control mice (no treatment). From the histology results, a normal bronchiolar/alveolar structure and epithelia were observed without evidence of oedema or mucus, or infiltration of inflammatory cells into the lumens (Figure 3.48). Rather, the normal fine lace structure the alveolar network and the single squamous epithelium of the alveolar wall were seen. Together, these results suggest that administration of bacteriophage (at this concentration/route) was not toxic to mice.

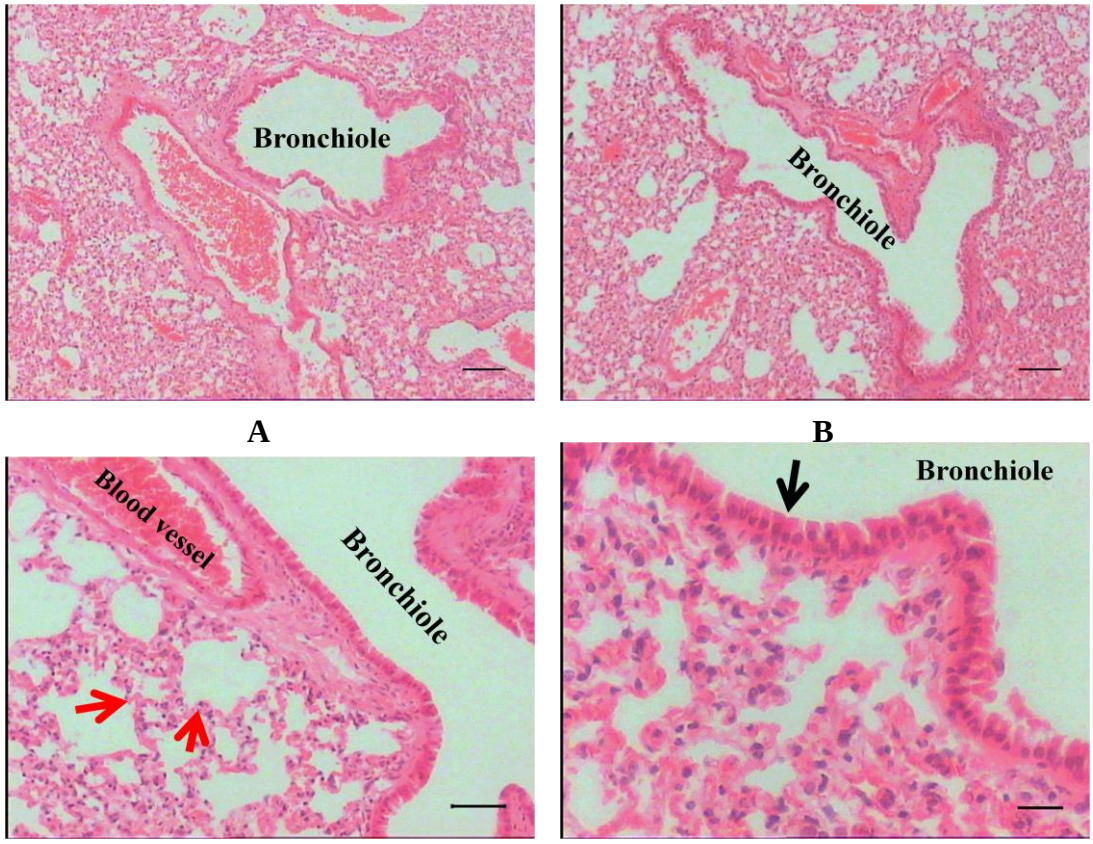

Figure 3.45. Lung histopathology of mice inoculated with an intermediate dose of *P. aeruginosa* followed with 2 nebulised doses of bacteriophageLung histopathology of mice adminstered bacteriophage solution intra-nasally. A-B, normal lace-like structure of the alveoli; C, red arrows show the single squamous epithelium of the alveoli; D, the arrow shows the normal columnar epithelium of the bronchiole. Scale bars for A/B, C and D are 10, 5, and 2 µm, respectively.

Chapter 4: Discussion

4.1. Encapsulation of bacteriophage in PLGA microspheres

4.1.1. Initial characterisation of bacteriophage loaded microspheres

Generally, the final size of polyester microspheres is affected by the stirring rate during emulsion preparation (Arshady, 1991; O'Donnell and McGinity, 1997). Some work has shown that the stirring rate during the secondary emulsion in particular affects microsphere size, rather than during the primary emulsion (Ito, et al., 2010). In the same study, the smaller droplet size produced during the primary emulsion increased 'drug' loading efficiency. Ito and co-workers (2008) also investigated the ratio of the droplet diameter of the primary emulsion (d_{pd}) against the secondary emulsion (d_{sd}), showing that the ratio (d_{sd}/d_{pd}) was linearly related to the loading efficiency of blue dextran. These results may help interpret the early data acquired in this study wherein a higher homogenisation speed resulted in an increase in the lytic activity of bacteriophage released from microspheres following encapsulation. That is, because of the constant rate of stirring during the secondary emulsion, it can be presumed that the smaller droplet size in the primary emulsion, as a consequence of increased stirring rate, might increase phage loading (consistent with an increase in the ratio d_{sd}/d_{pd}. Thus, although the data for lytic activity following high/low homogenisation was initially puzzling (since a higher homogenisation speed and smaller droplet size would increase phage denaturation at the oil/water interface), an increased encapsulation efficiency appears to provide a satisfactory explanation.

It should be noted that we used relatively short homogenisation times for the emulsion steps in this study to minimise the denaturation of phage at the interface. Ding and Shah

(2009) suggested that probiotic bacteria could better survive emulsification by reducing the speed of stirring rate and time of mixing during microencapsulation process (studying eight probiotic bacterial strains). They found that when the time of homogenisation during primary emulsion was decreased to 15 second, the loss of bacterial viability was largely avoided.

The smaller droplet size during primary emulsion, was also likely to be responsible for the smaller microsphere size, i.e. the homogenisation speed during the primary emulsion also influences on the size of microsphere. This result agrees with previous work by Zhao and co-workers (2007), showing that microspheres fabricated by w/o/w emulsion were reduced the size from 3.11 to 1.26 μm when the homogenisation speeds of the primary (or secondary) emulsion increased (Table 3.2).

With regard to the concentration of bacteriophage loaded during the primary emulsion (to maximize the amount of bacteriophage encapsulated), no change in microsphere size was observed. This is consistent with data for PLGA microparticles encapsulating ovalbumin (OVA) by w/o/w emulsion-solvent evaporation technique (as used here), which revealed that the microparticle size depended not on the concentration of OVA but on the volume of the aqueous phase in the primary emulsion (Jeffery, et al., 1993). Thus, in our studies, the different concentrations of bacteriophage had no effect on microsphere size because the loading volume for all emulsions was the same.

In these preliminary studies it was not found possible to easily quantify the loss of lytic activity following emulsification; the semi-quantitative tables using –P, P, +P, etc. are a result of this issue and explained in the results section. Therefore, although the lytic activity of bacteriophage following encapsulation was retained, it was clear that this was only a fraction of the positive control (the bacteriophage stock solution, Table 3.3).

Further investigation of this issue was made at a later date in this thesis, wherein alternative assays to the conventional plaque assay were sought.

In general, a formulation of a drug must contain a sufficient therapeutic dose. This is of course the case for bacteriophage too; i.e. an appropriate, therapeutically effective dose of phage is required in a given mass of microspheres that are intended for administration (e.g. through pulmonary delivery). Here a study by Capparelli and co-workers (2007) was chosen, which reported that 10^9 pfu of a particular bacteriophage (called M^{Sa}) could rescue mice infected with *S. aureus* strain A170, for both lethal bacterial loading 10^8 CFU/mouse and non-lethal loading 5 x 10^6 CFU/mouse. In brief, the mice treated with the highest phage dose (10^9 pfu/mouse) were all protected from death (5/5 mice). In contrast, 90 to 100% of mice injected with a dose of 10^8 CFU died within 4 days. Furthermore, the phage M^{Sa}, delivered inside macrophages by *S. aureus*, killed the intracellular staphylococci *in vivo*. Therefore, the number of phages that should be loaded in this study in a 'dose' of microsphere formulation would be considered to be 10^9 pfu.

4.1.2. The effect of lyophilisation on the lytic activity of bacteriophage

In recent years the challenge has been to devise microsphere formulations preserving the integrity (i.e. stability) of encapsulated proteins. It is becoming clear that the efficacy of these microspheres as protein delivery systems is highly dependent on the stability of the protein during microencapsulation and also in the course of the polymer degradation process (Crotts and Park, 1997). Therefore, we investigated the effect of the lyophilisation process on lytic activity of bacteriophage alone, because the final step of microsphere fabrication involves drying by lyophilisation.

Reconstitution of the microsphere dry powder with water and measurement of lytic activity by the plaque assay showed good retention of lytic activity of the bacteriophages for both lyophilisation periods (Table 3.4). Though, again, it is difficult to make a quantitative assessment of the absolute loss of lytic activity in this study, it can be said that the residual activity was comparable to the non-lyophilised bacteriophage under the phage assay method. Therefore, these results demonstrate that the lyophilisation step following microsphere fabrication does not appear to significantly affect the lytic activity of the bacteriophages used in this study. The loss of lytic activity is therefore due to poor encapsulation efficiencies and denaturation at the interface. A similar retention of stability has been reported for freeze drying of bacteriophage λ in the absence of excipient stabilisers (Jepson and March, 2004). The titre of bacteriophage λ decreased following freeze-drying from the initial phage count of around 2×10^{11} to 1×10^{10} pfu/mL. Although this represents an apparently large loss when expressed as fraction, in absolute terms, a pfu count of 10^{10} per ml remains high when assessed by plaque assay. Therefore, both studies indicate that lyophilisation of bacteriophage results in only small changes in lytic activity, so long as the initial phage count is high (10^9 pfu/ml or above). Therefore, lyophilisation would appear to be a convenient and effective method for the drying of bacteriophage-loaded microspheres.

4.1.3. Addition of bacteriophage during the secondary emulsion

To successfully develop PLGA microsphere as vehicles for the controlled release of bacteriophage, the stability and lytic activity of the bacteriophages must be retained. A modified double emulsion protocol was sought to reduce the exposure of protein coat of the bacteriophage to the oil(DCM)/water interface during primary emulsion process. This is because the oil/water interface is well known to be strongly denaturing to proteins (van de Weert, et al., 2000). Several approaches have been used to address this

problem such as: the type of surfactant or emulsifier used (Bouissou, et al., 2004); solid protein dispersions versus liquid emulsions (Castellanos, et al., 2001); buffering of the mildly acidic interior of the polyester matrix (Jiang and Zhu, 2002). However, given that the objective in this study was to fabricate microspheres suitable for inhalation (Mohamed and van der Walle, 2006), the approach adopted was to investigate the effect of addition of the bacteriophages during either the primary or secondary emulsion steps, the latter using a two-step secondary emulsion.

The plaque assay was used to provide information on the effect of the two different points of addition of phage in the fabrication process on the resultant lytic activity. The method wherein phages were added to the external aqueous phase of the initial secondary emulsion resulted in a greater phage activity when compared to the method wherein phages were added to the internal aqueous phase of the primary emulsion (Table 3.5). Since the primary emulsion is a water-in-oil system wherein the bacteriophages are concentrated within the small aqueous fraction, it is reasonable to assume a higher degree of exposure to the solvent interface. In contrast, the secondary emulsion is a oil-in-water system wherein the bacteriophages are more dispersed throughout the larger aqueous phase and less likely to come into contact with the solvent interface. However, the encapsulation efficiency will also decrease for increasing dispersion of the bacteriophages in the secondary aqueous phase. Therefore, a two-step secondary emulsion was adopted wherein a balance between bacteriophage dispersion and entrapment was maintained.

These results are consistent with previous work investigating the effect of organic solvent on phage infection, in which Matsubara and co-workers (2007) reported that phage infection was attenuated in relation to the concentration of the water-miscible organic solvent. The exposure time between phage and organic solvent in microsphere fabrication is therefore of concern in the development of phage-loaded microspheres.

Nevertheless, our data show that it is also important to take in to consideration the point at which phages are added to a double emulsion system. Ultimately, the lytic activity of the bacteriophage can be maintained during encapsulation into PLGA microspheres by simple modification of the double emulsion-solvent evaporation protocol to minimize exposure at the solvent interface, while retaining encapsulation efficiency.

4.1.4. Comparison of the lytic activity of both bacteriophage strains following encapsulation

Following initial experiments investigating the effect of emulsification and lyophilisation on the lytic activity of bacteriophages, the fabrication protocol described above was used to encapsulate bacteriophages selective for *S. aureus* and *P. aeruginosa*. Following encapsulation and release from the microspheres, the bacteriophage selective for *P. aeruginosa* showed a greater loss of lytic activity than the bacteriophage selective for *S. aureus* (Table 3.6). A simply interpretation would be that the former are either less stable during emulsification or are less efficiently encapsulated. However, it is also important to take into consideration the phenotype of the bacteria themselves, since this may affect the efficiency of phage infection and plaque formation. In contrast to *S. aureus* strain 8588, the *P. aeruginosa* strain 217M is a mucoid strain which produces exopolysaccharide. The exopolysaccharide produced (an alginate) by mucoid *P. aeruginosa* strains functions as a physical or electrostatic barrier, conferring resistance to antibiotics and phagocytes (Høiby, 2002; Høiby, et al., 2010). It has been reported that the digestion of the exopolysaccharide and a reduction in alginate viscosity has been shown to facilitate phage penetration of biofilms (Hanlon, et al., 2001; Suthereland, et al., 2004). With regard to the results here, the difference in lytic activity observed may therefore be in part due to exopolysaccharide secretion by the *P. aeruginosa* strain.

4.1.5. The stability of the bacteriophage-loaded microspheres

One putative advantage of encapsulating bacteriophage in PLGA microspheres is that immobilisation in the polymeric matrix may stabilise the phage. We therefore followed the stability of the bacteriophage encapsulated in the lyophilised microspheres over a period of 7 days, after which no further lytic activity was observed at either 4 °C or 22 °C storage (Table 3.7). The results are somewhat unexpected given the apparent stability following lyophilisation of the phage alone, and previous work showing that the half-life of bacteriophage λ at 20 °C was 20 days following lyophilisation of a simple aqueous suspension (Jepson and March, 2004). However, Ma and co-workers (2008) showed that air-drying of bacteriophage 'Felix O1' encapsulated in chitosan microspheres without protective agents resulted in near complete loss of phage survival over 6 weeks. In contrast, their microsphere formulation containing the lyo-protective agent, trehalose, resulted in a 12.6% survival rate of the bacteriophage after 6 weeks storage. It is interesting to note in this study that the loss of bacteriophage stability did not appear to be strongly dependent upon storage temperature. This suggests that the loss of integrity of the bacteriophages may have been due to a physical interaction at the surface of, or encapsulation within, the PLGA porous matrix. Further studies would be needed to demonstrate this, though it is not clear what techniques would be suitable for probing of the molecular mobility of immobilised bacteriophage.

4.1.6. Physical characterization of the bacteriophage-loaded microspheres

Many formulation parameters determine the size and morphology of PLGA microspheres such as the intrinsic viscosity of the polymer, the concentration and type of surfactant/stabiliser, the ratio of internal:external volume of aqueous phase, the

stirring rate, and the evaporation rate of organic solvent (Mohamed and van der Walle, 2008). Microspheres encapsulating phage selective for *S. aureus* or *P. aeruginosa* had median diameters around 10 μm, with the statistical test concluding that the particle size was independent of bacteriophage encapsulation. This result is in agreement with a report showing that the percentage drug loading does not have a significant influence on the mean microsphere size at a constant polymer concentration (Capan, et al., 1999). The size distribution profile of the microsphere batches showed a monomodal distribution. Where a minor peak at very small particle sizes was observed, this was assumed to be a consequence of 'fines' arising from grinding of the microspheres during hardening following secondary emulsion, or harvest following lyophilisation. The small size distribution (span) suggested that sufficient surfactant had been added to the emulsion, since too low a surfactant concentration would lead to poor stability of the surface tension, droplet coalescence and consequently a large range of measured particle sizes (in addition to an increase in particle size). It is acknowledged that the 1% PVA concentration used here is widely used in the preparation of protein-loaded microspheres in general, and one advantage of PVA is that it is a GRAS (Generally Recognized As Safe) listed excipient by the US Food and Drug Administration (FDA).

In this study, bacteriophage were incorporated in the secondary emulsion step, during which the internal aqueous phase droplets (distributed within the oil droplets) may coalescence if the primary emulsion was relatively unstable and so lead to the formation of an inner porous morphology (Nihant, et al., 1994; Rosca, et al., 2004). The greater the coalescence of the internal aqueous phase (w1) in the w/o/w emulsion, the greater the size of the internal pores of the microspheres (described as micro- to meso- to macro-porous by Florence and Attwood, 2006). As shown in Figure 4.1, the system is not thermodynamically stable and any collision between water droplets may be driven by bridging-flocculation or merely Brownian motion, leading to large vesicles. Consequently, the solvent diffuses from droplets to the continuous phase (w2) and then evaporates into the air. Following the solvent evaporation, the droplet of dispersed

phase (o) would enrich with polymer due to the precipitation and solidification (hardening) of the polymer.

As evidenced from the SEM and confocal micrographs in Figure 3.5 and 3.6, the microspheres' morphologies are altered by the addition of storage media to the emulsion (the thereby also for the addition of bacteriophage, since these are maintained in storage media). The shift away from an entirely hollow interior, produced by the use of Pluronic L92 as the stabiliser in the primary emulsion, indicates an increase in stability of the primary emulsion immediately prior to secondary emulsion and microsphere hardening (Florence and Attwood, 2006). It should be added that Pluronic L92 was found to be a very poor emulsifier of dichloromethane-water emulsions, and led to surface dimpling presumably because of the self-assembling nanoparticulate nature of the Pluronic L92 molecules (Bouissou, et al., 2004; Mohamed and van der Walle, 2006). Conversely, increasing the stability of the primary emulsion changes the internal structure of the microparticle from a multivesicular to microporous matrix-like structure (Nihant, et al., 1994). Similarly, increasing the homogenisation speed during the primary emulsion leads to a decreased internal porosity (Mao, et al., 2007).

It should be remembered that the secondary emulsion is very short lived and therefore the kinetics of droplet coalescence must be considered against the kinetics of polymer precipitation and hardening. The immobilisation of the bacteriophage is assumed to occur during polymer precipitation, though the degree of polymer mobility will exist during hardening of the outer surface followed by the inner matrix. It is unknown if bacteriophage can migrate within the hardening microsphere, possibly as a consequence of osmotic difference between the inner and outer aqueous phases, or a concentration gradient. However, with reference to the confocal photomicrographs, microspheres encapsulating fluorescein-labelled bacteriophage showed the distribution of bacteriophage to be almost entirely within the microsphere interior. Thus, bacteriophage

mobility during microsphere hardening must be minimal. Poor emulsion stability also leads to droplet coalescence between the inner (w1) and outer (w2) aqueous phases. In this case, bacteriophage incorporated in either the secondary or primary emulsion will be lost and result in low encapsulation efficiency. The confocal photomicrographs, however, show a punctuate staining, which is assumed to reflect the porosity of the microsphere interior, and would suggest that encapsulation was reasonably efficient.

The use of storage medium as the aqueous phase, rather than water, will impart an osmotic pressure between the primary and secondary aqueous phases. Herrmann and Bodmeier (1995) investigated the effects of buffers or salts added to the internal aqueous and/or external aqueous on the properties of somatostatin acetate-containing polylactide microspheres. The results indicated that addition of buffers or salts to the internal aqueous phase would produce the porous microsphere because there is the difference in osmotic pressure between internal and external aqueous phase. Another effect of the storage medium is that the gelatin component has itself (as any protein) an inherent emulsifying activity. Hence, the observed increase in the primary emulsion stability on addition of storage medium may be due to the presence of the gelatin.

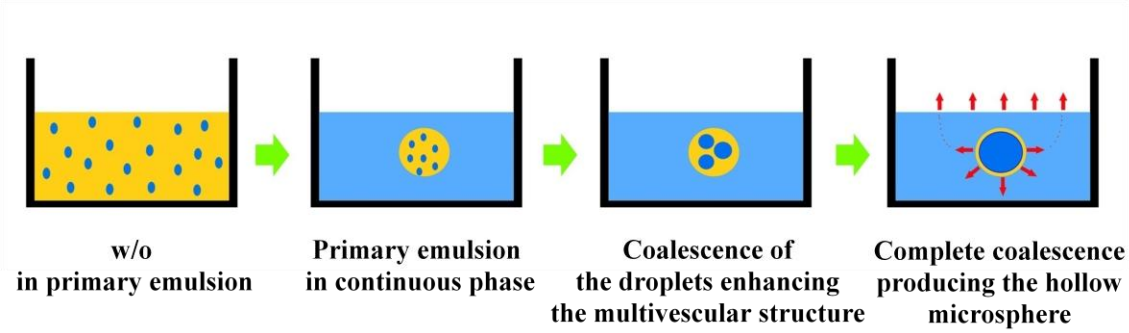

Figure 4.1. Schematic presenting the progression of droplet coalescence in the internal aqueous phase (w1). Poor stabilisers of the emulsion (namely Pluronic L92) lead to complete coalescence.

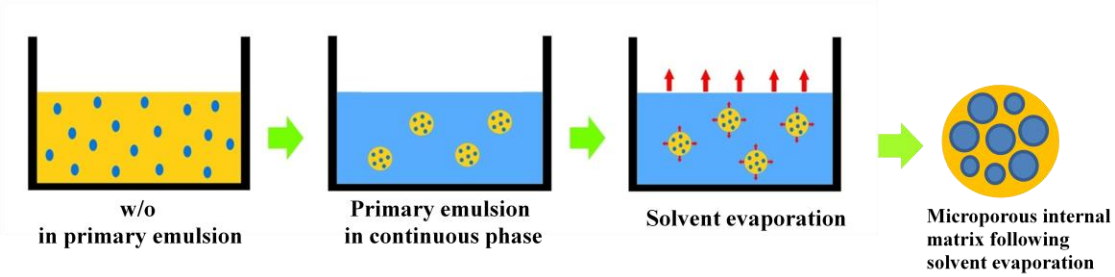

Figure 4.2. Schematic presenting the internal matrix structure with increasing homogenisation speeds or strong stabilisers of the solvent/water interface.

4.1.7. Powder flow, dispersion and deposition

A previous study determined that hollow, surface dimple microspheres prepared with Pluronic L92 has physical characteristics suitable for pulmonary delivery: an apparent density of 0.24 ± 0.04 g/cm^3, a measured diameter (d) of 7.85 µm and an aerodynamic diameter (d_a) of ~4 µm. The microspheres fabricated in this work had a lower apparent density of ~0.12 g/cm^3; this is despite SEM micrographs showing that the morphology of the microspheres was altered by inclusion of storage media into the emulsion. In particular, the internal porosity appeared macroporous, rather than entirely hollow, and would predict a higher apparent density. However, the measured diameter of the microspheres in this study was greater (10 µm) and therefore, on packing during the tapped density measurement, will occupy a greater volume, resulting in the lower apparent density. Direct measurement of density using a pycnometer may resolve this issue in future studies.

Plotting a probability log plot for particle distribution following cascade impaction (with the assumption that total powder recovery was 100%) yielded a particle cut-off size at

50% cumulative mass, equivalent to the geometric mean weight diameter (d_g). The d_g for the phage-loaded microspheres was nearly two-fold greater than the corresponding value of d_a and the value of d_g for the blank microspheres. The higher value of d_g for the phage-loaded microspheres was most likely due to the smooth surfaces of the microspheres (as shown in Figure 3.5) which would increase the surface area available for particle-particle interaction through electrostatic, capillary (residual moisture) electrostatic and/or van der Waal's forces; i.e. the phage-loaded microspheres appeared to aggregate following initial dispersion from the capsule. Further investigation of this cause of aggregation would require determination of particle surface and interaction using atomic force microscopy (Young, et al., 2002), and measurement of moisture content (e.g. by Karl Fisher titration). It is interesting to note a previous investigation of surface dimpling as a means to improve particle dispersion via reduction in particle-particle contact energies: namely 'corrugated' bovine serum albumin (BSA) particles (Chew and Chan, 2001). Fabrication of BSA particles progressing from smooth to highly corrugated surfaces has shown that only modest corrugations are required to considerably increase aerosol performance (Chew, et al., 2005).

With respect to delivering particles to the lung periphery via inhalation, aerosols are generally manufactured to meet an aerodynamic diameter of around 3-5 μm. Byron and Patton (1994) have reported an upper limit for particle aerodynamic diameter of 4.7 μm, for pulmonary delivery. Engineering particles with a d_a value in the appropriate range can be achieved by changing either particle size or density (porosity) and shape (e.g. surface roughness). Thus, it has been shown that microparticles engineered to have a large diameter, up 20 μm, can still have appropriate aerodynamic characteristics for pulmonary delivery (Edwards, et al., 1997; 1998): by increasing the porosity to such an extent that the resultant low density brings the d_a (or d_g) value down below 4.7 μm. It is inferred that the bacteriophage-loaded microspheres, with d_a values 3.3-3.75 μm, will have an aerodynamic characteristic wherein at least a fraction would likely approach the lung periphery on inhalation. Further development must address the issue of aggregation

but also, aim to decrease the size distribution (the span, or corresponding σ_g), to increase the fraction of microspheres deposited in the deep lung. Microspheres with uniform size distributions have been described for membrane emulsification (Ma, et al., 2003) and microchannel-mixing techniques (Freitas, et al., 2003). Ultimately, further testing of the bacteriophage-loaded microspheres in animal models of lung infection would be required to more fully characterise their therapeutic activity.

4.1.8. Release study of bacteriophage-loaded microspheres

To examine the rate of release of bacteriophage from the microspheres, fluorescently-labelled bacteriophages were employed to allow quantitative measurements. Although fluorescence labelling did not perturb the lytic activity of the bacteriophages (Table 4.1), it is accepted that, following formulation, this measurement will be unable to distinguish between active and inactive phages. Nevertheless, making the reasonable assumption that the rate of release for active and inactive bacteriophages is the same, this method allows a release profile to be constructed, which would otherwise not be possible for wild-type (non-labelled) phage. Although the bulky, hydrophobic fluorescein moiety would be expected to significantly change the physicochemical properties of a small peptide, for a bacteriophage order of magnitude larger, fluorescein labelling was not expected to perturb phage-matrix interactions or the release profile.

Table 4.1. Lytic activity of bacteriophage selective for *S. aureus* and *P. aeruginosa* before and after FITC labelling

Lytic activity of purified bacteriophage selective for *S. aureus* (pfu/mL)		Lytic activity of purified bacteriophage selective for *P. aeruginosa* (pfu/mL)	
before FITC labelling	after FITC labelling	before FITC labelling	after FITC labelling
2.1×10^{11}	2.56×10^{11}	9.82×10^{11}	1×10^{12}

Data show 1 sample for each phage.

Initially, a burst release was observed over the first 30 minutes followed by a slower sustained release phase; i.e. a biphasic release profile, which is commonly observed for proteins with similar non-homogenous distributions within the internal matrix (Bouissou, et al., 2004; Yang, et al., 1999). It is interesting that, although PLGA microspheres are purported to facilitate a steady, prolonged release of entrapped drug, this is generally not the case. Typically, a burst release occurs, wherein around 60-80% of the entrapped drug (e.g. protein) is released within the first 24 hours (Wang, et al., 2002). With reference to CSLM images for fluorescent protein in microspheres, protein is seen to be dispersed within the pores of the matrix, with the remainder within the PLGA matrix itself. The burst release is therefore thought to arise from drug (protein) loosely associated within the porous network of the microsphere matrix. Similarly, the non-homogenous deposition may facilitate the burst release of bacteriophages in this study if water was freely able reach the localised internal pores harbouring entrapped bacteriophage.

However, this simple mechanism proposed for the burst release has not been unequivocally proven despite studies aiming to mathematically model the erosion, pore tortuosity, water diffusivity and, ultimately, drug release (Batycky, et al., 1997; Faisant,

et al., 2002). It has been reported that microspheres in pH 7.4 buffer, show erosion behaviour with surface pitting and an increase in the number and size of channels with time (Li and Schwendeman, 2005). This behaviour is indicative of autocatalysis, where acidic oligomeric units accumulate and create a porous network within the microspheres, accelerating PLGA degradation. Microspheres incubated in buffer at higher pH (above the pKa value of lactic acid is 3.8) are thought to be heterogeneous in pH as a result of pockets of acidic PLGA oligomers which cause non-uniform degradation creating a porous microstructure.

To suggest that the release of bacteriophage from the mesoporous matrix was dominated by Fickian diffusion is attractive, since it is simple to model, but not necessarily correct. For example, Messaritaki et al. (2005) took CLSM images in real time for release of a fluorescently labelled protein from a microsphere trapped in a micro-well. They showed that the release of a drug distributed heterogeneously within the PLGA microsphere matrix was better modelled to a percolation process, which was dependent on swelling of the matrix and evolution of the pore structure. Sandor, et al. (2001) also investigated the affect of protein MW and protein loading on the subsequent release profile from PLGA microspheres, For low loadings (ca. 1%), release was dependent on protein MW, while for high loadings, release was independent of protein MW. Release of larger proteins was also dependent on pore interconnectivity, and presumably, pore evolution during erosion, similar to the work by Messaritaki, et al. Since the release of bacteriophage would be expected to occur as for large proteins, defining the underlying mechanisms of release would require detailed studies of pore evolution during microsphere erosion.

Additionally, the encapsulation efficiency of the bacteriophages, inferred from the release profiles near plateau, was around 18% and 27% for bacteriophages selective for *S. aureus* and *P. aeruginosa*, respectively. While this would suggest that the majority of the bacteriophages were lost during encapsulation (as describe in Session 4.1.5), the

apparent losses observed here are consistent with the encapsulation efficiency of some proteins (Bouissou, et al., 2004); though values for encapsulation efficiency are known to vary considerably depending on emulsification protocol and the nature of the drug entrapped (Castellanos, et al., 2001). It is noteworthy that the interaction between protein and polymer also enhance the encapsulation efficiency (Boury, et al., 1997). For example, proteins are generally capable of ionic interactions (dependent on their iso-electric point, pI, and buffer pH), so the encapsulated material with ionic charge is carefully considered. It is not possible at this stage to calculate a pI-equivalent value for the bacteriophage in this study since their molecular structure is not known. Nevertheless, a study of phage-polymer interactions would be interesting, as discussed above with respect to the rapid inactivation of entrapped phage during storage.

4.2. Stabilisation of bacteriophage during freeze drying

4.3.1. Morphology and lytic activity of bacteriophage

The lytic activity of the bacteriophages encapsulated in the microspheres was lost rapidly (within 7 days) while the results for lyophilised phage from Table 3.10-3.12 shows that the loss of lytic activity for both bacteriophages occurred after 30 days of storage at 4 °C. A loss of stability over this period is consistent with other work showing that the half-life of bacteriophage λ at 20 °C was 20 days, although assessment of the stability of bacteriophage λ at 4 °C was not performed (Jepson and March, 2004). Bacteriophages are classified to many types, such as tailed phage, poly hedral phages, filamentous phages, and pleomorphic phages. As noted by Ackermann, differing families of bacteriophage show distinct stabilities, with the 'tailed phages' seen to be most stable during long-term storage (Ackermann, et al., 2004). As shown in Figure 3.10, both bacteriophages used in this study were tailed phages.

It was interesting to note that the inclusion of gelatin did not appear to be beneficial in these studies. Rather than acting as a stabiliser during lyophilisation, the inclusion of gelatin was slightly detrimental to the stability of the bacteriophage, particularly phage active against *S. aureus*. From previous lyophilisation studies (Engel, et al., 1974), role of gelatin as a stabiliser is not entirely clear, and it is most likely that the inclusion of 5% sodium glutamate stabilized the freeze-dried bacteriophages. Yosha et al. (2008) also used the gelatin as a stabiliser for alginate bead preparation to stabilized emulsion droplet during incorporation of protein. However, gelatin is not successful to stabilise the lyophilised recombinant human growth hormone (rhGH) since the recovery of native rhGH from gelatin is less than using trehalose as a stabiliser in lyophilisation of this protein (Cleland and Jones, 1996). Therefore, there was no sound reason to include gelatin in the media immediately prior to lyophilisation of the particular bacteriophages under study, allowing the effect of sucrose and PEG to be studied in isolation.

The effect of the different excipients may be explained by comparison of their structure and mechanism of stabilisation. Lyo- and cryo-protection afforded by sucrose is thought to occur through its preferential exclusion from the protein/polypeptide surface (Kendrick, et al., 1997), thermodynamically favoring the folded state (Lee and Timasheff, 1981), or via hydrogen bonding with polar groups on the protein surface (Allison, et al., 1999). The level of stabilisation afforded by sugars is usually dependent on their bulk concentration.

The stabilisation mechanism of PEG may also occur through preferential exclusion wherein the PEG molecules remain randomly coiled and excluded from the protein surface, which in turn in preferentially hydrated (Bhat and Timasheff, 1992). However, PEG also appears to undergo hydrophobic interactions with non-polar protein residues, in contrast to sucrose (Lee and Lee, 1981). This leads to destabilisation of the system, phase separation and protein precipitation. The same underlying PEG-phage nonpolar interactions may therefore have a similar destabilized effect, though this requires further investigation. With the steric effect of PEG as above regarding the preferential hydration mechanism, it is possible that the interference of the interaction between bacteriophage and bacteria take place. So it is logical that the bacteriophage do not properly bind to the surface of specific/target bacteria resulting in less lytic activity with the addition PEG as shown in Table 3.11 and 3.12.

With the results in Table 3.10-3.12, the greater bacteriophage lytic activity in the extended drying cycle (primary and secondary) has been presented. The effect of the lyophilisation cycle was less clear and dependent on the bacteriophage. The review of Simpson (2010) suggests that 1 M sucrose can retain protein activity and prevent protein aggregation. However, in this study a higher concentration of sucrose caused a greater loss of lytic activity (Table 3.12). In practice there would appear to be little affect of the length of the secondary drying cycle on the final stability of bacteriophage freeze-dried

in the presence of 0.1 M sucrose. From a manufacturing perspective, the length of a typical secondary drying cycle makes this step relatively costly, so if an additive is desired an optimal formulation from the point of view of stability may be 0.1 M sucrose.

4.3.2. Physical characterization of freeze-dried bacteriophage/cakes

The appearance of the cake for bacteriophage lyophilised from storage media was poor, being entirely collapsed (Figure 3.11). The intention of adding a non-protein stabiliser was to produce a pharmaceutically acceptable, elegant freeze-dried cake for reconstitution. The cakes observed for bacteriophage lyophilised from 0.5 M sucrose and 5% PEG 6000 remained stable after pressure and temperature equilibration. It was noted that the bacteriophage themselves caused collapse of the cake for lower concentrations of sucrose (Figure 3.11), and the same effect was seen for 1% PEG 6000.

The cake appearance has shown that the collapse happen either in medium solution alone or in low concentration of additives (sucrose and PEG 6000). Therefore, high concentrations of PEG and sucrose are required to stabilise freeze-dried cakes containing bacteriophage. Similar behaviour is seen for lyophilised protein formulations (Pereira, et al., 2007). Note that an initial supercooling step was included wherein the shelf (not sample) temperature was lowered to −5 ^{o}C prior to further cooling to −30 ^{o}C at a moderate rate of 1 ^{o}C/min, slightly above the T_g of sucrose (−32 ^{o}C). The intention of this step was to improve the homogeneity of ice crystallization. Previous work has shown that supercooling and ice nucleation temperatures, but not cooling rates between 0.05 and 1^{o} C/min, are linked to the rate of primary drying (Searles, et al., 2001). The effect of this supercooling/ice nucleation step on phage adsorption to the ice/water interface and lytic activity needs to be determined. Ideally, the temperature during primary drying should remain below the T_g of sucrose but this also increases cycle time/cost. Collapse phenomenon can occur during primary drying above the

experimentally determined collapse temperature, due to loss of porous structure of an amorphous sample, but the stability of a protein may not always be affected by the collapse of the cake (Schersch, et al., 2010). Furthermore, there is no evidence to show that the aggregation happen from DLS and CLSM although the collapse appearance is seen from the images of bacteriophage freeze-dried cake.

4.2.3. Residual moisture content of the freeze-dried formulations

The glass transition temperature relates to glassy state of the amorphous formulation and its residual moisture content (Bell, et al., 1995). Increasing the moisture content in a formulation will decrease the Tg (the plasticizing effect of water). In this experiment, at 0.5 M sucrose, decreasing the moisture content of freeze-dried bacteriophage formulation relates to an increase in Tg. However, over drying of protein will also cause loss of stability (Hsu, et al., 1992). So an optimized moisture content, stability and bioactivity are required for each study.

As shown in Figure 3.21, the outlying value of moisture content (10.75% for storage media, without gelatin) may be due to the relatively low cake mass and poor porosity for drying. However, this large deviation does not change the overall trend observed. Correlating the data for the moisture content of the cakes with the corresponding lytic activities of the bacteriophages highlights the upper and lower limits for a ‘target’ moisture content for optimal retention of bacteriophage activity, which is broadly in agreement with previous data for lyophilised proteins (Jiang and Nail, 1998; Breen, et al., 2001).

It is interesting that higher concentrations of PEG or sucrose had lower residual moisture content of the final freeze-dried cakes following lyophilisation. This must indicate that the drying process for the higher concentration additives was more efficient. Similarly,

the residual water content of the cakes containing PEG alone (the controls) was much less than for PEG with bacteriophage. In both cases this can be explained by reference to the final appearance of the corresponding cakes (Figure 3.12 and 3.14). Clearly, in cases of collapse of the cake, that is, for addition of bacteriophage to 1% PEG and for 0.1 M sucrose, there will inevitably be a loss of porosity within the cake. Since efficient loss of non-frozen water during the secondary drying cycle is dependent on the maintenance of the porous structure of the cake, loss of porosity will result in higher residual moisture contents under the same lyophilisation procedure. Therefore, optimization of freeze-dried bacteriophage products would ideally include monitoring of the residual moisture content *in situ*, to a final moisture content of 4-6%, in this case.

4.3. *In vivo* studies

4.3.1. The rat model for bacteriophage therapy

4.3.1.1. Encapsulation of P. aeruginosa in agarose beads

The size of the agarose beads is important for tracheal instillation during the procedure. Generally, the diameters of the respiratory tube including trachea and upper bronchi are 1.5-2.5 cm and 4-1 mm, respectively. At the distal airways, the bronchioles have an apparent diameter much less than 1 mm (as shown in Figure 1.6). The average diameters of the *P. aeruginosa*-loaded and blank agarose beads were ~38 and 40 μm, respectively. In previous work, van Heeckeren and Schluchter (2002) fabricated the same agarose beads laden with *P. aeruginosa* but of 120 μm in diameter and reported that these beads successfully induced lung infection to the murine model. However, van Heeckeren and Schluchter used a surgical technique, wherein the trachea was severed and the beads instilled directly, before closure of the wound. In this study we sought to avoid surgery and instead attempted to use the tracheal insufflator device. With bead diameters of any several tens of micrometers, we anticipated that the beads would carry the bacteria to the deep lung and also be injectable through the insufflator device. The high agitation speeds used during emulsion in this study led to the smaller size of agarose bead. In our hands this agitation rate produced the most reproducible batches of beads and the bacteria remained viable. In addition, it was found that the rate of cooling influenced the size and shape of the beads, such that slow cooling produced a larger bead diameter and a greater size distribution. Possible contamination of the agarose beads through use of an aseptic technique (it was not practical to consider an entirely sterile technique) was also considered, with regard to secondary infection or opportunistic infection to the animal. However, the results demonstrated that the agarose beads could be stored at 4 °C up to one day before experiment, without fear of contamination from other bacteria.

4.3.1.2. Establishing lung infection in rats

The intra-tracheal dosing method used was non-invasive and therefore attractive with regard to ease of administration and severity of the procedure for the animal. The method delivers drug directly to the pulmonary system but because it is a 'blind technique', that is, the positioning of the insufflator is done larger by touch, the disadvantage is that different positions with the trachea may lead to inconsistencies and/or low success rate. In this case, the technique was first practiced on schedule-1 sacrificed rats, and was found to be entirely feasible. However, deep sedation of the live rats was required, since recovery from shallow sedation through inhaled halothane was too rapid; i.e. the rats tended to recover before positioning of the insufflator was confidently achieved. The clear advantage of the surgical method of van Heeckeren and Schluchter (2002) then is that consistent and reproducible dosing can be achieved and possibly with equal speed with an experienced surgical technique. In this study, it was clear that the technique was not precise and/or the rat responses to infection were inherently variable. This is in contrast to the van Heeckeren and Schluchter study which showed a correlation between bacterial concentration or number of beads and animal mortality. (Note that in the project licences it was not considered ethical to allow the animals to die of infection, rather the animals had to be sacrified when clearly defined clinical end-points were reached.) Furthermore, insertion of the insufflator device might have caused upper airway trauma and secondary inflammation or infection. Despite this, rats infected in this study did not appear to progress to clinical signs of infection, evidence of local bacterial infection was evident in the histology results. It was decided to move to a simpler model which allowed a greater number of animals to be infected/treated, in order to acquire statistically relevant data by which to assess bacteriophage therapy.

4.3.2. Mouse model for bacteriophage therapy

4.3.2.1. Establishing lung infection in mice

The lethal dose of *P. aeruginosa* determined in this study was 1.41×10^9 CFU/mouse, which is around a 100-fold greater than a recent report which determined an equivalent dose of 1×10^7 CFU/mouse, for a bioluminescent *P. aeruginosa* strain. It is reasonable to note that the difference in bacterial strains may clearly affect the clinical outcome, as of course may the strain of mouse, size and sex. Nevertheless, the bacterial dose required to lethally infect mice is generally distinguished in other studies as being lower: from 10^2 to 10^7 bacteria per animal (McVay, et al., 2007; Heo, et al., 2009; Debarbieux, et al., 2010). It has been previously reported that the mortality of mice depends on the strain of *P. aeruginosa*: a mucoid clinical strain PA M57-15 was found to be less lethal to animals than a mucoid laboratory strain PA 2192 (Van Heeckeren and Schluchter, 2002). It was considered important to establish upper and lower limits with respect to clinical outcomes. Ideally, the mice would become gradually more ill over time, and then recover with treatment. The upper dose of 1.41×10^9 CFU/mice brought the mice to their pre-defined clinical end points too quickly, that is, they were too ill the following day to be lightly aneasthetised and administered with bacteriophage. A 10-fold reduction in the dose was therefore used to define a lower limit. With this bacterial dosing, it was found that the mice did not present clinical signs and therefore recovery (or absence of) would be difficult to define. The intermediate dose (5.7×10^9 CFU/mouse) was found to cause clear clinical symptoms of infection without bringing the mice to end point symptoms. This dose was therefore used for investigation of bacteriophage therapy.

The clinical symptoms of infection were corroborated by histopathology. At high and intermediate doses of bacterial inoculation, the alveolar airspaces became filled with inflammatory cells and neutrophils, indicating a severe infection in the lung. Concomitant changes to the bronchioles, particularly a thickening of the wall were also

observed. Miyazaki and co-workers (2004) reported that the destruction or the alveolar walls (bringing about a coalescence) is mediated by proteolytic events and epithelial apoptosis. In particular infiltration by neutrophils and release of elastase which digests the basement membrane. It is also known that elastase is secreted by mucoid *P. aeruginosa* as part its pathogenic mechanism and virulence (Bejarano, et al., 1989). Oxidants produced in response to the bacterial infection have also been implicated in the destruction of the alveolar airspaces, loss of the alveolar septum and airspace enlargement (Taraseviciene-Stewart and Voelkel, 2008). Such coalescence of the alveoli and oedema would naturally lead to laboured breathing which was observed in mice succumbing to infection. The key clinical 'marker' used however was weight loss, with around 10% reduction in body commonly being observed before recovery in mice receiving an intermediate dose of bacteria. Body temperature was also monitored using an off-the-shelf digital thermometer, though more accurate and frequent data could in future be acquired with microchip transponders measuring subcutaneous tissue temperature. While the clinical and histological examination of tissue sections provided firm evidence of widespread infection in the lung, further work could also focus on other organs (i.e. the spread of infection) and/or the immune responses.

4.3.2.2. Bacteriophage therapy: treatment of infected mice.

The inherent toxicity of bacteriophage selective for *P. aeruginosa* was examined by intra-nasal administration of bacteriophage solutions. In this case, normal lung tissue was found from histological examination of lung sections, including the epithelium of the alveoli and bronchioles. These results are consistent with a recent toxicity study of bacteriophage lysate in chickens - the phage lysate being administered by intramuscular injection and clinical symptoms being monitored thereafter (Oliveira, et al., 2009). Over a 6 day period, the level of activity of the treated chickens was no different compared to the control group, indicating that the bacteriophage lysate was not toxic.

The histology and, particularly, the bacteriology of the infected lung revealed that bacteriophage treatment significantly reduced the bacterial load in the lung tissue. Neutrophil infiltration commonly found in lung sections and is a hallmark of bacterial infection, typical in chronic CF (Lyczak, et al., 2002). Neutrophil and macrophage infiltration of tissue was also observed in the infected mouse lung chronically exposed to pyocyanin (the green pigment) from *P. aeruginosa* strain PA01, the numbers of neutrophils significantly increased at weeks 6 and 12 (Caldwell, et al., 2009). As described above, destruction of the alveolar airspace and coalescence was clearly seen, so despite bacteriophage treatment, damage to the lung (e.g. loss of elasticity) was not prevented.

The bacteriology results suggested that intranasal administration of bacteriophage post-infection was more effective in clearance of bacteria than nebulisation, although the difference between the data were not significantly different ($p > 0.05$). Debarbieux and co-workers (2010) also reported that the bacteriophage instillation of infected Balb/c mice with luminescent bacteria provided the 100% survival of the infected animals. They also suggested that bacteriophage treatment should be provided with 2 hours post-infection. In this study, bacteriophage treatment was provided 24 h after infection, the longer incubation time would clearly facilitate establishment of the lung infection. Interestingly, the bacteriophage and bacteria used has ratio less than 1:10 due to the longer incubation time of bacteria in animal so it may cause of shorten survival of animal in this study (< 5 days). Similarly, Debarbieux and co-workers (2010) also noted that the ratio 1:10 of bacteriophage to bacteria provided the survival of animal within 5 days. With the higher ratio such as 1:1, mice would survive until day 12 of experiment. It indicated that the bacteriophage 1×10^9 pfu/mouse is not enough to treat the bacteria infection (with the initial amount 5×10^8 CFU/mouse) after 24 h. Moreover the lactate dehydrogenase showing the lung damage was also found equally between non-phage treated mice and phage-treated mice (3.7 and 3.1-fold, respectively) within 6 h of infection (Debarbieux, et al., 2010). It asserted that the duration we used (24 h) is too

long it may be cause of severe lung damage/infection whereas the dose of bacteriophage is not sufficient for this stage of infection.

The mucoid nature of the *P. aeruginosa* strain must also be considered, particularly with regard to the timing of bacteriophage treatment, since after overnight incubation *in vitro* mucoid colonies are clearly seen. As briefly mentioned previously, *P. aeruginosa* exopolysaccharide contributes to the aetiology of CF since it increases mucous viscosity and evokes an immune response (Pedersen, et al., 1990). The exopolysaccharide produced by mucoid strains confers added resistance to antibiotics and phagocytes by functioning as a physical or electrostatic barrier (Hoiby, 2002). Digestion of the exopolysaccharide with alginase increased diffusion of aminoglycosides (Hatch and Schiller, 1998), and a reduction in alginate viscosity facilitated phage penetration of biofilms (Hanlon, et al., 2001). Thus, the inability of the bacteriophage to eradicate the lung infection in mice may simply have been their inability to pass the mucoid barrier, which would be present after overnight incubation. This has implications for bacteriophage therapy of CF patients, since chronic infection in associated with mucoid strains. Future work then may well consider adjuvant therapy, not only with conventional antibiotics but also with an alginase which can break down the exopolysaccaride.

It was disappointing to see a high variability and apparent severity of infection for groups of mice receiving freeze dried bacteriophage formulations: either with or without 1% PEG as stabiliser. It can be interpreted that freeze-drying attenuates the lytic activity of the phage, and this is consistent with our *in vitro* data. However, this would not explain the high variability in these groups, which at present would require further experimentation to resolve.

Chapter 5: Conclusions and future work

5.1. Conclusions

The lytic activity of bacteriophage can be maintained during encapsulation within biodegradable polymer (PLGA) if the addition of phage is made to the external aqueous phase during the w/o/w emulsion-solvent extraction method. The modified emulsion protocol alters the microsphere morphology from a dimpled, hollow capsule to a macroporous internal matrix and smooth surface. The distribution study showed that the bacteriophages were entirely encapsulated within the microspheres, rather than on the surface of microspheres. The release profile showed an initial burst release over 30 min (55-63% of the total encapsulated) followed by slow sustained release to plateau at 6 h. The aerodynamic diameter of the microspheres containing bacteriophage was less than 4 µm, which would in principle allow the formulation to reach the lung periphery on inhalation. However, we found that the stability of the encapsulated bacteriophage was less than 7 days, either at 4 ^{o}C or 22 ^{o}C of storage.

Thus, a lyophilised bacteriophage formulation was developed to improve long term stability, optimising both the lyophilisation process and the excipients. We concluded that the lytic activity of the freeze dried bacteriophage was independent of the gelatin content in the storage medium. Sucrose would be a good candidate for bacteriophage lyophilisation since the retained lytic activity was greater than for PEG 6000. However, there was no need to add stabilisers to prolong the stability of the bacteriophage. High concentrations of additives (0.5 M sucrose and 5% PEG 6000) prevented collapse of the lyophilised cake, although the lytic activity of bacteriophage rapidly declined. Extension of the secondary drying cycle and addition of PEG 6000 yielded a lyophilised cake with a residual moisture content less than 4-6%. Changes in the activity of the lyophilised

bacteriophages correlated best with the moisture content of the cake; the interpretation being that a 4-6% moisture content is optimal for the bacteriophages studied here.

In the murine model of lung infection, treatment with bacteriophage solution administered either intra-nasally or by nebulisation reduced the bacterial load in the lung. This implied that phage therapy may be effective in lung infection. Unfortunately the reconstituted, formulated bacteriophage did not reduce the bacterial load.

5.2. Future work

Further development of microspheres containing bacteriophage should focus on improving the stability of the bacteriophage. It may be useful to modify the encapsulation method to increase the encapsulation efficiency and prevent the loss of bioactivity of bacteriophage. Furthermore, the deposition of the microspheres to the lung *in vivo* should be considered using imaging techniques.

Further studies on freeze-dried bacteriophage should focus on achieving a non-collapsed cake for as low an additive concentration as possible, monitoring the residual moisture content and the collapse temperature during lyophilisation *in situ*.

In further work, the monitoring of disease progression should be performed carefully with both the scoring system and a whole live-animal imaging system. The scoring system should consider the lethal dose of infection, but for monitoring disease progression, the imaging system would be necessary. In addition, the intensity of infection in the lung can also be visualized, so that data for pre and post treatment can be compared. Examination of the inflammatory responses, such as measurement of cytokines, would also support the histopathology results.

BIBLIOGRAPHY

Ackermann, H.W. (2003). Bacteriophage observations and evolution. *Research in Microbiology, 154* (4), 245-251.

Ackermann, H.W. (2005). Bacteriophage classification. In Kutter, A., Sulakvelidze, E. (eds.), *Bacteriophages: Biology and Applications*, CRC Press. Florida: 67-89.

Ackermann, H.W., Tremblay, D., Moineau, S. (2004). Long-term bacteriophage preservation. *World Federation for Culture Collections Newsletter, 38*, 35-40.

Alexis, N.E., Muhlebach, M.S., Peden, D.B., Noah, T.L. (2006). Attenuation of host defense function of lung phagocytes in young cystic fibrosis patients. *Journal of Cystic Fibrosis, 5*, 17-25.

Allison, S.D., Chang, B., Randolph, T.W., Carpenter, J.F. (1999). Hydrogen bonding between sugar and protein is responsible for inhibition of dehydration-induced protein unfolding. *Archives of Biochemistry and Biophysics, 365* (2), 289-298.

Allison, S.D., Dong, A., Carpenter, J.F. (1996). Counteracting effects of thiocyanate and sucrose on chymotrypsinogen secondary structure and aggregation during freezing, drying, and rehydration. *Biophysical Journal, 71* (4), 2022-2032.

Allison, S.D., Randolph, T.W., Manning, M.C., Middleton, K., Davis, A., Carpenter, J.F. (1998). Effects of drying methods and additives on structure and function of

actin: mechanisms of dehydration-induced damage and its inhibition. *Archives of Biochemistry and Biophysics, 358* (1), 171-181.

Amin, K., Dannenfelser, R., Zielinski, J., Wang, B. (2004). Lyophilization of polyethylene glycol mixtures. *Journal of Pharmaceutical Sciences, 93* (9), 2244-2249.

Amin, R., Subbarao, P., Jabar, A., Balkovec, S., Jensen, R., Kerrigan, S., Gustafsson, P., Ratjen, F. (2010). Hypertonic saline improves the LCI in paediatric patients with CF with normal lung function. *Thorax, 65* (5), 379-383.

Armstrong, D.S., Hook, S.M., Jamsen, K.M., Nixon, G.M., Carzino, R., Carlin, J.B., Robertson, C.F., Grimwood, K. (2005). Lower airway inflammation in infants with cystic fibrosis detected by newborn screening. *Pediatric Pulmonology, 40* (6), 500-510.

Arshady, R. (1991). Preparation of biodegradable microspheres and microcapsules: 2. Polyactides and related polyesters. *Journal of Controlled Release, 17* (1), 1-22.

Aso, Y., Yoshioka, S., Po, A., Terao, T. (1994). Effect of temperature on mechanisms of drug release and matrix degradation of poly(d,l-lactide) microspheres. *Journal of Controlled Release, 31* (1), 33-39.

Babalova, E.G., Katsitadze, K.T., Sakvarelidze, L.A., Imnaishvili, N.Sh., Sharashidze, T.G., Badashvili, V.A., Kiknadze, G.P., Meĭpariani, A.N., Gendzekhadze, N.D., Machavariani, E.V., Gogoberidze, K.L., Gozalov, E.I., Dekanosidze, N.G. (1968).

Preventive value of dried dysentery bacteriophage. *Zhurnal Mikrobiologii, Epidemiologii, i Immunobiologii, 45* (2), 143-145.

Bailey, A. G. (1997). The inhalation and deposition of charged particles within the human lung. *Journal of Electrostatics, 42*, 25-32.

Banerjee, D., Stableforth, D. (2000). The treatment of respiratory pseudomonas infection in cystic fibrosis: what drug and which way? *Drugs, 60* (5), 1053-1064.

Barman, S.P., Lunsford, L., Chambers, P., Hedley, M.L. (2000). Two methods for quantifying DNA extracted from poly(lactide-co-glycolide) microspheres. *Journal of Controlled Release, 69* (3), 337-344..

Bartlett, J., Fischer, A., McCray, P.J. (2008). Innate immune functions of the airway epithelium. *Contribution to Microbiology, 15*, 147-163.

Batycky, R., Hanes, J., Langer, R., Edwards, D. (1997). A theoretical model of erosion and macromolecular drug release from biodegrading microspheres. *Journal of Pharmaceutical Sciences, 86* (12), 1464-1477.

Beaulac, C., Clément-Major, S., Hawari, J., Lagacé, J. (1996). Eradication of mucoid Pseudomonas aeruginosa with fluid liposome-encapsulated tobramycin in an animal model of chronic pulmonary infection. *Antimicrobial Agents Chemotherapy, 40* (3), 665-669.

Bejarano, P., Langeveld, J., Hudson, B., Noelken, M. (1989). Degradation of basement membranes by Pseudomonas aeruginosa elastase. *Infection and Immunity, 57* (12), 3783–3787.

Bell, L.N., Hageman, M. J., Muraoka, L.M. (1995). Thermally induced denaturation of lyophilised bovine somatotropin and lysozyme as impacted by moisture and excipients. *Journal of Pharmaceutical Sciences, 84* (6), 707-712.

Benita, S., Benoit, J.P., Puisieux, F., Thies, C. (1984). Characterization of drug-loaded poly (d, l-lactide) microspheres. *Journal of Pharmaceutical Sciences, 73* (12), 1721-1724.

Bhat, R., Timasheff, S. (1992). Steric exclusion is the principal source of the preferential hydration of proteins in the presence of polyethylene glycols. *Protein Science, 1* (9), 1133-1143.

Bienenstock, J., Johnston, N. (1976). A morphologic study of rabbit bronchial lymphoid aggregates and lymphoepithelium. *Laboratory Investigation, 35* (4), 343-348.

Billon, A., Chabaud, L., Gouyette, A., Bouler, J.M., Merle, C. (2005). Vancomycin biodegradable poly (lactide-co-glycolide) microparticles for bone implantation. Influence of the formulation parameters on the size, morphology, drug loading and in vitro release. *Journal of Microencapsulation, 22* (8), 841-852.

Bjarnsholt T,J.P., Hansen, C., Andersen, C., Pressler, T., Givskov, M., Høiby, N. (2009). Pseudomonas aeruginosa biofilms in the respiratory tract of cystic fibrosis patients. *Pediatric Pulmonology, 44* (6), 547-558.

Blanco, D., Alonso, M.J. (1998). Protein encapsulation and release from poly (lactide-co-glycolide) microspheres: effect of the protein and polymer properties and of the co-encapsulation of surfactants. *European Journal of Pharmaceutics and Biopharmaceutics, 45* (3), 285-294.

Bogovazova, G., Voroshilova, N., Bondarenko, V., Gorbatkova, G., Afanas'eva, E., Kazakova, T., et al. (1992). Immunobiological properties and therapeutic effectiveness of preparations from Klebsiella bacteriophages. *Zhurnal Mikrobiologii, Epidemiologii, i Immunobiologii, 3*, 30-33.

Boucher, R. (2004). New concepts of the pathogenesis of cystic fibrosis lung disease. *The European Respiratory Journal, 23* (1), 146-158.

Bouissou, C., Potter, U., Altroff, H., Mardon, H., van der Walle, C. F. (2004). Controlled release of the fibronectin central cell binding domain from polymeric microspheres. *Journal of Controlled Release, 95* (3), 557-566.

Boury, F., Marchais, H., Proust, J. E., Benoit, J. (1997). Bovine serum albumin release from poly(α-hydroxy acid) microspheres: effects of polymer molecular weight and surface properties. *Journal Controlled Release, 45* (1), 75-86.

Brady, J. M., Cutright, D. E., Miller, R., Barristone, G. (1973). Resorption rate, route, route of elimination, and ultrastructure of the implant site of polylactic acid in the

abdominal wall of the rat. *Journal of Biomedical Materials Research, 7* (2), 155-166.

Braqonzi, A., Conese, M. (2002). Non-viral approach toward gene therapy of cystic fibrosis lung disease. *Current Gene Therapy, 2* (3), 295-305.

Breen, E., Curley, J., Overcashier, D., Hsu, C., Shire, S. (2001). Effect of moisture on the stability of a lyophilized humanized monoclonal antibody formulation. *Pharmaceutical Research, 18* (9), 1345-1353.

Brennan, S., Sly, P.D., Gangell, C.L., Sturges, N., Winfield, K., Wikstrom, M., Gard, S., Upham, J.W.; Arest CF.(2009). Alveolar macrophages and CC chemokines are increased in children with cystic fibrosis. *The European Respiratory Journal, 34* (3), 655-661.

Brody, S., Metzger, M., Danel, C., Rosenfeld, M., Crystal, R. (1994). Acute responses of non-human primates to airway delivery of an adenovirus vector containing the human cystic fibrosis transmembrane conductance regulator cDNA. *Human Gene Therapy, 5* (7), 821-836.

Byron, P.R., Patton, J.S. (1994). Drug delivery via the respiratory tract. *Journal of aerosol medicine, 7*(1), 49-75.

Cairns, B.J., Timms, A.R., Jansen, V.A.A., Connerton, I.F., Payne, R.J.H. (2009). Quantitative Models of In vitro Bacteriophage-Host Dynamics and Their Application to Phage Therapy. *PLoS Pathogens, 5*, e1000253.

Caldwell, C.C., Chen, Y., Goetzmann, H.S., Hao, Y., Borchers, M.T., Hassett, D.J., Young, L.R., Mavrodi, D.,Thomashow, L., Lau, G.W. (2009). Pseudomonas aeruginosa exotoxin pyocyanin causes cystic fibrosis airway pathogenesis. *The American Journal of Pathology, 175* (6), 2473-2488.

Cantin, A.M., Woods, D.E. (1999). Aerosolized prolastin suppresses bacterial proliferation in a model of chronic Pseudomonas aeruginosa lung infection. *American Journal of Respiratory and Critical Care Medicine, 160* (4), 1130-1135.

Capan, Y., Woo, B.H., Gebrekidan, S., Ahmed, S., DeLuca, P.P. (1999). Influence of formulation parameters on the characteristic of poly (D, L-lactide-co-glycolide) microspheres containing poly (L-lysine) complexed plasmid DNA. *Journal of Controlled Release, 60* (2-3), 279-286.

Caplen, N.J., Alton, E.W., Middleton, P.G., Dorin, J.R., Stevenson, B.J., Gao, X., Durham, S.R., Jeffery, P.K., Hodson, M.E., Coutelle, C. et al. (1995). Liposome-mediated CFTR gene transfer to the nasal epithelium of patients with cystic fibrosis. *Nature Medicine, 1* (1), 39-46.

Capparelli, R., Parlato, M., Borriello, G., Salvatore, P., Iannewlli, D. (2007). Experimental phage therapy against Staphylococcus aureus in Mice. *Antimicrobial Agents and Chemotherapy, 51* (8), 2765-2773.

Careri, G., Giansanti, A., Gratton, E. (1979). Lysozyme film hydration events: an IR and gravimetric study. *Biopolymers, 18*, 1187-1203.

Carpenter, J.F., Crowe, J.H., Arakawa, T. (1990). Comparison of Solute-Induce Protein Stabilization in Aqueous Solution and in the Frozen and Dried States. *Journal of Diary Science, 73* (12), 3627-3636.

Cash, H.A., Woods, D.E., McCullough, B., Johanson, W.G., Bass, J.A. (1979). A rat model of chronic respiratory infection with Pseudomonas aeruginosa. *The American Review of Respiratory Disease, 119* (3), 453-459.

Castellanos, I., Carrasquillo, K., Lopez, J.D., Alvarez, M., Griebenow, K. (2001). Encapsulation of bovine serum albumin in poly(lactide-co-glycolide) microspheres by the solid-in-oil-in-water technique. *The Journal of Pharmacy and Pharmacology, 53*, 167-178.

Cavalier, M., Benoit, J.P., Thies, C. (1986). The formation and characterization of hydrocortisone-loaded poly ((+/-)-lactide) microspheres. *The Journal of Pharmacy and Pharmacology, 34* (4), 249-253.

Chang, B.S., Reeder, G., carpenter, J.F. (1996). Development of a stable freeze-dried formulation of recombinant human interleukin-1 receptor antagonist. *Pharmaceutical Research, 13*, 243-249.

Chang, L., Shepherd, D., Sun, J., Tang, X., Pikal, M. (2005). Effect of sorbitol and residual moisture on the stability of lyophilized antibodies: Implications for the mechanism of protein stabilization in the solid state. *Journal of Pharmaceutical Sciences, 94* (7), 1445-1455.

Chapin, K.C., Lauderdale, T.L. (2007). Reagents, Stains, and Media: Bacteriology. In Murray, P.R. (ed.), *Manual of Clinical Microbiology*. 9th ed. ASM Press. Washington D.C.: 334-338.

Chen, A., Pu, X., Kang, Y., Liao, L., Yao, Y., Yin, G. (2007). Study of poly(L-lactide) microparticles based on supercritical CO2. *Journal of Materials Science. Materials in Medicine, 18* (12), 2339-2345.

Chen, B., Costantino, H., Liu, J., Hsu, C., Shire, S. (1999). Influence of calcium ions on the structure and stability of recombinant human deoxyribonuclease I in the aqueous and lyophilized states. *Journal of Pharmaceutical Sciences, 88* (4), 477-482.

Chen, W., Lu, D.R. (1999). Carboplatin-loaded PLGA microspheres for intracerebral injection: formulation and characterization. *Journal of Microencapsulation, 16* (5), 551-563.

Chew, N.Y., Chan, H.K. (2001). Use of solid corrugated particles to enhance powder aerosol performance. *Pharmaceutical Research, 18* (11), 1570-1577.

Chew, N.Y., Tang, P., Chan, H.K., Raper, J.A. (2005). How much particle surface corrugation is sufficient to improve aerosol performance of powders? *Pharmaceutical Research, 22* (1), 148-152.

Chmiel, J.F., Konstan, M.W., Knesebeck, J.E., Hilliard, J.B., Bonfield, T.L., Dawson, D.V., Berger, M. (1999). IL-10 attenuates excessive inflammation in chronic Pseudomonas infection in mice. *American Journal of Respiratory and Critical Care Medicine, 160* (6), 2040-2047.

Ciofu, O., Bagge, N., Høiby, N. (2002). Antibodies against beta-lactamase can improve ceftazidime treatment of lung infection with beta-lactam-resistant Pseudomonas aeruginosa in a rat model of chronic lung infection. *Acta Pathologica, Microbiologica, et Immunologica Scandinavica, 110* (12), 881-891.

Cisło, M., Dabrowski, M., Weber-Dabrowska, B., Woytoń, A. (1987). Bacteriophage treatment of suppurative skin infections. *Archivum Immunologiae et Therapiae Experimentalis, 35* (2), 175-83.

Clancy, J. (2009). Clinical trials of lipid-associated aerosolized amikacin: the AeikaceTM story. *Pediatric Pulmonology, 44* (32(suppl)), 186-187.

Cleland, J.L. (1997). Protein delivery from biodegradable microspheres. *Pharmaceutical Biotechnology, 10*, 1-43.

Cleland, J.L., Jones, A.J. (1996). Stable Formulations of Recombinant Human Growth Hormone and Interferon Gramma for microencapsulation in biodegradable microspheres. *Pharmaceutical Research, 13* (10), 1464-1475.

Cleland, J.L., Lam, X., Kendrick, B., Yang, J., Yang, T.H., Overcashier, D., Brooks, D., Hsu, C., Carpenter, J.F. (2001). A specific molar ratio of stabilizer to protein is required for storage stability of a lyophilized monoclonal antibody. *Journal of Pharmaceutical Sciences, 90* (3), 310-21.

Corveleyn, S., Vandenbossche, G., Remon, J. (1997). Near-infrared (NIR) monitoring of H2O2 vapor concentration during vapor hydrogen peroxide (VHP) sterilisation. *Pharmaceutical Research, 14* (3), 294-298.

Crotts, G., Park, T.G. (1997). Stability and release of bovine serum albumin encapsulated within poly(D,L-lactide-co-glycolode) microparticles. *Journal of Controlled Release, 44*, 123-134.

Crowe, J.H., Carpenter, J.F., Crowe, L.M. (1998). The role of vitrification in anhydrobiosis. *Annual Review of Physiology, 60*, 73-103.

Dagenais, A., Gosselin, D., Guilbault, C., Radzioch, D., Berthiaume, Y. (2005). Modulation of epithelial sodium channel (ENaC) expression in mouse lung infected with Pseudomonas aeruginosa. *Respiratory Research, 6*, 2-10.

Dancer, S.J., Robb, A., Crawford, A., Morrison, D. (2003). Oral streptogramins in the management of patients with methicillin-resistant Staphylococcus aureus (MRSA) infections. *The Journal of Antimicrobial Chemotherapy, 51* (3), 731-735.

Darquenne, C., Paiva, M., Prisk, G.K. (2000). Effect of gravity on aerosol dispersion and deposition in the human lung after periods of breath holding. *Journal of Applied Physiology, 89* (5), 1787-1792.

Dauletbaev, N., Lam, J., Eklove, D., Iskandar, M., Lands, L. (2010). Ibuprofen modulates NF-kB activity but not IL-8 production in cystic fibrosis respiratory epithelial cells. *Respiration, 79* (3), 234-42.

Davidson, D.J., Dorin, J.R. (2001). The CF mouse: an important tool for studying cystic fibrosis. *Expert Reviews in Molecular Medicine, 12*, 1-27.

Davies, J.C. (2002). Pseudomonas aeruginosa in cystic fibrosis: pathogenesis and persistence. *Paediatric Respiratory Reviews, 3*, 128-134.

Davies, O., Lewis, A., Whitaker, M., Tai, H., Shakesheff, K., Howdle, S. (2008). Applications of supercritical CO2 in the fabrication of polymer systems for drug delivery and tissue engineering. *Advanced Drug Delivery Reviews, 60* (3), 373-87.

de Boer, R., Knight, A.M., Spinner, R.J., Malessy, M.J., Yaszemski, M.J., Windebank, A.J. (2010). In vitro and in vivo release of nerve growth factor from biodegradable poly-lactic-co-glycolic-acid microspheres. *Journal of Biomedical Materials Research, Part A, Sep 28.* [Epub ahead of print].

Debarbieux, L., Leduc, D., Maura, D., Morello, E., Criscuolo, A., Grossi, O., Balloy, V., Touqi, L. (2010). Bacteriophages can treat and prevent Pseudomonas aeruginosa lung infections. *The Journal of Infectious Diseases, 201* (7), 1096-1104.

Degim, I.T., Celebi, N. (2007). Controlled delivery of peptides and proteins. *Current Pharmaceutical Design, 13* (1), 99-117.

DeGrazio, F., Flynn, K. (1992). Lyophilization closures for protein based drugs. *Journal of Parenteral Science and Technology, 46* (2), 54-61.

Deng, M., Uhrich, K. (2002). Effects of in vitro degradation on properties of poly(DL-lactide-co-glycolide) pertinent to its biological performance. *Journal of Materials Science. Materials in Medicine, 13* (11), 1091-1096.

Dill, K., Alonso, D., Hutchinson, K. (1989). Thermal stabilities of globular proteins. *Biochemistry, 28* (13), 5439-5449.

Ding, W., Shah, N. (2009). Effect of homogenization techniques on reducing the size of microcapsules and the survival od probiotic bacteria therein. *Journal of Food Science, 74*, M231-236.

Donaldson, S., Bennett, W., Zeman, K., Knowles, M., Tarran, R., Boucher, R. (2006). Mucus clearance and lung function in cystic fibrosis with hypertonic saline. *The New England Journal of Medicine, 354* (3), 241-250.

Donlan, R. (2009). Preventing biofilms of clinically relevant organisms using bacteriophage. *Trends in Microbiology, 17* (2), 66-72.

Dorin, J.R., Dickinson, P., Alton, E.W., Smith, S.N., Geddes, D.M., Stevenson, B.J., Kimber, W.L., Fleming, S.,Clarke, A.R., Hooper, M.L. (1992). Cystic fibrosis in the mouse by targeted insertional mutagenesis. *Nature, 359* (6392), 211-215.

Doring, G., Conway, S.P., Heijerman, H.G., Hodson, M.E., Hoiby, N., Smyth, A., Touw, D.J. (2000). Antibiotic against Pseudomonas aeruginosa in cystic fibrosis: a European consensus. *The European Respiratory Journal, 16(4)*, 749-767.

Döring, G., Hoiby, N.C. (2004). Early intervention and prevention of lung disease in cystic fibrosis: a European consensus. *Journal of Cystic Fibrosis, 3* (2), 67-91.

Döring, G., Meisner, C., Stern, M., (2007). A double-blind randomized placebo-controlled phase III study of a Pseudomonas aeruginosa flagella vaccine in cystic

fibrosis patients. *Proceedings of the National Academy of Sciences of the United States of America, 104* (26), 11020-11025.

Downey, D.G., Martin, S.L., Dempster, M., Moore, J.E., Keoqan, M.T., Starcher, B., Edgar, J., Bilton, D., Elborn, J.S. (2007). The relationship of clinical and inflammatory markers to outcome in stable patients with cystic fibrosis. *Pediatric Pulmonology, 42* (3), 216-220.

Drenkard, E., Ausubel, F.M. (2002). Pseudomonas biofilm formation and antibiotic resistance are linked to phenotypic variation. *Nature, 416* (6882), 740-743.

Duddu, S., Zhang, G., Dal Monte, P. (1997). The relationship between protein aggregation and molecular mobility below the glass transition temperature of lyophilized formulations containing a monoclonal antibody. *Pharmaceutical Research, 14* (5), 596-600.

Duncan, G., Jess, T.J., Mohamed, F., Price, N.C., Kelly, S.M., van der Walle, C.F. (2005). The influence of protein solubilisation, conformation and size on the burst release from poly(lactide-co-glycolide) microspheres. *Journal of Controlled Release, 110* (1), 34-48.

Dunn, M.M., Toews, G.B., Hart, D., Pierce, A.K. (1985). The effects of systemic immunization of pulmonary clearance of Pseudomonas aeruginosa. The *American Review of Respiratory Disease, 131* (3), 426-431.

Dunne, M., Bibby, D.C., Jones, J.C., Cudmore, S. (2003). Encapsulation of protamine sulphate compacted DNA in polylactide and polylactide-co-glycolide microparticles. *Journal of Controlled Release, 92*, 209-219.

Eberl, L. (2006). Quorum sensing in the genus Burkholderia. *International Journal of Medical Microbiology, 296* (2-3), 103-110.

Edwards, D.A., Ben-Jebria, A., Langer, R. (1998). Recent advances in pulmonary drug delivery using large, porous inhaled particles. *Journal of Applied Physiology, 85* (2), 379-385.

Edwards, D.A., Hanes, J., Caponnetti, G., Hrkach, J., Ben-Jebria, A., Eskew, M.L., Mintzes, J., Deaver, D., Lotan, N., Langer, R. (1997). Large porous particles for pulmonary drug delivery. *Science, 276* (5320), 1868-1871.

Elkins, M.R., Robinson, M., Rose, B.R., Harbour, C., Moriarty, C.P., Marks, G.B., Belousova, E.G., Xuan, W., Bye, P.T. (2006). A controlled trial of long-term inhaled hypertonic saline in patients with cystic fibrosis. The *New England Journal of Medicine, 354* (3), 229-240.

Engel, H., Smith, L., Berwald, L. (1974). The preservation of mycobacteriophages by means of freeze drying. The *American Review of Respiratory Disease, 109* (5), 561-566.

Faisant, N., Siepmann, J., Benoit, J. (2002). PLGA-based microparticles: elucidation of mechanisms and a new, simple mathematical model quantifying drug release. *European Journal of Pharmaceutical Sciences, 15* (4), 355-366.

Ferron, G. A. (1994). Aerosol properties and lung deposition. *The European Respiratory Journal, 7* (8), 1392-1394.

Finlay, W. H., Gehmlich, M. G. (2000). Inertial sizing of aerosol inhales from two dry powder inhalers with realistic breath patterns versus constant flow rates. *International Journal of Pharmaceutics, 210* (1-2), 83-95.

Fischer, D., Li, Y., Ahlemeyer, B., Krieglstein, J., Kissel, T. (2003). *In vitro* cytotoxicity testing of polycations: influence of polymer structure on cell viability and hemolysis. *Biomaterials, 24*, 1121-1131.

Florence, A. T., Attwood, D. (2006). Emulsions, suspensions and other disperse systems. *Physicochemical Principles of Pharmacy.* 4 th edn. Pharmaceutical Press. London: 229-272.

Flotte, T., Laube, B. (2001). Gene therapy in cystic fibrosis. *Chest, 120* (3 Suppl), 124S-131S.

Flotte, T.R., Afione, S.A., Conrad, C., McGrath, S.A., Solow, R., Oka, H., Zeitin, P.L., Guggino, W.B., Carter, B.J. (1993). Stable in vivo expression of the cystic fibrosis transmembrane conductance regulator with an adeno-associated virus vector. *Proceedings of the National Academy of Sciences of the United States of America, 90* (22), 10613-10617.

Flotte, T.R., Zeitlin, P.L., Reynolds, T.C., Heald, A.E., Pedersen, P., Beck, S., Conrad, C.K., Brass-Ernst, L., Humphires, M., Sullivan, K., Wetzel, R., Taylor, G., Carter, B. J., Guggino, W.B. (2003). Phase I trial of intranasal and endobronchial administration of a recombinant adeno-associated virus serotype 2 (rAAV2)-

CFTR vector in adult cystic fibrosis patients: a two-part clinical study. *Human Gene Therapy, 14* (11), 1079-1088.

Fonesca, F., Passot, S., Lieben, P., Martin, M. (2004). Collapse temperature of bacterial suspensions: the effect of cell type and concentration. *Cryo Letters, 25* (6), 425-434.

Franks, F. (1993). Solid aqueous-solutions. *Pure and Applied Chemistry*, 2527-2537.

Franz, M. N., Cohn, R. C., Wachonowsky-Diakiw, D. M., et al. (1994). Management of children and adults with cystic fibrosis: one center's approach. *Hospital Formulary, 29*, 364-378.

Frederiksen, B., Pressler, T., Hansen, A., Koch, C., Høiby, N. (2006). Effect of aerosolized rhDNase (Pulmozyme) on pulmonary colonization in patients with cystic fibrosis. *Acta Paediatrica, 95* (9), 1070-1074.

Freitas, S., Walz, A., Merkle, H., Gander, B. (2003). Solvent extraction employing a static micromixer: a simple, robust and versatile technology for the microencapsulation of proteins. *Journal of Microencapsulation, 20* (1), 67-85.

Fuchs, H.J., Borowitz, D.S., Christiansen, D.H., Morris, E.M., Nash, M.L., Ramsey, B.W., Rosenstein, B.J., Smith, A.L., Wohl, M.E. (1994). Effect of aerosolized recombinant human DNase on exacerbations of respiratory symptoms and on pulmonary function in patients with cystic fibrosis. The Pulmozyme Study Group. *The New England Journal of Medicine, 331* (10), 637-642.

Gebrekidan, S., Woo, B., DeLuca, P. (2000). Formulation and in vitro transfection efficiency of poly (D, L-lactide-co-glycolide) microspheres containing plasmid DNA for gene delivery. *AAPS PharmSciTech, 1* (4), E28.

Geller, D.E., Konstan, M.W., Smith, J., Noonberg, S.B., Conrad, C. (2007). Novel tobramycin inhalation powder in cystic fibrosis subjects: pharmacokinetics and safety. *Pediatric Pulmonology, 42* (4), 307-313.

Ghaderi, R., Artursson, P., Carlfors, J. (1999). Preparation of biodegradable microparticles using solution-enhanced dispersion by supercritical fluids (SEDS). *Pharmaceutical Research, 16* (5), 676-681.

Ghosal, S., Tayler, C.J., Colledge, W.H., Ratcliff, R., Evans, M.J. (2000). Sodium channel blockers and uridine triphosphate: effects on nasal potential difference in cystic fibrosis mice. *The European Respiratory Journal, 15* (1), 146-150.

Giovaqnoli, S., Blasi, P., Schoubben, A., Rossi, C., Ricci, M. (2007). Preparation of large porous biodegradable microspheres by using a simple double-emulsion method for capreomycin sulfate pulmonary delivery. *International Journal of Pharmaceutics, 333* (1-2), 103-111.

Glavac, D., Ravnik-Glavac, M., Potocnik, U., Dean, M., Wine, J. (2000). Screening methods for cystic fibrosis transmembrane conductance regulator (CFTR) gene mutations in non-human primates. *Pflugers Archive, 439* (3 Suppl), R12-13.

Goddard, C.A., Ratcliff, R., Anderson, J.R., Glenn, E., Brown, S., Gill, D.R., Hyde, S.C., MacVinish, L.J., Huang, L., Higgins, C.F., Cuthbert, A.W., Evans, M.J.,

Colledge, W.H. (1997). A second dose of a CFTR cDNA-liposome complex is as effective as the first dose in restoring cAMP-dependent chloride secretion to null CF mice trachea. *Gene Therapy, 4* (11), 1231-1236.

Golshahi, L., Lynch, K.H., Dennis, J.J., Finlay, W.H. (2010). *In vitro* lung delivery of bacteriophages KS4-M and ΦKZ using dry powder inhalers for treatment of *Burkholderia cepacia* complex and *Pseudomonas aeruginosa* infections in cystic fibrosis. *Journal of Applied Microbiology, 110,* 106-117.

Golshahi, L., Seed, K., Dennis, J.J., Finlay, W.H. (2008). Toward modern inhalational bacteriophage therapy: nebulization of bacteriophages of Burkholderia cepacia complex. *Journal of Aerosol Medicine and Pulmonary Drug Delivery, 21* (4), 351-360.

Gonda, I. (1990). Aerosols for delivery of therapeutic and diagnostic agents to the respiratory tract. *Critical Reviews in Therapeutic Drug Carrier Systems, 6* (4), 273-313.

Göpferich, A. (1996). Mechanisms of polymer degradation and erosion. *Biomaterials, 17* (2), 103-114.

Gould, S.J., Isaacson, P.G. (1993). Bronchus associated lymphoid tissue (BALT) in human fetal and infant lung. *The Journal of Pathology, 169* (2), 229-234.

Grandgirard, D., Loeffler, J.M., Fischetti, V.A., Leib, S.L. (2008). Phage lytic enzyme Cpl-1 for antibacterial therapy in experimental pneumococcal meningitis. *The Journal of Infectious Diseases, 197* (11), 1519-1522.

Graziano, G., Catanzano, F., Riccio, A., Barone, G. (1997). A reassessment of the molecular origin of cold denaturation. *Journal of Biochemistry, 122* (2), 395-401.

Griesenbach, U., Alton, E. (2009). Cystic fibrosis gene therapy: successes, failures and hopes for the future. *Expert Review of Respiratory Medicine, 3* (4), 363-371.

Hanlon, G., Denyer, S., Olliff, C., Ibrahim, L. (2001). Reduction in exopolysaccharide viscosity as an aid to bacteriophage penetration through Pseudomonas aeruginosa biofilms. *Applied and Environmental Microbiology, 67* (6), 2746-2753.

Harms, H.K., Matouk, E., Tournier, G., von der Hardt, H., Weller, P.H., Romano, L., Heijerman, H.G., FitzGerald, M.X., Richard, D., Strandvik, B., Kolbe, J., Kraemer, R., Michaisen, H. (1998). Multicenter, open-label study of recombinant human DNase in cystic fibrosis patients with moderate lung disease. DNase International Study Group. *Pediatric Pulmonology, 26* (3), 155-161.

Harris, M., Firsov, D., Vuagniaux, G., Stutts, M.J., Rossier, B.C. (2007). A novel neutrophil elastase inhibitor prevents elastase activation and surface cleavage of the epithelial sodium channel expressed in Xenopus laevis oocytes. *The Journal of Biological Chemistry, 282* (1), 58-64.

Harrison, F. (2007). Microbial ecology of the cystic fibrosis lung. *Microbiology, 153* (Pt 4), 917-923.

Harvey, B.G., Leopold, P.L., Hackett, N.R., Grasso, T.M., Williams, P.M., Tucker, A.L., Kaner, R.J., Ferris, B., Gonda, I., Sweeney, T.D., Ramalingam, R., Kovesdi, I., Shak, S., Crystal, R.G. (1999). Airway epithelial CFTR mRNA expression in

cystic fibrosis patients after repetitive administration of a recombinant adenovirus. *The Journal of Clinical Investigation, 104* (9), 1245-55.

Hasty, P., O'Neal, W.K., Liu, K.Q., Morris, A.P., Bebok, Z., Shumyatsky, G.B., Jilling, T., Sorscher, E.J., Bradley, A., Beaudet, A.L. (1995). Severe phenotypein mice with termination mutation in exon 2 of cystic fibrosis gene. *Somatic Cell and Molecular Genetics, 21* (3), 177-187.

Hatch, R., Schiller, N. (1998). Alginate lyase promotes diffusion of aminoglycosides through the extracellular polysaccharide of mucoid Pseudomonas aeruginosa. *Antimicrobial Agents and Chemotherapy, 42* (4), 974-977.

Hattori, Y. (2010). development of non-viral vector for cancer gene therapy. *Yakugaku Zasshi, 130* (7), 971-923.

Heller, M., Carpenter, J., Randolph, T. (1997). Manipulation of lyophilization-induced phase separation: implications for pharmaceutical proteins. *Biotechnology Progress, 13* (5), 590-596.

Heller, M., Carpenter, J., Randolph, T. (1999). Conformational stability of lyophilized PEGylated proteins in a phase-separating system. *Journal of Pharmaceutical Sciences, 88* (1), 58-64.

Heller, M., Carpenter, J., Randolph, T. (1999). Protein formulation and lyophilization cycle design: prevention of damage due to freeze-concentration induced phase separation. *Biotechnology and Bioengineering, 63* (2), 166-174.

Henry, R.L., Gibson, P.G., Carty, K., Cai, Y., Francis, J.L. (1998). Airway inflammation after treatment with aerosolized deoxyribonuclease in cystic fibrosis. *Pediatric Pulmonology, 26* (2), 97-100.

Heo, Y., Lee, Y., Jung, H., Lee, J., Ko, G., Cho, Y. (2009). Antibacterial efficacy of phages against Pseudomonas aeruginosa infections in mice and Drosophila melanogaster. *Antimicrobial Agents and Chemotherapy, 53* (6), 2469-2474.

Her, L., Nail, S. (1994). Measurement of glass transition temperatures of freeze-concentrated solutes by differential scanning calorimetry. *Pharmaceutical Research, 11* (1), 54-59.

Herrmann, J., Bodmeier, R. (1995). The effect of particle microstructure on the somatostatin release from poly(lactide) microspheres prepared by a W/O/W solvent evaporation method. *Journal of Controlled Release, 36* (1-2), 63-71.

Heyder, J. (1982). Particle transport onto human airway surfaces. *European Journal of Respiratory Diseases Supplement, 119*, 29-50.

Hickey, A.J., Thompson, D.C. (1992). Physiology of the airways. In Hickey, A. J. (ed.), *Pharmaceutical inhalation aerosol technology*. Marcel Dekker. New York : 1-27.

Hill, J., Shalaev, E., Zografi, G. (2005). Thermodynamic and dynamic factors involved in the stability of native protein structure in amorphous solids in relation to levels of hydration. *Journal of Pharmaceutical Sciences, 94* (8), 1636-1667.

Hodgson, A.E., Nelson, S.M., Brown, M.R., Gilbert, P. (1995). A simple in vitro model for growth control of bacterial biofilms. *The Journal of Applied Bacteriology*, *79* (1), 87-93.

Hodson, M.E., McKenzie,S., Harms, H.K., Koch, C., Mastella, G., Navarro, J., Stranvik, B. (2003). Dornase alfa in the treatment of cystic fibrosis in Europe: a report from the Epidemiologic Registry of Cystic Fibrosis. *Pediatric Pulmonology, 36* (5), 427-432.

Høiby, N. (2002). Understanding bacterial biofilms in patients with cystic fibrosis: current and innovative approaches to potential therapies. *Journal of Cystic Fibrosis, 1*(4), 249-254.

Høiby, N., Bjarnsholt, T., Givskov, M., Molin, S., Ciofu, O. (2010). Antibiotic resistance of bacterial biofilms. *International Journal of Antimicrobial Agents, 35* (4), 322-332.

Hoiby, N., Frederiksen, B., Pressler, T. (2005). Eradiation of early Pseudomonas aeruginosa infection. *Journal of Cystic Fibrosis, 4*, 49-54.

Hooton, J., Jones, M., Harris, H., Shur, J., Price, R. (2008). The influence of crystal habit on the prediction of dry powder inhalation formulation performance using the cohesive-adhesive force balance approach. *Drug Development and Industrial Pharmacy, 34* (9), 974-983.

Hooton, J., Jones, M., Price, R. (2006). Predicting the behavior of novel sugar carriers for dry powder inhaler formulations via the use of a cohesive-adhesive force balance approach. *Journal of Pharmaceutical Sciences, 95* (6), 1288-1297.

Houchin, M., Neuenswander, S., Topp, E. (2007). Effect of excipients on PLGA film degradation and the stability of an incorporated peptide. *Journal of Controlled Release, 117* (3), 413-420.

House, J., Mariner, J. (1996). Stabilisation of rinderpest vaccine by modification of the lyophilization process. *Developments in Biological Standardization, 87*, 235-244.

Hsu, C., Ward, C., Pearlman, R., Nguyen, H., Yeung, D., Curley, J. (1992). Determining the optimum residual moisture in lyophilized protein pharmaceuticals. *Developments in Biological Standardization, 74*, 255-70; discussion 271.

Hug, M. J., Bridges, R. J. (2001). pH regulation and bicarbonate transport of isolated porcine submucosal glands. *Journal of the Pancreas, 2* (4 Suppl), 274-279.

Hyman, P., Abedon, S. (2010). Bacteriophage host range and bacterial resistance. *Advances in Applied Microbiology, 70*, 217-248.

Inal, J. M. (2003). Phage therapy: a reappraisal of bacteriophages as antibiotics. *Archivum Immunologiae et Therapiae Experimentalis, 51* (4), 237-244.

Ioseliani, G., Meladze, G., Chkhetiia, N., Mebuke, M., Kiknadze, N. (1980). Use of bacteriophage and antibiotics for prevention of acute postoperative empyema in chronic suppurative lung diseases. *Grudnaia khirurgiia (Moscow, Russia), 6*, 63-67.

Ito, F., Fujimori, H., Honnami, H., Kawakami, H., Kanamura, K., Makino, K. (2010). Control of drug loading efficiency and drug release behavior in preparation of hydrophilic-drug-containing monodisperse PLGA microspheres. *Journal of Materials Science, Materials in Medicine, 21* (5), 1563-1571.

Ito, F., Fujimori, H., Makino, K. (2008). Factors affecting the loading efficiency of water-soluble drugs in PLGA microspheres. *Colloids and Surfaces. B, Biointerfaces, 61* (1), 25-29.

Iwata, M., Sato, A. (1991). Morphological and immunohistochemical studies of the lungs and bronchus-associated lymphoid tissue in a rat model of chronic pulmonary infection with Pseudomonas aeruginosa. *Infection and Immunity, 59* (4), 1514-1520.

Jeffery, H., Davis, S., O'Hagan, D. (1993). The preparation and characterization of poly(lactide-co-glycolide) microparticles. II. The entrapment of a model protein using a (water-in-oil)-in-water emulsion solvent evaporation technique. *Pharmaceutical Research, 10* (3), 362-8.

Jenkins, M.U., Egelhaaf, S.U. (2008). Confocal microscopy of colloidal particles: towards reliable, um coordinates. *Advances in Colloid and Interface Science, 136* (1-2), 65-92.

Jepson, C., March, J. (2004). Bacteriophage lambda is a highly stable DNA vaccine delivery vehicle. *Vaccine, 22* (19), 2413-2419.

Jiang, S., Nail, S. (1998). Effect of process conditions on recovery of protein activity after freezing and freeze-drying. *European Journal of Pharmaceutics and Biopharmaceutics, 45* (3), 249-257.

Jiang, H., Zhu, K. (2002). Bioadhesive fluorescent microspheres as visible carriers for local delivery of drugs. I: preparation and characterization of insulin-loaded PCEFB/PLGA microspheres. *Journal of Microencapsulation, 19* (4) , 451-461.

Johansen, H.K. (1996). Potential of preventing Pseudomonas aeruginosa lung infections in cystic fibrosis patients: experimental studies in animals. *APMIS Supplementum, 63*, 5-42.

Johansen, H., Gøtzsche, P. (2008). Vaccines for preventing infection with Pseudomonas aeruginosa in cystic fibrosis. *Cochrane Database of Systematic Reviews, 4*, CD001399.

Johansen, H.K., Hougen, H., Cryz, S.J., Rygaard, J., Høiby, N. (1995). Vaccination promotes TH1-like inflammation and survival in chronic Pseudomonas aeruginosa pneumonia in rats. *American Journal of Respiratory and Critical Care Medicine, 152* (4 Pt 1), 1337-1346.

Jones, M.D., Harris, H., Hooton, J.C., Shur, J., King, G.S., Mathoulin, C.A., Nichol, K., Smith, T.L., Dawson, M.L., Ferrie, A.R., Price, R. (2008). An investigation into the relationship between carrier-based dry powder inhalation performance and formulation cohesive-adhesive force balances. *European Journal of Pharmaceutics and Biopharmaceutics, 69* (2), 496-507.

Joo, N.S., Krouse, M.E., Wu, J.V., Saenz, Y., Jayaraman, S., Verkman, A.S., Wine, J.J. (2001). HCO3- transport in relation to mucus secretion from submucosal glands. *Journal of the Pancreas, 2* (4 Suppl), 280-284.

Joseph, P.M., O'Sullivan, B.P., Lapey, A., Dorkin, H., Oren, J., Balfour, R., Perricone, M.A., Rosenberg, M., Wadsworth, S.C., Smith, A.E., St George, J.A., Meeker, D.P. (2001). Aerosol and lobar administration of a recombinant adenovirus to individuals with cystic fibrosis. I. Methods, safety, and clinical implications. *Human Gene Therapy, 12* (11), 1369-1382.

Jung, T., Koneberq, R., Hunqerer, K.D., Kissel, T. (2002). Tetanus toxoid microspheres consisting of biodegradable poly (lactide-co-glycolide)-and ABA-triblock-copolymers: immune response in mice. *International Journal of Pharmaceutics, 234* (1-2), 75-90.

Kadouri, D., O'Toole, G. (2005). Susceptibility of biofilms to Bdellovibrio bacteriovorus attack. *Applied and Environmental Microbiology, 71* (7), 4044-4051.

Kalaji, N., Deloge, A., Sheibat-Othman, N., Boyron, O., About, I., Fessi, H. (2010). Controlled release carriers of growth factors FGF-2 and TGFbeta1: synthesis, characterization and kinetic modelling. *Journal of Biomedical Nanotechnology, 6* (2), 106-116.

Kellerman, D., Rossi Mospan, A., Engels, J., Schaberg, A., Gorden, J., Smiley, L. (2008). Denufosol: a review of studies with inhaled P2Y(2) agonists that led to Phase 3. *Pulmonary Pharmacology and Therapeutics, 21* (4), 600-7.

Kendrick, B.S., Chang, B.S., Arakawa, T., Peterson, B., Randolph, T.W., Manning, M.C., Carpenter, J.F. (1997). Preferential exclusion of sucrose from recombinant interleukin-1 receptor antagonist: role in restricted conformational mobility and compaction of native state. *Proceedings of the National Academy of Sciences of the United States of America, 94* (22), 11917-11922.

Kerem, B., Rommens, J. M., Buchanan, J. A., Markiewicz, D., Cox, T. K., Chakravarti, A., Buchwald, M., Tsui, L.C. (1989). Identification of the cystic fibrosis gene: genetic analysis. *Science, 245* (4922), 1073-1080.

Kerem, E. (2006). Mutation specific therapy in CF. *Paediatric Respiratory Reviews, 75*, S166-S169.

Kerem, E., Hirawat, S., Armoni, S., Yaakov, Y., Shoseyov, D., Cohen, M., Nissim-Rafinia, M., Blau, H., Rivlin, J., Aviram, M., Elfring, G.L., Northcutt, V.J., Miller, L.L., Kerem, B., Wilschanski, M. (2008). Effectiveness of PTC124 treatment of cystic fibrosis caused by nonsense mutations: a prospective phase II trial. *Lancet, 372* (9640), 719-727.

Kim, C., Kim, J., Park, H.Y., Park, H.J., Lee, J.H., Kim, C.K., Yoon, J. (2008). Furanone derivatives as quorum-sensing antagonists of Pseudomonas aeruginosa. *Applied Microbiology and Biotechnology, 80* (1), 37-47.

Kim, K.C., McCracken, K., Lee, B.C., Shin, C.Y., Jo, M.J., Lee, C.J., Ko, K.H.. (1997). Airway goblet cell mucin: its structure and regulation of secretion. *The European Respiratory Journal, 10*, 2644-2649.

Kishioka, C., Okamoto, K., Hassett, D.J., de Mello, D., Rubin, B.K. (1999). Pseudomonas aeruginosa alginate is a potent secretagogue in the isolated ferret trachea. *Pediatric Pulmonology, 27* (3), 174-179.

Kissel, T., Koneberq, R., Hilbert, A.K., Hunqerer, K.D. (1997). Microencapsulation of antigens using biodegradable polyesters: facts and phantasies. *Behring Institute Mitteilungen, 98*, 172-183.

Klinger, J.D., Cash, H.A., Wood, R.E., Miler, J.J. (1983). Protective immunization against chronic Pseudomonas aeruginosa pulmonary infection in rats. *Infection and Immunity, 39* (3), 1377-1384.

Klose, D., Siepmann, F., Elkharraz, K., Siepmann, J. (2008). PLGA-based drug delivery systems: importance of the type of drug and device geometry. *International Journal of Pharmaceutics, 354* (1-2), 95-103.

Knowles, M.R., Boucher, R.C. (2002). Mucus clearance as a primary innate defense mechanism for mammalian airways. *The Journal of Clinical Investigation, 109*, 571-577.

Kochetkova, V.A., Mamontov, A.S., Moskovtseve, R.L., Erastova, E.I., Trofimov, E.I., Popov, M.I., Dzhubalieva, S.K. (1989). Phagotherapy of postoperative suppurative-inflammatory complications in patients in patients with neoplasms. *Sovetskaia Meditsina, 6*, 23-26.

Kohlmeier, J., Woodland, D. (2009). Immunity to respiratory viruses. *Annual Review of Immunology, 27*, 61-82.

Koseki, T., Kitabatake, N., Doi, E. (1990). Freezing denaturation of ovalbumin at acid pH. *Journal of Biochemistry, 107* (3), 389-94.

Kostanski, J.W., Thanoo, B.C., DeLuca, P.P. (2000). Preparation, characterization, and in vitro evaluation of 1-and 4-month controlled release orntide PLA and PLGA microspheres. *Pharmaceutical Development and Technology, 5* (4), 585-596.

Kreilgaard, L., Frokjaer, S., Flink, J., Randolph, T., Carpenter, J. (1998). Effects of additives on the stability of recombinant human factor XIII during freeze-drying and storage in the dried solid. *Archives of Biochemistry and Biophysics, 360* (1), 121-34.

Kuni, C.C., Regelmann, W.E., duCret, R., Boudreau, R.J., Budd, J.R. (1992). Aerosol scintigraphy in the assessment of therapy for cystic fibrosis. *Clinical Nuclear Medicine, 17* (2), 90-93.

Kunzelmann, K., Mall, M. (2003). Pharmacotherapy of the ion transport defect in cystic fibrosis: role of purinergic receptor agonists and other potential therapeutics. *American Journal of Respiratory Medicine, 2* (4), 299-309.

Kuo, W.T., Huang, H.Y., Huang, Y.Y. (2010). Polymeric micelles comprising steric acid-grafted polyethyleneimine as nonviral gene carriers. *Journal of Nanoscience and Nanotechnology, 10* (9), 5540-5547.

Kutateladze, M., Adamia, R. (2008). Phage therapy experience at the Eliava Institute. *Médecine et Maladies Infectieuses, 38* (8), 426-430.

Kutter, E. (2009). Phage host range and efficiency of plating. *Methods in Molecular Biology, 501*, 141-149.

Kwarciński, W., Lazarkiewicz, B., Weber-Dabrowska, B., Rudnicki, J., Kamiński, K., Sciebura, M. (1994). Bacteriophage therapy in the treatment of recurrent subphrenic and subhepatic abscess with jejunal fistula after stomach resection. *Polski tygodnik lekarski, 49* (23-24), 535.

Lai, H.C., FitzSimmons, S.C., Allen, D.B., Kosorok, M.R., Rosenstein, B.J., Campbell, P.W.,Farrell, P.M. (2000). Risk of persistent growth impairment after alternate-day prednisone treatment in children with cystic fibrosis. *The New England Journal of Medicine, 342* (12), 851-859.

Lands, L., Milner, R., Cantin, A., Manson, D., Corey, M. (2007). High-dose ibuprofen in cystic fibrosis: Canadian safety and effectiveness trial. *The Journal of Pediatrics, 151* (3), 249-254.

Lebecque, P., Leal, T., Zylberberg, K., Reychler, G., Bossuyt, X., Godding, V. (2006). Towards zero prevalence of chronic Pseudomonas aeruginosa infection in children with cystic fibrosis. *Journal of Cystic Fibrosis, 5* (4), 237-244.

Le Brun, P.P., De Boer, A.H., Heijerman, H.G., Frijlink, H.W. (2000). A review of the technical aspect of drug nebulization. *Pharmacy World & Science, 22*, 75-81.

Lee, J., Lee, L. (1981). Preferential solvent interactions between proteins and polyethylene glycols. *The Journal of Biological Chemistry, 256* (2), 625-631.

Lee, J., Timasheff, S. (1981). The stabilization of proteins by sucrose. *The Journal of Biological Chemistry, 256* (14), 7193-7201.

Lee, S., Kim, M.S., Kim, J.S., Park, H.J., Woo, J.S., Lee, B.C., Hwang, S.J. (2006). Controlled delivery of a hydrophilic drug from a biodegradable microsphere system by supercritical anti-solvent precipitation technique. *Journal of Microencapsulation, 23* (7), 741-749.

Lenoir, G., Antypkin, Y.G., Miano, A., Moretti, P., Zanda, M., Varoli, G., Monici Preti, P.A., Aryayev, N.L. (2007). Efficacy, safety, and local pharmacokinetics of highly concentrated nebulized tobramycin in patients with cystic fibrosis colonized with Pseudomonas aeruginosa. *Paediatric Drugs, 9* (Suppl 1), 11-20.

Li, L., Schwendeman, S. (2005). Mapping neutral microclimate pH in PLGA microspheres. *Journal of Controlled Release, 101* (1-3), 163-173.

Li, Y., Ogris, M., Pelisek, J., Röedl, W. (2004). Stability and release characteristics of poly(D,L-lactide-co-glycolide) encapsulated CaPi-DNA coprecipitation. *International Journal of Pharmaceutics, 269* (1), 61-70.

Limberis, M., Wilson, J. (2006). Adeno-associated virus serotype 9 vectors transduce murine alveolar and nasal epithelia and can be readministered. *Proceedings of the National Academy of Sciences of the United States of America, 103* (35), 12993-12998.

Limberis, M., Vandenberghe, L., Zhang, L., Pickles, R., Wilson, J. (2009). Transduction efficiencies of novel AAV vectors in mouse airway epithelium in

vivo and human ciliated airway epithelium in vitro. *Molecular Therapy, 17* (2), 294-301.

LiPuma, J.J., Dasen, S.E., Nielson, D.W., Stern, R.C., Stull, T.L. (1990). Person-to-person transmission of Pseudomonas cepacia between patients with cystic fibrosis. *Lancet, 336*, 1094-1096.

Litvinova, A., Chtetsova, V., Kavtreva, I. (1978). Evaluation of efficacy of the use of coli-Proteus bacteriophage in intestinal dysbacteriosis in premature infants. *Voprosy Okhrany Materinstva i Detstva, 23* (9), 42-44.

Liu, F., Lizio, R., Schneider, U., Petereit, H., Blakey, P., Basit, A. (2009). SEM/EDX and confocal microscopy analysis of novel and conventional enteric-coated systems. *International Journal of Pharmaceutics, 369* (1-2), 1872-1878.

Lueckel, B., Helk, B., Bodmer, D., Leuenberger, H. (1998). Effects of formulation and process variables on the aggregation of freeze-dried interleukin-6 (IL-6) after lyophilization and on storage. *Pharmaceutical Development and Technology, 3* (3), 337-46.

Lührmann, A., Tschernig, T., Pabst, R. (2002-2003). Stimulation of bronchus-associated lymphoid tissue in rats by repeated inhalation of aerosolized lipopeptide MALP-2. *Pathobiology, 70* (5), 266-9.

Lugton, I. (1999). Mucosa-associated lymphoid tissues as sites for uptake, carriage and excretion of tubercle bacilli and other pathogenic mycobacteria. *Immunology and Cell Biology, 77* (4), 364-372.

Lui, R., Ma, G.-H., Wan, Y.-H., Su, Z.-G. (2005). Influence of process parameters on the size distribution of PLA microcapsules prepared by combining membrane emulsification technique and double emulsion-solvent evaporation method. *Colloids and Surfaces. B, Biointerfaces, 45* (3-4), 144-153.

Luten, J., van Nostrum, C.F., DeSmedt, S.C., Hennink, W.E. (2008). Biodegradable polymers as non-viral carriers for plasmid DNA delivery. *Journal of Controlled Release, 126*, 97-110.

Lyczak, J.B., Cannon, C.L., Pier, G.B. (2002). Lung infections associated with cystic fibrosis. *Clinical Microbiology Reviews, 15*, 194-222.

Ma, G., Su, Z., Omi, S., Sundberg, D., Stubbs, J. (2003). Microencapsulation of oil with poly(styrene-N,N-dimethylaminoethyl methacrylate) by SPG emulsification technique: effects of conversion and composition of oil phase. *Journal of Colloid and Interface Science, 266* (2), 282-294.

Ma, Y., Pacan, J.C., Wang, Q., Xu, Y., Huang, X., Korenevsky, A., Sabour, P.M. (2008). Microencapsulation of bacteriophage felix O1 into chitosan-alginate microspheres for oral delivery. *Applied and Environmental Microbiology, 74* (15), 4799-805.

Madeir, C., Mendes, R.D., Ribeiro, S.C., Boura, J.S., Aires-Barros, M.R., da Silva, C.L., Cabral, J.M.S. (2010). Nonviral Gene Delivery to Mesenchymal Stem Cells Using Cationic Liposomes for Gene and Cell Therapy. *Journal of Biomedicine and Biotechnology*, In Press.

Makino, K., Ohshima, H., Kondo, T. (1986). Mechanism of hydrolytic degradation of poly(L-lactide) microcapsules: effects of pH, ionic strength and buffer concentration. *Journal of Microencapsulation, 3* (3), 203-212.

Mall, M. (2009). Role of the amiloride-sensitive epithelial Na+ channel in the pathogenesis and as a therapeutic target for cystic fibrosis lung disease. *Experimental Physiology, 94* (2), 171-174.

Mao, S., Xu, J., Cai, C., Germershaus, O., Schaper, A., Kissel, T. (2007). Effect of WOW process parameters on morphology and burst release of FITC-dextran loaded PLGA microspheres. *International Journal of Pharmaceutics, 334* (1-2), 137-148.

Martin, A., Swarbrick, J., Cammarata, A. (1983). *Physical Pharmacy.* 3rd edn. Leise Febiger, Philadelphia: USA.

Marza, J.A., Soothill, J.S., Boydell, P., Collyns, T.A. (2006). Multiplication of therapeutically administered bacteriophages in Pseudomonas aeruginosa. *Burns, 32* (5), 644-646.

Markoishvili, K., Tsitlanadze, G., Katsarava, R., Morris, J.G.Jr., Sulakvelidze, A. (2002). A novel sustained-release matrix based on biodegradable poly(ester amide)s and impregnated with bacteriophages and an antibiotic shows promise in management of infected venous stasis ulcers and other poorly healing wounds. *International Journal of Dermatology, 41* (7), 453-458.

Massie, R.J., Delalycki, M., Bankier, A. (2005). Screening couples for cystic fibrosis carrier status: why are we waiting? *The Medical journal of Australia, 183* (10), 501-502.

Massie, R.J., Olsen, M., Glazner, J., Robertson, C.F., Francis, I. (2000). New born screening for cystic fibrosis in Victoria: 10 years experience (1989-1998). *The Medical journal of Australia, 172*, 584-587.

Mathee, K., Ciofu, O., Sternberg, C., Lindum, P.W., Campbell, J.I., Jensen, P., Johnsen, A.H., Givskov, M., Ohman, D.E., Molin, S., Høiby, N., Kharazmi, A. (1999). Mucoid conversion of Pseudomonas aeruginosa by hydrogen peroxide: a mechanism for virulence activation in the cystic fibrosis lung. *Microbiology, 145* (Pt 6), 1349-1357.

Matsubara, T., Emoto, W., Kawashiro, K. (2007). A simple two-transition model for loss of infectivity of phages on exposure to organic solvent. *Biomolecular Engineering, 24* (2), 269-271.

Matsui, H., Grubb, B.R., Tarran, R., Randell, S.H., Gatzy, J.T., Davis, C.W., Boucher, R.C. (1998). Evidence for periciliary liquid layer depletion, not abnormal ion composition, in the pathogenesis of cystic fibrosis airways disease. *Cell, 95* (7), 1005-1015.

Matsuyama, K., Mishima, K., Hayashi, K., Ishikawa, H., Matsuyama, H., Harada, T. (2003). Formation of microcapsules of medicines by the rapid expansion of a supercritical solution with nonsolvent. *Journal of Applied Polymer Science, 89*, 742-752.

Matthews, L.W., Doershuk, C.F. (1967). Inhalation therapy and postural drainage for the treatment of cystic fibrosis. *Bibliotheca Paediatrica, 86,* 297-314.

McManus, C., Mohan, K., Ledson, M.J., Walshaw, M.J. (2005). Increasing antibiotic resistance amongst pseudomonas strains in one UK adult CF unit. *Journal of Cystic Fibrosis, 4* (210), S34-S58.

McVay, C., Velásquez, M., Fralick, J. (2007). Phage therapy of Pseudomonas aeruginosa infection in a mouse burn wound model. *Antimicrobial Agents and Chemotherapy, 51* (6), 1934-8.

Meers, P., Neville, M., Malinin, V., Scotto, A.W., Sardaryan, G., Kurumunda, R., Mackinson, C., James, G., Fisher, S., Perkins, W.R. (2008). Biofilm penetration, triggered release and in vivo activity of inhaled liposomal amikacin in chronic Pseudomonas aeruginosa lung infections. *The Journal of Antimicrobial Chemotherapy, 61* (4), 859-868.

Meladze, G.D., Mebuke, M.G., Chkhetia, N.S., Kiknadze, N.I., Koguashvili, G.G., Timoshuk, I.I., et al. (1982). The efficacy of Staphylococcal bacteriophage in treatment of purulent diseases of lungs and pleura. *Grudnaia Khirurgiia, 1,* 53-56.

Merril, C.R., Scholl, D., Adhya, S. (2006). Phage therapy. In Calendar, R. (ed.), *The bacteriophages* 2nd ed., Oxford University Press. New York: 725-741.

Messaritaki, A., Black, S.J., van der Walle, C.F., Rigby, S.P. (2005). NMR and confocal microscopy studies of the mechanisms of burst drug release from PLGA microspheres. *Journal Controlled Release, 108,* 271-281.

Meyer, K.C., Lewandoski, J.R., Zimmerman, J.J., Nunley, D., Calhoun, W.J., Dopico, G.A. (1991). Human neutrophil elastase and elastase/alfa-antiprotease complex in cystic fibrosis: comparison with interstitial lung disease and evaluation of the effectof intravenously administered antibiotic therapy. The *American Review of Respiratory Disease, 144* (3Pt1), 580-585.

Michel-Briand, Y., Baysse, C. (2002). The pyocins of Pseudomonas aeruginosa. *Biochimie, 84* (5-6), 499-510.

Miliutina, L., Vorotyntseva, N. (1993). Current strategy and tactics of etiotropic therapy of acute intestinal infections in children. *Antibiotics and Chemotherapy, 38* (1), 46-53.

Mishima, K., Matsuyama, K., Tanabe, D., Yamauchi, S., Young, T., Johnston, K.P. (2000). Microencapsulation of proteins by rapid expansion of supercritical solution with a nonsolvent. *American Institute of Chemical Engineers Journal, 46*, 857.

Mitomo, K., Griesenbach, U., Inoue, M., Somerton, L., Meng, C., Akiba, E., Tabata, T., Ueda, Y., Frankel, G.M., Farley, R.,Singh, C., Chan, M., Munkonge, F., Brum, A., Xenariou, S., Escudero-Garcia, S., Hasegawa, M., Alton, E.W. (2010). Toward gene therapy for cystic fibrosis using a lentivirus pseudotyped with Sendai virus envelopes. *Molecular Therapy, 18* (6), 1173-82.

Miyazaki, H., Kuwano, K., Yoshida, K., Maeyama, T., Yoshimi, M., Fujita, M., Hagimoto, N., Yoshida, R., Nakanishi,Y. (2004). The perforin mediated apoptotic

pathway in lung injury and fibrosis. *Journal of Clinical Pathology, 57* (12), 1292-8.

Mohamed, F., van der Walle, C. (2008). Engineering biodegradable polyester particles with specific drug targeting and drug release properties. *Journal of Pharmaceutical Sciences, 97* (1), 71-87.

Mohamed, F., van der Walle, C. (2006). PLGA microcapsules with novel dimpled surfaces for pulmonary delivery of DNA. *International Journal of Pharmaceutics , 311* (1-2), 97-107.

Mollica, F., Biondi, M., Muzzi, S., Ungaro, F., Quaglia, F., LaRotonda, M.I., Netti, P.A. (2008). Mathematical modelling of the evolution of protein distribution within single PLGA microspheres: prediction of local concentration profiles and release kinetics. *Journal of Material Sciences. Materials in Medicine, 19* (4), 1587-1593.

Moss, R.B., Milla, C., Colombo, J., Accurso, F., Zeitlin, P.L., Clancy, J.P., Spencer, L.T., Pilewski, J., Waltz, D. A., Dorkin, H.L., Ferkol, T., Pian, M., Ramsey, B., Carter, B.J., Martin, D.B., Heald, A.E. (2007). Repeated aerosolized AAV-CFTR for treatment of cystic fibrosis: a randomized placebo-controlled phase 2B trial. *Human Gene Therapy, 18* (8), 726-732.

Moss, R.B., Rodman, D., Spencer, L.T., Aitken, M.L., Zeitlin, P.L., Waltz, D., Milla,C., Brody, A.S., Clancy, J.P., Ramsey, B., Hamblett, N., Heald, A.E. (2004). Repeated adeno-associated virus serotype 2 aerosol-mediated cystic fibrosis transmembrane regulator gene transfer to the lungs of patients with cystic

fibrosis: a multicenter, double-blind, placebo-controlled trial. *Chest, 125* (2), 509-521.

Mozhaev, V., Martinek, K. (1984). Structure-stability relationships in proteins: new approaches to stabilizing enzymes. *Enzyme and Microbial Technology, 6* (2), 50-59.

Mueller, C., Flotte, T. (2008). Gene therapy for cystic fibrosis. *Clinical Reviews in Allergy & Immunolog , 35* (3), 164-78.

Mukhopadhyay, S., Singh, M., Cater, J.I., Ogston, S., Franklin, M., Olver, R.E. (1996). Nebulised antipseudomonal antibiotic therapy in cystic fibrosis; a meta analysis of benefit and risk. *Thorax, 51*, 364-368.

Mundargi, R.C., Srirangarajan, S., Agnihotri, S.A., Patil, S.A., Ravindra, S., Setty, S.B., Aminabhavi, T.M. (2007). Development and evaluation of novel biodegradable microspheres based on poly(d, l-lactide-co-glycolide) and poly (epsilon-caprolactone) for controlled delivery of doxycycline in the treatment of human periodontal pocket; in vitro and in vivo studies. *Journal of Controlled Release*, *119* (1), 59-68.

Murase, N., Franks, F. (1989). Salt precipitation during the freeze-concentration of phosphate buffer solutions. *Biophysical Chemistry, 34* (3), 293-300.

Nacucchio, M.C., Cerquetti, M.C., Meiss, R.P., Sordelli, D.O. (1984). Short communication. Role of agar beads in the pathogenicity of Pseudomonas aeruginosa in the rat respiratory tract. *Pediatric Research, 18* (3), 295-296.

Nail, S., Johnson, W. (1992). Methodology for in-process determination of residual water in freeze-dried products. *Developments in Biological Standardization, 74*, 137-150.

Newman, S.P. (1985). Aerosol deposition considerations in inhalation therapy. *Chest, 88* (2 suppl), 1525-1605.

Nihant, N., Schugens, C., Grandfils, C., Jérôme, R., Teyssié, P. (1994). Polylactide microparticles prepared by double emulsion/evaporation technique. I. Effect of primary emulsion stability. *Pharmaceutical Research, 11* (10), 1479-1484.

Nixon, G.M., Armstrong, D.S., Carzino, R., Carlin, J.B., Olinsky, A., Robertson, C.F., Grimwood, K. (2001). Clinical outcome after early Pseudomonas aeruginosa infection in cystic fibrosis. The *Journal of Pediatrics, 138* (5), 699-704.

O'Donnell, P.B., McGinity, J.W. (1997). Preparation of microspheres by the solvent evaporation technique. *Advanced Drug Delivery Reviews, 28*(1), 25-42.

Okada, H., Doken, Y., Ogawa, Y., Toquchi, H. (1994). Preparation of three-month depot injectable microspheres of leuprorelin acetate using biodegradable polymers. *Pharmaceutical Research, 11* (80), 1143-1147.

Okada, H., Toquchi, H. (1995). Biodegradable microspheres in drug delivery. *Critical Reviews in Therapeutic Drug Carrier Systems, 12* (1), 1-99.

Oliveira, A., Sereno, R., Nicolau, A., Azeredo, J. (2009). In vivo toxicity study of phage lysate in chickens. *British Poultry Science, 50* (5), 558-63.

O'Neal, W.K., Hasty, P., McCray, P.B., Casey, B., Rivera-Pérez, J., Welsh, M.J., Beaudet, A.L., Bradley, A. (1993). A severe phenotype in mice with a duplication of exon 3 in the cystic fibrosis locus. *Human Molecular Genetics, 2* (10), 1561-1569.

Pabst, R., Tschernig, T. (2010). Bronchus-associated lymphoid tissue: an entry site for antigens for successful mucosal vaccinations? *American Journal of Respiratory Cell and Molecular Biology, 43* (2), 137-141.

Pai, V.B., Nahata, M.C. (2001). Efficacy and safety of aerosolized tobramycin in cystic fibrosis. *Pediatric Pulmonology, 32* (4), 314-327.

Pang, Y., Sakagami, M., Byron, P.R. (2005). The pharmacokinetics of pulmonary insulin in the isolated perfused rat lung: implications of metabolism and regional deposition. *European Journal of Pharmaceutical Sciences, 25* (4-5), 369-378.

Panyam, J., Dali, M.M., Sahoo, S.K., Ma, W., Chakravarthi, S.S., Amidon, G.L., Levy, R.J., Labhasetwar, V. (2003). Polymer degradation and in vitro release of a model protein from poly(D,L-lactide-co-glycolide) nano- and microparticles. *Journal of Controlled Release, 92* (1-2), 173-187.

Parikh, B.V., Upadrashta, S.M., Neu, S.H., Nuessle, N.O. (1993). Oestrone loaded poly(L-lactic acid) microspheres: preparation, evaluation and in vitro release kinetics. *Journal of Microencapsulation, 10* (2), 141-153.

Park, T. (1995). Degradation of poly(lactic-co-glycolic acid) microspheres: effect of copolymer composition. *Biomaterials, 16* (15), 1123-30.

Paschoal, I.A., de Oliveira Villalba, W., Bertuzzo, C.S., Cerqueira, E.M., Pereira, M.C. (2007). Cystic fibrosis in Adults. *Lung, 185* (2), 81-87.

Passerini, N., Craig, D. (2001). An investigation into the effects of residual water on the glass transition temperature of polylactide microspheres using modulated temperature DSC. *Journal of Controlled Release, 73* (1), 111-115.

Patton, J.S. (1996). Mechanisms of macromolecule absorption by the lungs. *Advanced Drug Delivery Reviews, 19*, 3-36.

Payne, R., Jansen, V. (2001). Understanding bacteriophage therapy as a density-dependent kinetic process. *Journal of Theoretical Biology, 208* (1), 37-48.

Payne, R., Jansen, V. (2003). Pharmacokinetic principles of bacteriophage therapy. *Clinical Pharmacokinetics, 42* (4), 315-325.

Pedemonte, N., Lukacs, G.L., Du, K., Caci, E., Zegarra-Moran, O., Galietta, L.J., Verkman, A.S. (2005). Small-molecule correctors of defective DeltaF508-CFTR cellular processing identified by high-throughput screening. *The Journal of Clinical Investigation, 115* (9), 2564-2571.

Pedersen, S.S., Shand, G.H., Hansen, B.L., Hansen, G.N. (1990). Induction of experimental chronic Pseudomonas aeruginosa lung infection with P. aeruginosa entrapped in alginate microspheres. *Acta Pathologica, Microbiologica, et Immunologica Scandinavica, 98* (3), 203-211.

Pennington, J.E., Hickey, W.F., Blackwood, L.L., Arnaut, M.A. (1981). Active immunization with lipopolysaccharide Pseudomonas antigen for chronic Pseudomonas bronchopneumonia in guinea pigs. *The Journal of Clinical Investigation, 68* (5), 1140-1148.

Pereira, P., Kelly, S.M., Cooper, A., Mardon, H.J., Gellert, P.R., van der Walle, C.F. (2007). Solution formulation and lyophilisation of a recombinant fibronectin fragment. *European Journal of Pharmaceutics and Biopharmaceutics, 67* (2), 309-319.

Perepanova, T.S., Darbeeva, O.S., Kotliarova, G.A., Kondrat'eva, E.M., Maĭskaia, L.M, Malysheva, V.F., Baiguzina, F.A., Grishkova, N.V. (1995). The efficacy of bacteriophage preparations in treating inflammatory urologic diseases. *Urologiia͡ i nefrologiia͡, 5,* 14-17.

Pickles, R. (2004). Physical and biological barriers to viral vector-mediated delivery of genes to the airway epithelium. *Proceedings of the American Thoracic Society, 1* (4), 302-308.

Pikal, M.J., Shah, S. (1990). Transport mechanisms in iontophoresis. III. An experimental study of the contributions of electroosmotic flow and permeability change in transport of low and high molecular weight solutes. *Pharmaceutical Research, 7* (3), 222-229.

Pikal, M.J., Shah, S. (1997). Intravial distribution of moisture during the secondary drying stage of freeze drying. *PDA Journal of Pharmaceutical Science and Technology, 51* (1), 17-24.

Pikal, M.J., Roy, M.L., Shah, S. (1984). Mass and heat transfer in vial freeze-drying of pharmaceuticals: role of the vial. *Journal of Pharmaceutical Sciences, 73* (9), 1224-1237.

Pikal, M.J., Shah, S., Roy, M.L., Putman, R. (1990). The secondary drying stage of freeze drying-drying kinetics as a function of temperature and chamber pressure. *International Journal of Pharmaceutics, 60*, 203-217.

Plesch, B., Gamelkoorn, G., van de Ende, M. (1983). Development of bronchus associated lymphoid tissue (BALT) in the rat, with special reference to T- and B-cells. *Developmental and Comparative Immunology, 7* (1), 179-188.

Porteous, D.J., Dorin, J.R., McLachlan, G., Davidson-Smith, H., Davidson, H., Stevenson, B., Carothers, A.D., Wallace, W.A., Moralee, S., Hoenes, C., Kallmeyer, G., Michaelis, U., Naujoks, K., Ho, L.P., Samways, J.M., Imrie, M., Greening, A.P., Innes, J.A. (1997). Evidence for safety and efficacy of DOTAP cationic liposome mediated CFTR gene transfer to the nasal epithelium of patients with cystic fibrosis. *Gene Therapy, 4* (3), 210-8.

Puapermpoonsiri, U., Spencer, J., van der Walle, C.F. (2009). A freeze-dried formulation of bacteriophage encapsulated in biodegradable microspheres. *European Journal of Pharmaceutics and Biopharmaceutics, 72* (1), 26-33.

Puchelle, E., Bajolet, O., Abely, M. (2002). Airway mucus in cystic fibrosis. *Paediatric Respiratory Reviews, 3* (2), 115-119.

Quan, J.M., Tiddens, H.A., Sy, J.P., McKenzie, S.G., Montgomery, M.D., Robinson, P.J., Wohl, M.E., Konstan, M.W., (2001). A two-year randomized, placebo-controlled trial of dornase alfa in young patients with cystic fibrosis with mild lung function abnormalities. *The Journal of Pediatrics, 139* (6), 813-820.

Rahman, N.A., Mathiowitz, E. (2004). Localization of bovine serum albumin in double-walled microspheres. *Journal of Controlled Release, 94* (1), 163-175.

Randall, T.D. (2010). Bronchus-associated lymphoid tissue (BALT) structure and function. *Advances in Immunology, 107*, 187-241.

Ratjen, F. (2006). Restoring airway surface liquid in cystic fibrosis. *The New England Journal of Medicine, 354*, 291-293.

Ratjen, F. (2009). Cystic fibrosis: pathogenesis and future treatment strategies. *Respiratory Care, 54* (5), 595-605.

Ravilly, S., Olesen, H.V., Quinton, H.B., Viviani, L., Wiedemann, B., Le Roux, E., et al. (2005). Study on cystic fibrosis mortality in 5 countries. *Journal of Cystic Fibrosis, 4* (450), S119-S125.

Riordan, J.R., Rommens, J.M., Kerem, B., Alon, N., Rozmahel, R., Grezelczak, Z., Zielenski, J., Lok, S., Plavsic, N., Chou, J.L., et al. (1989). Identification of the cystic fibrosis gene: cloning and characterization of complementary DNA. *Science, 245* (4922), 1066-1073.

Robert, R., Carlile, G., Pavel, C., Liu, N., Anjos, S., Liao, J., Luo, Y., Zhang, D., Thomas, D.Y., Hanrahan, J.W. (2008). Structural analog of sildenafil identified as a novel corrector of the F508del-CFTR trafficking defect. *Molecular Pharmacology, 73* (2), 478-489.

Rodgers, H.C., Knox, A.J. (2001). Pharmacological treatment of the biochemical defect in cystic fibrosis airways. *The European Respiratory Journal, 17* (6), 1314-1321.

Rosca, I., Watari, F., Uo, M. (2004). Microparticle formation and its mechanism in single and double emulsion solvent evaporation. *Journal of Controlled Release, 99* (2), 271-280.

Rosenecker, J., Huth, S., Rudolph, C. (2006). Gene Therapy for Cystic Fibrosis Lung Disease: Current Status and Future Perspectives. *Current Opinion in Molecular Therapeutics, 8* (5), 439-445.

Rosenfeld, M.A., Gibson, R.L., McNamara, S., Emerson, J., Burns, J.L., Castile, R., Hiatt, P., McCoy, K., Wilson, C.B., Inglis, A., Smith, A., Martin, T.R., Ramsey, B.W. (2001). Early pulmonary infection, inflammation, and clinical outcomes in infants with cystic fibrosis. *Pediatric Pulmonology, 32* (5), 356-366.

Rosenfeld, M.A., Siegfried, W., Yoshimura, K., Yoneyama, K., Fukayama, M., Stier, L.E., Pääkkö, P.K., Gilardi, P., Stratford-Perricaudet, L.D., Perricaudet, M.,et al. (1991). Adenovirus-mediated transfer of a recombinant alpha 1-antitrypsin gene to the lung epithelium in vivo. *Science, 252* (5004), :431-434.

Rosenfeld, M.A., Yoshimura, K., Trapnell, B.C., Yoneyama, K., Rosenthal, E.R., Dalemans, W., Fukayama, M., Bargon, J., Stier, L.E., Stratford-Perricaudet, L. et

al. (1992). In vivo transfer of the human cystic fibrosis transmembrane conductance regulator gene to the airway epithelium. *Cell, 68* (1), 143-155.

Rouse, J., Mohamed, F., van der Walle, C. (2007). Physical ageing and thermal analysis of PLGA microspheres encapsulating protein or DNA. *International Journal of Pharmaceutics, 339* (1-2), 112-120.

Rozmahel, R., Wilschanski, M., Matin, A., Plyte, S., Oliver, M., Auerbach, W., Moore, A., Forstner, J., Durie, P., Nadeau, J., Bear, C., Tsui, L.C. (1996). Modulation of disease severity in cystic fibrosis transmembrane conductance regulator deficient mice by a secondary genetic factor. *Nature Genetics, 12* (3), 280-287.

Rozov, T., de Oliveira, V.Z., Santana, M.A., Adde, F.V., Mendes, R.H., Paschoal, I.A., Caldeira Reis, F.J., Higa, L.Y., Toledo, A.C. Jr., Pahl, M. (2010). Dornase alfa improves the health-related quality of life among Brazilian patients with cystic fibrosis--a one-year prospective study. *Pediatric Pulmonology, 45* (9), 874-82.

Ruan, G., Frenq, S.S. (2003). Preparation and characterization of poly (lactic acid)-poly (ethylene glycol)-poly (lactic acid) (PLA-PEG-PLA) microspheres for controlled release of paclitaxel. *Biomaterials, 24* (27), 5037-5044.

Ruiz, F.E., Clancy, J.P., Perricone, M.A., Bebok, Z., Hong, J.S., Cheng, S.H, Meeker, D.P.,Young, K.R., Schoumacher, R.A., Weatherly, M.R., Wing, L., Morris, J.E., Sindel, L., Rosenberg, M., van Ginkel, F.W., McGhee, J.R., Kelly, D., Lyrene, R.K., Sorcher, E.J. (2001). A clinical inflammatory syndrome attributable to

aerosolized lipid-DNA administration in cystic fibrosis. *Human Gene Therapy, 12* (7), 751-61.

Rupley, J., Careri, G. (1991). Protein hydration and function. *Advances in Protein Chemistry, 41*, 37-172.

Sakagami, M., Byron, P.R., Venitz, J., Rypacek, F. (2002). Solute disposition in the rat lung in vivo and in vitro: determining regional absorption kinetics in the presence of mucociliary clearance. *Journal of Pharmaceutical Sciences, 91* (2), 594-694.

Sakandelidze, V.M. (1991). The combine use of specific phages and antibiotics indifferent infectious allergoses. *Vrachebnoe Delo, 3*, 60-63.

Saleki-Gerhardt, A., Zografi, G. (1994). Nonisothermal and isothermal crystallization of sucrose from the amorphous state. *Pharmaceutical Research, 11*, 1166-1173.

Salunkhe, P., Smart, C.H., Morgan, J.A., Panagea, S., Walshaw, M.J., Hart, C.A., Geffers, R., Tümmler, B., Winstanley, C. (2005). A cytic fibrosis epiodemic strain of Pseudomonas aeruginosa displays enhanced virulence and antimicrobial resistance. *Journal of Bacteriology, 187*, 4908-4920.

Sambrook, J. and Russell, D.W. (2001a). Purification of Bacteriophage λ Particles by Isopyonic Centrifugation through CsCl Gradients. *Molecular Cloning: A Laboratory Manual.* Cold Spring Harbour Laboratory Press, New York: 2.47-2.51.

Sanders, N., Franckx, H., De Boeck, K., Haustraete, J., De Smedt, S., Demeester, J. (2006). Role of magnesium in the failure of rhDNase therapy in patients with cystic fibrosis. *Thorax, 61* (11), 962-968.

Sandor, M., Enscore, D., Weston, P., Mathiowitz, E. (2001). Effect of protein molecular weight on release from micron-sized PLGA microspheres. *Journal of Controlled Release , 76* (3), 297-311.

Sapru, K., Stotland, P.K., Stevenson, M.M. (1999). Quantitative and qualitative differences in bronchoalveolar inflammatory cells in Pseudomonas aeruginosa-resistant and -susceptible mice. *Clinical and Experimental Immunology, 115* (1), 103-109.

Sarciaux, J., Mansour, S., Hageman, M., Nail, S. (1999). Effects of buffer composition and processing conditions on aggregation of bovine IgG during freeze-drying. *Journal of Pharmaceutical Sciences, 88* (12), 1354-1361.

Schersch, K., Betz, O., Garidel, P., Muehlau, S., Bassarab, S., Winter, G. (2010). Systematic investigation of the effect of lyophilizate collapse on pharmaceutically relevant proteins I: stability after freeze-drying. *Journal of Pharmaceutical Sciences, 99* (5), 2256-2278.

Schook, L., Carrick, L. J., Berk, R.S. (1977). Experimental pulmonary infection of mice by tracheal intubation of Pseudomonas aeruginosa: the use of antineoplastic agents to overcome natural resistance. *Canadian Journal of Microbiology, 23* (6), 823-826.

Scott, A.E., Timms, A.R., Connerton, P.L., Loc Carrillo, C., Adzfa, R.K., Connerton, I.F. (2007). Genome Dynamics of *Campylobacter jejuni* in Response to Bacteriophage Predation. *PLoS Pathogens*, *3*, e119.

Searles, J., Carpenter, J., Randolph, T. (2001). The ice nucleation temperature determines the primary drying rate of lyophilization for samples frozen on a temperature-controlled shelf. *Journal of Pharmaceutical Sciences, 90* (7), 860-871.

Sener, B., Cakar, A., Ozcelik, U., Dogru, D., Yalcin, E., Gur, D., Aslan, A., Kiper, N. (2005). Hypermutable Pseudomonas aeruginosa strains in cystic fibrosis patients; A link with antibiotic resistance. *Journal of Cystic Fibrosis, 4* (Supplement1), S56.

Shah, P., Scott, S., Geddes, D., Hodson, M. (1995). Two years experience with recombinant human DNase I in the treatment of pulmonary disease in cystic fibrosis. *Respiratory Medicine*, *89* (7), 499-502.

Shalaev, E., Johnson-Elton, T., Chang, L., Pikal, M. (2002). Thermophysical properties of pharmaceutically compatible buffers at sub-zero temperatures: implications for freeze-drying. *Pharmaceutical Research, 19* (2), 195-201.

Shi, S., Hickey, A. (2010). PLGA microparticles in respirable sizes enhance an in vitro T cell response to recombinant Mycobacterium tuberculosis antigen TB10.4-Ag85B. *Pharmaceutical Research, 27* (2), 350-360.

Shih, C., Waldron, N., Zentner, G. (1996). Quantitative analysis of ester linkages in poly(-lactide) and poly(-lactide-co-glycolide). *Journal of Controlled Release, 38*, 69-73.

Shortle, D. (1996). The denatured state (the other half of the folding equation) and its role in protein stability. *FASEB Journal, 10* (1), 27-34.

Simões, S., Filipe, A., Faneca, H., Mano, M., Penacho, N., Düzgünes, N., de Lima, M.P. (2005). Cationic liposomes for gene delivery. *Expert Opinion on Drug Delivery, 2* (2), 237-254.

Simpson, R. J. (2010). Stabilization of proteins for storage. *Cold Spring Harbor Protocols,* (5), pdb.top79.

Singh, M., O'Hagan, D. (1998). The preparation and characterization of polymeric antigen delivery systems for oral administration. *Advanced Drug Delivery Reviews, 34* (2-3), 285-304.

Sinha, V. R., Trehan, A. (2005). Biodegradable microspheres for parenteral delivery. *Critical Reviews in Therapeutic Drug Carrier Systems, 22* (6), 535-602.

Skurnik, M., Pajunen, M., Kiljunen, S. (2007). Biotechnological challenges of phage therapy. *Biotechnology Letters, 29* (7), 995-1003.

Smith, H.W., Huggins, M.B. (1982). Successful treatment of experimental Escherichaia coli infections in mice using phages: its general superiority over antibiotics. *Journal of General Microbiology, 128*, 307-318.

Snouwaert, J.N., Brigman, K.K., Latour, A.M., Malouf, N.N., Boucher, R.C., Smithies, O., Koller, B.H. (1992). An animal model for cystic fibrosis made by gene targeting. *Science, 257* (5073), 1083-1088.

Song, Z., Kharazmi, A., Wu, H., Faber, V., Moser, C., Krogh, H. K., Rigaard, J., Hoiby, N. (1998). Effects of ginseng treatment on neutrophil chemiluminescence and immunoglobulin G subclasses in a rat model of chronic Pseudomonas aeruginosa pneumonia. *Clinical and Diagnostic Laboratory Immunology, 5* (6), 882-887.

Song, Z., Wu, H., Mygind, P., Raventos, D., Sonksen, C., Kristensen, H. H., Høiby, N. (2005). Effects of intratracheal administration of novispirin G10 on a rat model of mucoid Pseudomonas aeruginosa lung infection. *Antimicrobial Agents and Chemotherapy, 49* (9), 3868-3874.

Soothill, J., Hawkins, C., Anggard, E., Harper, D. (2004). Therapeutic use of bacteriophages. *The Lancet Infectious Diseases, 4*, 544-545.

Sprent, J., Surh, C. (2002). T cell memory. *Annual Review of Immunology, 20*, 551-579.

Starke, J.R., Edwards, M.S., Langston, C., Baker, C.J. (1987). A mouse model of chronic pulmonary infection with Pseudomonas aeruginosa and Pseudomonas cepacia. *Pediatric Research, 22* (6), 698-702.

Stoltz, D.A., Meyerholz, D.K., Pezzulo, A.A., Ramachandran, S., Rogan, M.P., Davis, G.J.,Hanfland, R.A., Wohlford-Lenane, C., Dohrn, C.L., Barlett, J.A., Nelson, G.A., Chang, E.H., Taft, P.J., Ludwig, P.S., Estin, M., Hornick, E.E., Launspach, J.L., Samuel, M., Rokhlina, T., Karp, P.H., Ostegaard, L.S., Uc, A., Starner, T.D., Horswill, A.R., Brogden, K.A., Prather, R.S., Richter, S.S. Shilyansky, J., McCray, P.B.Jr., Zabner, J., Welsh, M.J. (2010). Cystic fibrosis pigs develop lung disease and exhibit defective bacterial eradication at birth. *Science Translational Medicine, 2* (29), 29ra31.

Stotland, P.K., Radzioch, D., Stevenson, M.M. (2000). Mouse models of chronic lung infection with Pseudomonas aeruginosa: models for the study of cystic fibrosis. *Pediatric Pulmonology, 30* (5), 413-424.

Strambini, G., Gabellieri, E. (1996). Proteins in frozen solutions: evidence of ice-induced partial unfolding. *Biophysical Journal, 70* (2), 971-976.

Strój, L., Weber-Dabrowska, B., Partyka, K., Mulczyk, M., Wójcik, M. (1999). Successful treatment with bacteriophage in purulent cerebrospinal meningitis in a newborn. *Neurologia i Neurochirugia Polska, 33* (3), 693-698.

Sulakvelidze, A., Alavidze, Z., Morris, J.G. (2001). Bacteriophage therapy. *Antimicrobial Agents and Chemotherapy, 45* (3), 649-659.

Suri, R. (2005). The use of human deoxyribonuclease (rhDNase) in the management of cystic fibrosis. *BioDrugs. , 19* (3), 135-144.

Suthereland, I., Hughes, K., Skillman, L., Tait, K. (2004). The interaction of phage and biofilms. *FEMS Microbiology Letters, 232* (1), 1-6.

Tang, X., Pikal, M. (2004). Design of freeze-drying processes for pharmaceuticals: practical advice. *Pharmaceutical Research, 21* (2), 191-200.

Tang, X., Pikal, M. (2005). Measurement of the kinetics of protein unfolding in viscous systems and implications for protein stability in freeze-drying. *Pharmaceutical Research, 22* (7), 1176-85.

Tarran, R., Grubb, B.R., Gatzy, J.T., Davis, C., Boucher, R.C. (2001). The relative roles of passive surface forces and active ion transport in the modulation of airway surface liquid volume and composition. *The Journal of General Physiology, 118* (2), 223-236.

Tarran, R., Grubb, B.R., Parsons, D., Picher, M., Hirsh, A., Davis, C.W., Boucher, R.C. (2001). The CF salt controversy: in vivo observations and therapeutic approaches. *Molecular Cell, 8* (1), 149-158.

Taraseviciene-Stewart, L., Voelkel, N. (2008). Molecular pathogenesis of emphysema. *The Journal of Clinical Investigation, 118* (2), 394-402.

Taylor, R.F., Hodson, M.E. (1993). Cystic fibrosis: Antibiotic prescribing practices in the United Kingdom and Eire. *Respiratory Medicine, 87* (7), 535-539.

Teitelbaum, R., Schubert, W., Gunther, L., Kress, Y., Macaluso, F., Pollard, J.W., McMurray, D.N., Bloom, B.R. (1999). The M cell as a portal of entry to the lung for the bacterial pathogen Mycobacterium tuberculosis. *Immunity, 10* (6), 641-50.

Teper, A., Jaques, A., Charlton, B. (2010). Inhaled mannitol in patients with cystic fibrosis: A randomised open-label dose response trial. *Journal of Cystic Fibrosis*, Sep 29, [Epub ahead of print].

Thomas, C., Gupta, V., Ahsan, F. (2010). Particle size influences the immune response produced by hepatitis B vaccine formulated in inhalable particles. *Pharmaceutical Research, 27* (5), 905-919.

Thomassen, M.J., Klinger, J. D., Winnie, G. B., Wood, R.E., Burtner, C., Tomashefski, J.F., Horowitz, J.G., Tandler,B. (1984). Pulmonary cellular response to chronic irritation and chronic Pseudomonas aeruginosa pneumonia in cats. *Infection and Immunity, 45* (3), 741-747.

Thorsson, L., Geller, D. (2005). Factors guiding the choice of delivery device for inhaled corticosteroids in the long-term management of stable asthma and COPD: Focus on budesonide. *Respiratory Medicine, 99*, 836-849.

Toro, H., Price, S.B., McKee, A.S., Hoerr, F.J., Krehling, J., Perdue, M., Bauermeister, L. (2005). Use of bacteriophages in combination with competitive exclusion to reduce Salmonella from infected chickens. *Avian Diseases, 49* (1), 118-124.

Touw, D. J., Brimicombe, R. W., Hodson, M., Heijerman, H. G., Bakker, W. (1995). Inhalation of antibiotics in cystic fibrosis. *The European Respiratory Journal, 8* (9), 1594-1604.

Townsend, M., DeLuca, P. (1990). Stability of ribonuclease A in solution and the freeze-dried state. *Journal of Pharmaceutical Sciences, 79* (12), 1083-1086.

Tronde, A., Norden, B.M., Wendel, A.K., Lennernas, H., Bengtsson, U.H. (2003). Pulmonary absorption rate and bioavailability of drugs in vivo in rats: structure absorption relationships and physiochemical profiling of inhaled drugs. *Journal of Pharmaceutical Sciences, 92* (6), 1216-1233.

Tschernig, T., Pabst, R. (2000). Bronchus-associated lymphoid tissue (BALT) is not present in the normal adult lung but in different diseases. *Pathobiology, 68* (1), 1-8.

Tsuda, A., Butter, J.P., Fredberq, J.J. (1994). Effect of aveolated duct structure on aerosol kinetics II. Gravitational sedimentation and inertial impaction. *Journal of Applied Physiology, 76* (6), 2510-2516.

van de Weert, M., van 't Hof, R., van der Weerd, J., Heeren, R.M., Posthuma, G., Hennink, W.E., Crommelin, D.J. (2000). Lysozyme distribution and conformation in a biodegradable polymer matrix as determined by FTIR techniques. *Journal of Controlled Release, 68*, 31-40.

Van Goor, F., Straley, K.S., Cao, D., González, J., Hadida, S., Hazlewood, A., Joubran J., Knapp, T., Makings, L.R., Miller, M., Neuberger, T., Olson, E., Panchenko, V.,

Rader, J., Singh, A., Stack, J.H., Tung, R., Grootenhuis, P.D., Negulescu, P. (2006). Rescue of DeltaF508-CFTR trafficking and gating in human cystic fibrosis airway primary cultures by small molecules. *American Journal of Physiology. Lung Cellular and Molecular Physiology, 290* (6), L1117-30.

van Heeckeren, A., Ferkol, T., Tosi, M. (1998). Effects of bronchopulmonary inflammation induced by pseudomonas aeruginosa on adenovirus-mediated gene transfer to airway epithelial cells in mice. *Gene Therapy, 5* (3), 345-351.

Van Heeckeren, A., Schluchter, M. (2002). Murine models of chronic Pseudomonas aeruginosa lung infection. *Laboratory Animals, 36* (3), 291-312.

Wall, D. (1995). Pulmonary absorption of peptides and proteins. *Drug Delivery, 2*, 1-10.

Walters, R., Grunst, T., Bergelson, J., Finberg, R., Welsh, M., Zabner, J. (1999). Basolateral localization of fiber receptors limits adenovirus infection from the apical surface of airway epithelia. *The Journal of Biological Chemistry, 274* (15), 10219-10226.

Wang, J., Wang, B.M., Schwendeman, S.P. (2002). Characterization of the initial burst release of a model peptide from poly(D,L-lactide-co-glycolide) microspheres. *Journal of Controlled Release, 82* (2-3), 289-307.

Wang, W. (1999). Instability, stabilization, and formulation of liquid protein pharmaceuticals. *International Journal of Pharmaceutics, 185* (2), 129-188.

Wang, W. (2000). Lyophilization and development of solid protein pharmaceuticals. *International Journal of Pharmaceutics, 203* (1-2), 1-60.

Wang, Y.J., Chen, H., Busch, M., Baldwin, P.A. (1997). Headspace analysis for parenteral products: Oxygen permeation and integrity test. *Pharmaceutical Technology, 21* (3), 108-122.

Washington, N., Washington, C., Wilson, C.G. (2001). Pulmonar Drug Delivery. *Physiological Pharmaceutics Barriers to Drug Absorption.* 2nd edn. Taylor and Francis Inc. New York: 222-247.

Weber-Dabrowska, B., Dabrowski, M., Slopek, S. (1987). Studies on bacteriophage penetration in patients subjected to phage therapy. *Archivum Immunologiae et Therapiae Experimentalis, 35* (5), 563-568.

Weber-Dabrowska, B., Mulczyk, M., Gorski, A. (2003). Bacteriophages as an efficient therapy for antibiotic-resistant septicemia in man. *Transplantation Proceedings, 35* (4), 1385-1386.

Weibel, E.R. (1979). Morphometry of the human lungs: the state of the art after two decades. *Bulletin Européen de Physiopathologie Respiratoire, 15* (5), 999-1013.

Welsh, M.J. (1994). The path of discovery in understanding the biology of cystic fibrosis and approaches to therapy. *The American Journal of Gastroenterology, 89* (8), S97-S105.

Welsh, M., Ramsey, B., Accurso, F., Cutting, G. (2001). Cystic fibrosis. In Scriver, C., Beaudet, A., Sly, W., Valle, D. C. (eds.), *The metabolic and molecular bases of inherited disease.* McGraw-Hill, New York: 5121-5188.

Wiley, J.A., Richert, L.E., Swain, S.D., Harmsen, A., Barnard, D.L., Randall, T.D., Jutila, M., Douglas, T., Broomell, C., Young, M. (2009). Inducible bronchus-associated lymphoid tissue elicited by a protein cage nanoparticle enhances protection in mice against diverse respiratory viruses. *Public Library of Science One, 4* (9), e7142.

Williams, N., Lee, Y., Polli, G., Jennings, T. (1986). The effects of cooling rate on solid phase transitions and associated vial breakage occurring in frozen mannitol solutions. *Journal of Parenteral Science and Technology, 40* (4), 135-141.

Williams, S., Gebhart, D., Martin, D., Scholl, D. (2008). Retargeting R-type pyocins to generate novel bactericidal protein complexes. *Applied and Environmental Microbiology, 74* (12), 3868-3876.

Wills, P. (2007). Inhaled mannitol in cystic fibrosis. *Expert Opinion on Investigational Drugs, 16* (7), 1121-1126.

Witschi, C., Doelker, E. (1998). Influence of the microencapsulation method and peptide loading on poly (lactic acid) and poly (lactic-co-glycolic acid) degradation during in vitro testing. *Journal of Controlled Release, 51* (2-3), 327-341.

Wright, A., Hawkins, C., Anggård, E., Harper, D. (2009). A controlled clinical trial of a therapeutic bacteriophage preparation in chronic otitis due to antibiotic-resistant

Pseudomonas aeruginosa; a preliminary report of efficacy. *Clinical Otolaryngology, 34* (4), 349-357.

Wu, H., Song, Z., Givskov, M., Doring, G., Worlitzsch, D., Mathee, K., Rigaard, J., Høiby, N. (2001). Pseudomonas aeruginosa mutations in lasI and rhlI quorum sensing systems result in milder chronic lung infection. *Microbiology, 147* (Pt 5), 1105-1113.

Wu, H., Song, Z., Givskov, M., Høiby, N. (2004). Effects of quorum-sensing on immunoglobulin G responses in a rat model of chronic lung infection with Pseudomonas aeruginosa. *Microbes and Infection , 6* (1), 34-37.

Wu, H., Song, Z., Hentzer, M., Andersen, J., Molin, S., Givskov, M., Høiby, N. (2004). Synthetic furanones inhibit quorum-sensing and enhance bacterial clearance in Pseudomonas aeruginosa lung infection in mice. *The Journal of Antimicrobial Chemotherapy, 53* (6), 1054-1061.

Yang, F., Song, F.L., Pan, Y.F., Wang, Z.Y., Yang, Y.Q., Zhao, Y.M., Liang, S.Z., Zhang, Y.M. (2010). Preparation and characteristics of interferon-alpha poly(lactic-co-glycolic acid) microspheres. *Journal of Microencapsulation, 27* (2), 133-141.

Yang, T.H., Dong, A., Meyer, J., Johnson, O.L., Cleland, J.L., Carpenter, J.F. (1999). Use of infrared spectroscopy to assess secondary structure of human growth hormone within biodegradable microspheres. *Journal of Pharmaceutical Sciences, 88* (2), 161-165.

Yosha, I., Shani, A., Magdassi, S. (2008). Slow Release of Pheromones to the Atmosphere from Gelatin-Alginate Beads. *Journal of Agricultural and Food Chemistry, 56*, 8045-8049.

Yoshioka, S., Aso, Y., Kojima, S. (1997). dependence of the molecular mobility and protein stability of freeze-dried γ-globulin formulations on the molecular weight of dextran. Pharmaceutical Research, 14, 736-741.

Yoshioka, T., Kawazoe, N., Tateishi, T., Chen, G. (2008). In vitro evaluation of biodegradation of poly(lactic-co-glycolic acid) sponges. *Biomaterials, 29* (24-25), 3438-3443.

Young, P.M., Cocconi, D., Colombo, P., Bettini, R., Price, R., Steele, D.F., Tobyn, M.J. (2002). Characterization of a surface modified dry powder inhalation carrier prepared by "particle smoothing". *The Journal of Pharmacy and Pharmacology, 54* (10), 1339-1344.

Zhao, H., Gagnon, J., Häfeli, U.O. (2007). Process and formulation variables in the preparation of injectable and biodegradable magnetic microspheres. *Biomagnetic Research and Technology, 5*, 2.

Zhao, K., Li, G.X., Jin, Y.Y., Wei, H.X., Sun, Q.S. Huang, T.T., Wang, Y.F., Tong, G.Z. (2010). Preparation and immunological effectiveness of a Swine influenza DNA vaccine encapsulated in PLGA microspheres. *Journal of Microencapsulation, 27* (2), 178-186.

Zhukov-Verezhnikov, N., Peremitina, L., Berillo, E., Komissarov, V., Bardymov, V. (1978). Therapeutic effect of bacteriophage preparations in the complex treatment of suppurative surgical diseases. *Sovetskaia Meditsina, 12*, 64-66.

Ziady, A., Kelley, T., Milliken, E., Ferkol, T., Davis, P. (2002). Functional evidence of CFTR gene transfer in nasal epithelium of cystic fibrosis mice in vivo following luminal application of DNA complexes targeted to the serpin-enzyme complex receptor. *Molecular Therapy, 5* (4), 413-419.

Zolnik, B., Leary, P., Burgess, D. (2006). Elevated temperature accelerated release testing of PLGA microspheres. *Journal of Controlled Release, 112* (3), 293-300.